

**BRØNSTED ACID PROMOTED OLEFIN FUNCTIONALIZATION
(ANTI-AMINOHYDROXYLATION) AND PROGRESS TOWARD
(+)-ZWITTERMICIN A**

By

Ki Bum Hong

Dissertation

Submitted to the Faculty of the
Graduate School of Vanderbilt University
in partial fulfillment of the requirements

for the degree of

DOCTOR OF PHILOSOPHY

In

Chemistry

May, 2010

Nashville, Tennessee

Approved:

Jeffrey N. Johnston

Gary A. Sulikowski

Carmelo J. Rizzo

Eva Harth

Copyright © 2010 by Ki Bum Hong
All Rights Reserved

To my parents and younger brother.

ACKNOWLEDGEMENTS

First and foremost I would like to thank my research advisor, Dr. Jeffrey Johnston, for his guidance, encouragement, enthusiasm for research and support throughout my six years graduate life both at Indiana and Vanderbilt University. His mentorship and passion for chemistry inspired me to strive to be a better scientist. I would also like to thank the past and present members of the Johnston group for their intellectual contributions to my research as well as their friendships. I would like to specifically acknowledge Dr. Matthew Donahue for his participation in some of this work. I am indebted to Dr. Jeong-Seok Han, Dr. Julie Pigza, Dr. Ryan Yoder, Dr. Timothy Troyer, Dr. Jayasree Srinivasan, Dr. Bo Shen, and Dr. Anand Singh for their helpful discussions, critiques, and friendships throughout my graduate career. I want to thank all my lab mates and colleagues; especially, Mark Dobish and Tyler Davis for their friendship.

Finally, I want to acknowledge and thank Dr. Gary A. Sulikowski, Dr. Carmelo J. Rizzo, Dr. Eva Harth for their participation on my graduate advisory committee.

TABLE OF CONTENTS

Chapter I.....	1
The Development of <i>anti</i> -Aminohydroxylation	1
1.1. Molecules Containing a <i>Vicinal</i> 1,2-Aminoalcohols	1
1.1.1. Naturally Occurring <i>Vicinal</i> 1,2-Aminoalcohols	1
1.1.2. Synthetic, Pharmacologically Active <i>Vicinal</i> -1,2-Aminoalcohols within Ligands and Chiral Auxiliaries.....	2
1.2. Olefin Functionalization: <i>vicinal</i> 1,2-Aminoalcohols	4
1.3. Organic Azides: Valuable Intermediate in Organic Synthesis	8
1.3.1. 1,3-Dipoles and Cycloaddition (Natural Product Synthesis)	8
1.3.2. Reactions of Organic Azides: Lewis Acid, and High Pressure	15
1.4. Triazoline Decomposition.....	24
1.4.1. Triazoline: Versatile Reaction Intermediate	24
1.4.2. Thermal Decomposition of Triazoline.....	25
1.4.3. Acid- and Base-Induced Decomposition of Triazoline	28
1.4.4. Photodecomposition of Triazoline	30
1.5. Brønsted Acid Promoted Olefin Functionalization	32
1.5.1. Brønsted Acid Promoted [3+2] Cycloaddition.....	32
1.5.2. Acceptor Design	37
1.5.3. β -Alkyl Substituted Imide Derivatives.....	38
1.5.4. α -Alkyl Substituted Imide Derivatives.....	52
1.5.5. β -Aryl Substituted Imide Derivatives: Microwave-Assisted [3+2] Cycloaddition.	58
1.6. Conclusion.....	65
Chapter 2.....	66
Secondary Catalysis by Water (Hydronium Triflate).....	66
2.1. Organic Reactions in Water	66

2.2. Water-Accelerated Organic Transformations	68
2.2.1. Internal Quenching Agent	68
2.2.2. Hydrolyzing Agent Leading to Secondary Catalyst	70
2.2.3. Lewis Acid Activator, Brønsted Acid-Base Cooperative Activation	78
2.2. Fragmentation of Triazoline by Brønsted Acid: Secondary Catalysis by Water (Hydronium Triflate)	83
2.3. Use of Comparative Triazolium Triflate Fragmentation Rates as a Tool to Assay Relative Competency of Brønsted Bases in $N \rightarrow N$ Proton Transfer	97
2.4. Conclusion	102
Chapter 3	104
Studies Towards the Synthesis of (+)-Zwittermicin A	104
3.1. Background	104
3.1.1 Introduction to (+)-Zwittermicin A and Biosynthesis of (+)-Zwittermicin A ..	104
3.1.2. Previous Synthetic Efforts	105
3.1.3. Retrosynthetic Analysis	106
3.2. Results and Discussions	107
3.2.1 Diastereoselective Intermolecular [3+2] Azide-Olefin Cycloadditions	107
3.2.2 Model System: Intramolecular [3+2] Cycloaddition	115
3.2.3 Progress Toward Double-Addition Strategy	118
3.3. Conclusion	135
Chapter IV	136
Experimental Procedures	136
Chapter V	207
Appendix	207

LIST OF TABLES

Table 1. Olefin Aziridination using Benzyl Azide and Methyl Vinyl Ketone: The Effect of Solvent	34
Table 2. Olefin Aziridination using Benzyl Azide and Methyl Vinyl Ketone: The Effect of Lewis Acid	35
Table 3. Scope: Aziridination with Various Azides	36
Table 4. β -Substituted Imides Preparation.....	39
Table 5. Olefin Functionalization using Benzyl Azide and Imide: The Effect of Lewis Acid.....	40
Table 6. The Scope of β -alkyl substituted acceptors: Aminohydroxylation	41
Table 7. The Effect of Additives: Triazoline vs Oxazolidine Dione	43
Table 8. Acid Promoted/Thermal [3+2] cycloaddition, Acid Promoted Triazoline Fragmentation	44
Table 9. . Scope: Aminohydroxylation with Various Azides	46
Table 10. Optimization of Chiral <i>trans</i> -Triazoline Fragmentation to Corresponding Aziridine.....	50
Table 11. Acid Promoted Iminoacetoxylation: α -Substituted Imides	54
Table 12. High Pressure Assisted [3+2] Cycloaddition: α -Substituted Imides	56
Table 13. Acid Promoted [3+2] Cycloaddition: α -Substituted Imides.....	57
Table 14. Acid Promoted Triazoline Fragmentation: α -Substituted Triazolines	58
Table 15. Microwave-Assisted [3+2] Cycloaddition: The Effect of Solvent.....	60
Table 16. Microwave-Assisted [3+2] Cycloaddition: The Effect of Solvent.....	61
Table 17. Microwave-Assisted [3+2] Cycloaddition: The Effect of Reaction Time and Temperature	62
Table 18. Microwave-Assisted [3+2] Cycloaddition: The Effect of Reaction Time and Concentration	63
Table 19. Microwave-Assisted [3+2] Cycloaddition: β -Aryl Substituted Imides	64
Table 20. Acid Promoted Triazoline Fragmentation: β -Aryl Substituted Triazolines.....	65
Table 21. Kinetics and Selectivity of Diels-Alder Reaction	66
Table 22. Enhanced Selectivity of Diels-Alder Reaction in Water	67

Table 23. Stereoselective Conjugate Addition of Stannylcuprate to Acetylenes	69
Table 24. Diastereoselective Allylzinc Additions to Imines	70
Table 25. Effect of Water on the Proline Catalyzed Aldol Reaction	77
Table 26. Effect of Added Water on the Product Distribution of Triflic Acid Promoted Azide-Olefin Additions at Low Temperature – Substituted Imide	84
Table 27. Effect of Added Water on the Product Distribution of Triflic Acid Promoted Azide-Olefin Additions at Low Temperature – Unsubstituted Imide	85
Table 28. Additive Effects in the Conversion of Triazolinium to Oxazolidine Dione ^a	99
Table 29. Comparison of Stoichiometric and Substoichiometric Additive Effects in the Conversion of Triazolinium to Oxazolidine Dione ^a	101
Table 30. Enolate Alkylation Approach to Bisimide Synthesis	119

LIST OF FIGURES

Figure 1. Naturally occurring amino acids and dipeptides Containing 1,2-Aminoalcohols	1
Figure 2. Naturally Occurring Lipids Containing 1,2-Aminoalcohols	2
Figure 3. Synthetic Molecules containing 1,2 Aminoalcohols	3
Figure 4. Chiral Auxiliaries Containing 1,2-Aminoalcohols	3
Figure 5. Natural Compounds Containing Aziridine Functionality	14
Figure 6. Modes of Triazoline Conversion	25
Figure 7. Azide-Olefin 1,3-Dipolar Cycloaddition and Triazoline Fragmentation	32
Figure 8. Substrate Design	33
Figure 9. Mechanistic Hypothesis of <i>anti</i> -Triazoline Fragmentation to <i>anti</i> -Oxazolidine Dione	48
Figure 10. Assignment of <i>cis</i> -Relative Stereochemistry by NOESY Analysis of Aziridine 257	51
Figure 11. Stereoselective Conjugate Addition of Cuprate to α,β -Acetylenic Esters	68
Figure 12. Rate Acceleration Effect in DMP Oxidation	71
Figure 13. Rate Acceleration by Addition of Water	72
Figure 14. Enantioselective Nitroaldol Reaction	72
Figure 15. Proposed Mechanism of Rate Acceleration	73
Figure 16. Proline Based Catalyst	75
Figure 17. Proposed Mechanism of Zirconium Catalyzed <i>anti</i> -Aldol Reaction	81
Figure 18. Reaction Course Observed by <i>in situ</i> IR Spectroscopy (Thermal, Anhydrous Variation)	87
Figure 19. Reaction Course Observed by <i>in situ</i> IR Spectroscopy (Water Additive Variation)	88
Figure 20. Reaction Course Observed by Monitoring Oxazolidine Dione 245a·TfOH Formation (1830 cm^{-1} , <i>in situ</i> IR) from Triazoline 246a using (a) Thermal or (b) Water-Catalyzed Conditions	89
Figure 21. Comparison of 245a (^{16}O) and 245a ₃ ($^{18}\text{O}:^{16}\text{O} = 2:1$), and H ₂ ¹⁸ O-catalyzed Experiments	92

Figure 22. Comparison of Water Catalyzed Triazolium Fragmentations	96
Figure 23. (+)-Zwittermicin A.....	104
Figure 24. Conformational Depiction of <i>anti-anti</i> (401) and <i>syn-anti</i> Triazoline (402).....	110
Figure 25. Observed Regional NOESY Correlations for <i>anti-anti</i> Triazoline (401)	111
Figure 26. Observed Regional NOESY Correlations for <i>syn-anti</i> Triazoline (402).....	112
Figure 27. Depiction of <i>anti-anti</i> (405) and <i>syn-anti</i> Oxazolidine-Dione (406).....	113
Figure 28. Observed Regional NOESY Correlations for <i>anti-anti</i> Oxazolidine Dione (405)	113
Figure 29. Observed Regional NOESY Correlations for <i>syn-anti</i> Oxazolidine Dione (406).....	114
Figure 30. Observed NOESY Correlations for <i>syn</i> -Aziridine 413 and <i>syn-anti</i> Oxazolidine Dione 414....	117
Figure 31. Depiction of <i>anti-anti</i> (444) and <i>syn-anti</i> Oxazolidine-Dione (445).....	126
Figure 32. Observed NOESY Correlations for <i>anti-anti</i> Oxazolidine Dione (444).....	126
Figure 33. Dipiction of <i>anti-anti</i> (446) and <i>syn-anti</i> Triazoline (447).....	128
Figure 34. Observed NOESY Correlations for <i>syn-anti</i> Triazoline (446)	129
Figure 35. Depiction of <i>anti-anti</i> Triazoline (393) and Observed NOESY Correlations	132
Figure 36. Depiction of <i>anti-anti</i> Oxazolidine Dione (392) and Observed NOESY Correlations	133

Chapter I

The Development of *anti*-Aminohydroxylation

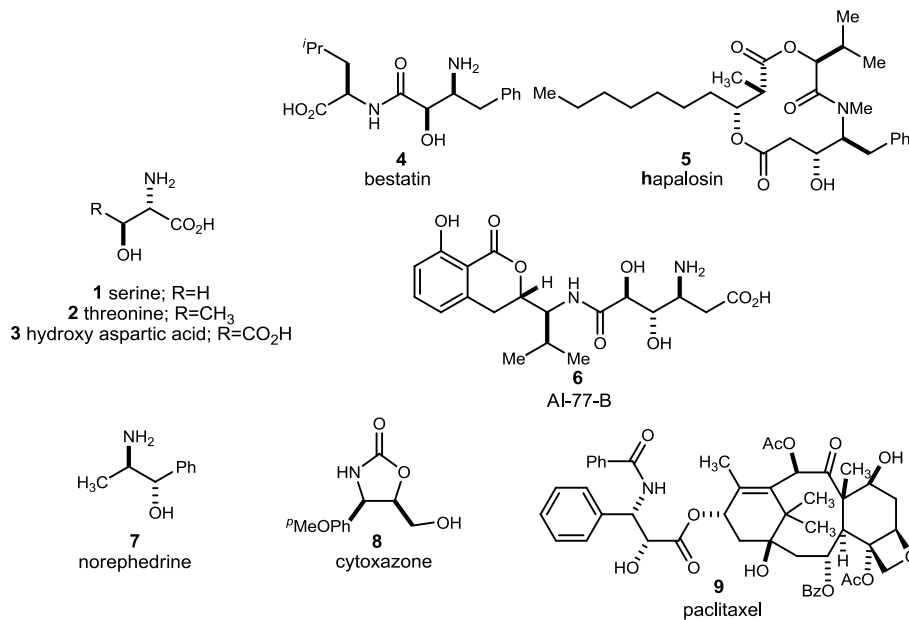
1.1. Molecules Containing a *Vicinal* 1,2-Aminoalcohols

The *vicinal* aminoalcohol moiety is a common structural motif in various groups of natural products, pharmaceuticals, ligands for metals, and chiral auxiliaries.¹

1.1.1. Naturally Occurring *Vicinal* 1,2-Aminoalcohols

One of the most important small molecules containing the 1,2-aminoalcohol moiety are hydroxyl amino acids (Figure 1). Examples of naturally occurring hydroxyamino acids are bestatin, hapalosin, and AI-77-B.² The dipeptide bestatin (**4**) is an

Figure 1. Naturally Occurring Amino Acids and Dipeptides Containing 1,2-Aminoalcohols



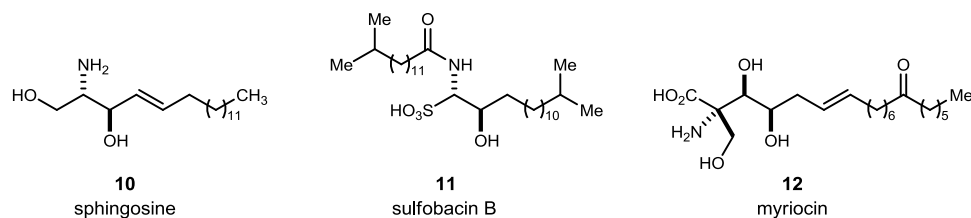
¹ Bergmeier, S. C. *Tetrahedron* **2000**, *56*, 2561.

² Sallach, H. J.; Kornguth, M. L. *Biochim. Biophys. Acta* **1959**, *34*, 582. Kornguth, M. L.; Sallach, H. J. *Arch. Biochem. Biophys.* **1960**, *91*, 39. Mokotoff, M.; Bagaglio, J. F.; Parikh, B. S. *J. Med. Chem.* **1975**, *18*, 354.

aminopeptidase inhibitor and exhibits immunomodulatory activity and is used as an adjuvant in cancer chemotherapy.³ Hapalosin (**5**) shows an ability to inhibit multidrug resistance in drug resistant cancer cells.⁴ AI-77-B (**6**) exhibits gastroprotective activity.⁵

Another class of molecules containing the vicinal aminoalcohol moiety is lipids and lipid-like molecules (Figure 2). Sphingosine (**10**) and its analogue sulfobacin B (**11**) are a von Willebrand factor receptor antagonist and antithrombotic agent.⁶

Figure 2. Naturally Occurring Lipids Containing 1,2-Aminoalcohols



1.1.2. Synthetic, Pharmacologically Active Vicinal-1,2-Aminoalcohols within Ligands and Chiral Auxiliaries

A variety of synthetic molecules containing 1,2-aminoalcohols are used as drugs or pharmacological agents. Often these molecules are analogues of naturally occurring aminoalcohols (Figure 3). For example, the peptidomimetic saquinavir (**13**), which contains a hydroxyethylene isostere, showed HIV protease inhibition, and is well established peptide analogue. Aminoalcohol **14** has been reported to selectively interact

³ Feng, D.-Z.; Song, Y.-L.; Jiang, X.-H.; Chen, L.; Long, Y.-Q. *Org. Biomol. Chem.* **2007**, *5*, 2690. Ghorai, M. K.; Das, K.; Kumar, A. *Tetrahedron Lett.* **2007**, *48*, 2471.

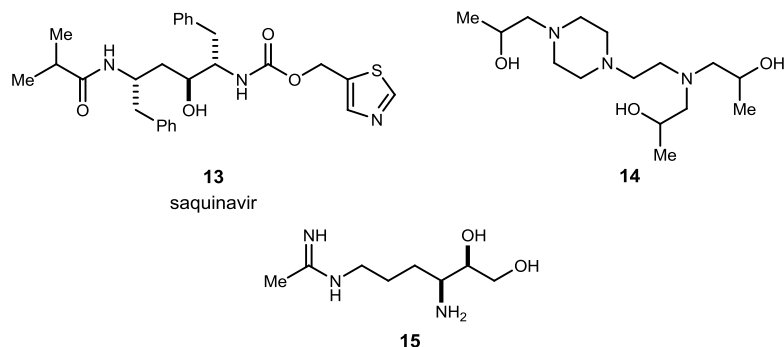
⁴ Gottesman, M. M.; Pastan, I.; Ambudkar, S. V. *Curr. Opin. Genet. Dev.* **1996**, *6*, 610. Atadja, P.; Watanabe, T.; Xu, H.; Cohen, D. *Cancer Metastasis Rev.* **1998**, *17*, 163.

⁵ Shimojima, Y.; Hayashi, H.; Ooka, T.; Shibukawa, M.; Iitaka, Y. *Tetrahedron Lett.* **1982**, *23*, 5435.

⁶ Mislow, K. *J. Am. Chem. Soc.* **1952**, *74*, 5155. Devant, R. M. *Kontakte (Darmstadt)* **1992**, *11*. Koskinen, P. M.; Koskinen, A. M. P. *Synthesis* **1998**, 1075. Hannun, Y. A.; Linaudic, C. M. *Biochim. Biophys. Acta* **1993**, *1154*, 223.

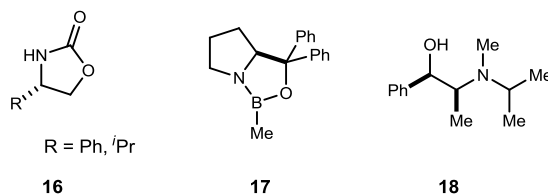
with RNA. Additionally, amidine containing molecule **15** is reported to be an inhibitor of nitric oxide synthetase.

Figure 3. Synthetic Molecules Containing 1,2-Aminoalcohols



A number of enantiomerically pure aminoalcohols have been used as ligands and chiral auxiliaries (Figure 4). The most important examples are the ‘Evans auxiliaries’.⁷ Additionally, aminoalcohol derived oxazolidinones have been used for various types of organic reactions. Oxazaborolidine **17** and ephedrine derivative **18** have been used for various asymmetric transformations.⁸

Figure 4. Chiral Auxiliaries Containing 1,2-Aminoalcohols



⁷ Evans, D. A.; Bartroli, J.; Shih, T. L. *J. Am. Chem. Soc.* **1981**, *103*, 2127. Evans, D. A.; Ennis, M. D.; Mathre, D. J. *J. Am. Chem. Soc.* **1982**, *104*, 1737. Ager, D. J.; Prakash, I.; Schaad, D. R. *Chem. Rev.* **1996**, *96*, 835.

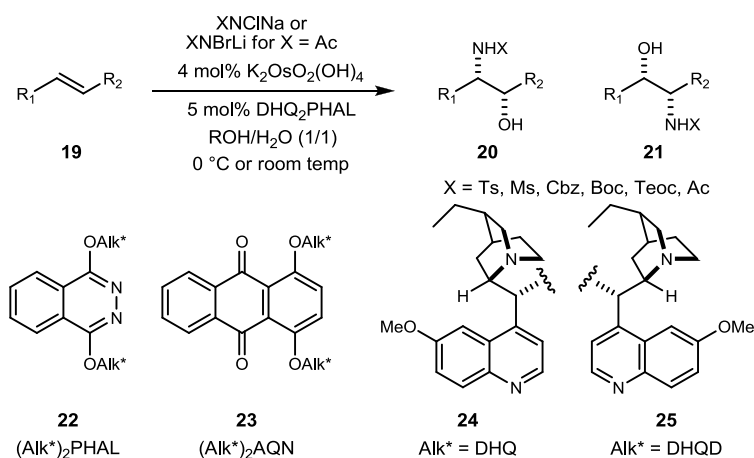
⁸ Itsuno, S.; Ito, K.; Hirao, A.; Nakahama, S. *J. Chem. Soc., Chem. Commun.* **1983**, 469. Itsuno, S.; Ito, K.; Hirao, A.; Nakahama, S. *J. Org. Chem.* **1984**, *49*, 555. Corey, E. J.; Bakshi, R. K.; Shibata, S. *J. Am. Chem. Soc.* **2002**, *109*, 5551. Corey, E. J.; Loh, T. P. *J. Am. Chem. Soc.* **2002**, *113*, 8966.

Due to the importance of the enantiomerically pure aminoalcohol functionality, the synthetic organic community has devoted significant effort to the development of methods for their synthesis of *vicinal* aminoalcohols. Since an abundance of articles on the topic of *vicinal* amino alcohol synthesis has been discussed, methods based on olefin functionalization reactions to vicinal aminoalcohol will be discussed in this chapter.

1.2. Olefin Functionalization: *vicinal* 1,2-Aminoalcohols

The heterofunctionalization of olefins is a well-studied area of organic chemistry. The area of most relevance to this particular research is the aminohydroxylation (or oxyamination, hydroxyamination) of olefins. The genesis of this type of functional group manipulation lies in the chemistry developed by Sharpless (Scheme 1).^{9,10} Many other aminohydroxylation protocols are variations of the Sharpless aminohydroxylation.

Scheme 1. Overview of Sharpless Asymmetric Aminohydroxylation

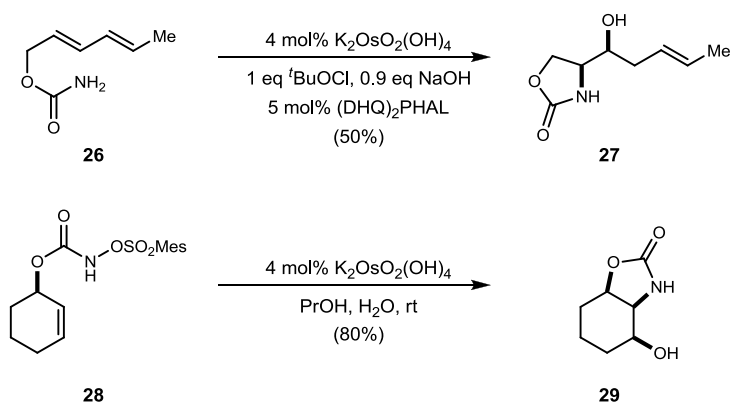


⁹ Sharpless, K. B.; Patrick, D. W.; Truesdale, L. K.; Biller, S. A. *J. Am. Chem. Soc.* **1975**, *97*, 2305. Guigen, L.; Han-Ting, C.; Sharpless, K. B. *Angew. Chem., Int. Ed.* **1996**, *35*, 451. Valery, V. F.; Sharpless, K. B. *Angew. Chem. Int. Ed.* **2001**, *40*, 3455. Malin, A. A.; Robert, E.; Valery, V. F.; Sharpless, K. B. *Angew. Chem. Int. Ed.* **2002**, *41*, 472.

¹⁰ selected review; Peter, O. B. *Angew. Chem. Int. Ed.* **1999**, *38*, 326. Bodkin, J. A.; McLeod, M. D. *J. Chem. Soc. Perkin Trans 1* **2002**, 2733. Dirk, V. D.; Kilian, M. *Chem. Eur. J.* **2004**, *10*, 2475. Christie, S. D. R.; Warrington, A. D. *Synthesis* **2008**, *2008*, 1325.

In addition to osmium based aminohydroxylation protocol, Donohoe and coworkers have demonstrated a tethered aminohydroxylation of cyclic allylic carbamates to overcome the regioselectivity issue with unsymmetrical alkenes which using the Sharpless protocol.¹¹ Use of intramolecular tethered carbamates **26** and **28** furnished aminoalcohols **27** and **29**, respectively. They also demonstrated an improved tethered aminohydroxylation using *N*-sulfonyloxy carbamates as reoxidant variations (Scheme 2).

Scheme 2. Tethered Aminohydroxylation Reaction



Aside from the Sharpless protocol, Bäckvall, Trost and Sorensen independently developed Pd-catalyzed olefin functionalizations. Seminal work involving stoichiometric Pd(II)-catalyzed nitrogen addition to alkene was reported by Bäckvall.¹² Trost reported epoxides from the olefin used as an intermediate to achieve hydroxyamination in the presence of Pd catalyst.¹³ Reaction of vinyl epoxides **30** with nitrogen nucleophile

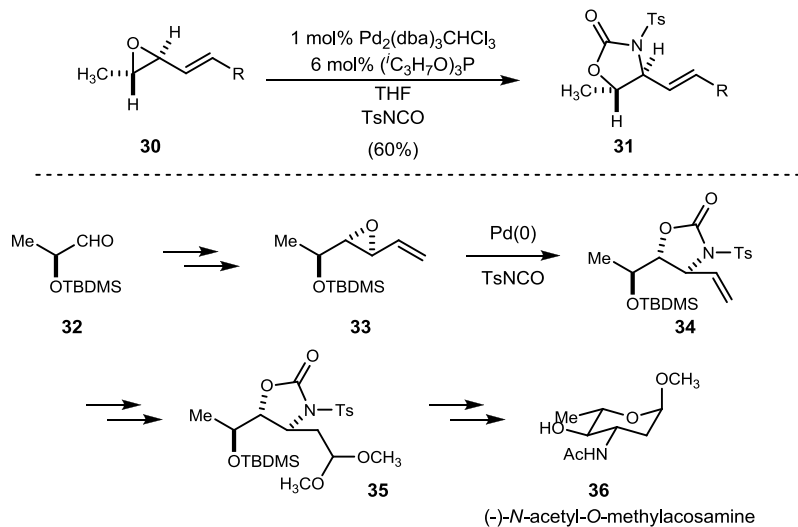
¹¹ Donohoe, T. J.; Johnson, P. D.; Cowley, A.; Keenan, M. *J. Am. Chem. Soc.* **2002**, *124*, 12934. Donohoe, T. J.; Johnson, P. D.; Pye, R. J.; Keenan, M. *Org. Lett.* **2004**, *6*, 2583. Donohoe, T. J.; Chughtai, M. J.; Klauber, D. J.; Griffin, D.; Campbell, A. D. *J. Am. Chem. Soc.* **2006**, *128*, 2514. Donohoe, T. J.; Bataille, C. J. R.; Gattrell, W.; Kloesges, J.; Rossignol, E. *Org. Lett.* **2007**, *9*, 1725.

¹² Bäckvall, J.-E. *Tetrahedron. Lett.* **1975**, *16*, 2225. Bäckvall, J. E.; Bjoerkman, E. E. *J. Org. Chem.* **2002**, *45*, 2893.

¹³ Trost, B. M.; Sudhakar, A. R. *J. Am. Chem. Soc.* **2002**, *109*, 3792.

isocyanate produces the initial *O*-alkylation intermediate which can be converted to oxazolidinone **31**. This protocol was successfully applied to the synthesis of (-)-acosamine **36** (Scheme 3).

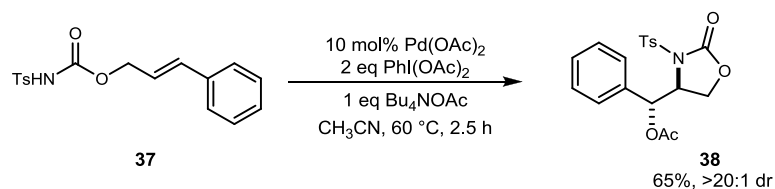
Scheme 3. Trost's Hydroxyamination: Application to the Synthesis of (-)-Acosamine



Sorensen demonstrated Pd-catalyzed ring-forming aminoacetoxylation of alkenes by using *N*-tosyl carbamate.¹⁴ The alkyl-palladium intermediate could be oxidized with $\text{PhI}(\text{OAc})_2$, followed by C-O bond forming reductive elimination furnishing aminoacetoxylation adduct **38** in a highly diastereoselective fashion (Scheme 4).

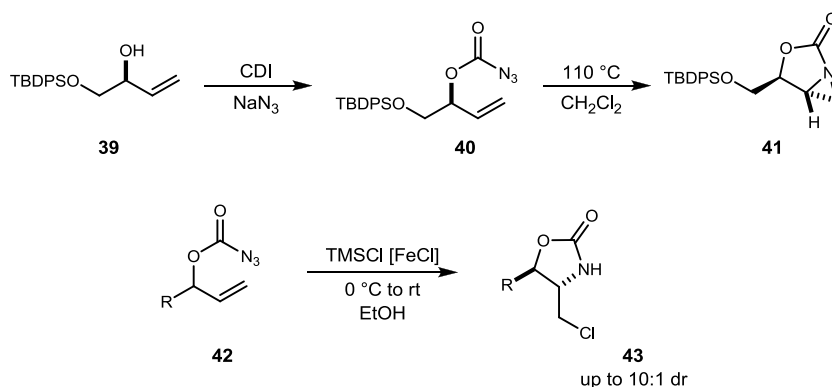
¹⁴ Alexanian, E. J.; Lee, C.; Sorensen, E. J., *J. Am. Chem. Soc.* **2005**, *127*, 7690.

Scheme 4. Palladium-Catalyzed Ring-Forming Aminoacetoxylation



The tandem intramolecular aziridination of olefin and ring opening method is also a well known approach to 1,2-aminoalcohols. For example, Bergmeier reported the thermal decomposition of alkenyl azidoformate **40** yielding a bicyclic aziridine intermediate which underwent a facile ring opening to substituted oxazolidinone **41**.¹⁵ Bach and co-workers also reported a metal-catalyzed intramolecular nitrogen transfer reaction to form oxazolidinone **43** (Scheme 5).¹⁶

Scheme 5. Intramolecular Aziridination and Ring Opening: Thermal and Metal Catalyzed Reactions



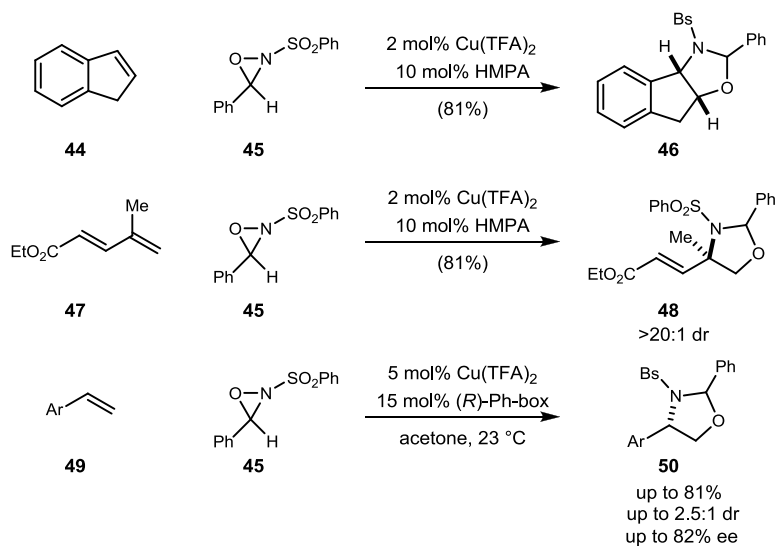
More recently, Yoon and coworkers reported olefin aminohydroxylation by using oxaziridine as both the source of electrophilic oxygen and nucleophilic nitrogen. Under the reaction conditions, a diverse range of styrenes (**44**, **49** and 1,3-diene **47**)

¹⁵ Bergmeier, S. C.; Seth, P. P. *J. Org. Chem.* **1997**, *62*, 2671. Bergmeier, S. C.; Stanchina, D. M. *J. Org. Chem.* **1999**, *64*, 2852.

¹⁶ Bach, T.; Schlummer, B.; Harms, K. *Chem.-Eur. J.* **2001**, *7*, 2581.

regioselectively produced the 1,2-aminoalcohols (Scheme 6).¹⁷ An enantioselective variation was also reported by using copper-bisoxazoline complexes.¹⁸

Scheme 6. Copper(II) Catalyzed Aminohydroxylation.



1.3. Organic Azides: Valuable Intermediate in Organic Synthesis

1.3.1. 1,3-Dipoles and Cycloaddition (Natural Product Synthesis)

The chemistry between a 1,3-dipole and an alkene has been used for more than 100 years in the synthesis of five-membered ring systems.¹⁹ A 1,3-dipole is defined as zwitterionic a-b-c structure that undergoes a 1,3-dipolar cycloaddition reaction with a multiple bond system as described by two different dipolar structures (Scheme 7).

Two different types of dipoles exist: the allyl anion type and the propargyl anion type.

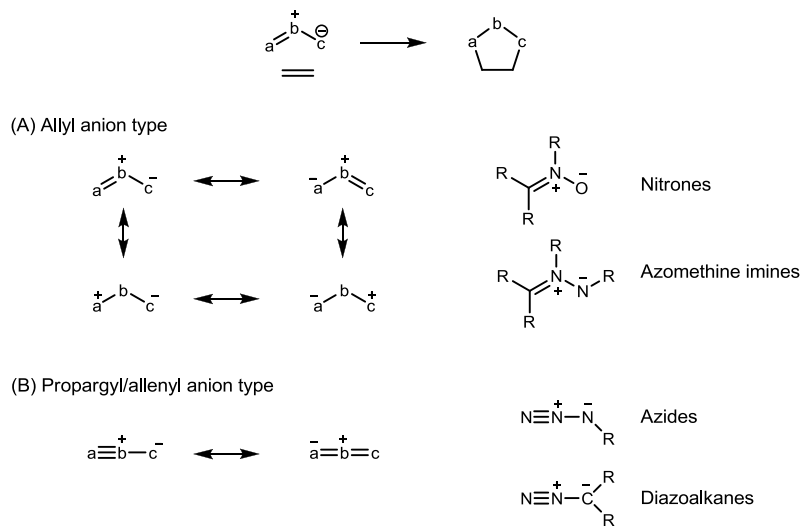
¹⁷ Michaelis, D. J.; Shaffer, C. J.; Yoon, T. P. *J. Am. Chem. Soc.* **2007**, *129*, 1866. Michaelis, D. J.; Ischay, M. A.; Yoon, T. P. *J. Am. Chem. Soc.* **2008**, *130*, 6610.

¹⁸ Michaelis, D. J.; Williamson, K. S.; Yoon, T. P. *Tetrahedron* **2009**, *65*, 5118.

¹⁹ Padwa, A., In *1,3-Dipolar Cycloaddition Chemistry, Vol. 1*, Padwa, A., Ed. Wiley: New York, 1984; p 817pp. Lwowski, W., In *1,3-Dipolar Cycloaddition Chemistry, Vol. 2*, Padwa, A., Ed. Wiley: New York, 1984; p 704 pp. Sha, C. K.; Mohanakrishnan, A. K., In *Synthetic Applications of 1,3-Dipolar Cycloaddition Chemistry Toward Heterocycles and Natural Products*, Padwa, A.; Pearson, W. H., Eds. Wiley: New York, 2002; p 940 pp.

The allyl anion type is described by having four electrons in three p-orbitals on three atoms. Two resonance structures are possible; one is an electron octet for all three centers, while the other is an electron sextet for each end. Due to this sextet structure, these allyl anion type dipoles can be both electrophilic and nucleophilic, which is key to understanding the dipole's reactivity. The propargyl anion type has an extra p-orbital located in the plane orthogonal to the allenyl type anion. Furthermore, the 1,3-dipole is linear and the central atom b is limited to a nitrogen atom.²⁰

Scheme 7. 1,3-Dipoles



The organic azide is one of the propargyl anion type 1,3-dipole, and has been used for preparation of many nitrogen containing heterocycles such as carbazoles,²¹ furoxanes,²² azepines,²³ triazoline,²⁴ triazole,²⁵ and aziridine.²⁶ Azide-alkene cycloaddition can expel

²⁰ Gothelf, K. V.; Jorgensen, K. A. *Chem. Rev.* **1998**, *98*, 863.

²¹ He, P.; Zhu, S. Z. *Tetrahedron* **2005**, *61*, 12398.

²² Stadlbauer, W.; Fiala, W.; Fischer, M.; Hojas, G. *J. Heterocycl. Chem* **2000**, *37*, 1253. Ouali, M. S.; Vaultier, M.; Carrie, R. *Tetrahedron* **1980**, *36*, 1821.

²³ Leyva, E.; Sagredo, R. *Tetrahedron* **1998**, *54*, 7367.

²⁴ Yao, L.; Smith, B. T.; Aube, J. *J. Org. Chem.* **2004**, *69*, 1720.

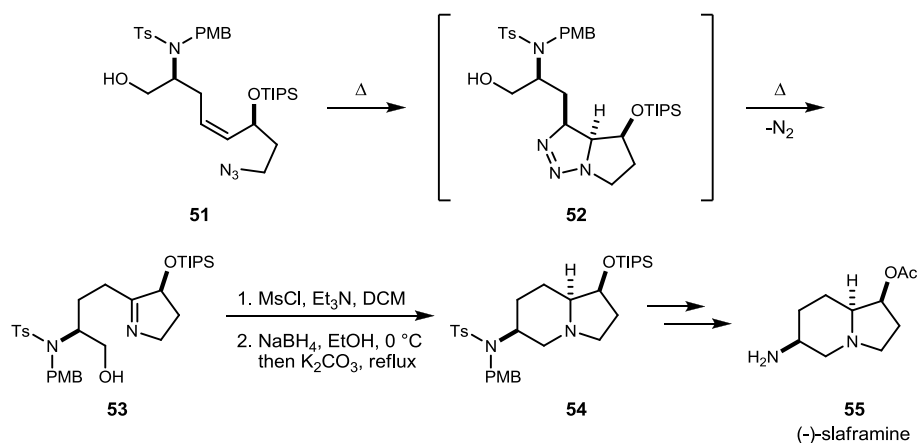
²⁵ Binder, W. H.; Kluger, C. *Cur. Org. Chem.* **2006**, *10*, 1791.

²⁶ Lin, Z. W.; Kadaba, P. K. *J. Heterocycl. Chem* **1997**, *34*, 1645.

molecular nitrogen to form aziridine or imine, depending on the substrate and reaction conditions. Due to the ability to deliver a nitrogen atom to molecules, the azide-alkene cycloaddition became a useful tool in target synthesis, specifically in nitrogen containing natural product synthesis. These heterocycles and natural products have been obtained by cycloaddition of organic azide with subsequent decomposition of the intermediate triazoline. Detailed triazoline decomposition will be discussed in the next section.

Cha and coworkers reported the enantioselective synthesis of (-)-slaframine (**55**) via an intramolecular azide dipolar cycloaddition as the key step.²⁷ Azide-alkene thermolysis produced imine **53** subsequent bicyclic ring closure was achieved by mesylation and NaBH₄ reduction to produce the protected slaframine derivative **54** (Scheme 8).

Scheme 8. Enantioselective Synthesis of (-)-Slaframine



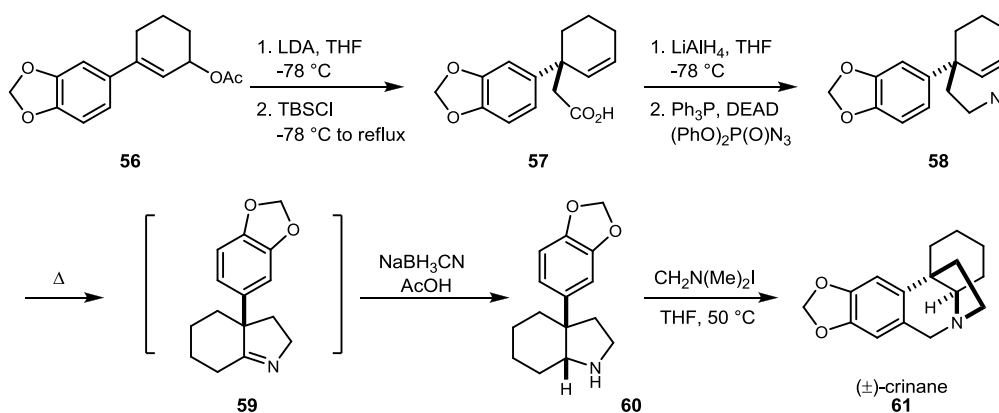
Pearson and coworkers utilized the azide dipolar cycloaddition to achieve a synthesis of *rac*-crinane (**61**).²⁸ The conversion of acetate **56** into the carboxylic acid **57** via an Ireland-Claisen rearrangement was followed by reduction and aziridination to furnish

²⁷ Choi, J.-R.; Han, S.; Cha, J. K. *Tetrahedron. Lett.* **1991**, 32, 6469.

²⁸ Schkeryantz, J. M.; Pearson, W. H. *Tetrahedron* **1996**, 52, 3107.

precursor **58**. Thermolysis of the azido-olefin generated the triazoline intermediate, which furnished imine **59** upon rapid extrusion of molecular nitrogen furnished imine **59**. Reduction of imine **59** with NaBH_3CN in acetic acid occurred stereoselectively to provide the *cis*-octahydroindole **60** in 81% yield. Warming amine **60** with Eschenmoser's salt afforded (\pm)-crinane (**61**) (Scheme 9).

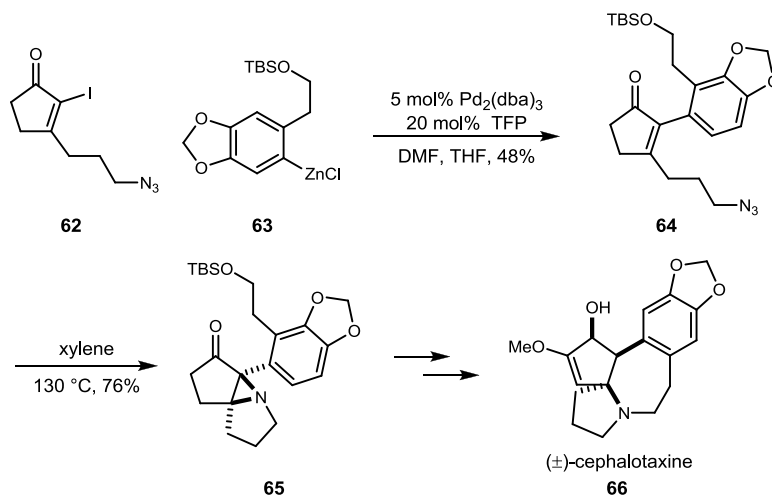
Scheme 9. Synthesis of (\pm)-Crinane Using an Intramolecular Azide-Olefin Cycloaddition



Molander has utilized the intramolecular azide-enone cycloaddition reaction in the synthesis of azaspirocyclic ketoaziridine **65** which can serve as the intermediate for cephalotaxine (**66**) (Scheme 10).²⁹

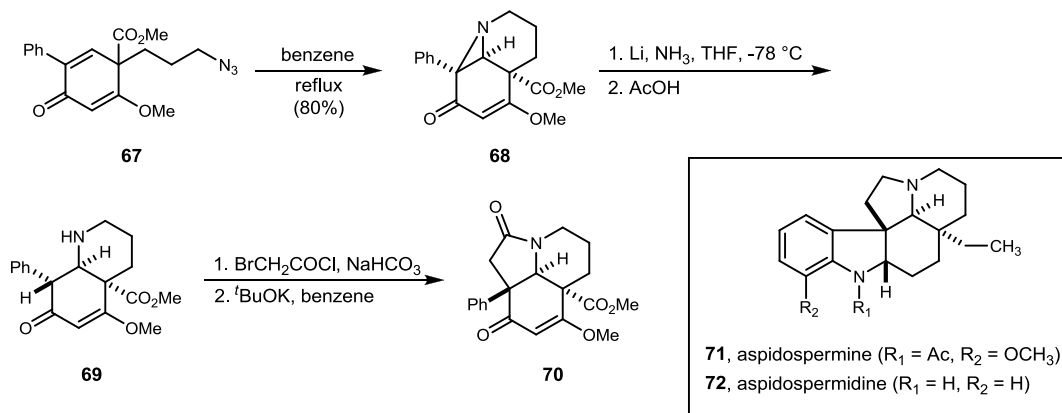
²⁹ Molander, G. A.; Hiersemann, M. *Tetrahedron. Lett.* **1997**, 38, 4347.

Scheme 10. Synthesis of Intermediates for the Total Synthesis of (±)-Cephalotaxine



Schultz and coworkers have employed the intramolecular azide-enone cycloaddition to construct the core of the aspidospermine alkaloids.³⁰ In refluxing conditions, azido-enone **67** was converted to aziridine product **68** in 80% yield with complete regio- and stereocontrol (Scheme 11). The production of aziridine **68** rather than the triazoline was attributed to the triazoline's instability, which led to accelerated nitrogen extrusion.

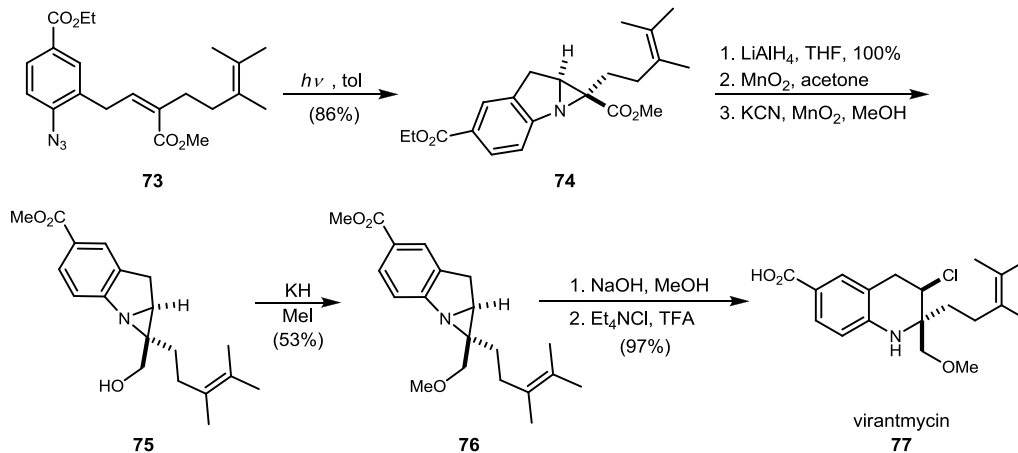
Scheme 11. Synthesis of the Tricyclic Core of Aspidospermine



³⁰ Guo, Z.; Schultz, A. G. *Tetrahedron Lett.* **2004**, *45*, 919.

Another example of intramolecular azide-enone cycloaddition was demonstrated in the total synthesis of the natural product (\pm)-virantmycin (**77**).³¹ Stereospecific photochemical nitrene addition of aryl azide **73** gave the tricyclic aziridine derivative **74**, which was converted into methyl benzoate derivative **76** by functional group manipulations. Aziridine **76** was transformed regioselectively and stereoselectively into (\pm)-virantmycin (**77**) under basic conditions (Scheme 12).

Scheme 12. Total Synthesis of (\pm)-Virantmycin



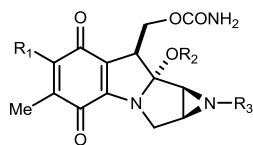
More importantly, there are many natural compounds which contain the aziridine functionality. For example, FR-900482 (**84**) and FR-66979 (**85**), which were isolated from *Streptomyces sandaensis* No. 6897, are among a class of antibiotics which exhibit potent antitumor activity.^{32, 33} Mitomycin C (**80**) is a potent antitumor agent now used in

³¹ Omura, S.; Nakagawa, A. *Tetrahedron. Lett.* **1981**, 22, 2199. Morimoto, Y.; Matsuda, F.; Shirahama, H. *Tetrahedron. Lett.* **1990**, 31, 6031.

³² Uchida, I.; Takase, S.; Kayakiri, H.; Kiyoto, S.; Hashimoto, M.; Tada, T.; Koda, S.; Morimoto, Y. *J. Am. Chem. Soc.* **1987**, 109, 4108. Iwami, M.; Kiyoto, S.; Terano, H.; Kohsaka, M.; Aoki, H.; Imanaka, H. *J. Antibiot.* **1987**, 40, 589. Hirai, O.; Shimomura, K.; Mizota, T.; Matsumoto, S.; Mori, J.; Kikuchi, H. *J. Antibiot.* **1987**, 40, 607. Shimomura, K.; Hirai, O.; Mizota, T.; Matsumoto, S.; Mori, J.; Shibayama, F.; Kikuchi, H. *J. Antibiot.* **1987**, 40, 600. Terano, H.; Takase, S.; Hosoda, J.; Kohsaka, M. *J. Antibiot.* **1989**, 42, 145.

clinical chemotherapy (Figure 5).

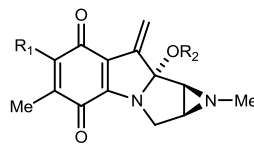
Figure 5. Natural Compounds Containing Aziridine Functionality



78: mitomycin A, R₁ = OMe, R₂ = Me, R₃ = H

79: mitomycin B, R₁ = OMe, R₂ = H, R₃ = Me

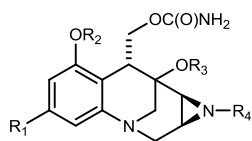
80: mitomycin C, R₁ = NH₂, R₂ = Me, R₃ = Me



81: mitomycin G, R₁ = NH₂, R₂ = Me

82: mitomycin H, R₁ = OMe, R₂ = H

83: mitomycin K, R₁ = OMe, R₂ = Me



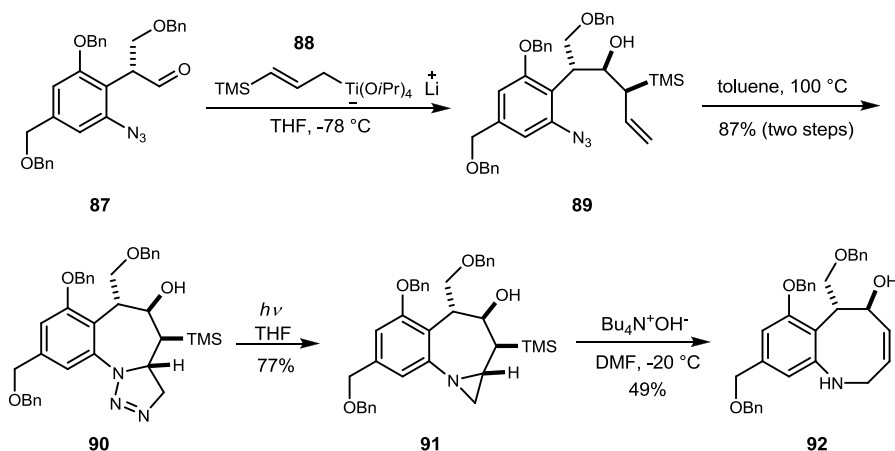
84: FR-900482, R₁ = CHO, R₂ = R₃ = R₄ = H

85: FR-66979, R₁ = CH₂OH, R₂ = R₃ = R₄ = H

86: FR-70496, R₁ = CHO, R₂ = Me, R₃ = H, R₄ = Ac

Ciufolini and coworkers utilized an intramolecular cycloaddition as a key step in their total synthesis of FR-66979.³⁴ After selective addition of allyl compound **88** to azide containing aldehyde **89**, diastereoselective 1,3-dipolar cycloaddition gave tricyclic

Scheme 13. Total Synthesis of FR66979



³³ Sweeney, J. B. *Chem. Soc. Rev.* **2002**, 31, 247.

³⁴ Ducray, R.; Ciufolini, M. A. *Angew. Chem., Int. Ed.* **2002**, 41, 4688.

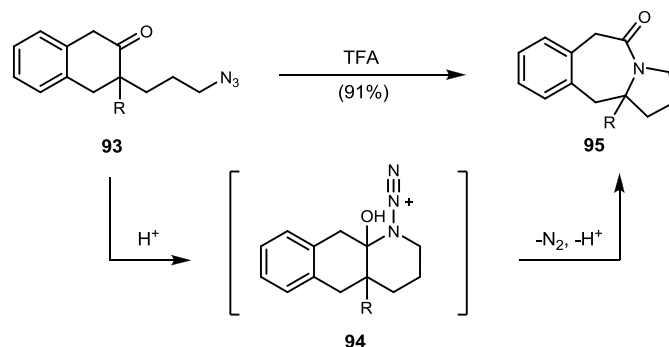
triazoline **90**. Following photochemical nitrogen extrusion from the triazoline and subsequent ring contraction to the aziridine **91**, a homo-Brook-triggered fragmentation formed benzazocenol **92** (Scheme 13).

As detailed above, many synthetic efforts have demonstrated the utility of azide cycloadditions with olefins to make alkaloid natural products and intermediates.

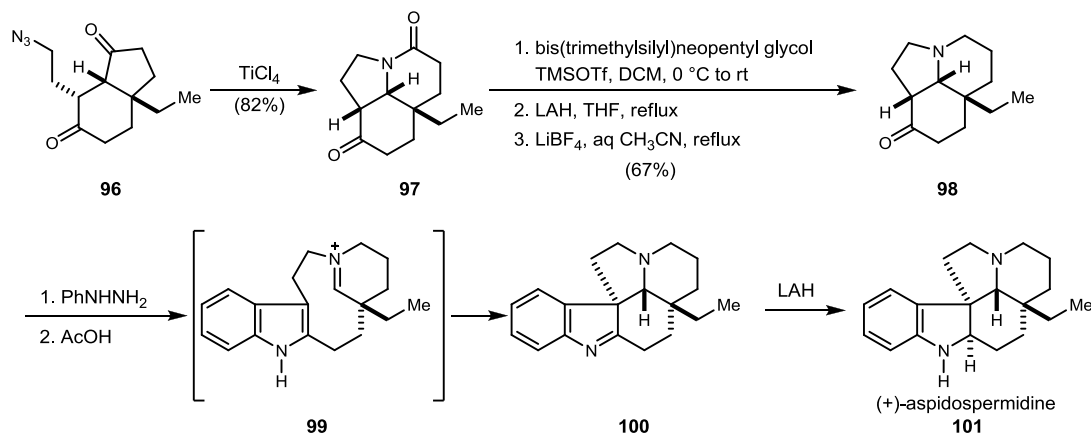
1.3.2. Reactions of Organic Azides: Lewis Acid, and High Pressure

Beyond their use in 1,3-dipolar cycloaddition with alkenes and natural product synthesis, organic azides have seen utilized in other transformations due to their ability to deliver a nitrogen to a molecule. In general, thermally and photochemically induced azide and olefin cycloaddition are the main strategies for this type of transformation. However, there are several unique examples of Lewis acid catalyzed azide transformation reactions. For example, Aubé and co-workers have used Lewis acids for the reaction of azides with various cyclic ketones. They utilized a range azides, such as alkyl azide and hydroxyl azide, with ketones and aldehydes for different reaction pathways. The first example of intramolecular Schmidt reaction was reported in 1991.³⁵ In the presence of TFA, various cyclic azido-ketone derivatives (**93**) formed intermediate aminal (**94**), which then underwent ring expansion to furnish lactam **95** (Scheme 14).

³⁵ Aube, J.; Milligan, G. L. *J. Am. Chem. Soc.* **2002**, *113*, 8965.

Scheme 14. Intramolecular Schmidt Reaction of Alkyl Azide

The Lewis acid catalyzed intramolecular Schmidt reaction was utilized for the synthesis of fused, nitrogen-containing heterocycles such as (+)-aspidospermidine³⁶ and (\pm)-stenine.³⁷ Azido-ketone **96** underwent a selective intramolecular Schmidt cyclization, followed by deprotection to furnish ketone **97**. The synthesis was completed using Stork's classic Fischer indolization to afford (+)-aspidospermidine (**101**) (Scheme 15).

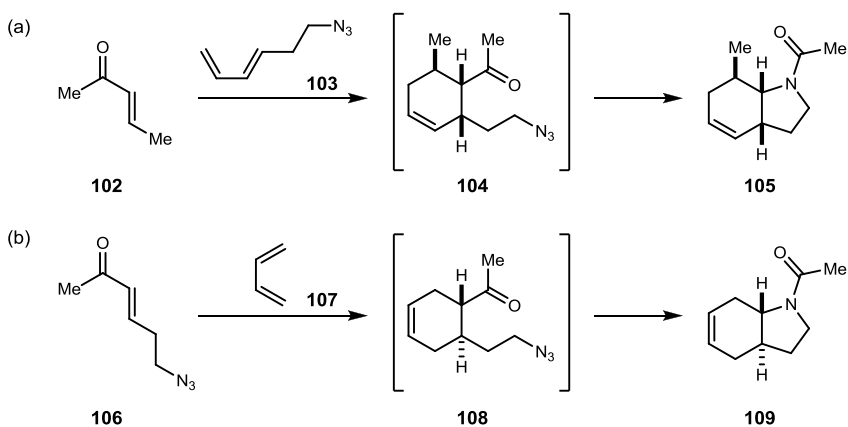
Scheme 15. Total Synthesis of (+)-aspidospermidine

³⁶ Iyengar, R.; Schildknegt, K.; Aube, J. *Org. Lett.* **2000**, 2, 1625. Iyengar, R.; Schildknegt, K.; Morton, M.; Aube, J. *J. Org. Chem.* **2005**, 70, 10645.

³⁷ Zeng, Y.; Aube, J. *J. Am. Chem. Soc.* **2005**, 127, 15712. Frankowski, K. J.; Golden, J. E.; Zeng, Y.; Lei, Y.; Aube, J. *J. Am. Chem. Soc.* **2008**, 130, 6018.

Another example of a Lewis acid catalyzed reaction was the combination of the intramolecular Schmidt reaction with the Diels-Alder reaction.³⁸ Since the reactivity of the intermolecular Schmidt reaction is substantially lower than the intramolecular version, the reaction was designed to attach azide functionality on the dienophile or diene. The use of Diels-Alder reaction brings the two pieces together, then the subsequent azido-Schmidt reaction takes place (Scheme 16).

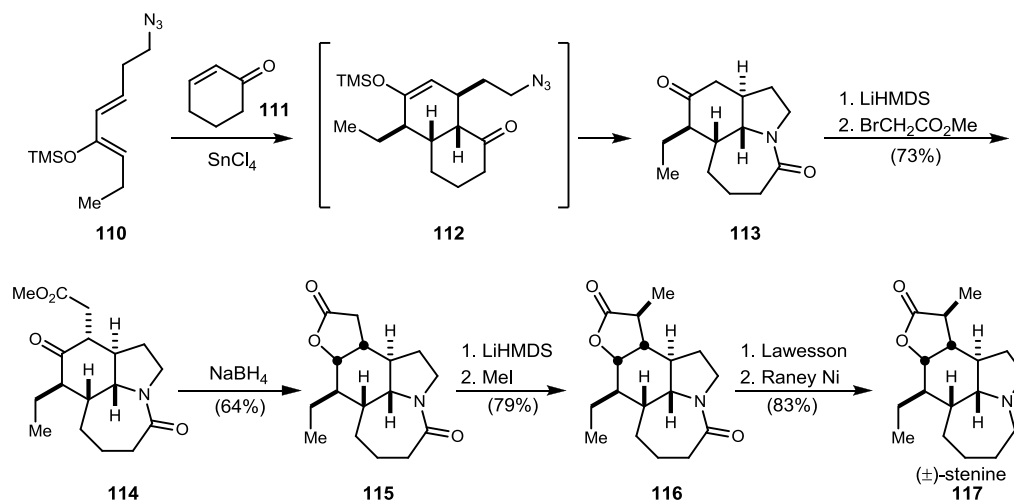
Scheme 16. Designed Domino Reaction



After initial investigation, the domino Diels-Alder and Schmidt reaction was applied to the synthesis of stemona alkaloid (\pm)-stenine (**117**). Treatment of azido-diene **110** with cyclohexenone **111** and SnCl_4 afforded a 3:1 ratio of desired lactam **113** in moderate yield (Scheme 17). The remaining stereocenters were generated by two highly selective substrate-controlled reactions: axially directed alkylation and reduction afforded lactone **115**, then another alkylation and decarbonylation furnished (\pm)-stenine (**117**).

³⁸ Zeng, Y.; Reddy, D. S.; Hirt, E.; Aube, J. *Org. Lett.* **2004**, *6*, 4993. Frankowski, K. J.; Hirt, E. E.; Zeng, Y.; Neuenswander, B.; Fowler, D.; Schoenen, F.; Aube, J. *J. Comb. Chem.* **2007**, *9*, 1188.

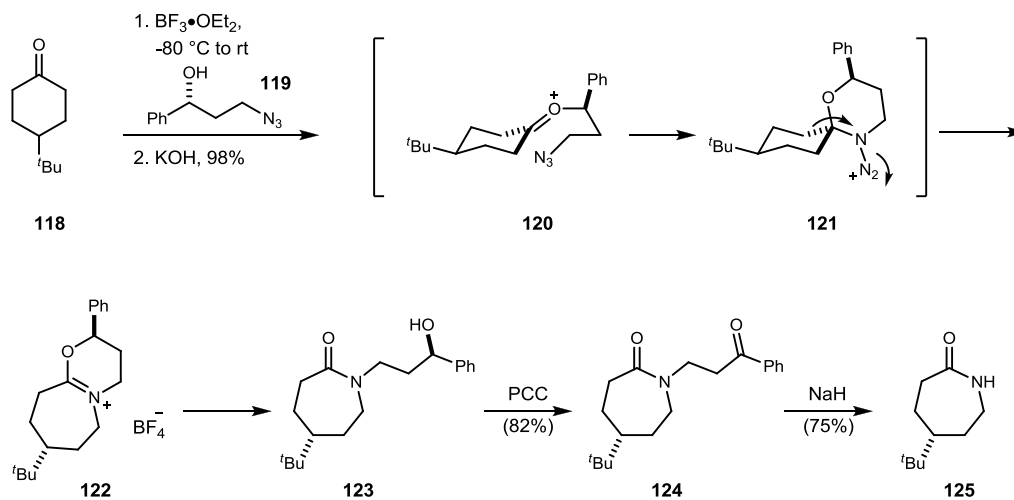
Scheme 17. Total Synthesis of (±)-Stenine



Not long after the intramolecular version of the Schmidt reaction, a $\text{BF}_3 \cdot \text{OEt}_2$ mediated intermolecular reaction of cyclic ketones with hydroxyalkyl azides to afford *N*-alkyl lactams was also reported by Aubé and co-workers.³⁹ Activation of the carbonyl group of ketone **118** by a Lewis acid promoted the formation of oxonium ion **120** after dehydration. Intramolecular azide addition to the oxonium ion followed by a rearrangement and the loss of N_2 furnished the intermediate iminium ion **122**. Achiral ketone **118** could be converted to chiral lactam **125** after hydrolysis. Chiral hydroxyl alkyl azide can lead to a selective asymmetric nitrogen ring expansion via the Schmidt rearrangement.

³⁹ Gracias, V.; Milligan, G. L.; Aube, J. *J. Org. Chem.* **1996**, *61*, 10. Furness, K.; Aube, J. *Org. Lett.* **1999**, *1*, 495. Sahasrabudhe, K.; Gracias, V.; Furness, K.; Smith, B. T.; Katz, C. E.; Reddy, D. S.; Aube, J. *J. Am. Chem. Soc.* **2003**, *125*, 7914.

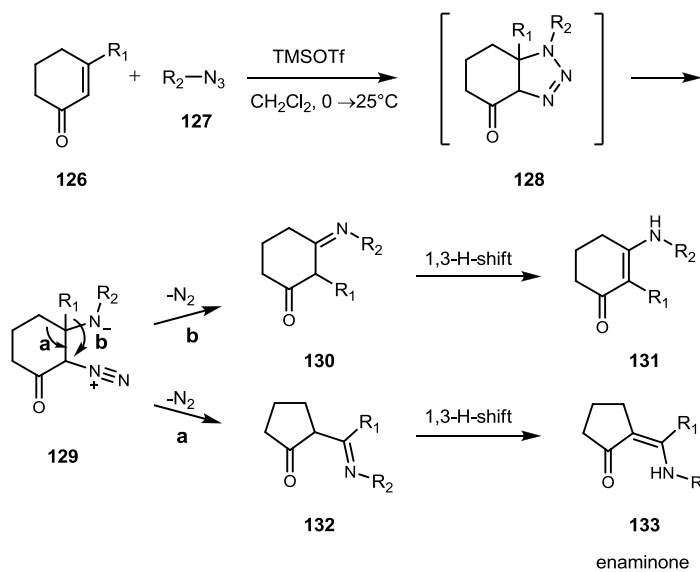
Scheme 18. Asymmetric Induction in a Nitrogen Ring Expansion



More recently, Aubé has reported that Lewis acid promoted [3+2] cycloaddition with an α,β -unsaturated ketone affords the ring contraction product via triazolone intermediate **128**. Under these reaction conditions, the unstable triazolone intermediate **128** underwent decomposition to produce a zwitterionic species **129** that can rearrange via pathway a or b. In pathway a, antiperiplanar migration followed by 1,3-hydrogen shift gave exocyclic ring contracted enaminone **133**. In contrast to pathway a, migration of the alkyl group onto an axial diazonium species gave endocyclic enaminone **131**. In general, normal cycloadditions require heating for long periods of time for activation, but in this reaction, Lewis acids are sufficient to activate the carbonyl group toward cycloaddition at low temperatures (Scheme 19).⁴⁰

⁴⁰ Reddy, D. S.; Judd, W. R.; Aube, J. *Org. Lett.* **2003**, *5*, 3899.

Scheme 19. Lewis acid Promoted [3+2] Cycloaddition with an α,β -Unsaturated Ketone



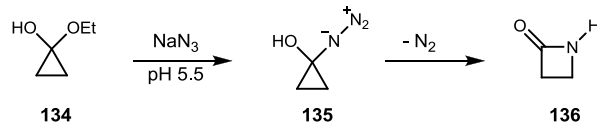
Another example of an intermolecular azide addition was reported in 2000. The Lewis acid promoted reaction of cyclopropanone acetals with alkyl azides furnished diazo derivatives **144** and β -lactams **145**, where the product was dependent on the structure of cyclopropanone (Scheme 20).⁴¹ In the 1970s, Wasserman and coworkers demonstrated that cyclopropanones react with sodium azide to afford β -lactam **136**.⁴² In this study, Lewis acid promoted ring opening of cyclopropanone reacted in a [3+3] cycloaddition with the alkyl azide to produce 1,2,3-triazine-5-one intermediate **142**. Subsequent ring fragmentation produced both diazo **144** and lactam **145**.

⁴¹ Desai, P.; Aube, J., *Org. Lett.* **2000**, 2, 1657. Grecian, S.; Desai, P.; Mossman, C.; Poutsma, J. L.; Aube, J. *J. Org. Chem.* **2007**, 72, 9439.

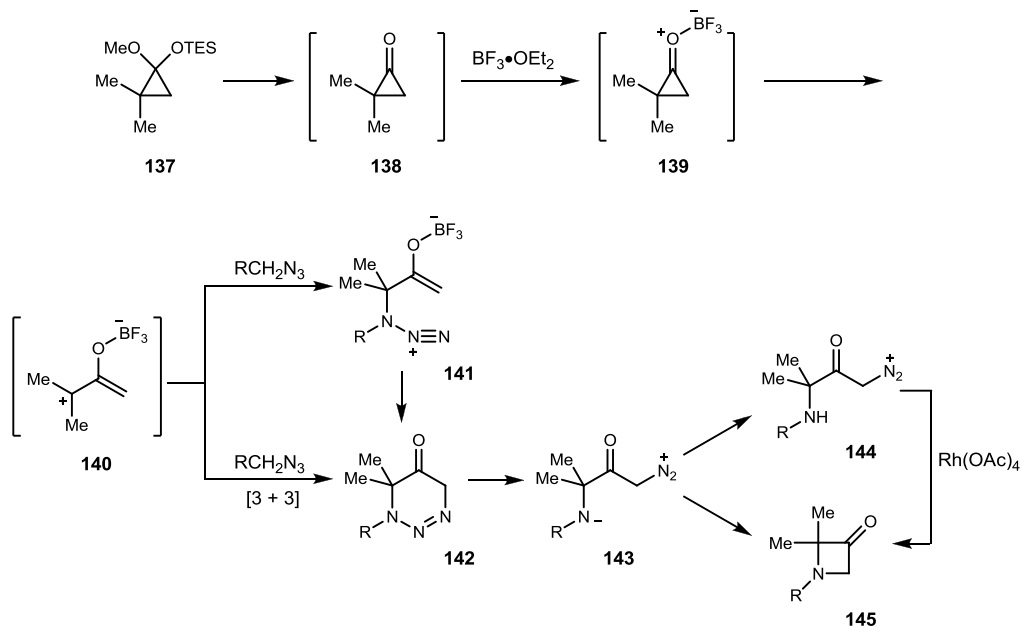
⁴² Wasserman, H. H.; Adickes, H. W.; Espejo de Ochoa, O., *J. Am. Chem. Soc.* **1971**, 93, 5586. Wasserman, H. H.; Glazer, E., *J. Org. Chem.* **1975**, 40, 1505.

Scheme 20. Reactions of Cyclopropanone Acetals with Alkyl Azides

(a) Wasserman and coworkers



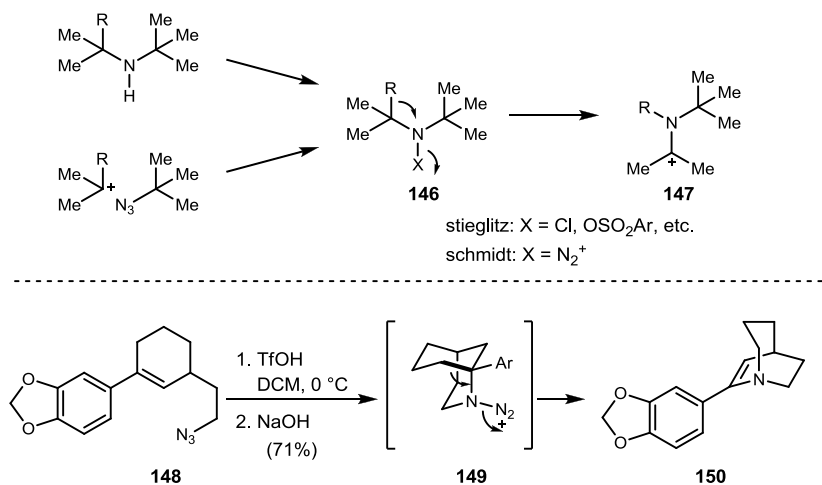
(b) Aubé and coworkers



As Aubé continues to demonstrate the power of azide addition to the carbonyl functional group (azido-Schmidt), Pearson outlined the extensive chemistry triggered by carbenium ion addition to an electron rich azide. Treatment of azidoalkene **148** with a protic acid such as triflic acid affords the bicyclic alkene **150** as the sole product. Protonation of alkene **148** produces the tertiary benzylic carbocation, which can be captured by the azide to form aminodiazonium ion **149**. Subsequent migration of an alkyl group and proton transfer that lead to bicyclic alkene **150** (Scheme 21).⁴³

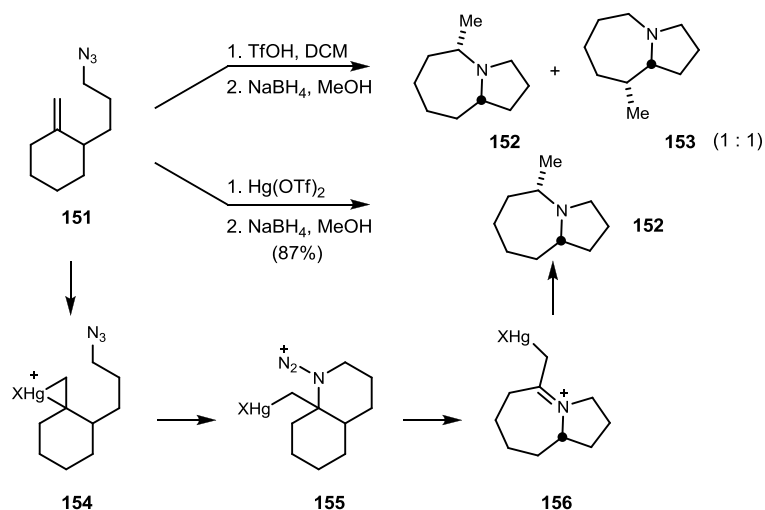
⁴³ Pearson, W. H.; Schkeryantz, J. M. *Tetrahedron. Lett.* **1992**, 33, 5291. Pearson, W. H.; Walavalkar, R.; Schkeryantz, J. M.; Fang, W. K.; Blickensdorf, J. D., *J. Am. Chem. Soc.* **1993**, 115, 10183.

Scheme 21. Intramolecular Schmidt Reaction of an Alkyl Azide



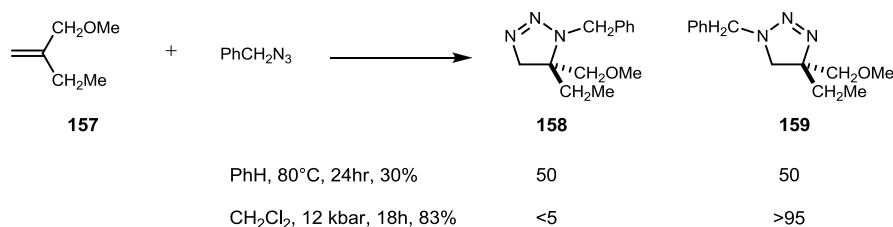
However, the proton promoted intramolecular Schmidt reaction of azidoalkene can undergo cation rearrangement to form a more stable cation. The result of cation rearrangement affords the mixture of regioisomeric products **152** and **153** (Scheme 22). Additionally, acid sensitive functional groups were not tolerated under strong acidic conditions. To avoid functional group intolerance and the regioselectivity issue, various electrophiles were screened. Among the various nonprotic electrophiles, stoichiometric amounts of Hg(OTf)₂ promoted the rearrangement; subsequent reduction with sodium borohydride to afford **152** as a single regioisomer.⁴³

Scheme 22. Mercury Promoted Schmidt Reaction



Asides from the Lewis acid promoted azide and carbonyl/alkene reactions, another unique example of cycloaddition of azide and olefin was reported by Weinreb and co-workers.⁴⁴ They utilized high pressure to overcome general reaction problems such as long reaction times and partial conversion. Additionally, they found that traditional thermal conditions afforded a 1:1 mixture of regioisomers in poor yield. However, at high pressure isomer **159** was produced with over 95% selectivity in good yield (Scheme 23).

Scheme 23. High Pressure Assisted Azide Olefin Cycloaddition



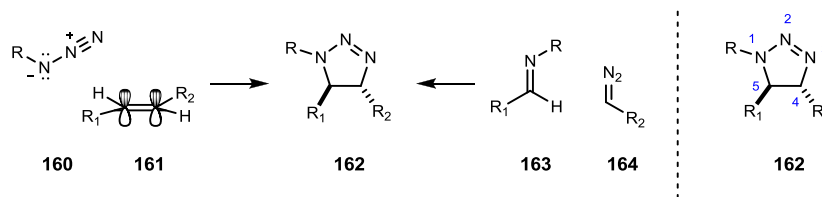
⁴⁴ Anderson, G. T.; Henry, J. R.; Weinreb, S. M. *J. Org. Chem.* **1991**, *56*, 6946.

1.4. Triazoline Decomposition

1.4.1. Triazoline: Versatile Reaction Intermediate

Since the preparation of triazoline **162** in 1912,⁴⁵ the fragmentation of Δ^2 -1,2,3-triazolines (hereafter triazolines) has been investigated by the organic synthetic community. In general, the preparation of triazolines often involves a [3+2] cycloaddition of azide (**160**) and an olefin (**161**) or cycloaddition of an imine (**163**) and a diazoalkane (**164**) (Scheme 24).

Scheme 24. Triazoline Formation and Conformational Depiction

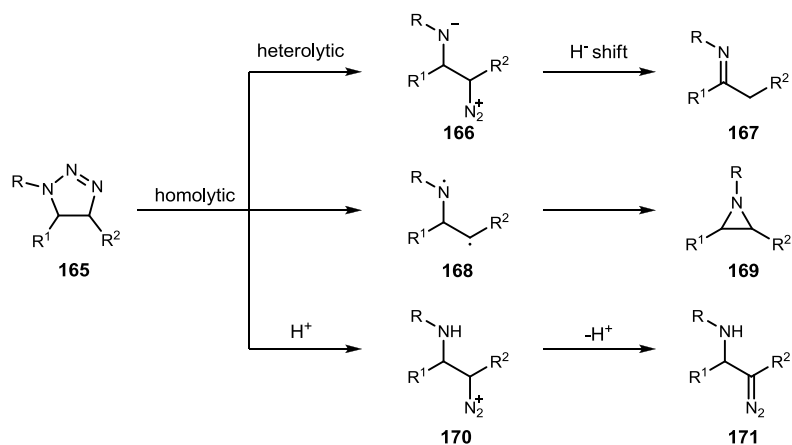


Since basic nitrogen (N1) provides reaction pathways by homolytic and heterolytic fragmentation, triazoline **165** can be converted to azomethine **167**, aziridine compounds **169** after expelling nitrogen under mild conditions and diazo compounds **171** (Figure 6). Three different types of triazoline decomposition will be discussed: 1) thermal, 2) acid and base catalyzed, and 3) photodecomposition.⁴⁶

⁴⁵ Wolff, L. Ann., **1912**, 394, 60.

⁴⁶ Scheiner, P., Triazoline Decomposition. In *Selective Organic Transformations*, Thyagarajan, B. S., Ed. Wiley-Interscience: New York, USA, 1970; Vol. 1.

Figure 6. Modes of Triazoline Conversion

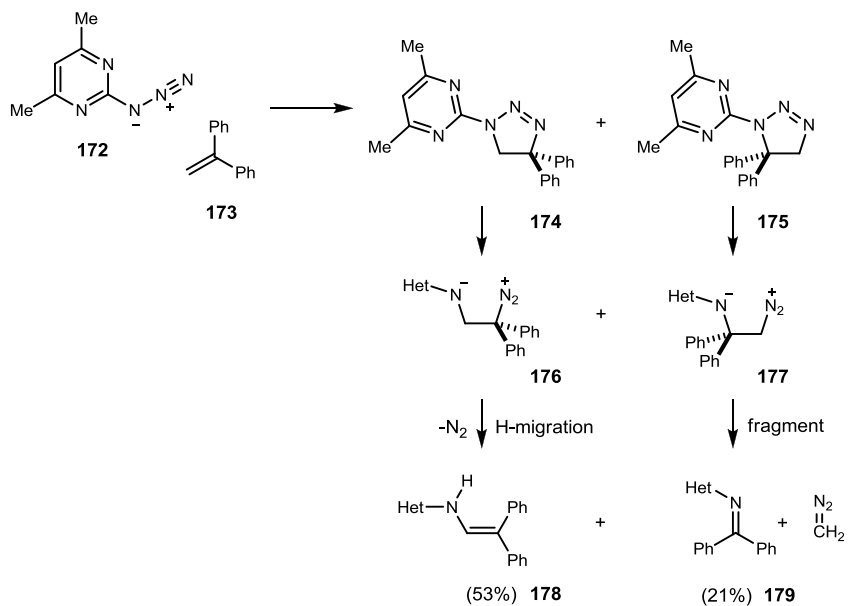


1.4.2. Thermal Decomposition of Triazoline

Early study of triazoline decomposition was based on the distribution of products that included imine, aziridine, and diazo compounds. Especially in the case of thermal decomposition, product distributions are entirely dependent on the structure of triazoline and the solvent used. For example, triazolines from unactivated and unstrained olefin **173** with aryl azide **172** decompose spontaneously at room temperature to the corresponding enamine **178** and imine **179** (Scheme 25).⁴⁷

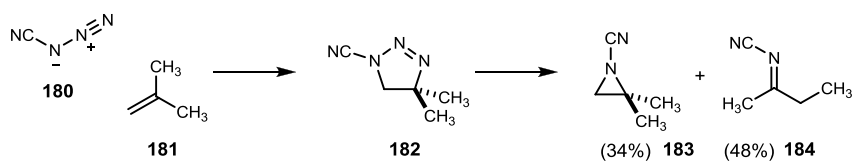
⁴⁷ Huisgen, R.; Fraunberg, K. v.; Sturm, H. J. *Tetrahedron. Lett.* **1969**, *10*, 2589.

Scheme 25. Thermal Decomposition of Unactivated and Unstrained Olefins



In the case of cyanogen azide addition to unactivated olefin **181**, intermediate triazoline **182** decomposed to aziridine **183** and alkyl shifted imine **184** due to the electron withdrawing effect of cyano group (Scheme 26). A diverse range of olefins were investigated with cyanogen azide to verify the reaction rate of cycloaddition.

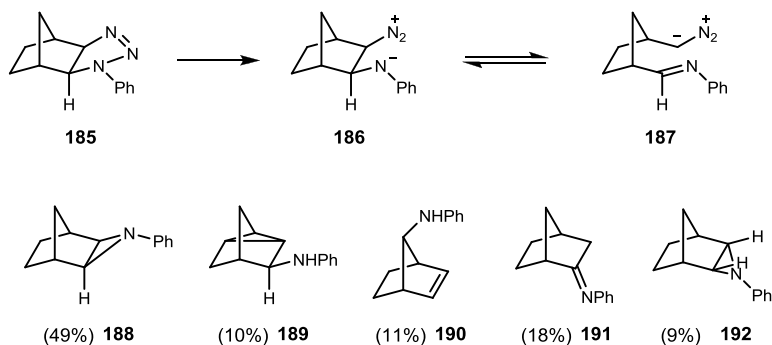
Scheme 26. Cyanogen Azide Addition to Unactivated Olefin



Additionally, the strained olefin norbornene formed exo adduct **185**, then decomposition of triazoline **186** gave five major products (Scheme 27). Unlike the photochemically induced decomposition which gave 100% yield of **188**, thermal

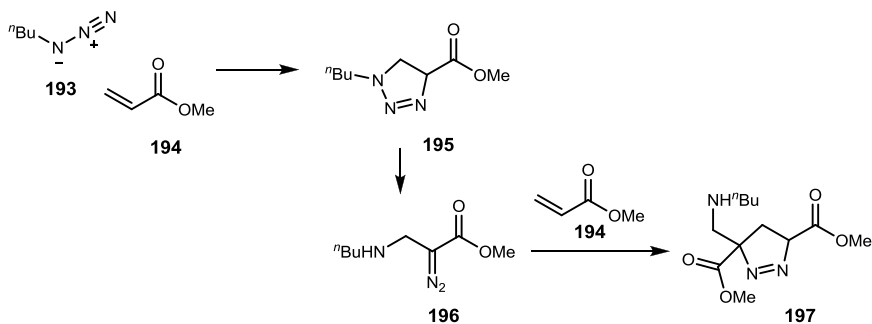
decomposition of the triazoline produced a wide range of products dependent on its structure and electronics.⁴⁸

Scheme 27. Thermal Decomposition of Norbornene Derivative Triazoline



Various types of electron-poor olefins were also investigated. For examples, methyl acrylate cycloaddition with phenylazide gave the mixture of triazoline **195** and aminodiazole compound **196**. The α -diazo ester can react further with another molecule of acrylate **194**, to produce pyrazoline **197** (Scheme 28).⁴⁹

Scheme 28. Azide Addition to Electron Deficient Olefin



As listed here, early study of thermal triazoline decomposition mainly focused on to the

⁴⁸ McDaniel, R. S.; Oehlschlager, A. C. *Tetrahedron* **1969**, 25, 1381. Hale, R. L.; Zalkow, L. H. *Tetrahedron* **1969**, 25, 1393.

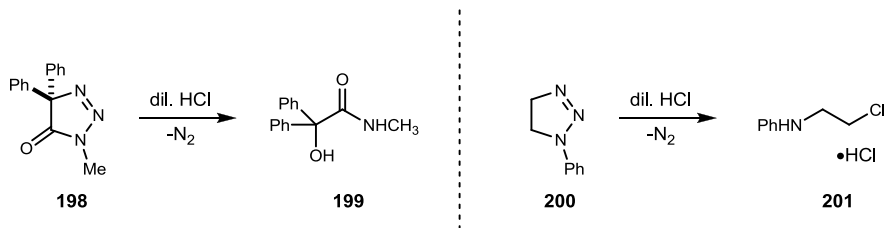
⁴⁹ Broeckx, W.; Overbergh, N.; Samyn, C.; Smets, G.; L'Abbé, G. *Tetrahedron* **1971**, 27, 3527.

rate of triazoline formation with various types of olefin. The decomposition pathways were hypothesized from product distributions alone.

1.4.3. Acid- and Base-Induced Decomposition of Triazoline

Earlier study of acid-induced triazoline decomposition focused on the structural features and the reaction conditions. Multiple reaction pathways are characterized based on the reaction conditions. For example, displacement of diazonium nitrogen by external nucleophiles has been reported.⁵⁰ Triazoline **198** decomposed to amide **199** while **200** gave aniline hydrochloride **201** (Scheme 29).

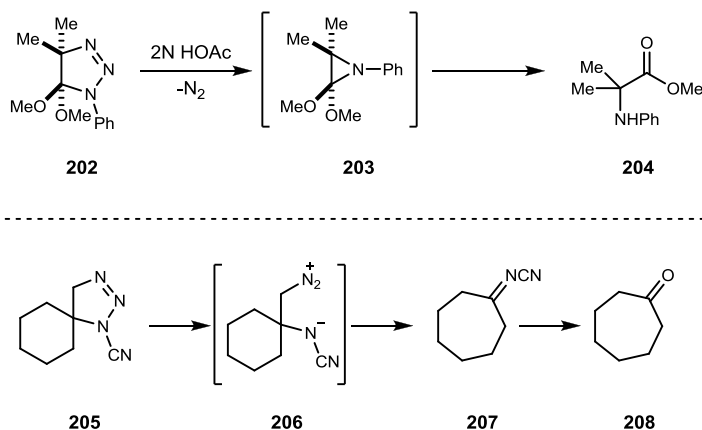
Scheme 29. Acid-Induced Triazoline Decomposition: External Nucleophiles



Acid induced decomposition of triazoline **202** produced aziridine **203** then facile acid-cleavage of aziridine furnished amine **204**. Additionally, migration of the alkyl group produced the corresponding ring expanded ketone **208** (Scheme 30).

⁵⁰ Hohenlohe-Oehringen, K. *Monatsh* **1958**, 89, 588. Backer, H. J. *Rec. Trav. Chim* **1950**, 69, 1223.

Scheme 30. Acid-Induced Triazoline Decomposition



Additionally, the effect of base on the decomposition of triazoline has been investigated by Huisgen.⁵¹ Following the pathway outlined in Scheme 28, triazolines containing acyl, carboxyl, and nitrile groups at the 4-position readily isomerized to the corresponding diazo compounds in the presence of base. The diazo compound could then react in another cycloaddition, or be subjected to further functional group manipulation.

In the early 1990's, systematic experimental and theoretical investigations of acid- or base-induced decomposition of triazoline to aziridinium ion were reported.⁵² Smith and coworkers extensively studied the acid promoted triazoline and triazene decomposition.⁵³ Calculations have determined N3-protonation can be favored over N1 by as much as 10 kcal/mol, but N1 protonation is in equilibrium and leads to irreversible triazoline decomposition.

⁵¹ Huisgen, R. Szeimies, G. Mobius, L. *Chem. Ber.*, **1966**, *99*, 475. Szeimies, G. Huisgen, R. *Chem. Ber.*, **1966**, *99*, 491.

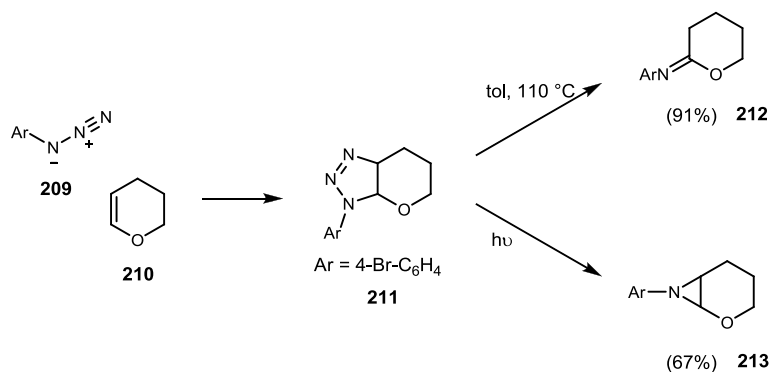
⁵² Michejda, C. J.; Denlinger, C. L.; Kupper, R.; Koepke, S. R.; Smith, R. H. *J. Am. Chem. Soc.* **1984**, *106*, 1056. Smith, R. H.; Denlinger, C. L.; Kupper, R.; Mehl, A. F.; Michejda, C. J. *J. Am. Chem. Soc.* **1986**, *108*, 3726. Schmiedekamp, A.; Smith, R. H.; Michejda, C. J. *J. Org. Chem.* **1988**, *53*, 3433.

⁵³ Ozment, J. L.; Schmiedekamp, A. M.; Schultz-Merkel, L. A.; Smith, R. H.; Michejda, C. J. *J. Am. Chem. Soc.* **1991**, *113*, 397. Wladkowski, B. D.; Smith, R. H.; Michejda, C. J. *J. Am. Chem. Soc.* **1991**, *113*, 7893. Smith, R. H.; Wladkowski, B. D.; Taylor, J. E.; Thompson, E. J.; Pruski, B.; Klose, J. R.; Andrews, A. W.; Michejda, C. J. *J. Org. Chem.* **1993**, *58*, 2097.

1.4.4. Photodecomposition of Triazoline

Unlike thermal and acid-induced triazoline fragmentation, photodecomposition displays a high selectivity for the corresponding aziridine. Photodecomposition of triazoline was extensively investigated in the mid 1960s. Unlike thermal decomposition of the norbornenyl derivative *exo* triazoline (Scheme 27), photolysis provided an aziridine as a sole product with 100% yield. In addition to the norbornene like strained ring systems,⁵⁴ Scheiner demonstrated parallel experiments to compare selectivity of thermal and photodecomposition.⁵⁵ Dihydropyran derivative triazoline **211** was converted to imine **212** in 91% yield under thermal conditions. In contrast to thermolysis, photodecomposition furnished aziridine **213** as a sole product in 67% yield (Scheme 32).

Scheme 31. Decomposition Selectivity: Thermal vs Photochemical



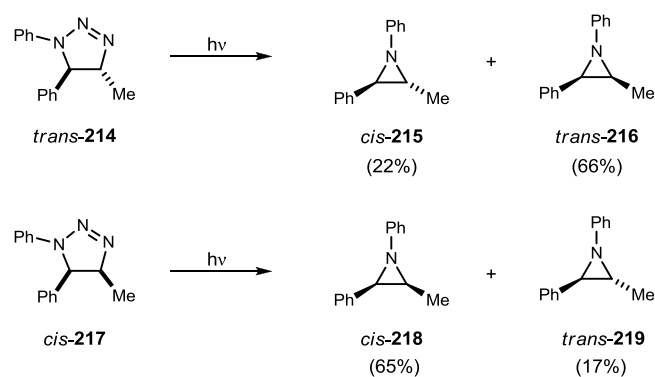
Stereochemistry had not been studied in the mechanism of thermal and acid-induced decomposition of triazoline. However, in 1968, Scheiner reported the stereochemistry and mechanism of aziridine formation from the photodecomposition of triazoline (Scheme

⁵⁴ Scheiner, P. *Tetrahedron* **1968**, *24*, 2757. Hale, R. L.; Zalkow, L. H. *Tetrahedron* **1969**, *25*, 1393.

⁵⁵ Scheiner, P. *J. Org. Chem.* **1967**, *32*, 2022.

32).⁵⁶ Under photolytic conditions, predominant retention of triazoline geometry in the aziridine formation was observed. Photolytic decomposition may occur via homolytic cleavage of the N1-N2 bond and involve a diradical intermediate (**168**, Figure 6). The observed selectivity of triazoline photodecomposition is a consequence of its homolytic nature of cleavage.

Scheme 32. Triazoline Photodecomposition



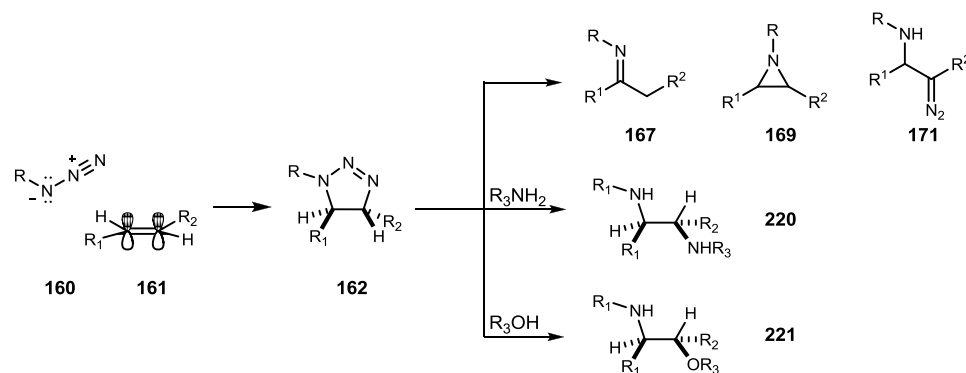
⁵⁶ Scheiner, P. *J. Am. Chem. Soc.* **1968**, *90*, 988.

1.5. Brønsted Acid Promoted Olefin Functionalization

1.5.1. Brønsted Acid Promoted [3+2] Cycloaddition

As mentioned in previous sections, the combination of azides and olefins which undergo a 1,3-dipolar cycloaddition reaction has been extensively studied with a wide range of target molecules.⁵⁷ For the most part, this interest stems from the ability to transform the resulting triazoline **162** to a range of derivatives, including aziridine **169** and diazo compound **171**. The triazoline can also be transformed by various nucleophiles such as amines or alcohols into a number of synthetically useful intermediates such as *vicinal* diamines **220** or *vicinal* aminoalcohols **221** (Figure 7).

Figure 7. Azide-Olefin 1,3-Dipolar Cycloaddition and Triazoline Fragmentation

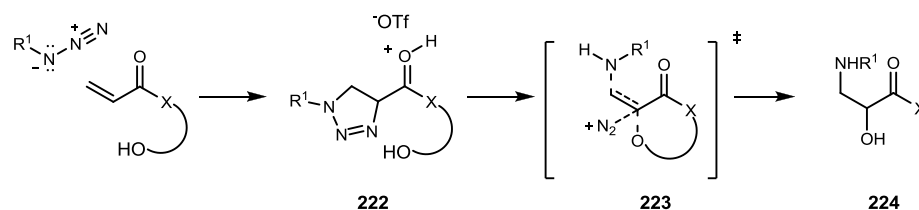


As discussed in Section 3.1.2 and 3.1.3, all previously reported methods for reacting azides with alkenes were thermal reactions at varying temperatures, used Lewis acid catalysts, or were run at high pressure. Although these reactions have already been shown to form the cycloaddition product, improvements can still be made. We hypothesized that Brønsted acid catalysts in combination with substrate design would allow us to reach this

⁵⁷ Scriven, E. F. V.; Turnbull, K. *Chem. Rev.* **1988**, *88*, 297.

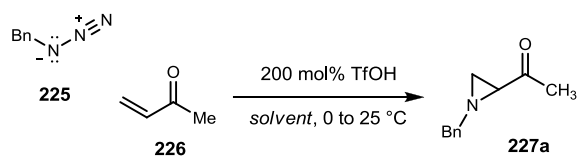
goal. First of all, the main object is to develop a mild and efficient substrate activation to overcome generally long reaction times and the limited means to activate substrates (thermal, photochemical). The use of catalysts would also provide an opportunity to achieve absolute stereocontrol. Second, we were interested in the use of substrates that would provide opportunity for further stereocontrolled functionalization.

Figure 8. Substrate Design



The basis for developing the protic acid catalyzed 1,3-dipolar cycloaddition reaction began from the methyl vinyl ketone as an electron deficient olefin with electron rich benzyl azide. Due to lack of activation of simple olefins, the reaction was designed and tested with the carbonyl group as an activating group for promoting the cycloaddition reaction with various azides. In order to convert alkene to triazolone (**222**), we started our investigation with various solvent screen. The protic acid catalyzed cycloaddition reaction with azide gave aziridine **227a** as the major product (Table 1).⁵⁸ As in previously reported articles, the stability of the resulting triazolone allows for spontaneous decomposition to aziridine (**227a**). However, the addition of Brønsted acid allows for a faster reaction time than thermal conversion. The acetonitrile reaction proceeded cleanly with a high yield while diethyl ether and dichloromethane gave satisfactory yields. Notably, protic solvents such as methanol and aprotic DMF gave no reaction.

⁵⁸ Mahoney, J. M.; Smith, C. R.; Johnston, J. N. *unpublished results*.

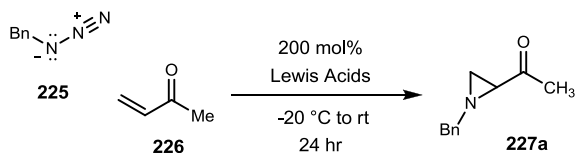
Table 1. Olefin Aziridination Using Benzyl Azide and Methyl Vinyl Ketone: The Effect of Solvent

entry ^a	Solvent	% yield ^b
1	MeCN	79
2	Et ₂ O	58
3	CH ₂ Cl ₂	49
4	THF	35
5	CHCl ₃	33
6	MeOH	N.R.
7	DMF	N.R.

^aAll reactions were 0.3 M in substrate. ^bIsolated yield after chromatography.

Secondly, a Lewis acid screen was carried out to determine if Lewis acids could efficiently catalyze the direct formation of aziridine **227a** (Table 2).⁵⁹ Several Lewis acids such as Cu(OTf)₂, BF₃·OEt₂ and TMSOTf gave an appreciable yield in both CH₃CN and CH₂Cl₂ solvents. All others gave at best no reaction with many giving complex reaction mixtures as judged by ¹H NMR of the crude reaction mixtures.

⁵⁹ Hong, K. B.; Johnston, J. N. *unpublished results*.

Table 2. Olefin Aziridination Using Benzyl Azide and Methyl Vinyl Ketone: The Effect of Lewis Acid

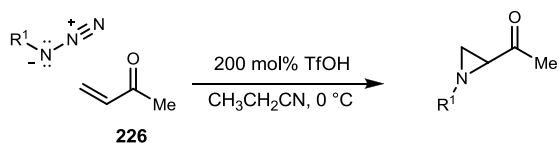
Lewis acid ^a	% yield ^b	
	CH ₃ CN	CH ₂ Cl ₂
MgBr ₂	<5	<5
Cu(OTf) ₂	18	17
YbCl ₃	<5	<5
LaCl ₃	<5	<5
ZnCl ₂	<5	<5
TiCl ₄	13	6
BF ₃ •OEt ₂	22	22
SnCl ₄	6	6
TMSOTf	23	20
TfOH	75	48

^aAll reactions were 0.3 M in substrate. ^bIsolated yield after chromatography.

Next, with this condition, we set out to study the scope of the aziridination with different azides (Table 3).⁶⁰ Various azides were examined and gave generally good yields. Among them, benzyl azide engaged the olefin to produce the *N*-benzyl protected terminal aziridine **227a** in 79% isolated yield. Since benzyl is a common protecting group for nitrogen, benzyl azide was chosen as the standard nitrogen donor. Alternatively, the aziridine may be isolated in slightly higher yield (92%) by direct crystallization of the triflic acid salt (Table 3, entry 2). More hindered azides are also effective, including diphenylmethyl azide **227c** and adamantyl azide **227d**. Azides such as *tert*-butyl glycinyl azide can be smoothly converted to the aziridine **227f** without identifiable ester hydrolysis. Finally, a variety of allylic azides formed their derived aziridines **227g**, **227h** in good yield.

⁶⁰ Mahoney, J. M.; Smith, C. R.; Johnston, J. N. *J. Am. Chem. Soc.* **2005**, *127*, 1354.

Table 3. Scope: Aziridination with Various Azides

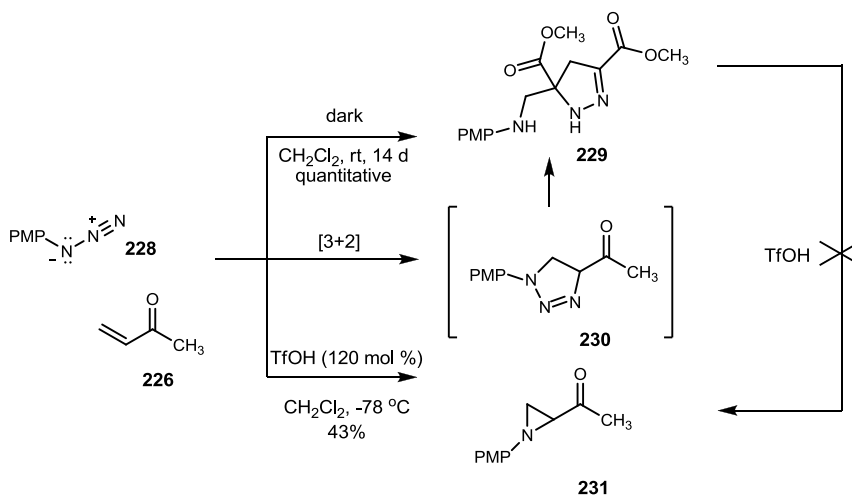


entry ^a	R ¹		% yield ^b
1	Bn	227a	79
2	Bn	227b	92 ^c
3	Ph ₂ CH	227c	49
4	Ad	227d	93
5	<i>p</i> -MeOC ₆ H ₄	227e	43 ^d
6	^t BuO ₂ CCH ₂	227f	66
7	EtO ₂ CCH=CHCH ₂	227g	76
8	Me ₂ C=CHCH ₂	227h	68

^aAll reactions were 0.30 M in substrate and proceeded to complete conversion. ^bIsolated yield after chromatography. ^cYield of the crystalline **227a** triflic acid salt. ^dReaction run in CH₂Cl₂ at -78 °C to minimize trimeric azide byproduct.

In order to probe the mechanism of the aziridination, a detailed study of the reaction between *p*-methoxyphenyl azide **228** and methyl vinyl ketone was undertaken (Scheme 33). With 1.2 equivalents of triflic acid in dichloromethane, a 43% yield of the aziridine **231** was obtained. In the absence of triflic acid at room temperature, the thermal cycloaddition gave a quantitative yield of pyrazole **229**.

Scheme 33.

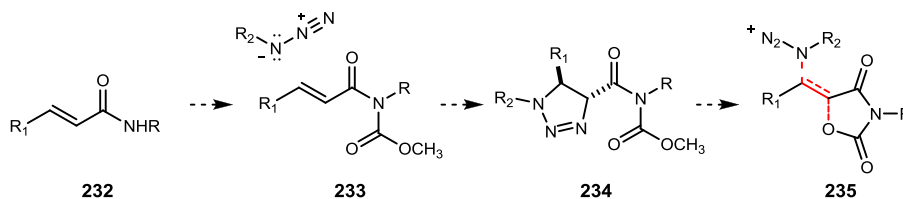


This latter behavior is preceded and believed to arise via the isomerization of the triazolone to an α -diazo intermediate which can then undergo [3+2] cycloaddition with another equivalent of methyl vinyl ketone. This pyrazole was not converted to aziridine with TfOH and therefore lies after any potential common intermediate.

1.5.2. Acceptor Design

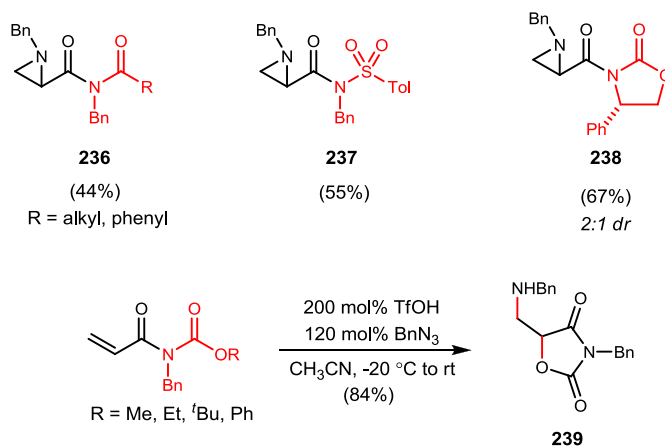
The ease with which the aziridine triflic acid salt **227b** could be formed and isolated led us to consider the possibility that an oxygen nucleophile might be internally delivered by an activated ester heteroatom **233** (Scheme 34).

Scheme 34.



To verify our hypothesis, different types of active esters such as imide **236**, sulfonamide **237**, and cyclic oxazolidinone **238** were synthesized and tested under standard condition. Under these conditions, the aziridination reaction was tolerated with different functional groups. Finally, to deliver various heteroatoms to olefin functionalization, oxygen nucleophiles such as carbamate type active esters were synthesized and tested to form desired oxazolidinone dione **239** with various ester derivatives (Scheme 35).

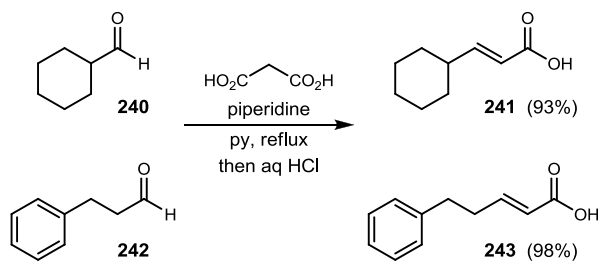
Scheme 35. Olefin Aziridination Using Benzyl Azide and Various Active Esters



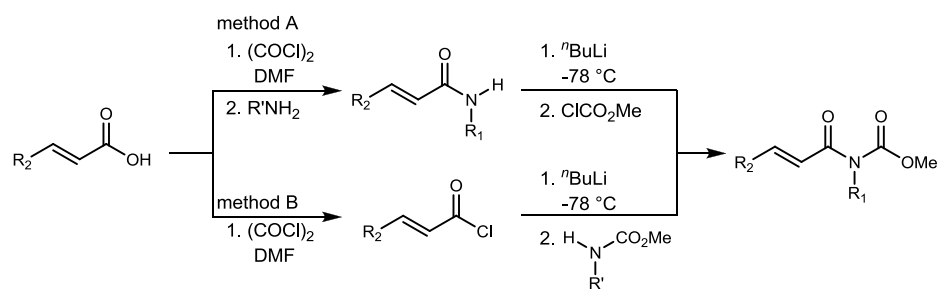
1.5.3. β -Alkyl Substituted Imide Derivatives.

The starting materials were prepared in one to two steps. Amides were prepared by coupling benzyl amine or aniline with the acid chloride. These reactions usually worked cleanly and the products were isolated as crystalline solids (Table 4). The amides were further functionalized by lithiating the amide and then reacting it with methyl chloroformate. In the case of β -cyclohexane derivative **241** and β -hydrocinnamoyl derivative **243**, the requisite carboxylic acid was prepared from the corresponding aldehyde using a Knoevenagel condensation (Scheme 36).⁶¹

Scheme 36. Carboxylic Acid Preparation: Knoevenagel Condensation



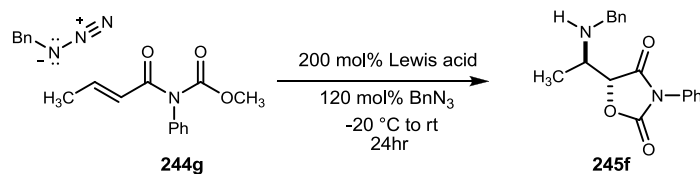
⁶¹ Jessup, P. J.; Petty, C. B.; Roos, J.; Overman, L. E. *Organic Syntheses*; Wiley: New York, 1988; Collect. Vol. 6, p 95.

Table 4. β -Substituted Imides Preparation

entry ^a	R ₁	R ₂	method	imide	yield (%) ^b
1	Bn	H	A	244a	85
2	Bn	Me	A	244b	87
3	Bn	Et	A	244c	90
4	Bn	<i>i</i> Pr	B	244d	43
5	Bn	Cy	B	244e	64
6	Bn	C ₈ H ₉	A	244f	25
7	Ph	Me	A	244g	72
8	Ph	Et	A	244h	73
9	Ph	<i>i</i> Pr	B	244i	60
10	Ph	Cy	A	244j	27
11	Ph	C ₈ H ₉	A	244k	71
12	Ph	Ph	A	244l	59

^aAll reactions were 0.25 M in substrate and proceeded to complete conversion. ^bIsolated yield after chromatography.

With these Michael acceptors in hand, Lewis acids were screened to determine if Lewis acids could efficiently catalyze the direct formation of oxazolidine dione **245f** (Table 5). Using the same selection that was used with methyl vinyl ketone **226**, several Lewis acids such as TiCl₄, SnCl₄ and TMSOTf gave an appreciable yield in both CH₃CN and CH₂Cl₂ solvents. It was also confirmed that TfOH afforded the most efficient transformation to the desired oxazolidine dione. All others resulted in either no reaction or a complex reaction mixture as judged by ¹H NMR of the crude reaction mixtures.

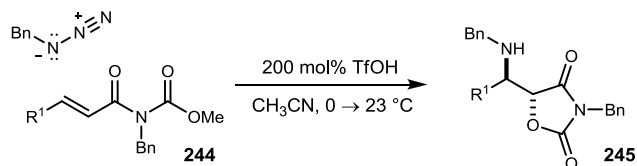
Table 5. Olefin Functionalization Using Benzyl Azide and Imide: The Effect of Lewis Acid

Lewis acid ^a	% yield ^b	
	CH ₃ CN	CH ₂ Cl ₂
MgBr ₂	<5	<5
Cu(OTf) ₂	<5	<5
YbCl ₃	<5	10 ^c
LaCl ₃	<5	<5
ZnCl ₂	<5	<5
TiCl ₄	35	34
BF ₃ •OEt ₂	15	45
SnCl ₄	26	26
TMSOTf	36	35
TfOH	67	43

^aAll reactions were 0.3 M in substrate. ^bIsolated yield after chromatography. ^cTriazoline was isolated.

Using these *N*-Bn protected carbamates, the standard aziridination reaction was investigated. The crotonyl derivative of *N*-benzyl methyl carbamate **244b** was subjected to the standard aziridination conditions which delivered oxazolidinone dione **245b** as a single regioisomer (>20:1, ¹H NMR). The scope of the β-alkyl substituted acceptor for this process was studied and the results are shown in Table 6. All of the alkyl substituted *N*-Bn imides gave good diastereoselectivity and moderate yield. However, the cinnamoyl imide derivative **245i** gave only the product of imide hydrolysis.

Table 6. The Scope of β -alkyl Substituted Acceptors: Aminohydroxylation

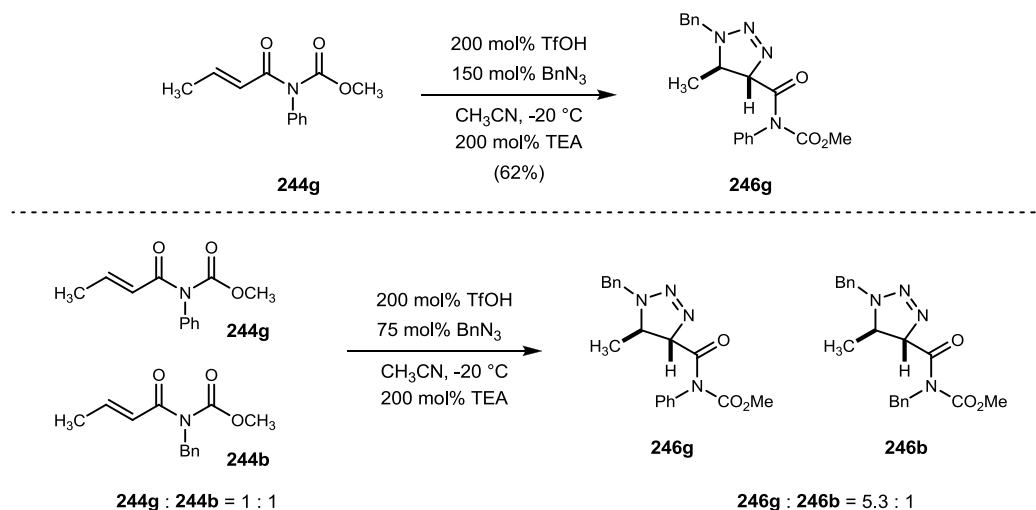


entry ^a	R ¹	dr	% yield ^b
1	Me 245b	> 20:1	94
2	Et 245c	15:1	82
3	ⁱ Pr 245d	> 20:1	61
4	Ph 245l		0

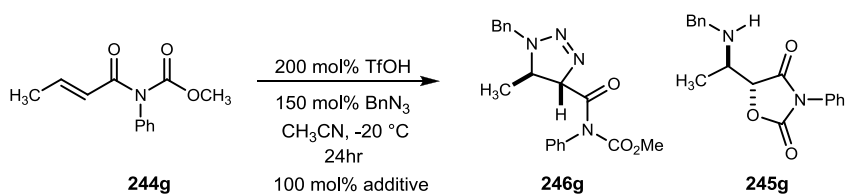
^aAll reactions were 0.25 M in substrate and proceeded to complete conversion. ^bIsolated yield after chromatography.

Considering the fact that these reactions are accelerated by Lewis acids, we sought a more electron deficient carbamate electrophile and targeted **244g** for synthesis and evaluation. After screening reaction variables, *trans*-triazoline **246g** was isolated as a single diastereomer when the reaction was maintained and quenched at -20°C with triethylamine (Scheme 37). *N*-Bn carbamate was also converted and isolated. Additionally, a competition experiment proved that the more electron deficient *N*-Ph carbamate reactivity was five times faster than the corresponding *N*-Bn carbamate.

Scheme 37. Competition Experiment: *N*-Bn Carbamate vs *N*-Ph Carbamate



Our initial protocol was performed with commercial TfOH without purification and the reaction was initiated at low temperature but then allowed to warm to room temperature. After finding the new reaction variation with low temperature, however, running several reactions starting from the imide side by side under identical conditions revealed that this reaction did not consistently show the same ratio of triazoline to oxazolidine dione. Due to this fact, the next set of experiments were performed to verify the effect of additives for formation of triazoline and oxazolidine dione (Table 7).

Table 7. The Effect of Additives: Triazoline vs Oxazolidine Dione

entry ^a	Additives	% conversion ^b	ratio (TA : AH)
1	MeOH	80	0 : 100
2	EtOH	80	0 : 100
3	^t PrOH	72	0 : 100
4	CF ₃ CH ₂ OH	100	0 : 100 (58%) ^c
5	Et ₂ O	100	13 : 87
6	DMF	40	40 : 60
7	NMP	42	42 : 58
8	none	100	100 : 0 (64%) ^c

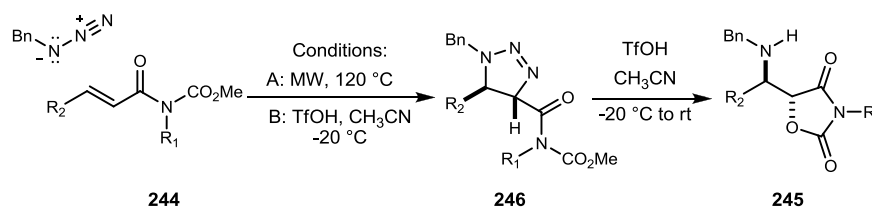
^aAll reactions were 0.25 M in substrate and proceeded to complete conversion.

^bMeasured by ¹H NMR analysis of the crude reaction mixture after reaction quench (Et₃N, 2 equiv.) at the reaction temperature. ^cIsolated yield after chromatography.

First, using various alcohol additives showed over 70% conversion from imide to oxazolidinedione without forming triazoline. Even at low temperature, alcohol additives can activate this reaction pathway to convert triazoline to oxazolidinedione. Additionally, other non protic additives such as Et₂O, DMF and NMP showed an acceleration of the transformation to oxazolidine dione. However, DMF and NMP showed only 50% conversion and around 50:50 mixtures of triazoline and oxazolidine dione. Without an additive, the reaction gave only triazoline formation in 64% yield. More detailed mechanism and the effect of additives will be discussed in Chapter 2.

This observation held true for β -substituted *N*-phenyl and *N*-benzyl carbamates, leading to their corresponding triazolines in good yield. The scope of the β -alkyl substituted acceptor for this process was studied and the results are shown in Table 8. The formation of triazoline was dependent on the temperature and freshly distilled TfOH (entry 1-3, 6-8). Additionally, unlike the conventional heating method, microwave can facilitate the promotion of [3+2] cycloaddition in a short period of time (entry 4-5, 9-10).

Table 8. Acid Promoted/Thermal [3+2] Cycloaddition, Acid Promoted Triazoline Fragmentation



entry	R ₁	R ₂		yield (%)		yield (%) ^c
1	Bn	H	246a	54 ^b	245a	92
2	Bn	Me	246b	73 ^b	245b	62
3	Bn	Et	246c	78 ^b	245c	72
4	Bn	<i>i</i> Pr	246d	75 ^b	245d	70
5	Bn	Cy	246e	70 ^a	245e	75
6	Bn	C ₈ H ₉	246f	76 ^a	245f	74
7	Ph	Me	246g	62 ^b	245g	56
8	Ph	Et	246h	73 ^b	245h	63
9	Ph	<i>i</i> Pr	246i	65 ^b	245i	54
10	Ph	Cy	246j	60 ^a	245j	50
11	Ph	C ₈ H ₉	246k	41 ^a	245k	51

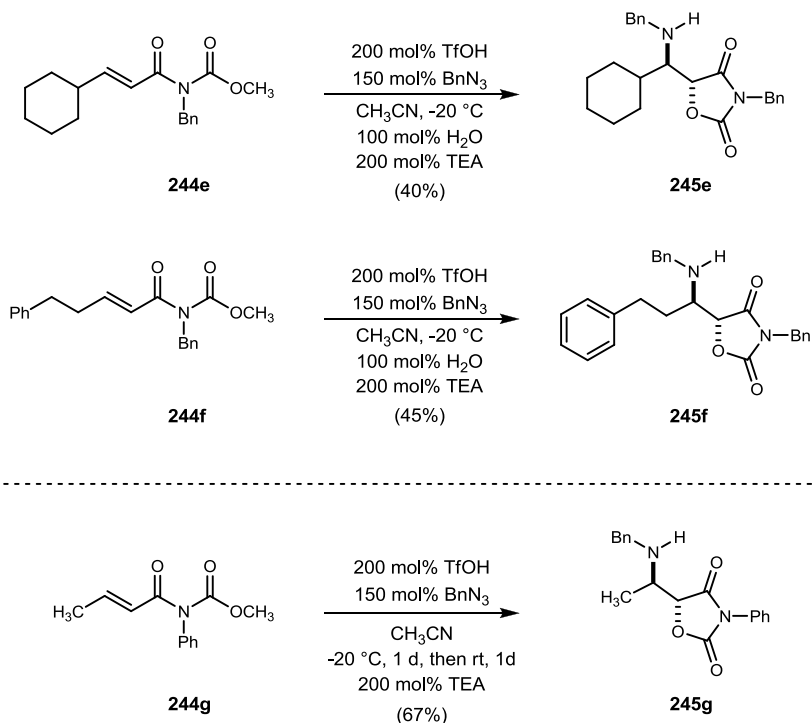
^aGeneral condition A: Reactions were run with 0.2 mmol of imide and 80 equiv. of BnN₃ at 120 - 150 °C. ^bGeneral condition B: BnN₃ (1.5 equiv.) and the olefin (1 equiv.) in CH₃CN (0.33 M) were treated with triflic acid at -20 °C, then quenched with TEA (2.0 equiv) at -20 °C. ^cTriazoline (1 equiv.) in CH₃CN (0.33 M) was treated with triflic acid at -20 °C and warmed to room temperature.

Both protocols were generally efficient, leading to a good yield of triazoline **246** with high diastereoselectivity (>20:1, ¹H NMR) in both *N*-Bn and *N*-Ph protected imides. Sterically unencumbered methyl **246b**, ethyl **246c**, and isopropyl **246d** gave slightly better results than hindered cyclohexyl **246e**, and hydrocinnamoyl **246f**. The isolated

triazolines were then resubjected to standard acid promoted conversion to the corresponding oxazolidine diones. In general, various alkyl substituted triazoline series showed moderate conversion to oxazolidine dione.

We can also control the reactivity of the carbamate imide dependent on the additive and temperature. Utilizing this fact, the desired oxazolidine dione can be obtained under various conditions (Scheme 38). For example, under the low temperature, imides **244e** and **244f** furnished oxazolidine dione **245e** and **245f** with 1 equivalent of water as an additive.

Scheme 38. One Step Synthesis of Oxazolidine Dione

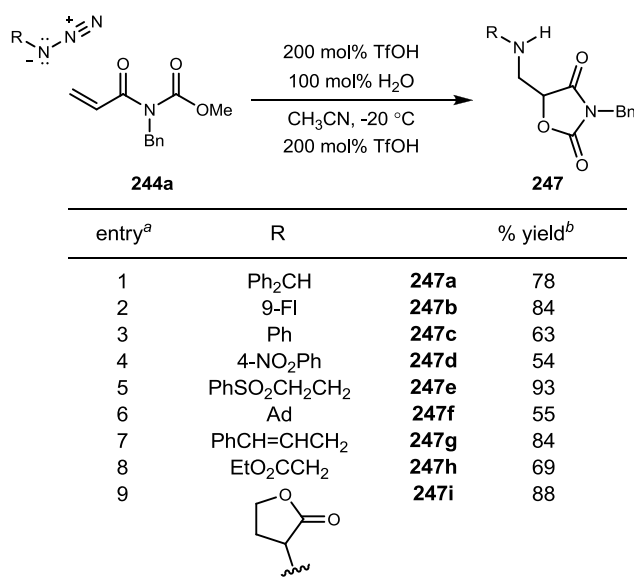


However, in the presence of water, the competition reaction between triazoline fragmentation and imide hydrolysis resulted in lower yield than direct conversion from triazoline to oxazolidine dione. Additionally, imide **244g** can convert to triazoline under

low temperature, then warming to room temperature to afford oxazolidine dione **245g** in 67% yield.

Next, using acryloyl derivative *N*-Bn carbamate **244a**, a range of functionalized azide additions were investigated (Table 9). Various azides were screened and gave generally good yields. More hindered azides are also effective, including diphenylmethyl azide **247a**, fluorenyl azide **247b**, and adamantyl azide **247f**. Azides such as ethyl glycinyl azide **247h** and cyclic ester derivative azide **247i** can be smoothly converted to the oxazolidine dione without identifiable ester hydrolysis. Finally, a variety of functional group such as 4-nitrophenyl azide, sulfone functionalized alkyl azide formed their derived oxazolidine dione **247d**, **247e** in good yields.

Table 9. Scope: Aminohydroxylation with Various Azides

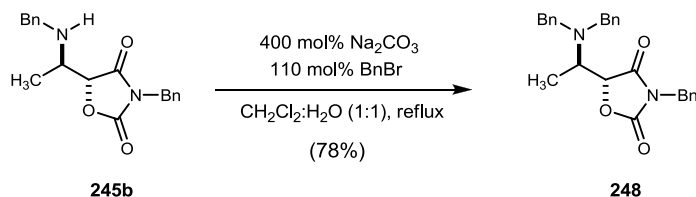


^aAll reactions were 0.30 M in substrate and proceeded to complete conversion. ^bIsolated yield after chromatography. ^cAbbreviations: Ad = adamantyl, Fl = fluorenyl.

The X-ray crystal structure of **248** established the relative stereochemistry as *anti* for these products. We hypothesized that there is an intermediate *trans*-triazoline which

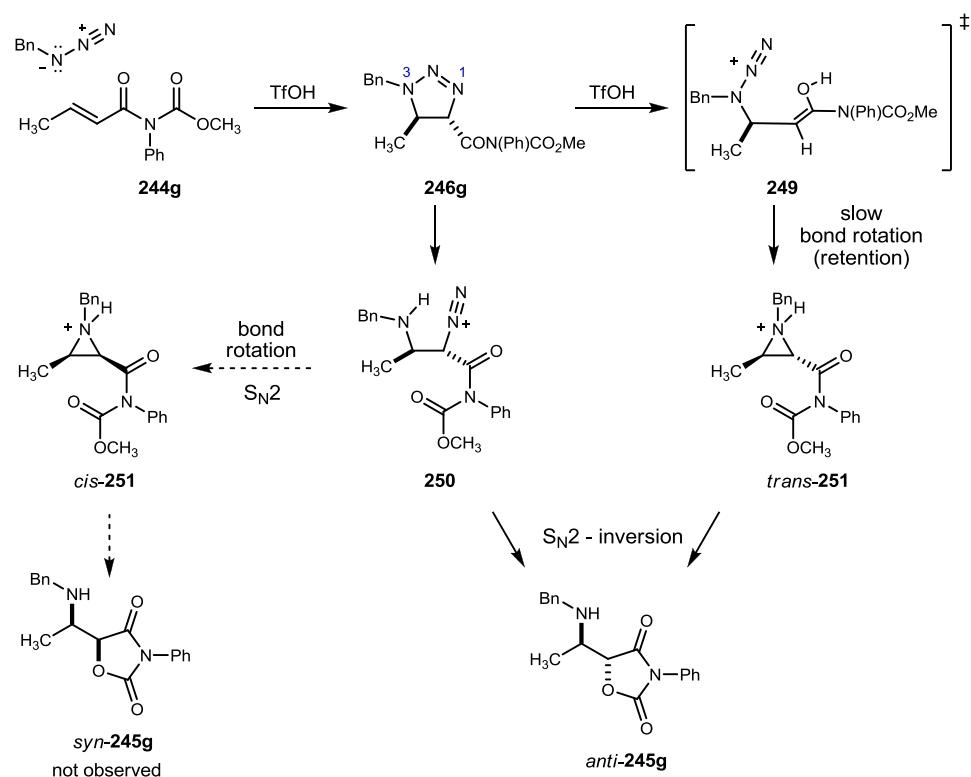
under our reaction conditions would allow us to obtain relative stereochemistry were the *trans*-triazoline fragments to a *trans*-oxazolidine dione.

Scheme 39.



The triazolines formed in thermal azide-olefin cycloadditions were analyzed by 1D and 2D NMR, which showed the product to be the *trans*-triazoline **246g**. The proposed mechanism, for the conversion of the *trans*-triazoline **246g** to *anti*-**245g** via either diazonium **250** or *trans*-aziridine **251** is shown in Figure 9. Under acidic conditions, the more basic nitrogen of the triazoline is protonated, which activates it toward ring opening. In the first pathway, N3 of the triazoline is protonated, followed by isomerization to the β -amino- α -diazonium imide. Intermediate **250** is then susceptible to $\text{S}_{\text{N}}2$ attack by the carbonyl, expelling N_2 , and leading to the *anti*-oxazolidine dione **245g**. However, another pathway exists to *anti*-**245g** through amino diazonium intermediate **249**, which could undergo aziridination to *trans*-**251**, and finally produce the *anti*-aminohydroxylation product *anti*-**245g**. The difference between these pathways is the fragmentation pathway from triazoline **246g**; N-N bond cleavage forms diazonium **250**, whereas C-N bond fragmentation leads to aminodiazonium **249**. In work with triazolines derived from fumarate esters, we have found that diazonium ions similar to **250** typically form *cis*-aziridine such as *cis*-**251**.

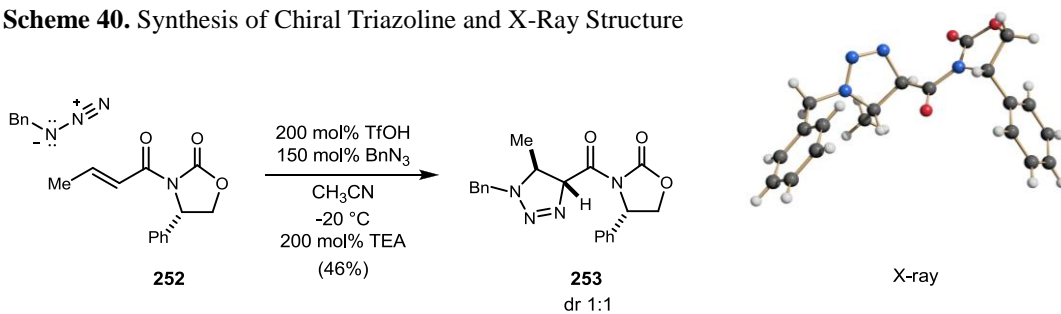
Figure 9. Mechanistic Hypothesis of *anti*-Triazoline Fragmentation to *anti*-Oxazolidine Dione



Therefore, it is highly interesting that triazoline **246g** does not proceed through *cis*-**251**, as determined by the exclusive production of *anti*-**245g** from **244g**. A possible mechanistic hypothesis for this different behavior is the faster rate of cyclization of **250** to *anti*-**245g** versus bond rotation and cyclization leading to *cis*-**251** (if **250** is an intermediate).

The next step in determining the stereochemical and hypothesized mechanistic pathways for both the cycloaddition and aminohydroxylation was investigated by using chiral oxazolidinone **252** and studying the decomposition of chiral triazoline **253** (Scheme 40).

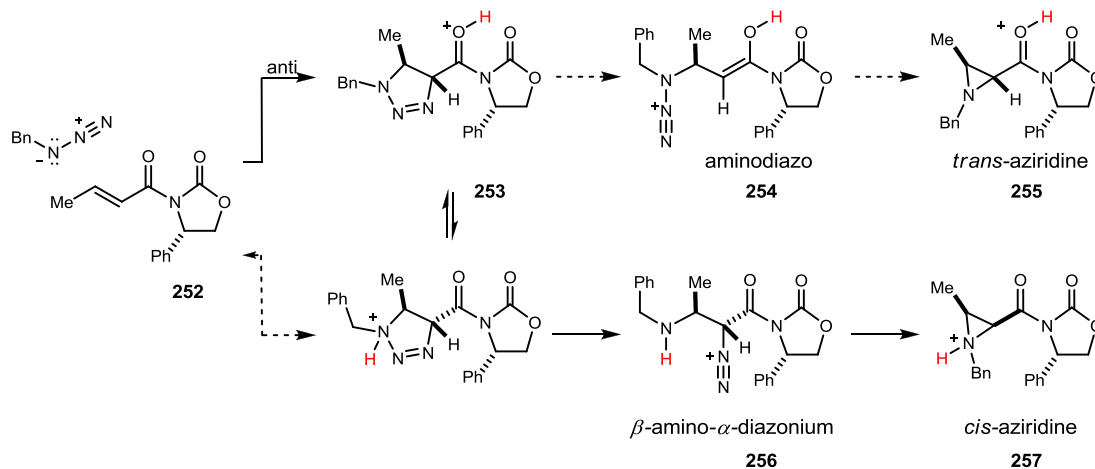
Scheme 40. Synthesis of Chiral Triazoline and X-Ray Structure



Chiral oxazolidinone **252** was reacted with benzyl azide under the same conditions to afford chiral triazoline **253** in 45% yield with 1:1 dr. A crystal of one diastereomer was grown from toluene and petroleum ether, and the relative stereochemistry was determined by X-ray crystallography.

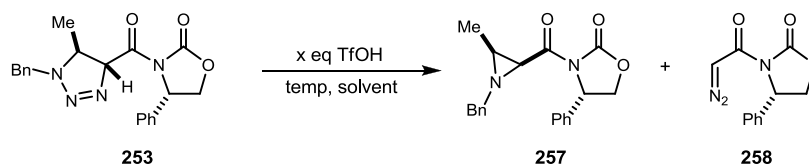
If the intermediate of this reaction is aminodiazonium **254**, *trans*-aziridine **255** should result from treatment of **253** with TfOH. In contrast to imide Michael acceptors **254**, the nucleophile in this chiral oxazolidinone acceptor is incapable of cyclization. However, if the reaction intermediate is β -amino- α -diazonium **256**, *cis*-aziridine **257** should result (Scheme 41).

Scheme 41. Mechanistic Hypothesis of Chiral *anti*-Triazoline Fragmentation to Aziridine



In an attempt to convert a *trans*-triazoline **253** to the corresponding aziridine, standard acid promoted conditions were applied. The *trans*-triazoline was treated with 2 equivalents of TfOH and 1 equivalent of water, followed by a quench with 2 equivalents of triethylamine at low temperature (Table 10, entry 1).

Table 10. Optimization of Chiral *trans*-Triazoline Fragmentation to Corresponding Aziridine



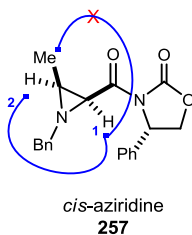
entry	TfOH	temp	solvent	ratio (%yield ^a)
1	2	-20 °C	CH ₃ CN	43% (258 only)
2	1	-20 °C to rt	CH ₃ CN	258 only
3	1	-78 °C	EtCN	75% (258 only)
4	1	0 °C	CCl ₄	258 only
5	1	rt	CH ₃ CN	258 only
6	1	rt	CCl ₄ : EtCN (1:2)	257 : 258 = 1 : 2
7	1	rt	CCl ₄ : EtCN (2:1)	257 : 258 = 1 : 1
8	1	0 °C	CCl ₄ : EtCN (10:1)	257 : 258 = 0.6 : 1
9	1	-20 °C	CCl ₄ : EtCN (1:1)	257 : 258 = 1 (~30% ^b) : 5
10	1	-78 °C	EtCN	258 only (75%)
11	1	-20 °C	CCl ₄ : EtCN (10:1)	257 (30% ^c)

^a% Conversion was measured by ¹H NMR of the triazoline H _{α} and aziridine H _{α} . ^b60% yield of diazo. ^c60% yield of hydrolysis.

Unfortunately, the product was α -diazo imide **258** resulting from a retro-Mannich fragmentation of the intermediate β -amino- α -diazonium ion. Warming of the reaction gave the same result (Table 10, entry 2). Various temperatures and solvents (Table 10, entry 3-5) were not successful. Finally, the combination of CCl₄ and EtCN solvent with 1 equivalent TfOH started to afford desired aziridine **257** based on ¹H NMR analysis of the crude reaction mixture (Table 10, entry 6). However, several variations of the solvent system were unable to prevent the retro-Mannich pathway (Table 10, entry 7-9). Additionally, isolated aziridine **257** was a mixture with an unknown impurity which

could not be easily separated by column chromatography. Repeated column chromatography, however, did yield relatively pure aziridine **257** which was fully characterized by 1D and 2D NMR analysis (Figure 10).

Figure 10. Assignment of *cis*-Relative Stereochemistry by NOESY Analysis of Aziridine **257**.

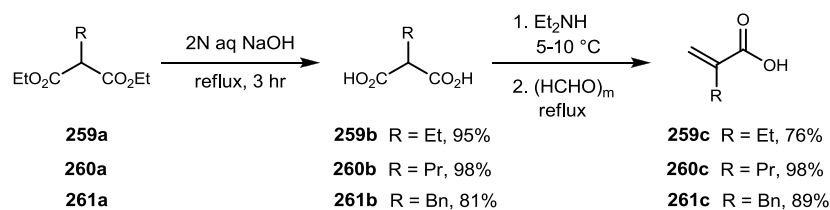


Based on the stereochemical outcome from the conversion of *trans*-triazoline **253** to *cis*-aziridine **257**, the reaction pathway of *anti*-aminohydroxylation and reaction intermediate were confirmed. The *trans*-triazoline **253** decomposed to β -amino- α -diazonium **256**, then subsequent ring closure furnished *cis*-aziridine **257**. In the case of *anti*-oxazolidine dione formation (Figure 9), the more basic nitrogen of the triazoline is protonated, which activates it toward ring opening. This leads to intermediate **250** which is susceptible to S_N2 attack by the carbamate carbonyl, expelling N_2 , and leading to the *anti*-oxazolidine dione **245g**. Additionally, *cis*-aziridine **257** formation through aminodiazonium **249** was not supported by these findings, since it should be converted to *trans*-aziridine **251**.

1.5.4. α -Alkyl Substituted Imide Derivatives.

Preparation of the α -substituted Michael acceptor was less straightforward, since only methacrylic acid is commercially available. α,β -Unsaturated carboxylic acids were prepared in a two step sequence.⁶² Starting from 2-alkylmalonate derivatives, such as ethylmalonic acid **259b**, obtained by base hydrolysis of diethyl ethylmalonate **259a**, and was subjected to a Mannich reaction with diethylamine and paraformaldehyde to produce 2-methylenebutyric acid **259c** in 76% yield (Scheme 42).

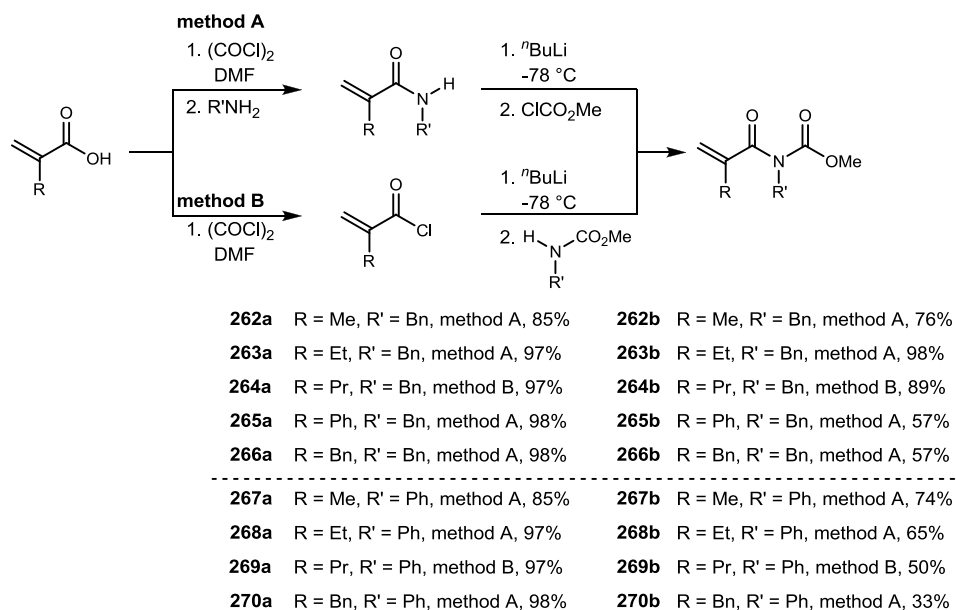
Scheme 42. Carboxylic Acid Preparation



Imides were prepared by 1) coupling benzylamine or aniline with the acid chloride, followed by acylation with methyl chloroformate, or 2) in situ generation of the acid chloride, then coupling with lithiated *N*-protecting carbamates. These reactions usually worked cleanly and the products were isolated as oils (Scheme 43).

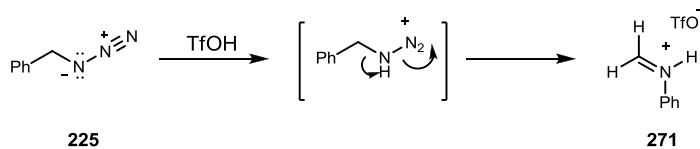
⁶² Kuang, Y. Y; Chen, F. E. *Org. Prep. Proced. Int.*, **2004**, 37, 184.

Scheme 43. α -Substituted Imides Preparation

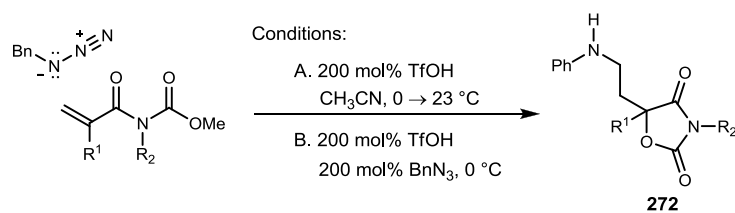


In contrast to the β -alkyl substituted *N*-Bn carbamate, α -substitued *N*-Bn carbamates followed a different reaction pathway. During the reaction, the triflic acid catalyzed azide rearrangement was faster than [3+2] cycloaddition. Presumably, the reaction occurred *via* a [1,2]-phenyl shift to **271** via an intermediate aminodiazonium ion (Scheme 44).

Scheme 44. Azide Rearrangement: Acid Promoted Aza-Schmidt



α -Substituted acrylates led to generally high yields of oxazolidine diones **272a-272e** (Table 11, entries 1-5). Additionally, a protocol in which generation of aminodiazonium ion **271** preceded imide addition was also effective to convert imide to iminoacetoxylation product (Table 11, entry 6-9).

Table 11. Acid Promoted Iminoacetoxylation: α -Substituted Imides

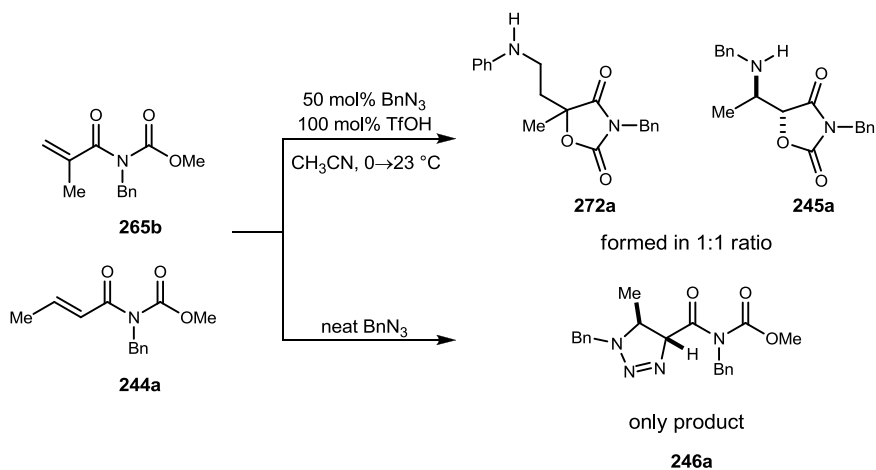
entry	R ₁	R ₂		yield (%) ^c
1	Bn ^a	Me	272a	84
2	Bn ^a	Et	272b	88
3	Bn ^a	Pr	272c	61
4	Bn ^a	Ph	272d	60
5	Bn ^a	Bn	272e	86
6	Ph ^b	Me	272f	64
7	Ph ^b	Et	272g	76
8	Ph ^b	Pr	272h	56
9	Ph ^b	Bn	272i	47

^aGeneral condition A: BnN₃ (1.5 equiv.) and the olefin (1 equiv) in CH₃CN (0.33 M) were treated with triflic acid at 0 °C, then warmed to room temperature.

^bGeneral condition B: BnN₃ (2.0 equiv.) in CH₃CN (0.33 M) were treated with triflic acid at 0 °C, then the olefin (1 equiv) was added and the reaction temperature was maintained until completion.

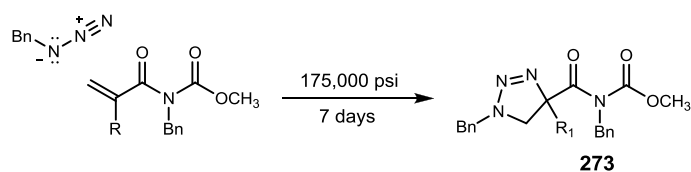
To understand the reactivity difference between β -alkyl substituted *N*-Bn carbamate and α -substituted *N*-Bn carbamates, competitive thermal triazoline formation with the α - and β -methyl acceptors (**256b**, **244a**) was performed and gave only the β -substituted triazoline. In contrast to this, Brønsted acid with only 0.5 equivalents of benzyl azide leads to a 1:1 mixture of aminohydroxylated product **245a** and iminoacetoxylation product **272a** (Scheme 45) in a competition reaction. Additionally, triazoline **246a** failed to thermally convert to aziridine or oxazolidine dione, but its exposure to triflic acid led to clean low-temperature (-20 °C) conversion to **245a**.

Scheme 45. Competition Experiment: α -Substituted Imide vs β -Substituted Imide



Since the triflic acid-catalyzed reaction of azide with α -substituted carbamate led solely to a Schmidt/iminoacetoxylation reaction, we explored the use of high pressure to access the triazoline, and then determine whether the triazoline could serve as precursor to the oxazolidine dione. A series of α -substituted carbamates were subjected to high pressure conditions with benzyl azide (with S. Weinreb, Penn. State. U.) (Table 12). These efficiency of this [3+2] cycloaddition dropped as the size of the α -substituent increased. For example, sterically favored methyl substituted **273a** gave better results than ethyl **273b** and propyl **273c**. Ph **273d** and Bn **273d** substituted products gave similar results. Although these experiments were not normally replicated, in the ethyl case (**273b**), we were performed two experiments to improve the yield of formation but the results were identical (23% and 20%, respectively). In all cases, seven days were required for substantial triazoline formation. When using ethyl and propyl substituents, considerably lower yields were observed. It is not clear whether the lower yields represent a modest steric effect, or if the limitations of the apparatus and handling contributed.

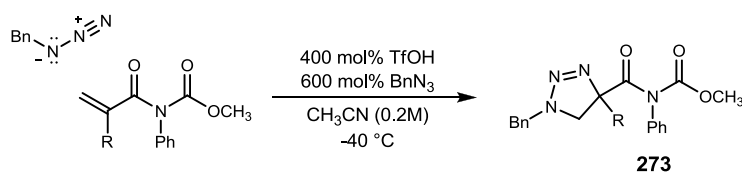
Table 12. High Pressure Assisted [3+2] Cycloaddition: α -Substituted Imides



entry ^a	R		%yield ^b
1	Me	273a	70
2	Et	273b	23
3	Pr	273c	15
4	Ph	273d	54
5	Bn	273e	52

^aA solution of the olefin in azide 1.1 mL was sealed in a 5 mL plastic Luerlok syringe and subjected to 175,000 psi of pressure for 7 days at ambient temperature in a LECO Model PG-200-HPC apparatus. ^bIsolated yield after chromatography.

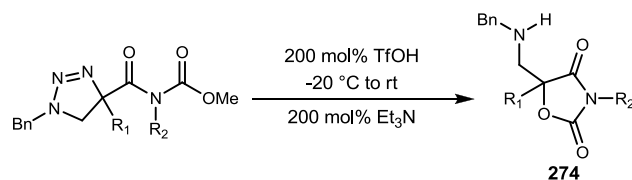
We observed that variation of temperature and equivalents of triflic acid and benzyl azide can control the reactivity of α -substituted carbamate to lead to triazoline as a sole product. Under optimized conditions, various α -substituted imides were converted to corresponding triazolines (Table 13). Although α -substituted *N*-Ph carbamates can be converted to triazoline under Brønsted acid promoted reaction conditions, the same protocol with *N*-Bn carbamates produced an inseparable mixture of triazoline and oxazolidine dione (iminoacetoxylation).

Table 13. Acid Promoted [3+2] Cycloaddition: α -Substituted Imides

entry ^a	R		yield (%) ^b
1	Me	273f	73
2	Et	273g	83
3	Pr	273h	68
4	Bn	273i	61

^aGeneral procedure: BnN₃ (6.0 equiv.) and the triflic acid (4.0 equiv.) in solvent (0.2 M) were treated with olefin (1.0 equiv.) for 7 days at -40 °C. ^bIsolated yield after chromatography.

Using these triazolines, the acid-promoted conversions of triazoline to aminohydroxylation were investigated (Table 14). These transformations were generally efficient, leading to good yields of β -amino-oxazolidine dione **274** in all cases. For example, aliphatic substrates **273a-c** provided oxazolidine diones **274a-c** in 90%, 70%, and 71% yield (Table 14, entries 1-3). Using the α -phenyl carbamate, oxazolidine dione **274d** was formed in 54% yield (Table 14, entry 4). And finally, benzyl substituent **273e** furnished the product in 80% yield. It was also found that *N*-Ph protected triazoline derivatives gave moderate yield of oxazolidine diones (Table 14, entry 6-9).

Table 14. Acid Promoted Triazoline Fragmentation: α -Substituted Triazolines

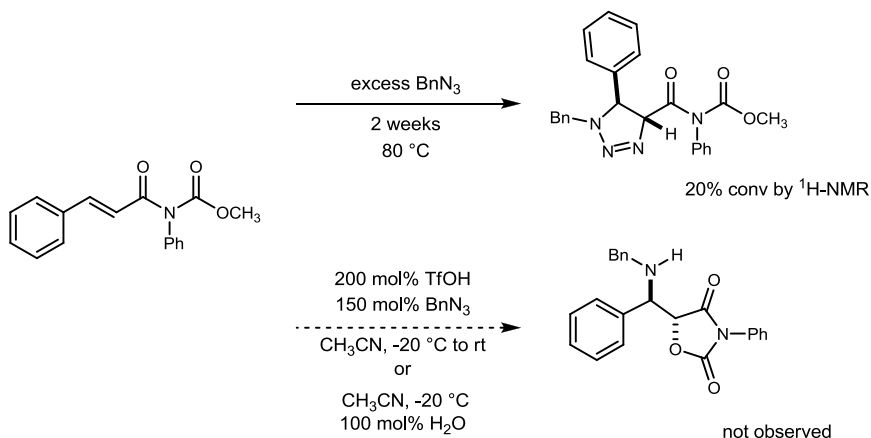
entry ^a	R ₁	R ₂		yield (%) ^b
1	Bn	Me	274a	90
2	Bn	Et	274b	70
3	Bn	Pr	274c	71
4	Bn	Ph	274d	54
5	Bn	Bn	274e	80
6	Ph	Me	274f	56
7	Ph	Et	274g	74
8	Ph	Pr	274h	53
9	Ph	Bn	274i	63

^aTriflic acid (2.0 equiv.) in solvent (0.2 M) were treated with olefin (1.0 equiv.) at -20 °C. ^bIsolated yield after chromatography.

1.5.5. β -Aryl Substituted Imide Derivatives: Microwave-Assisted [3+2] Cycloaddition.

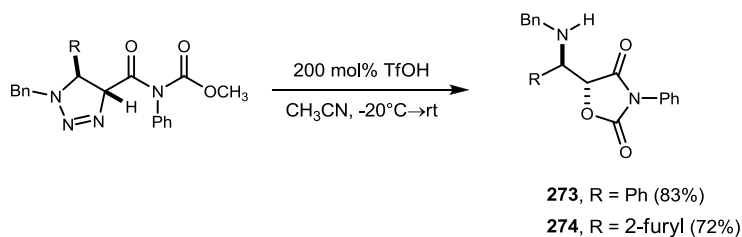
We set out to study the effects of Lewis acids and additives on the formation of either triazoline or aminohydroxylated product. Based on the results of section 5.1.3, 5.1.4, all *N*-Bn and *N*-Ph substituted β -aromatic acceptors such as cinnamoyl and 4-methoxycinnamoyl imides were investigated (Scheme 46). However, due to the low reactivity of β -aromatic acceptors, conventional heating conditions provided only 20% conversion, as measured by ¹H NMR after 2 weeks at 80 °C. Additionally, different temperature variations and standard acid promoted conditions were not effective in these reactions. When the acceptor's β position was an alkyl substituent, the aminohydroxylation pathway was much faster than the competing reactions, particularly imide hydrolysis. In contrast to β -alkyl acceptors, the β -aromatic substrates are rapidly hydrolyzed.

Scheme 46.



A second set of experiments were performed to isolate thermal triazoline product and to further convert it to the aminohydroxylation product. Even though at 80°C thermal conditions produced the product after 2 weeks, the triazoline yield was only around 30%. In spite of the low reactivity of imide to triazoline, this triazoline showed moderate reactivity with long reaction times at room temperature (Scheme 47).

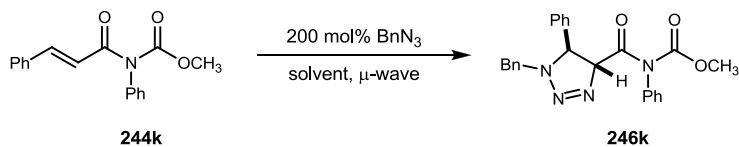
Scheme 47.



In order to accelerate thermal triazoline formation for β -aromatic acceptors, microwave-assisted conditions were considered. Since triazoline formation in a microwave was unprecedented, conditions similar to those used in triazole synthesis were initially tested. First, various solvents were tested such as DMF, benzene, dioxane,

cyclohexane, 1,2-dimethoxyethane and 1,2-dichloroethane. Based on the operating system of the microwave, the temperature was set near the boiling point to prevent the automatic shut down of the microwave. Various high temperatures were also tested with DMF as the solvent; however, DMF gave only starting material and unidentified decomposed product. The other five solvents gave only ~5% conversions by ¹H NMR (Table 15).

Table 15. Microwave-Assisted [3+2] Cycloaddition: The Effect of Solvent



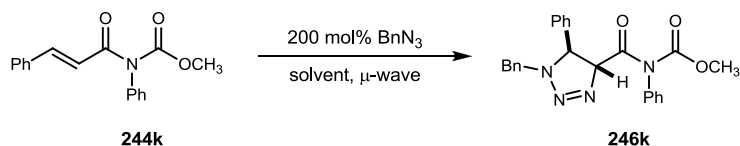
entry ^a	solvent	microwave conditions		
		time (hr)	temp (°C)	conversion(%) ^b
1	DMF	1	150	SM only
2	DMF	1	140	SM only
3	DMF	1	130	SM only
4	DMF	1	120	SM only
5	benzene	4	70	<5
6	dioxane	4	90	<5
7	C ₆ H ₁₂	4	70	<5
8	CH ₃ OCH ₂ CH ₂ OCH ₃	4	70	<5
9	ClCH ₂ CH ₂ Cl	4	70	<5

^aGeneral procedure: BnN₃ (1.5 equiv.) and olefin (1.0 equiv.) in solvent (0.2 M) were heated with microwave at various temperatures. ^bMeasured by ¹H NMR analysis of the crude reaction mixture.

Based on these experiments, instead of using polar solvents such as DMF, we assumed that nonpolar solvents such as toluene or xylene could give the desired pathway to triazolone formation. The following experiment was tested with toluene and xylene as solvents and various temperatures and reaction times (Table 16). First, using toluene, mild reaction conditions were tested near the boiling point of the solvent. Six hours at low temperature gave only ~5% conversion (Table 16, entry1-3); however, allowing the

reaction to go for 12 hours gave 13% conversion by NMR (Table 16, entry 4). Finally, after 60 hours the reaction showed 60% conversion of imide to triazoline (Table 16, entry 5). Xylene was also effective in terms of increasing the temperature to facilitate conversion and decreasing reaction time (Table 16, entry 6-8).

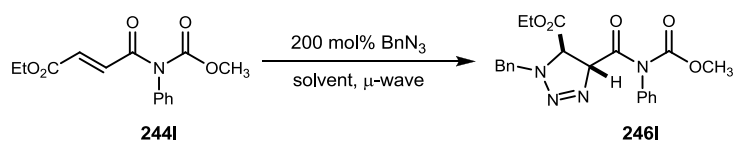
Table 16. Microwave-Assisted [3+2] Cycloaddition: The Effect of Solvent



entry ^a	solvent	microwave conditions		
		time (hr)	temp (°C)	conversion(%) ^b
1	toluene	2	100	5
2	toluene	4	100	5
3	toluene	6	90	5
4	toluene	12	90	13
5	toluene	60	90	60
6	xylene	4	140	36
7	xylene	4	130	40
8	xylene	12	130	50

^aGeneral procedure: BnN₃ (1.5 equiv.) and olefin (1.0 equiv.) in solvent (0.2 M) were heated with microwave at various temperatures. ^bMeasured by ¹H NMR analysis of the crude reaction mixture.

Based on this observation, different *N*-Ph carbamates were tested under similar conditions. However, in contrast to the β-Ph carbamate case, β-ester **244l** showed no reaction under the same conditions (Table 17, entry 1). Several different temperature variations were tested to find improved conversion of this imide (Table 17.). The best conversion was observed at 100 °C after 4 hours (entry 3). However, longer reaction time or higher temperature gave only decomposition with no triazoline. Under these same conditions, trifluorotoluene also gave a similar result to xylene.

Table 17. Microwave-Assisted [3+2] Cycloaddition: The Effect of Reaction Time and Temperature

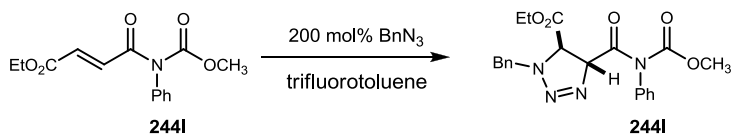
entry ^a	microwave conditions		
	time (hr)	temp (°C)	conversion(%) ^b
1	4	130	0
2	8	120	<5
3	4	100	70
4	6	100	decomposed

^aGeneral procedure: BnN₃ (1.5 equiv.) and olefin (1.0 equiv.) in solvent (0.2 M) were heated with microwave at various temperatures.

^bMeasured by ¹H NMR analysis of the crude reaction mixture.

Despite obtaining optimal results in xylene, microwave synthesis typically employs solvents that contain a strong dipole in order to better absorb the microwave. In an attempt to better optimize this microwave absorption, further investigation into this reaction was performed with trifluorotoluene.

Various reaction conditions and reaction scales were tested with trifluorotoluene (Table 18). Depending on the reaction scale and concentration, different results were obtained. For example, at the same temperature, longer reaction times always gave decomposed byproduct exclusively. However, shorter reaction times with various reaction scales showed around 70% conversion at best. Different substrates, such as β -furanyl and thiophenyl also showed similar results such as incomplete and inconsistent conversion.

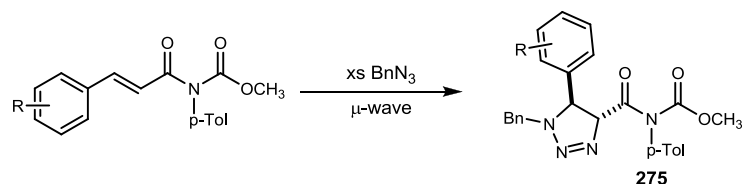
Table 18. Microwave-Assisted [3+2] Cycloaddition: The Effect of Reaction Time and Concentration

Entry ^a	Microwave conditions		concentration (M)	conversion(%) ^b
	time (hr)	temp (°C)		
1	12	100	0.1	decomposed
2	12	100	0.1	decomposed
3	2	100	0.1	75
4	4	100	0.25	decomposed
5	4	100	0.5	60
6	4	100	0.5	65
7	4	100	0.05	52
8	2	100	0.1	60
9	3	100	0.1	60
10	4	100	0.1	62

^aGeneral procedure: BnN₃ (1.5 equiv.) and olefin (1.0 equiv.) in solvent (0.2 M) were heated with microwave at various temperatures. ^bMeasured by ¹H NMR analysis of the crude reaction mixture.

Finally, similar to the thermal conversion, benzyl azide was used as solvent. Under these neat conditions, β -aromatic acceptors showed better conversion and reactivity compared with other solvents. Although the issue of incomplete conversion was not resolved, various β -aryl carbamates also converted the corresponding triazolines (Table 19). Dependent on the substrates, conversion and isolated yield varied. Under the standard reaction conditions, in general, around 80% conversions to triazoline were observed by ¹H NMR. In general, electron donating groups in the acceptors such as **275a**, **275b**, **275h**, and **275i** gave good conversion and relatively high yields. However, in the case of electron withdrawing group acceptors, low to moderate yield were generally observed (Table 19, entry 2-6, 10-11).

Table 19. Microwave-Assisted [3+2] Cycloaddition: β -Aryl Substituted Imides



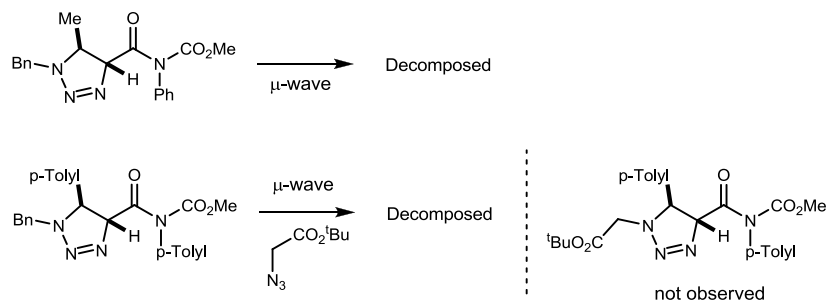
entry ^a	R	%yield ^b	
1	4-CH ₃ -C ₆ H ₄	275a	81 %
2	4-CH ₃ O-C ₆ H ₄	275b	82 %
3	4-F-C ₆ H ₄	275c	42 %
4	4-Cl-C ₆ H ₄	275d	48 %
5	4-Ph-C ₆ H ₄	275e	36 %
6	4-CF ₃ -C ₆ H ₄	275f	43 %
7	4-NO ₂ -C ₆ H ₄	275g	82 %
8	2-CH ₃ -C ₆ H ₄	275h	67 %
9	2-CH ₃ O-C ₆ H ₄	275i	54 %
10	2-CF ₃ -C ₆ H ₄	275j	57 %
11	2-Cl-C ₆ H ₄	275k	46 %
12	C ₇ H ₆ O ₂	275l	45 %
13	3,4,5-CH ₃ O-C ₆ H ₂	275m	35 %

^aAll reactions were run with 0.2 mmol of imide and 10 eq of benzyl azide at 120 - 150 °C for 5 - 10 min.

^bIsolated yield after chromatography.

Due to this incomplete conversion with different substrates, the isolated triazoline was re-subjected to the reaction conditions to identify the stability of the triazoline to the reaction conditions. After 4 hours, the crude NMR showed no triazoline starting material and complete decomposition to an unknown product. During this reaction course, some point after formation of triazoline, formation and decomposition of triazoline occurred simultaneously due to the nature of triazoline. Additionally, the possibility of a reversible

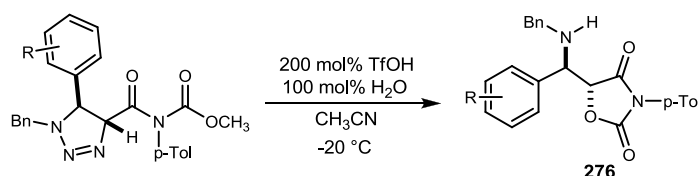
Scheme 48.



reaction pathway was not supported by scrambling experiments (Scheme 48).

However, using these triazolines, the acid-promoted conversions of triazoline to aminohydroxylation were investigated (Table 20). These transformations were generally efficient, leading to good yields of oxazolidine dione in all cases except entry 12 and entry 13.

Table 20. Acid Promoted Triazoline Fragmentation: β -Aryl Substituted Triazolines



entry	R		%yield
1	4-CH ₃ -C ₆ H ₄	276a	62 %
2	4-CH ₃ O-C ₆ H ₄	276b	95 %
3	4-F-C ₆ H ₄	276c	56 %
4	4-Cl-C ₆ H ₄	276d	72 %
5	4-Ph-C ₆ H ₄	276e	60 %
6	4-CF ₃ -C ₆ H ₄	276f	70 %
7	4-NO ₂ -C ₆ H ₄	276g	64 %
8	2-CH ₃ -C ₆ H ₄	276h	50 %
9	2-CH ₃ O-C ₆ H ₄	276i	57 %
10	2-CF ₃ -C ₆ H ₄	276j	86 %
11	2-Cl-C ₆ H ₄	276k	81 %
12	C ₇ H ₆ O ₂	276l	47 %
13	3,4,5-CH ₃ O-C ₆ H ₂	276m	37 %

^aAll reactions were run with 0.2 mmol of imide and 10 eq of benzyl azide at 120 -150 °C for 5 - 10 min.

^bIsolated yield after chromatography.

1.6. Conclusion

In conclusion, a diastereoselective synthesis of α -hydroxy- β -amino acid derivatives was achieved using Brønsted acid promoted azide-olefin [3+2] cycloaddition and triazoline fragmentation using thermal and water catalyzed protocols. Additionally, microwave assisted [3+2] cycloaddition was utilized to promote unreactive β -aryl imide and α -alkyl imide to the corresponding triazolines.

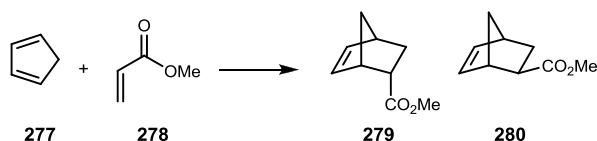
Chapter 2.

Secondary Catalysis by Water (Hydronium Triflate)

2.1. Organic Reactions in Water

Water is the most abundant molecule on earth and a universal reaction medium in enzyme active sites, where water can play a key role during catalyst.⁶³ However, water is not generally considered as a solvent for organic reactions because most organic molecules are insoluble in aqueous medium. In the 1980s, water was reconsidered by Breslow and Grieco as a solvent for organic reactions because of its positive effects on selectivity and rate enhancement.⁶⁴

Table 21. Kinetics and Selectivity of Diels-Alder Reaction



condition	rate constant	endo 279 /exo 280
isooctane	5.94	3.85
MeOH	75.5	8.5
H ₂ O with cyclodextrin	10900	22.5

Breslow reported dramatic rate acceleration in the aqueous reaction of cyclopentadiene **277** with methyl vinyl ketone **278** (Table 21) when compared to

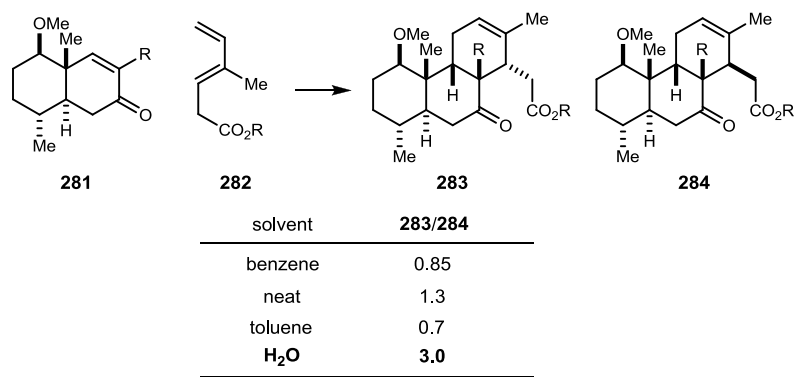
⁶³ Poulos, T. L. Peroxidases and Cytochrome P450. In *The Porphyrin Handbook*; Kadish, K. M.; Smith, K. M.; Guillard, R., Eds.; 2000; Vol. 4, Chapter 32, pp 189-218. Dunford, H. B., *Heme Peroxidases*; Wiley-VCH: New York, 1999. Gajhede, M., In *The Handbook of Metalloproteins*; Messerschmidt, A., Huber, R., Poulos, T., Wieghardt, K., Eds.; Wiley: New York, 2001; Vol. 1, pp 195-210.

⁶⁴ Rideout, D. C.; Breslow, R. *J. Am. Chem. Soc.* **1980**, *102*, 7816. Grieco, P. A.; Garner, P.; He, Z.-m. *Tetrahedron. Lett.* **1983**, *24*, 1897.

nonpolar solvents. This rate acceleration was explained by hydrophobic packing of the reactants in the presence of water.

Another seminal example of the effect of water was reported by Grieco in 1983 (Table 22). Grieco found that when the Diels-Alder reaction was performed in water, a higher reaction rate and selectivity were observed, compared to hydrocarbon solvents such as benzene and toluene. The observed rate acceleration was described by the relative orientation of the reactants in a micelle which lowered the entropy requirement for this bimolecular reaction.

Table 22. Enhanced Selectivity of Diels-Alder Reaction in Water



Since these seminal reports, significant progress has been made using water or aqueous media for many organic reactions.⁶⁵ Various organic reactions and transformations accelerated by water in stoichiometric and substoichiometric amounts will be discussed in this chapter.

⁶⁵ Lindstrom, U. M. *Chem. Rev.* **2002**, *102*, 2751. Lubineau, A.; Auge, J., *Top. Curr. Chem.*, **1999**, *206*, 1. Sinou, D., *Top. Curr. Chem.*, **1999**, *206*, 41. Li, C. J.; Chan, T. H., *Tetrahedron*, **1999**, *55*, 611. Fringuelli, F.; Piermatti, O.; Pizzo, F., *Heterocycles*, **1999**, *50*, 611. Engberts, J. B. F. N.; Feringa, B. L.; Keller, E., Otto, S., *Recl. Trav. Chim. Pays-Bas*, **1996**, *15*, 457. Lubineau, A.; Auge, J.; Queneau, Y., *Synthesis*, **1994**, 741. Li, C. J., *Chem. Rev.*, **1993**, *93*, 2023.

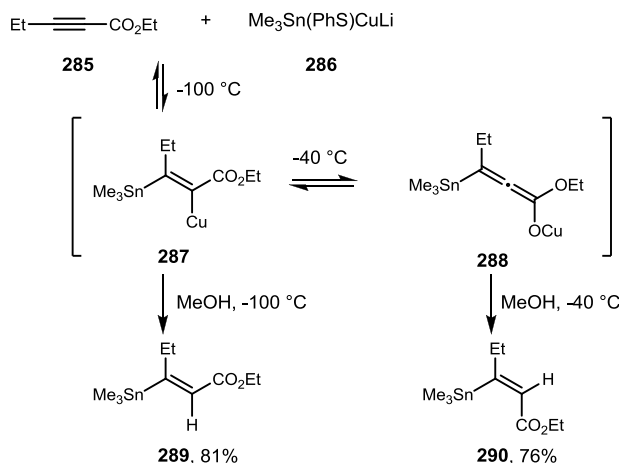
2.2. Water-Accelerated Organic Transformations

Water can exhibit special properties such as rate acceleration and enhancement of selectivity as a solvent in organic reactions. Additionally, stoichiometric or substoichiometric quantities of water resulting in the same effect have been reported in the literature.⁶⁶ The role of water in this type of organic transformation is categorized into three distinct classes based on activation mode: 1) water used as an internal quenching agent to drive chemical equilibria, 2) water as a hydrolyzing agent leading to a secondary catalyst, and 3) water serving as a Lewis-acid activator or Brønsted acid-base cooperative activator.

2.2.1. Internal Quenching Agent

In 1980, Piers and coworkers described the first example of an addition of a proton source such as MeOH and EtOH for stannylcupration of α,β -acetylenic esters (Figure 11).⁶⁷ At low temperature, kinetic intermediate **287** is reasonably stable and isomerizes

Figure 11. Stereoselective Conjugate Addition of Cuprate to α,β -Acetylenic Esters



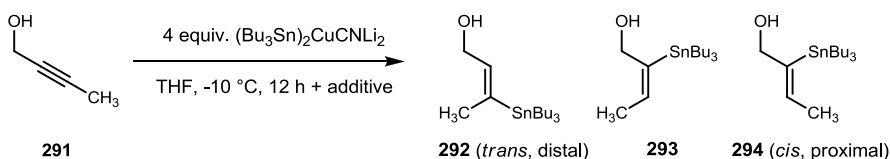
⁶⁶ Ribe, S.; Wipf, P. *Chem. Commun.* **2001**, 299. Pan, C. F.; Wang, Z. Y. *Coord. Chem. Rev.* **2008**, 252, 736.

⁶⁷ Piers, E.; Morton, H. E. *J. Org. Chem.* **1980**, 45, 4263. Piers, E.; Chong, J. M.; Morton, H. E. *Tetrahedron. Lett.* **1981**, 22, 4905. Piers, E.; Chong, J. M.; Keay, B. A. *Tetrahedron. Lett.* **1985**, 26, 6265. Piers, E.; Chong, J. M.; Morton, H. E. *Tetrahedron* **1989**, 45, 363. Piers, E.; Wong, T.; Ellis, K. A. *Can. J. Chem.* **1992**, 70, 2058.

very slowly, producing mostly (*E*)-isomer **289**. However, at higher temperature, isomerization of **287** to **288** can occur, and produces (*Z*)-isomer **290**. This isomerization can be minimized by the presence of a proton source such as MeOH or water.

Stereoselective stannylation of alkynes was also demonstrated by this author and others by using MeOH addition (Table 23).⁶⁸ Both of these studies clearly demonstrated stereoselectivity, by trapping of the kinetic intermediate prior to isomerization, to the (*E*)-derivatives.

Table 23. Stereoselective Conjugate Addition of Stannylcuprate to Acetylenes

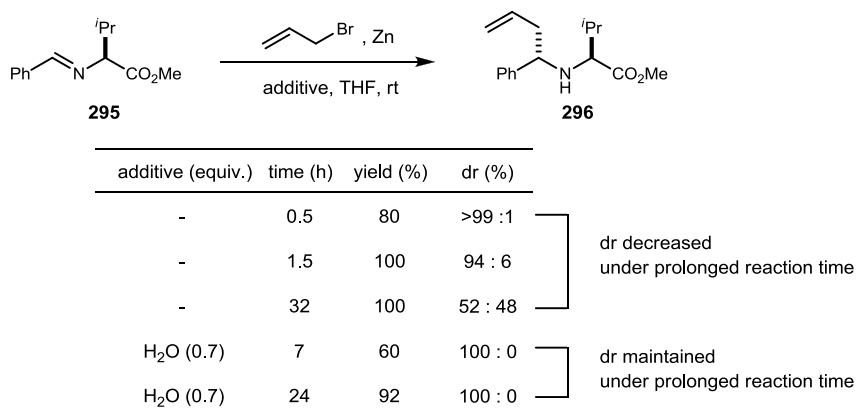


additive (equiv.)	yield (%)	292 (%)	293 (%)	294 (%)
none	82	30	0	70
MeOH (110)	70	100	0	0
H ₂ O (10)	97	85	15	0

A proton source can also increase the diastereoselectivity of Barbier type additions of allylzinc to imines (Table 24).⁶⁹ Under anhydrous conditions, diastereoselectivity decreases over extended reaction times due to the reversible nature of the addition step. However, in the presence of a proton source, this equilibrium can be avoided by protonation of the zinc salt intermediate.

⁶⁸ Betzer, J.-F.; Delalogue, F.; Muller, B.; Pancrazi, A.; Prunet, J. *J. Org. Chem.* **1997**, *62*, 7768. Betzer, J.-F.; Pancrazi, A. *Synlett* **1998**, 1998, 1129. Betzer, J.-F. o.; Pancrazi, A. *Synthesis* **1999**, 629. Barbero, A.; Pulido, F. *J. Chem. Soc. Rev.* **2005**, *34*, 913.

⁶⁹ Basile, T.; Bocoum, A.; Savoia, D.; Umani-Ronchi, A. *J. Org. Chem.* **2002**, *59*, 7766.

Table 24. Diastereoselective Allylzinc Additions to Imines

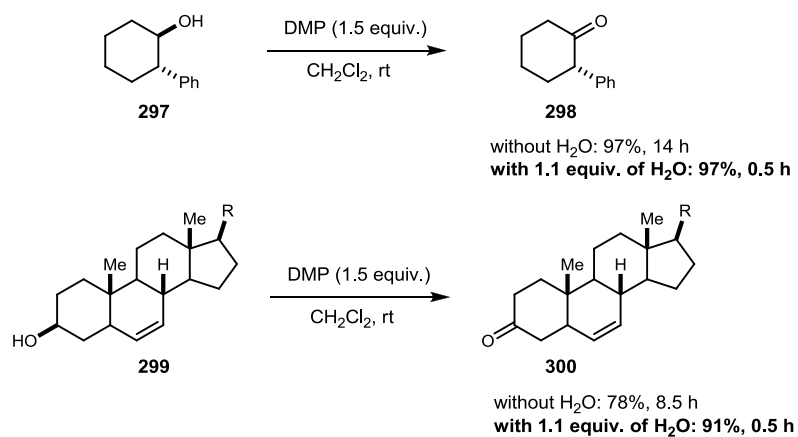
2.2.2. Hydrolyzing Agent Leading to Secondary Catalyst

More recently, a dramatic rate effect of water addition on the Dess-Martin Periodinane oxidation was reported.⁷⁰ After a serendipitous discovery of ‘aged’ DMP reagent, it was observed that addition of 1 equivalent of water to the reaction accelerated the oxidation dramatically (Figure 12). As an analogue of water addition, Schreiber and Meyer demonstrated the rate acceleration effect by replacing an acetoxy group of DMP reagent with hydroxide through the addition of one equivalent of water.⁷¹

⁷⁰ Romo, D.; Meyer, S. D.; Johnson, D. D.; Schreiber, S. L. *J. Am. Chem. Soc.* **1993**, *115*, 7906.

⁷¹ Meyer, S. D.; Schreiber, S. L. *J. Org. Chem.* **1994**, *59*, 7549.

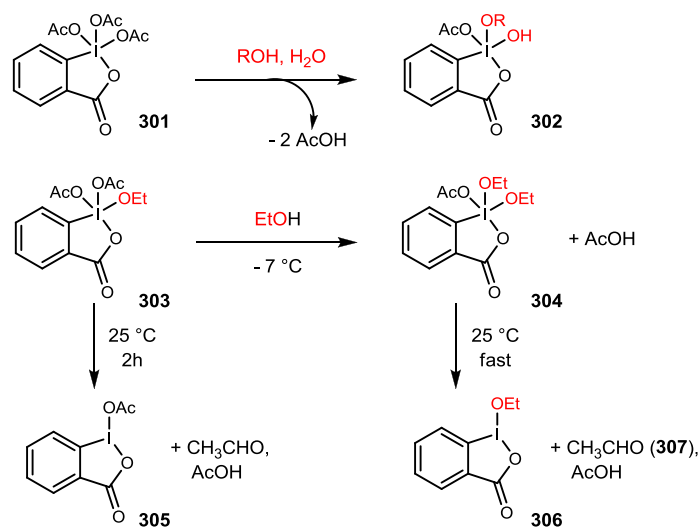
Figure 12. Rate Acceleration Effect in DMP Oxidation



The inspiration of using water as an additive came from earlier work in which Dess and Martin observed a rate enhancement in the oxidation of ethanol by adding a second equivalent of ethanol (Figure 13).⁷² A proposed rationale for this rate acceleration was that the increased electron donating ability of an alkoxy substituent in place of an acetyl group can enhance the overall rate of dissociation of the remaining acetate ligand, leading to the production of **306** and corresponding aldehyde **307**.

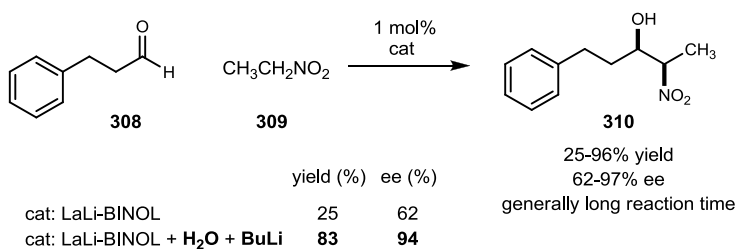
⁷² Dess, D. B.; Martin, J. C. *J. Org. Chem.* **1983**, *48*, 41, 4155. Dess, D. B.; Martin, J. C. *J. Am. Chem. Soc.* **1991**, *113*, 7277.

Figure 13. Rate Acceleration by Addition of Water



Similar types of rate acceleration and enhancement of catalyst reactivity by addition of water were reported by Shibasaki.⁷³ Through the combined use of LaLi-BINOL, BuLi, and 1 equivalent of water as the catalyst system, the asymmetric nitroaldol reaction was greatly accelerated (Figure 14.).

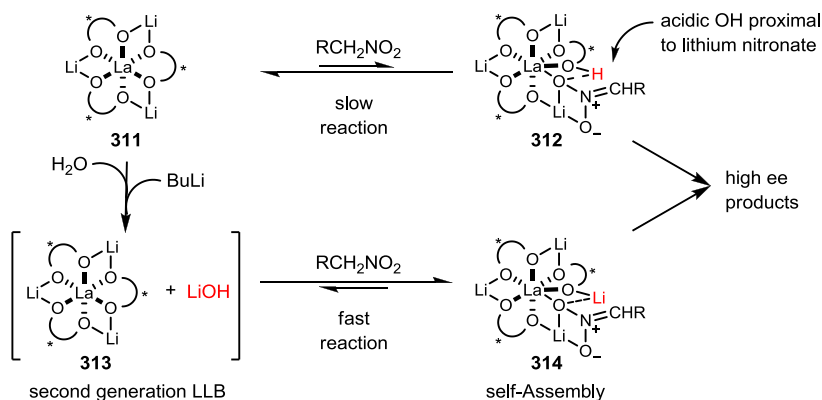
Figure 14. Enantioselective Nitroaldol Reaction



⁷³ Sasai, H.; Suzuki, T.; Arai, S.; Arai, T.; Shibasaki, M. *Ibid.* **1992**, *114*, 4418. Sasai, H.; Suzuki, T.; Itoh, N.; Arai, S.; Shibasaki, M. *Tetrahedron. Lett.* **1993**, *34*, 2657. Sasai, H.; Suzuki, T.; Itoh, N.; Shibasaki, M. *Tetrahedron. Lett.* **1993**, *34*, 851. Sasai, H.; Suzuki, T.; Itoh, N.; Tanaka, K.; Date, T.; Okamura, K.; Shibasaki, M. *J. Am. Chem. Soc.* **1993**, *115*, 10372. Sasai, H.; M.A. Yamada, Y.; Suzuki, T.; Shibasaki, M. *Tetrahedron* **1994**, *50*, 12313. Arai, T.; Yamada, Y. M. A.; Yamamoto, N.; Sasai, H.; Shibasaki, M. *Chem. Eur. J.* **1996**, *2*, 1368.

This proposed mechanism for the rate enhancement and improved catalytic activity for the asymmetric nitroaldol reaction catalyzed by heterobimetallic lanthanoid complexes is shown in Figure 15. In the initial step, the nitroalkane component is deprotonated and the resulting lithium nitronate coordinates to the lanthanoid complex **311**. However, a slow rate of catalyst turnover and overall reaction rate was observed due to the high degree of aggregation of LaLi-BINOL and lithium nitronate **312**. In contrast, with the addition of BuLi and H₂O, the lanthanoid catalyst reacted with carbonyl compounds much faster than intermediate **312**.

Figure 15. Proposed Mechanism of Rate Acceleration

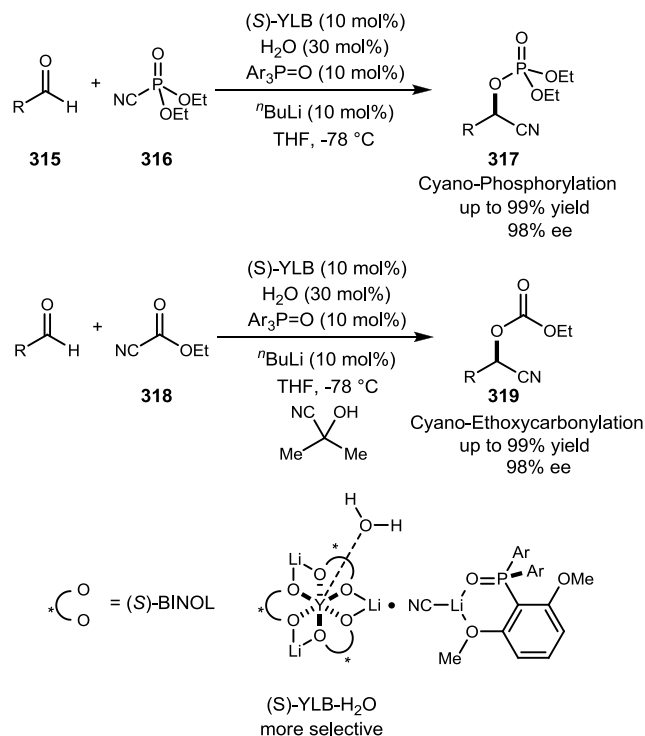


The same type of activation in cyanoethoxycarbonylation⁷⁴ and cyanophosphorylation⁷⁵ was also reported by Shibasaki (Scheme 49).

⁷⁴ Tian, J.; Yamagiwa, N.; Matsunaga, S.; Shibasaki, M. *Angew. Chem. Int. Ed.* **2002**, *41*, 3636. Tian, J.; Yamagiwa, N.; Matsunaga, S.; Shibasaki, M. *Org. Lett.* **2003**, *5*, 3021. Yamagiwa, N.; Tian, J.; Matsunaga, S.; Shibasaki, M. *J. Am. Chem. Soc.* **2005**, *127*, 3413.

⁷⁵ Abiko, Y.; Yamagiwa, N.; Sugita, M.; Tian, J.; Matsunaga, S.; Shibasaki, M. *Synlett* **2004**, 2434. Yamagiwa, N.; Abiko, Y.; Sugita, M.; Tian, J.; Matsunaga, S.; Shibasaki, M. *Tetrahedron: Asymmetry* **2006**, *17*, 566.

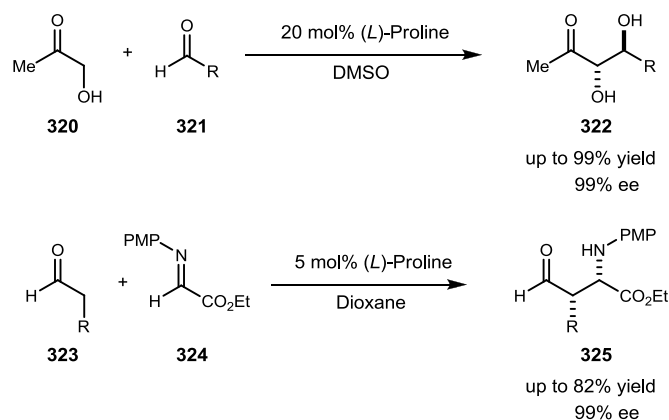
Scheme 49. Cyanoethoxycarbonylation and Cyanophosphorylation



Similar observations were also made with organocatalyst systems either on water or in water by various research groups. Barbas and coworkers reported a proline catalyzed aldol and Mannich type reaction in the presence of water (Scheme 50).⁷⁶ They mentioned that the reaction yield and both enantioselectivity and diastereoselectivity were improved with less than 4 vol% of water in DMSO.

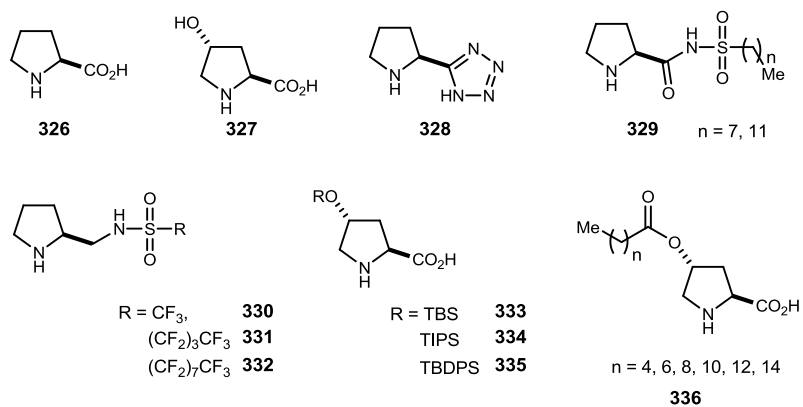
⁷⁶ Sakthivel, K.; Notz, W.; Bui, T.; Barbas, C. F. *J. Am. Chem. Soc.* **2001**, *123*, 5260. Notz, W.; Tanaka, F.; Watanabe, S.-i.; Chowdari, N. S.; Turner, J. M.; Thayumanavan, R.; Barbas, C. F. *J. Org. Chem.* **2003**, *68*, 9624.

Scheme 50. Proline Catalyzed Aldol and Mannich Reaction



Afterwards, many other modifications of the catalysts were reported, for which water is a beneficial additive or co-solvent and can lead to higher yield, rate, and selectivity. Hayashi and Yamamoto independently reported proline-surfactant organocatalysts for aqueous direct cross-aldol reaction of aldehyde and direct aldol reaction (Figure 16).⁷⁷

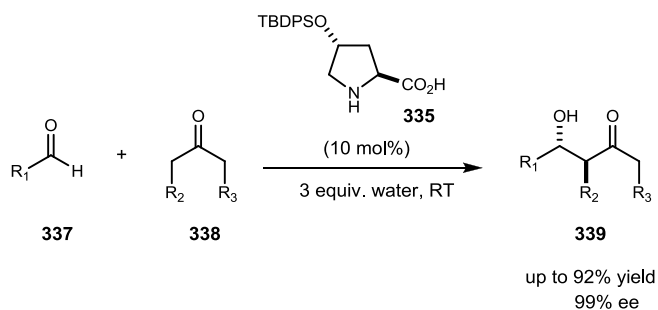
Figure 16. Proline Based Catalyst



⁷⁷ Yujiro, H. *Angew. Chem. Int. Ed.* **2006**, *45*, 8103. Yujiro, H.; Seiji, A.; Tsubasa, O.; Junichi, T.; Tatsunobu, S.; Mitsuru, S. *Angew. Chem. Int. Ed.* **2006**, *45*, 5527. Hayashi, Y.; Aratake, S.; Itoh, T.; Okano, T.; Sumiya, T.; Shoji, M. *Chem. Commun.* **2007**, 957. Aratake, S.; Itoh, T.; Okano, T.; Usui, T.; Shoji, M.; Hayashi, Y. *Chem. Commun.* **2007**, 2524. Seiji, A.; Takahiko, I.; Tsubasa, O.; Norio, N.; Tatsunobu, S.; Mitsuru, S.; Yujiro, H. *Chem. Eur. J.* **2007**, *13*, 10246. Hiromi, T.; Masakazu, N.; Kazuaki, I.; Susumu, S.; Hisashi, Y. *Angew. Chem. Int. Ed.* **2004**, *43*, 1983.

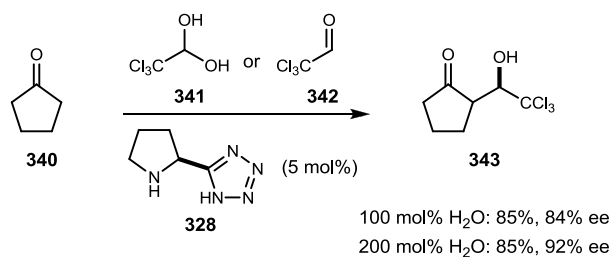
Hayashi and coworkers examined various types of proline based catalyst and found that sulfonamides **329** and siloxyprolines **333-335** gave high yields and selectivities (Scheme 51). The effect of water was verified using a different amount of water. The yield and selectivity was improved by addition of water.

Scheme 51. Siloxyproline Catalyzed Direct Aldol Reaction



Yamamoto also reported that the addition of 1 equivalent of water using tetrazole attached proline type of catalyst, enhanced reaction rate and enantioselectivity (Scheme 52). However, a catalytic amount of water failed to show the acceleration effect, and the exact role of water in this reaction remains unclear.

Scheme 52. Tetrazoleproline Catalyzed Direct Aldol Reaction

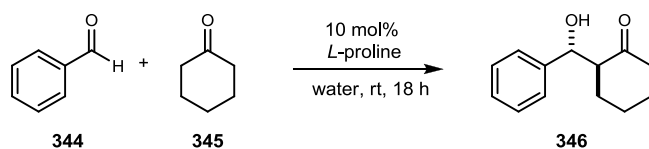


In 2006, a systematic study of the effect of water as an additive on the proline catalyzed aldol reaction was demonstrated by Pihko.⁷⁸ The reaction showed rate

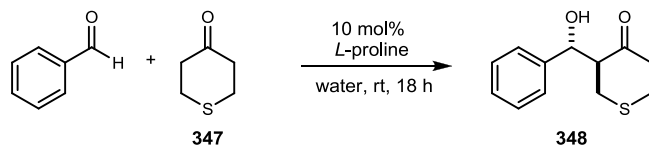
⁷⁸ Pihko, P. M.; Laurikainen, K. M.; Usano, A.; Nyberg, A. I.; Kaavi, J. A. *Tetrahedron* **2006**, *62*, 317.

acceleration and increased enantioselectivity depending on the amount of water. They found that water can play at least two important roles in the proline catalyzed aldol reaction: 1) water might help to increase the solubility of the reaction mixture, and 2) water might assist in the hydrolysis of intermediate oxazolidinone to facilitate catalytic cycles.

Table 25. Effect of Water on the Proline Catalyzed Aldol Reaction



water (mol%)	yield	ee
0	61	89
100	87	97
200	84	97
10000	84	>99



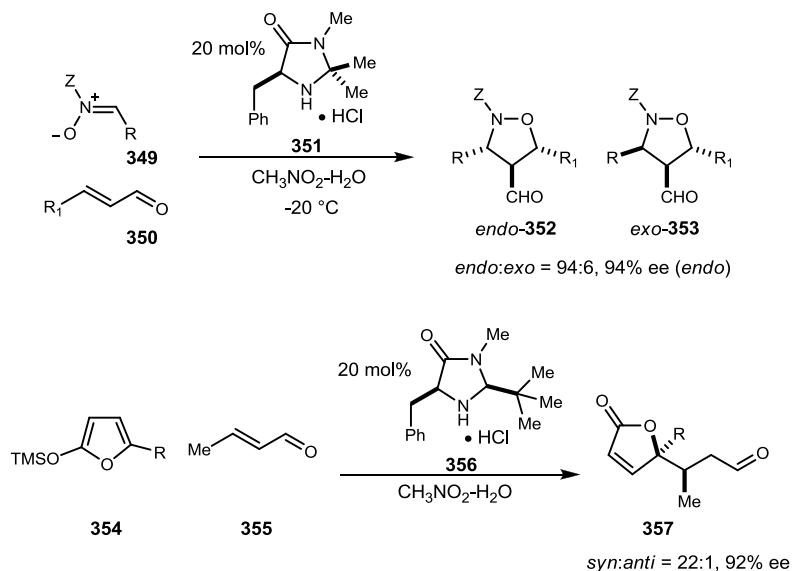
water (mol%)	Conv	ee
0	3	65
100	22	86
200	37	93
500	60	98

MacMillan and coworkers also achieved a highly enantioselective organocatalytic 1,3-dipolar cycloaddition reaction and a Mukaiyama-Michael reaction in the presence of water.⁷⁹ The water played an important role in the regeneration of catalyst by hydrolyzing the iminium ion to improve the turnover of imidazolidinone catalyst **351** and **356**, thereby

⁷⁹ Ahrendt, K. A.; Borths, C. J.; MacMillan, D. W. C. *J. Am. Chem. Soc.* **2000**, *122*, 4243. Jen, W. S.; Wiener, J. J. M.; MacMillan, D. W. C. *J. Am. Chem. Soc.* **2000**, *122*, 9874. Brown, S. P.; Goodwin, N. C.; MacMillan, D. W. C. *J. Am. Chem. Soc.* **2003**, *125*, 1192.

increasing yield and enantioselectivity.

Scheme 53. 1,3-Dipolar Cycloaddition Reaction and a Mukaiyama-Michael Reaction



2.2.3. Lewis Acid Activator, Brønsted Acid-Base Cooperative Activation

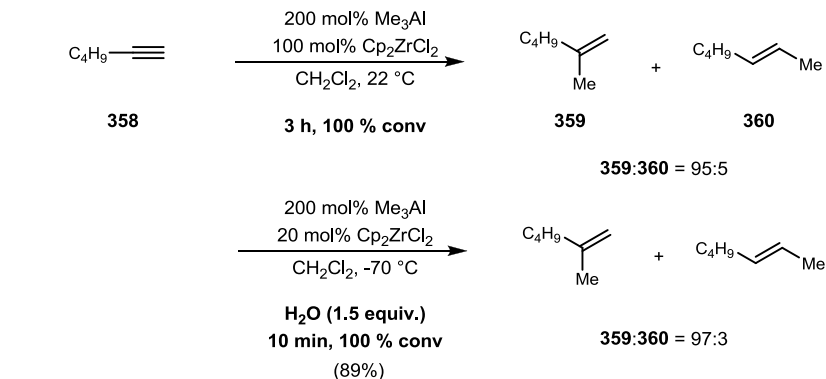
The first example of water acting as a Lewis acid activator is in Wipf's alkyne carboalumination reaction.⁸⁰ In the course of reaction optimization, they discovered that the addition of 1-2 equivalent of water led to significant rate acceleration. The reaction as previously reported exhibited low reactivity even at room temperature.⁸¹ In contrast, Wipf's protocol showed that even at -70 °C methylalumination of 1-hexyne **358** was completed in 10 minutes in the presence of 1 equivalent of water (Scheme 54). The rate enhancement of water was further evaluated to protic additives such as H_2S , alcohols, silanols. All other additives such as H_2S , alcohols, silanols failed to reproduce the effect

⁸⁰ Peter, W.; Sungtaek, L. *Angew. Chem., Int. Ed.* **1993**, 32, 1068.

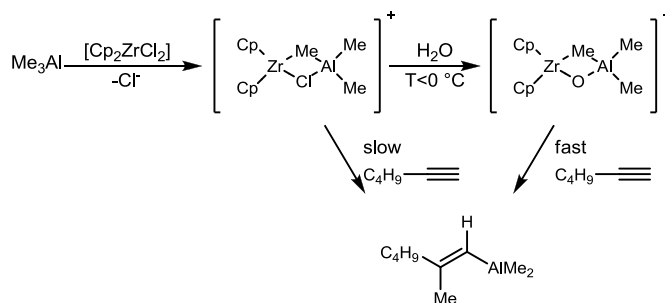
⁸¹ Kondakov, D. Y.; Negishi, E.-i. *J. Am. Chem. Soc.* **2002**, 117, 10771. Kondakov, D. Y.; Negishi, E.-i. *J. Am. Chem. Soc.* **1996**, 118, 1577.

of water.

Scheme 54.



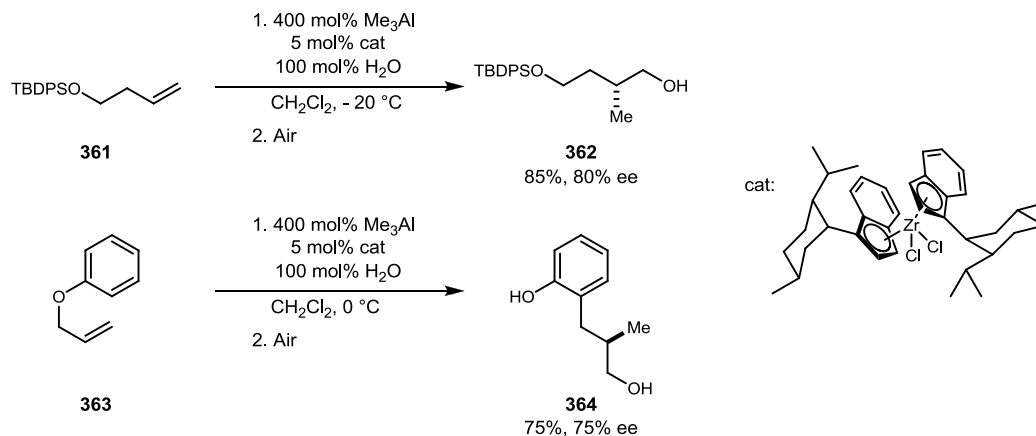
via



Similar examples of this type of effect were also observed in the asymmetric olefin methylalumination of olefin and tandem Claisen rearrangement-carboalumination reaction.⁸² As with the carboalumination reaction with alkynes, water showed the same acceleration effect with olefin methylalumination. Although the level of enantioselectivity was moderate, the accelerating effect of water was not interfering with chirality transfer by Erker's zirconocene catalyst. Additionally, allyl aryl ether **363** underwent Claisen rearrangement-methylalumination sequence in the presence of water and aluminoxane.

⁸² Wipf, P.; Ribe, S. *Org. Lett.* **2000**, 2, 1713. Wipf, P.; Ribe, S. *Org. Lett.* **2001**, 3, 1503. Peter, W.; Sonia, R. *Adv. Synth. Catal.* **2002**, 344, 434.

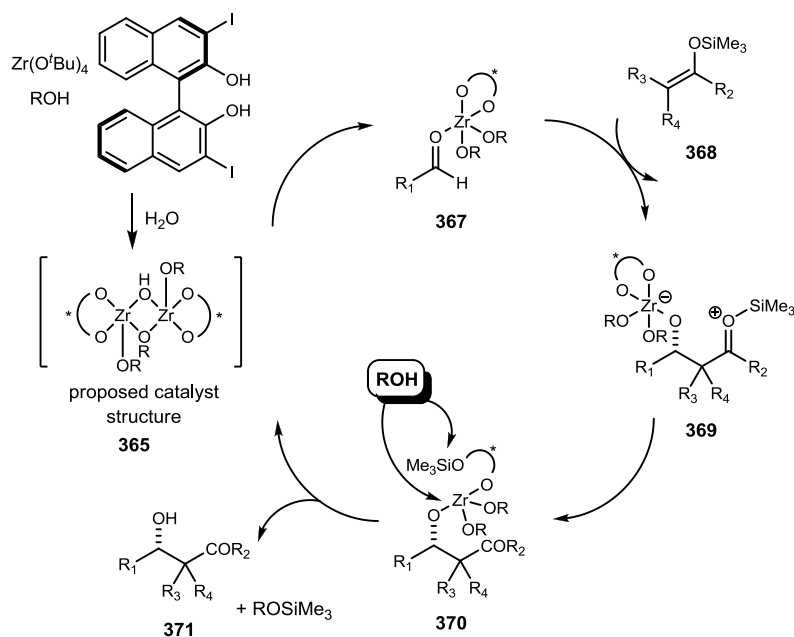
Scheme 55.



In the area of Lewis acid catalyzed organic reactions, water can also play an important role in reactivity and selectivity. Kobayashi and coworkers have reported a chiral zirconium catalyzed *anti*-aldol reaction using water in the preparation of the active catalyst.⁸³ Addition of a catalytic amount of a protic solvent such as alcohol and water can accelerate the formation of active catalyst **365** and promote regeneration of the catalyst. Addition of 5-20 mol% water improved the yield and enantioselectivity, but over 40 mol% water inhibited the reaction. It was assumed that the role of water was to generate the active catalyst structure.

⁸³ Ishitani, H.; Yamashita, Y.; Shimizu, H.; Kobayashi, S. *J. Am. Chem. Soc.* **2000**, *122*, 5403. Yamashita, Y.; Ishitani, H.; Shimizu, H.; Kobayashi, S. *J. Am. Chem. Soc.* **2002**, *124*, 3292.

Figure 17. Proposed Mechanism of Zirconium Catalyzed *anti*-Aldol Reaction



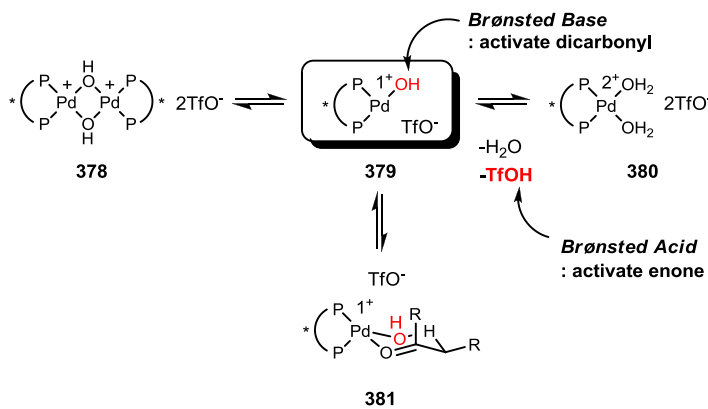
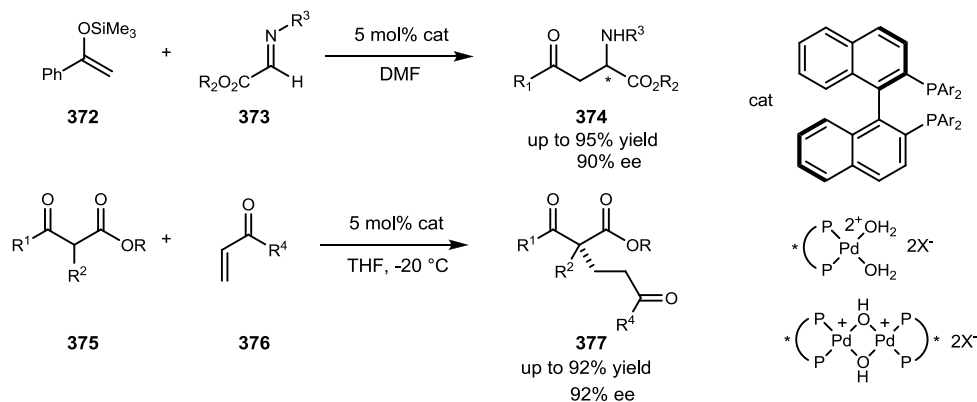
Shibasaki reported the first example of a catalytic asymmetric aldol reaction that occurred via a Pd(II) enolate which was modified by water.⁸⁴ They found that the cationic active catalyst was generated from Pd-BINAP and AgOTf in wet DMF. Various control experiments proved that water played an important role in this reaction. Sodeoka also demonstrated highly enantioselective catalytic Mannich and Michael type reactions using chiral Pd-hydroxo complex **378** (Scheme 56).⁸⁵ When substrates reacted with the catalyst, which acted as a Brønsted base, to form a chiral Pd enolate complex, the formation of a strong Brønsted acid (TfOH) could effectively activate electrophilic imines and enols to

⁸⁴ Sodeoka, M.; Ohrai, K.; Shibasaki, M. *J. Org. Chem.* **2002**, *60*, 2648. Sodeoka, M.; Tokunoh, R.; Miyazaki, F.; Hagiwara, E.; Shibasaki, M. *Synlett* **1997**, 1997, 463.

⁸⁵ Hagiwara, E.; Fujii, A.; Sodeoka, M. *J. Am. Chem. Soc.* **1998**, *120*, 2474. Fujii, A.; Hagiwara, E.; Sodeoka, M. *J. Am. Chem. Soc.* **1999**, *121*, 5450. Hamashima, Y.; Hotta, D.; Sodeoka, M. *J. Am. Chem. Soc.* **2002**, *124*, 11240. Tsuchiya, Y.; Hamashima, Y.; Sodeoka, M. *Org. Lett.* **2006**, *8*, 4851. Dubs, C.; Hamashima, Y.; Sasamoto, N.; Seidel, T. M.; Suzuki, S.; Hashizume, D.; Sodeoka, M. *J. Org. Chem.* **2008**, *73*, 5859. Hamashima, Y.; Yagi, K.; Takano, H.; Tamas, L.; Sodeoka, M. *J. Am. Chem. Soc.* **2002**, *124*, 14530.

achieve the desired C-C bonding reactions.

Scheme 56.



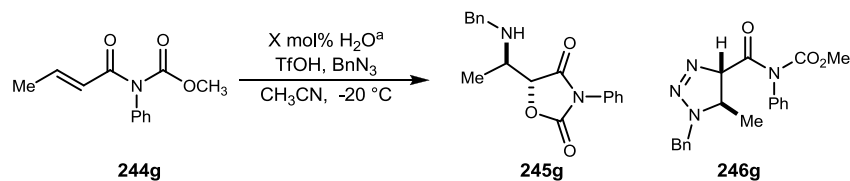
2.2. Fragmentation of Triazoline by Brønsted Acid: Secondary Catalysis by Water (Hydronium Triflate)

Our initial studies of olefin aziridination and anti-aminohydroxylation using triflic acid were performed with commercial triflic acid and handling that followed standard laboratory protocols (section 5.1.1).⁸⁶ Additionally, these reactions were initiated at -20 °C, but then allowed to warm slowly to room temperature at the reaction's end prior to quench and purification. After some scrutinization of the reaction variables, a new reaction product was observed, isolated, and structurally characterized as triazoline **246g**.

The initial reaction performed with commercial triflic acid showed various level of reactivity with selectivity depending on the substrates. Due to this fact, we hypothesized that the small amount of water content in the triflic acid might control overall reactivity and selectivity. This behavior suggested that adventitious water promoted the formation of **245a** and **245g**, and this hypothesis was confirmed by several experiments in which water was intentionally added to reactions (Table 26, Table 27). To prove this hypothesis, two different approaches were tested. First, water was added to the reaction directly. Second, pre-mixed water and triflic acid stock solution was added to the reaction (Table 26). Additionally, unsubstituted acryloyl imide **244a** was also tested with the contents of water in the reaction (Table 27). Due to the reactivity difference between substituted and unsubstituted imide, more reactive unsubstituted imide was chosen for further experimentation.

⁸⁶ Mahoney, J. M.; Smith, C. R.; Johnston, J. N. *J. Am. Chem. Soc.* **2005**, *127*, 1354.

Table 26. Effect of Added Water on the Product Distribution of Triflic Acid Promoted Azide-Olefin Additions at Low Temperature – Substituted Imide



entry	X	245g:246g^b
<i>water added directly</i>		
1 ^c	0	95:5
2	0	5:95
3	10	33:67
4	100	78:22
5	200	95:5
<i>water premixed with TfOH</i>		
6	10	50:50
7	50	95:5
8	100	95:5
9	1000	- ^d

^aGeneral conditions: BnN₃ (1.5 equiv.) and the olefin (1 equiv) in CH₃CN (0.33 M) were treated with triflic acid at -20 °C. The triflic acid was first premixed with the indicated amount of water to create a stock solution. For additional procedural variations, resulting in similar observations, see the Supporting Information. ^bMeasured by ¹H NMR analysis of the crude reaction mixture after reaction quench (Et₃N, 2 equiv.) at the reaction temperature and removal of volatiles by high vacuum. ^cReaction mixture was warmed to room temperature prior to quench. ^dOnly hydrolysis of imide observed.

We first verified our earlier observation that warming of the reaction mixture, even with strictly anhydrous conditions, produces the oxazolidine dione selectively (Table 26, Table 27, entry 1) as measured by ¹H NMR of the crude reaction mixture after reaction quench by the addition of dry triethylamine. The protocol involving maintenance of the reaction and quench (triethylamine) at -20 °C, however, provided *solely* triazolone **246g**, **246a** when no water is added to the reaction, and again using anhydrous triflic acid (Table 26, Table 27, entry 2). Increasing amounts of added water provided a corresponding shift in the ratio toward oxazolidine dione **245g**, **245a** formation when reaction time was held constant (Table 26, Table 27, entries 3-5), and oxazolidine dione

245g, 245a eventually became the sole product. Addition of water beyond the 200 mol % level ultimately led to complete hydrolysis of **244g, 244a** without production of either triazoline or oxazolidine dione. This result highlighted the direct correlation between water and a three-way balance of the product distribution (triazoline, oxazolidine dione, and hydrolysis products).

This intermediate triazoline **246a** could be isolated as the sole product when the following constraints were carefully followed: (1) the triflic acid was dried and distilled (from Tf₂O) prior to use, (2) transfer of the triflic acid prevented absorption of ambient humidity, (3) the reaction temperature was carefully maintained at -20 °C or below, and (4) reaction quenching by anhydrous triethylamine was performed at -20 °C. Following the reaction quench, the exclusion of water was not as critical, but purification by flash chromatography (SiO₂) immediately followed, with the removal of volatiles *in vacuo* as the only intervening step. This procedure reproducibly furnished the analytically pure

Table 27. Effect of Added Water on the Product Distribution of Triflic Acid Promoted Azide-Olefin Additions at Low Temperature – Unsubstituted Imide

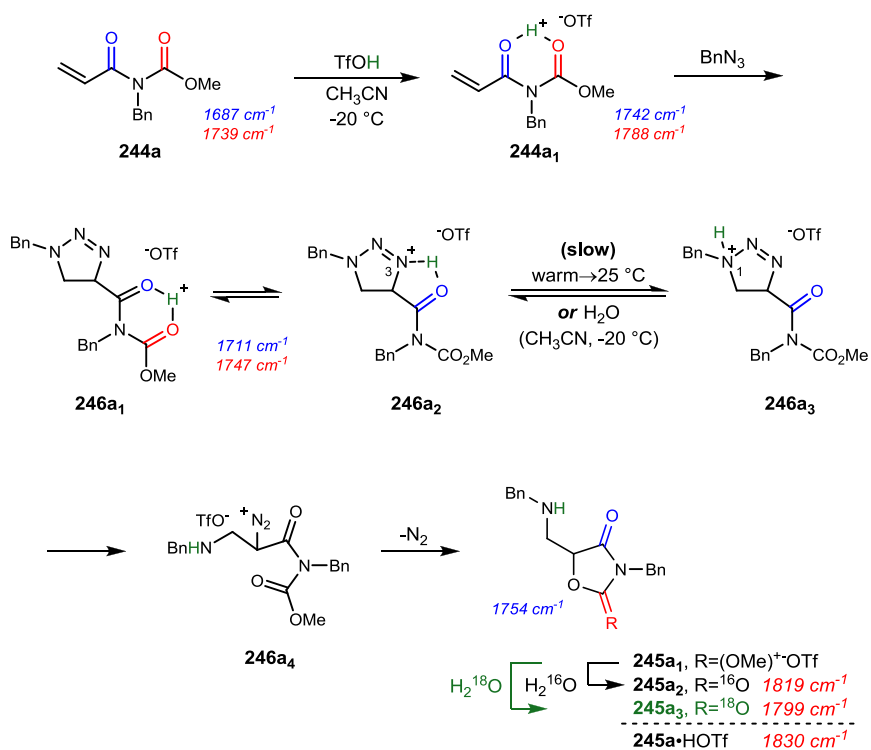
entry	X	245a:246a ^b
1 ^c	0	95:5
2	0	5:95
3	10	71:29
4	100	90:10
5	200	95:5

^aGeneral conditions: BnN₃ (1.5 equiv.) and the olefin (1 equiv.) in CH₃CN (0.33 M) were treated with triflic acid at -20 °C. The triflic acid was first premixed with the indicated amount of water to create a stock solution. For additional procedural variations, resulting in similar observations, see the Supporting Information. ^bMeasured by ¹H NMR analysis of the crude reaction mixture after reaction quench (Et₃N, 2 equiv.) at the reaction temperature and removal of volatiles by high vacuum. ^cReaction mixture was warmed to room temperature prior to quench.

triazoline **246a** in 54% yield.

To more accurately characterize the effect of water as an additive, the mechanistic proposal outlined in Scheme 57 was hypothesized on the basis of the behavior described to this point and in Table 27. We turned to *in situ* IR spectroscopy as a means to monitor the reaction course across a series of procedural changes; 1) our earlier observation that warming of the reaction mixture prior to quench lead to the formation of **245a**, and 2) maintaining the temperature at -20 °C and adding 1 equivalent of water led to the formation of **245a**.

Scheme 57. Mechanistic Picture of Triazoline Fragmentation

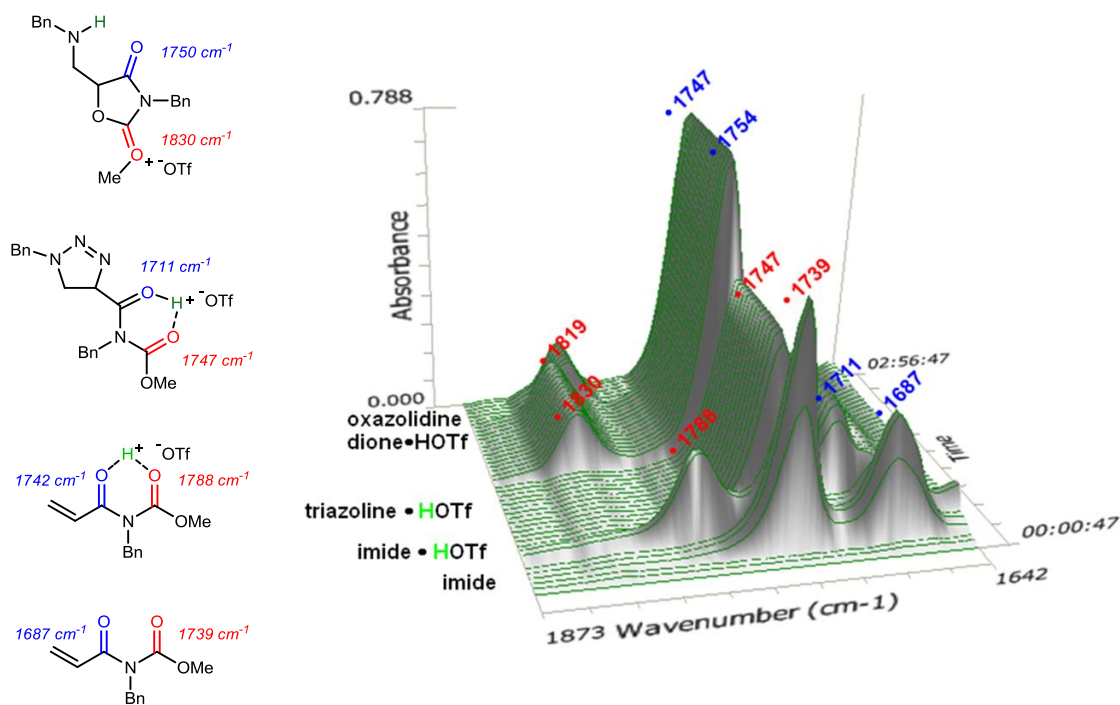


Several initial exploratory experiments were used to identify distinctive carbonyl peak observed by *in situ* IR spectroscopy, and these were assigned by correlation to the

carbonyl peaks observed for salt and free base forms of authentic samples. In the beginning, complexation of imide **244a₁** was evident from the shift of the carbamate carbonyl from 1739 to 1788 cm^{-1} upon addition of triflic acid to a cold ($-20\text{ }^{\circ}\text{C}$) acetonitrile solution of **244a**.

Once benzyl azide was added, immediate movement of this carbamate absorption to 1747 cm^{-1} was observed, and complete conversion was achieved within a matter of minutes. Assignment of this new species to triazolone salt **246a** is consistent with absorptions at 1711 cm^{-1} (amide C=O [proton bound]) and 1747 cm^{-1} (carbamate C=O [proton bound]). This absorption was matched with corresponding absorptions in free triazolone **246a**'s amide C=O 1704 and carbamate C=O 1740 cm^{-1} , respectively. Intermediate **246a-c** was indefinitely stable at $-20\text{ }^{\circ}\text{C}$ in solution, and triazolone **246a** was isolated when this reaction mixture was quenched with triethylamine.

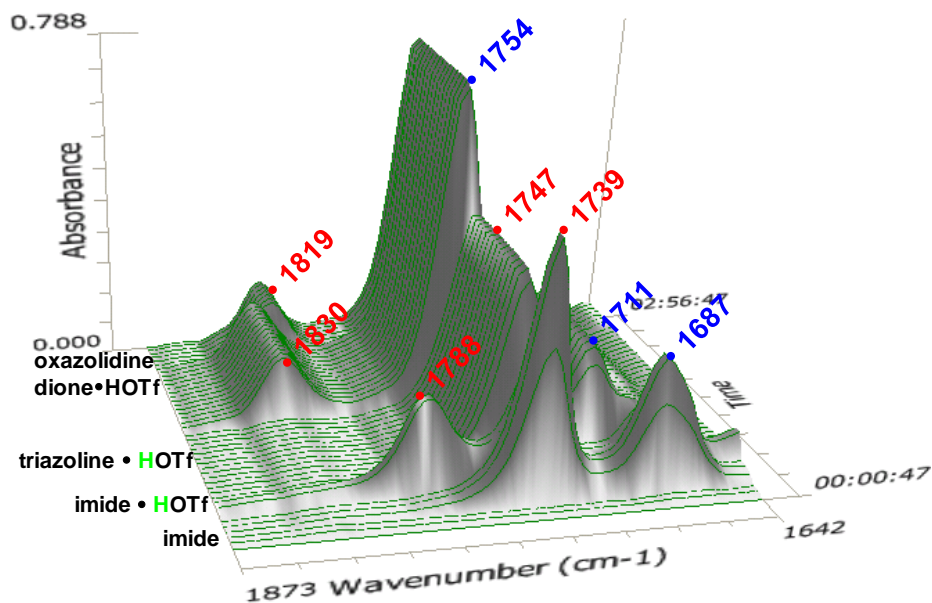
Figure 18. Reaction Course Observed by *in situ* IR Spectroscopy (Thermal, Anhydrous Variation)



After these initial experiments, two different sets of experiment were designed to verify the effect of water. First, we investigated our earlier observation during warming of the reaction mixture prior to quench. When the low temperature bath was replaced with a 25 °C water bath, a change in the IR spectrum occurred within several minutes (Figure 18).

The aforementioned peaks were replaced by new absorptions at 1830 and 1750 cm^{-1} . Gas evolution (N_2) was visually observed when the reaction temperature was in the 0-25 °C range. Importantly, nitrogen evolution consistently paired with the appearance of the 1830/1754 cm^{-1} IR absorptions. The IR spectrum of the new species is consistent with product **245a**·HOTf, which was converted to its free base in the crude reaction mixture by triethylamine addition.

Figure 19. Reaction Course Observed by *in situ* IR Spectroscopy (Water Additive Variation)

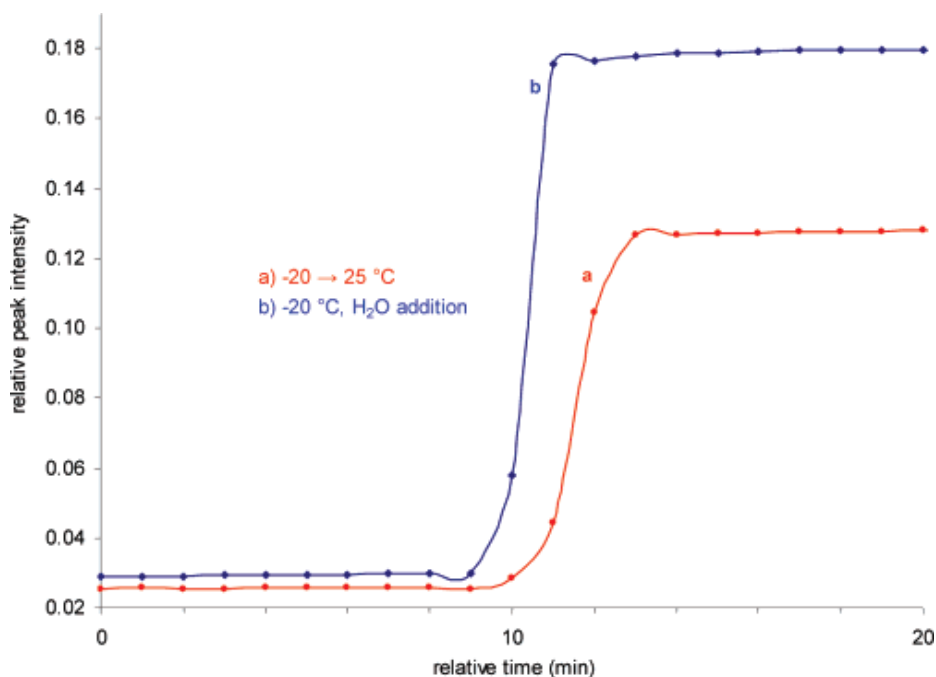


In a separate experiment (Figure 19), the same conditions and procedures were applied until the stability of **246a** was again apparent. Instead of warming the reaction

mixture at this point, one equivalent of water was added to the reaction mixture ($[\text{H}_2\text{O}]_{\text{max}} = 0.4 \text{ mM}$). The changes in the IR spectrum were both immediate and identical to those induced by warming of the reaction mixture to room temperature. In most cases, the conversion was complete within several minutes, and no further change was observed by IR. Neutralization of the reaction mixture again led to observation of **245a** by ^1H NMR.

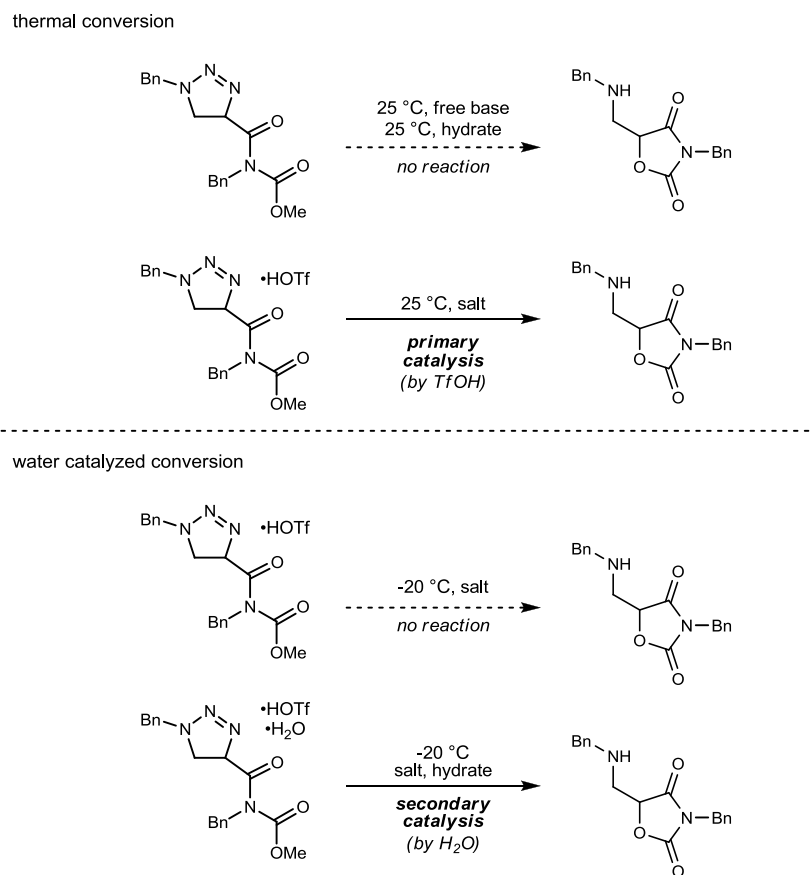
The rate of decomposition of triazoline **246a**, and the formation of **245a** were compared, as a function of time (a) when the temperature was raised and (b) when water was added to initiate the conversion but the temperature was maintained at -20°C (Figure 20). Additional control experiments confirmed that isolated triazoline behaved identically to that formed *in situ* (as in the experiments above), and that water alone, without TfOH present, returned only unmodified triazoline even at room temperature.

Figure 20. Reaction Course Observed by Monitoring Oxazolidine Dione **245a**·TfOH Formation (1830 cm^{-1} , *in situ* IR) from Triazoline **246a** Using (a) Thermal or (b) Water-Catalyzed Conditions



The role of water therefore, is secondary to triflic acid which can catalyze the conversion of **246a/245a** unassisted, if the proper amount of thermal energy (above -20 °C) is supplied. Water alone is not a competent catalyst, but the combination of triflic acid and water will promote the conversion at -20 °C, clearly requiring less thermal energy (Scheme 58).

Scheme 58. Secondary Catalysis by Water: Observations and Logic Supporting the Characterization



To generate free oxazolidinone **245a**, demethylation by thermal and water assisted cleavage was also monitored by IR spectroscopy. Thermal decomposition of triazolone **246a** resulted in, cleavage of the methyl-oxygen bond by S_N2 attack of a nucleophile (e.g.,

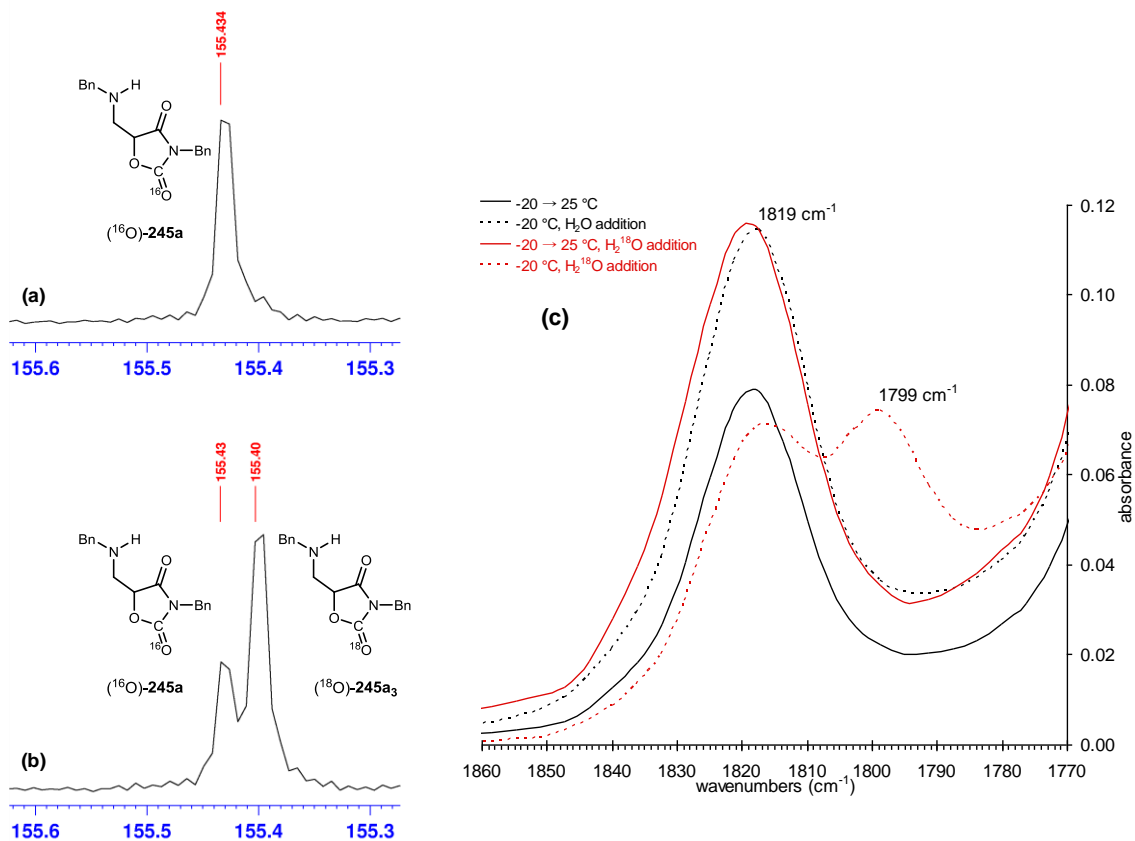
CH₃CN), which was supported by detection of Ritter-type intermediate **382** (Scheme 59). A change in the mechanism to form oxazolidine dione is believed to occur when water is present. In this case, hydrolysis of the oxonium intermediate leads to the production of MeOH. This was also monitored by IR spectroscopy by using labeled water. Since oxazolidine dione **245a**·TfOH was the next spectroscopically observed and isolated product from both anhydrous thermal and low temperature water catalyzed reactions, its formation under these very different conditions from putative intermediate salt **245a₁** needed to be rectified. The operative pathways were identified using two experiments and the use of H₂¹⁸O; 1) the thermal procedure for decomposition of the intermediate triazoline **246a** was applied, and H₂¹⁸O was added at room temperature prior to the usual quench, and 2) oxazolidine dione formation by H₂¹⁸O-catalyzed triazoline decomposition at -20 °C (Figure 21).

The thermal procedure for decomposition of the intermediate triazoline was applied, and H₂¹⁸O was added prior to the usual quench. In this case, the spectra (¹³C NMR and IR) of **245a** (¹⁶O) observed (Figure 21a,c) was similar to the analogous case when H₂¹⁶O was used for decomposition of triazoline. This behavior is consistent with nucleophilic cleavage of the methyl-oxygen bond by acetonitrile solvent during the thermal decomposition protocol. Indeed, an absorption at 2418 cm⁻¹ in this experiment (*in situ* IR) prior to reaction quench is consistent with the formation of a nitrilium intermediate [CH₃CNCH₃]⁺. When the heavy isotope was used as the water additive at -20 °C, the IR of the oxazolidine dione that resulted was similar to that observed when using H₂¹⁶O, but with the carbamate C=O shifted from 1819 to 1799 cm⁻¹, consistent with **245a₃** (Figure 21c). The ¹³C NMR analysis for **245a₃** also exhibits the characteristic isotope-induced chemical shift (-0.03 ppm) for the carbamate oxygen, consistent with 66% ¹⁸O

enrichment (Figure 21b). The transformations depicted in Scheme 59 summarize this behavior in the context of mechanism following the triazolium fragmentation.

Figure 21. Comparison of **245a** (^{16}O) and **245a₃** ($^{18}\text{O}:^{16}\text{O} = 2:1$), and H_2^{18}O -Catalyzed Experiments. ^{13}C NMR (125 MHz) Spectra of Oxazolidine Dione.

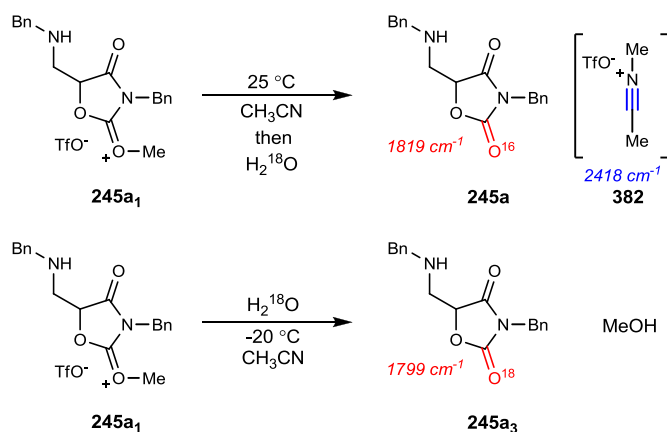
(a) **245a** (^{16}O) formed from thermal triazoline decomposition (H_2^{18}O quench at room temperature), and (b) **245a₃** formed by H_2^{18}O -catalyzed triazoline decomposition at $-20\text{ }^\circ\text{C}$ (reaction quench with Et_3N at $-20\text{ }^\circ\text{C}$); (c) IR of oxazolidine diones formed from the thermal experiment and three variations, including H_2^{18}O catalyzed triazoline decomposition leading to ^{18}O incorporation.



We propose two roles for water in this reaction. A full equivalent is ultimately consumed in the hydrolysis of oxonium intermediate **245a₁**. Additionally, the evidence suggests that water accelerates the triazoline fragmentation, particularly by catalyzing the

preceding isomerization (a nonhydrolytic process). The irreversible expulsion of nitrogen allows these two roles to be deconvoluted since the visual evolution of N₂ allows us to pinpoint rate acceleration at the triazoline ring-opening step. Was this not the case, an alternate explanation for the observed water effect would normally be the existence of an equilibrium whose product is consumed by water in a chemical reaction, thereby leading to the disappearance of the monitored species through reconstitution of the equilibrium.

Scheme 59. Isotope Labeling Experiments to Ascertain Role and Fate of Water in Both Thermal and Water-Catalyzed Triazolinium Fragmentations



These observations are consistent with *secondary catalysis* of the triazoline decomposition step by water. It is also important to note that reactions to which water is added at the beginning typically result in slower overall conversion of **244a/245a**. Since the first step is Lewis acid catalyzed, this behavior is consistent with hydronium triflate's lower Lewis acidity relative to triflic acid. This character is clearly reversed in the second step where the Lewis acidity of hydronium triflate and triflic acid are unchanged, but their mobility is the determinant of rate.

The free base is indefinitely stable to water in the absence of added Brønsted acid. In

our experience, the triazoline free base is also indefinitely thermally stable up to temperatures of (at least) 100 °C. This behavior contrasts that of the triflic acid salt, which is indefinitely stable at low temperature (-20 °C) when anhydrous, but will convert concomitant with nitrogen evolution when warmed to room temperature. These three behaviors indicate that the triazoline stability is primarily controlled by the polarization provided by Brønsted acid. However, the effect of water further accelerates the rate of triazoline decomposition, and this can be clearly quantified at -20 °C. The overall transformation produces oxonium ion **245a₁**, which then consumes one equivalent of water. Water is still a catalyst for the triazolinium fragmentation, since the individual isomerization and cyclization steps do not consume water. The evolution of nitrogen provides a visual cue to correlate with triazolinium consumption observed simultaneously by IR indicating that fragmentation is catalyzed under these conditions.

It was not clear to us why the triazolinium intermediate might exhibit this behavior, since its stability would need to be rationalized by a reluctant proton transfer. Calculations have determined N3-protonation can be favored over N1 by as much as 10 kcal/mol, but N1 protonation is in equilibrium and leads to irreversible triazoline decomposition in studies of the triazoline-aziridine interconversion.⁸⁷ The stability of **246a₁/246a₂** is therefore surprising, particularly since a number of capable proton carriers can be identified in the reaction mixture, including a second triazolinium or simply the abundant acetonitrile solvent. Proton “immobilization” is often perceived to require the design of special Brønsted bases that bear no resemblance to the intermediates at play

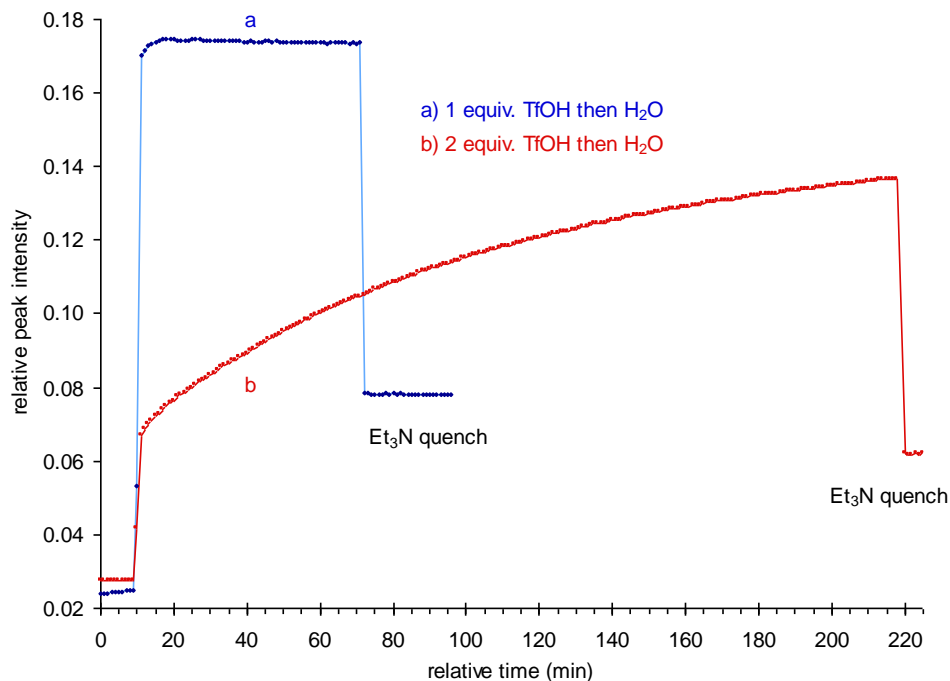
⁸⁷ Smith, R. H.; Wladkowski, B. D.; Taylor, J. E.; Thompson, E. J.; Pruski, B.; Klose, J. R.; Andrews, A. W.; Michejda, C. J. *J. Org. Chem.* **1993**, 58, 2097. Hunig, S.; Schmitt, M. *Liebigs Ann.* **1996**, 559. Schmiedekamp, A.; Smith, R. H.; Michejda, C. J. *J. Org. Chem.* **1988**, 53, 3433.

here.⁸⁸

A final test of this reasoning was made by monitoring the water catalysis phenomenon under conditions of excess triflic acid. If protonation at N3 is nonlabile and electronically stabilizes the triazoline toward N1-N2 fragmentation, then excess triflic acid would not be expected to overcome this effect; although protonation at N1 might be possible (to form the doubly protonated triazoline), protonation at N3 would prevent proper polarization for N1-N2 fragmentation. Furthermore, addition of water to the bis(salt) would enhance proton mobility, but oxazolidine dione formation might be slower because of protonation of the carbamate oxygen in the cyclization step or because of slower triazoline fragmentation (via formation of monosalt **246a₃** from a bis(salt)). Both of these predictions were confirmed by experiment (Figure 22.). The triazoline was indefinitely stable toward two equivalents of triflic acid at -20 °C in the absence of water. And addition of water promoted triazoline fragmentation again, but oxazolidine dione formation was markedly slower (Figure 22.b) than the rate observed with a single equivalent of triflic acid (Figure 22.a).

⁸⁸ Cheney, J.; Lehn, J. M. *J. Chem. Soc. Chem. Comm.* **1972**, 487. Alder, R. W.; Goode, N. C.; Miller, N.; Hibbert, F.; Hunte, K. P. P.; Robbins, H. J. *J. Chem. Soc. Chem. Comm.* **1978**, 89.

Figure 22. Comparison of Water Catalyzed Triazolium Fragmentations (Monitoring Oxazolidine Dione Formation at 1830 cm^{-1}) Using a) 1 Equivalent, and b) 2 Equivalents of Triflic Acid

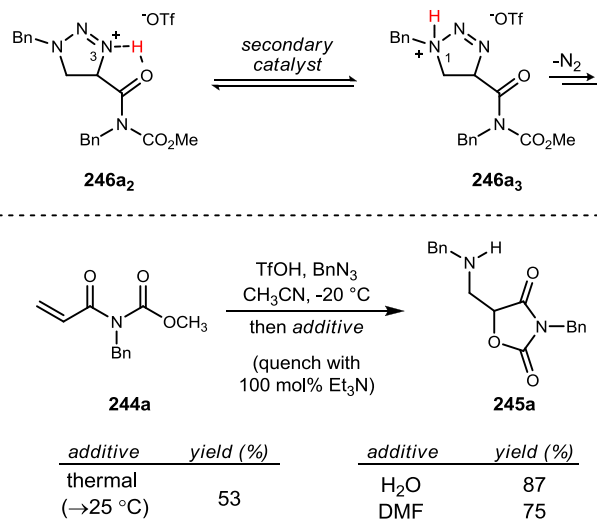


Water may specifically lower the barrier to isomerization of **246a₂** to **246a₃**. The stability of **246a₂** may be a general phenomenon of anhydrous triazoline salts or may be due to a bidentate proton chelate. It is not possible to further discriminate details of the isomerization process. For example, the water molecule could shuttle the proton (as hydronium) from N3 to N1 of the triazoline. Alternatively, it could competitively bind to the carbamate system, allowing an agent such as solvent to play the role of shuttle. Although the mechanism advanced in Scheme 57 suggests a discrete diazonium ion **246a₄**, we cannot exclude the possibility that this intermediate is bypassed by a single transition state in which carbon-oxygen bond formation is concomitant with triazoline fragmentation. The depressed rate of formation of oxazolidine dione observed when using excess triflic acid is consistent with this possibility as well.

2.3. Use of Comparative Triazolinium Triflate Fragmentation Rates as a Tool to Assay Relative Competency of Brønsted Bases in $N \rightarrow N$ Proton Transfer

We described the use of triazoline fragmentation as a tool to identify a *secondary catalysis* effect of water as an additive. We sought additional candidates for the secondary catalyst role, both protic and aprotic, so we investigated various additives that might similarly function as proton shuttles. A number of additives, particularly those containing the amide functional group were tested first. The amide functional group provided a more effective agent for proton transfer to convert the intermediate triazoline to product oxazolidine dione (Scheme 60).

Scheme 60. Additive-Accelerated Fragmentation of Triazolinium Triflates

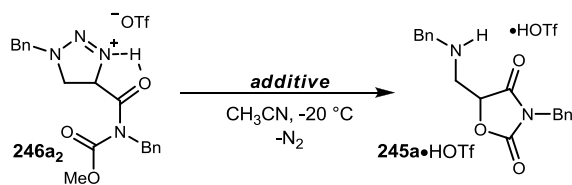


Our benchmark system used either thermal conversion or a stoichiometric amount of water (-20 °C, isothermal) to promote the formation of oxazolidine dione **245a** (as its triflic acid salt prior to reaction quench), and was used here to screen additives that might provide a similar function - that of a proton transfer agent. For example, the polar aprotic additive dimethyl formamide (DMF) was found to accelerate triazolinium fragmentation at -20 °C, and following a low temperature quench, oxazolidine dione **245a** was retrieved

in 75% isolated yield. By analogy, this suggested that water's Brønsted basicity at oxygen might be more important than its Brønsted acidity in the proton transfer step.

As a measure of relative ability to stimulate proton transfer, we monitored either oxazolidine dione carbamate carbonyl formation or triazoline carbamate carbonyl decomposition as a function of time. First of all, electronically different water and alcohol additives were investigated to identify the exact functional group's ability to transfer the proton (summarized in Table 28, entries 1-5).

Under standard experimental conditions for this series, water promoted the conversion with a triazolinium half-life of 33 minutes, and apparent completion at 210 minutes (Table 28, entry 1). Deuterated water appeared to behave similarly, with a half-life of 58 minutes and time to completion at approximately 231 minutes (Table 28, entry 2). The behavior is consistent with the attenuated Brønsted basicity (and increased Brønsted acidity) of D₂O relative to H₂O. By comparison, methanol promotes the proton transfer more efficiently, leading to a triazolinium half-life of 2 minutes, and time to completion of 4 minutes (Table 28, entry 3). If the oxygen bears two alkyl groups as in diethyl ether, the triazolinium stability appears unaffected (Table 28, entry 4). Similarly, trifluoroethanol failed to promote the conversion (Table 28, entry 5). Acetic acid caused seemingly characteristic changes in the IR spectrum, but nitrogen evolution was not observed (Table 28, entry 6). Similar to acetic acid, ethyl acetate and phenol failed to promote the conversion (Table 28, entry 7, 8).

Table 28. Additive Effects in the Conversion of Triazolium to Oxazolidine Dione^a

entry	additive	t _{1/2} (min) ^b
1	H ₂ O	33
2	D ₂ O	58
3	CH ₃ OH	2
4	(CH ₃ CH ₂) ₂ O	- ^c
5	CF ₃ CH ₂ OH	- ^c
6	AcOH	- ^c
7	ethyl acetate	- ^c
8	phenol	- ^c

9	DMF	2
10	CH ₃ C(O)NH ₂	1
11	<i>N</i> -Me-oxazolidinone	46
12	<i>N</i> -Me-imidazole	3
13	imidazole	2
14	pyridine	2
15	DBU	2
16	ⁱ PrNH ₂	3

^aThe intermediate triazolium salt was prepared in situ using 200 mol% TfOH, and maintained for >20 minutes to establish its stability in the absence of additive. ^bTimes were measured from the point of addition of the additive. When conversion was observed by IR, nitrogen evolution was also noted. Entries 8, 10-11, 13-14 monitored the decomposition of the triazolium using the absorption at 1711 cm⁻¹. Entries 1-3, 7, 9, 12 monitored the growth of the oxazolidine dione absorption at 1830 cm⁻¹. ^cChanges in the IR spectrum occurred at the addition point, but no gas (nitrogen) evolution was observed.

Under this standard reaction condition, even though some experiments failed to show immediate conversion to oxazolidine dione, we observed the nitrogen evolution during the course of quenching with triethylamine. This phenomenon can be explained by simple acid-base neutralization or proton transfer during the course of addition of triethylamine. However, in terms of comparison of relative rate of triazolium decomposition, these additives failed to show their ability to shuttle the proton.

These behaviors suggested that the Brønsted basicity of the oxygen in these additives

(not their Brønsted acidity) is the most important determinant of triazolium stability and proton transfer. Moreover, the Brønsted basicity can be modulated using both steric (ether) and inductive effects (trifluoroethanol, ethyl acetate, phenol, acetic acid).

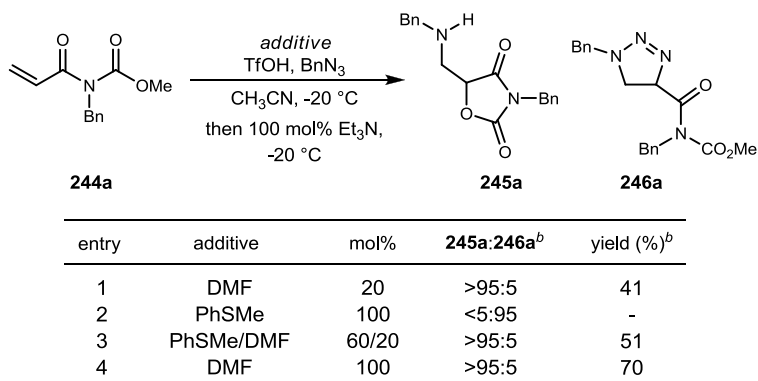
We expanded our search for effective proton transfer agents based on the observation that methanol was superior to water (c.f. entry 1 & 3, Table 28), and that polar aprotic additives such as DMF did not adversely affect the overall reaction (Scheme 60). This series continued with Brønsted basic oxygen donors (Table 28, entries 9-11). The immediate evolution of nitrogen, appearing as a gaseous eruption, was a characteristic of the most effective additives, and continued with other oxygen donors such as dimethyl formamide and acetamide (Table 28, entries 9-10). *N*-Methyl oxazolidinone (entry 11), however, exhibited only moderate activity that was on par with the behavior of water.

We next turned to Brønsted basic nitrogen donors. The behavior of all of these places them in the class of most effective additives and is again consistent with their ability to function as a proton shuttle (Table 28, entries 10-14). It is important to note that the fragmentation rate, which requires positive charge generation at N1, increases when Brønsted basic nitrogen additives are employed, despite the fact that these same additives would attenuate Brønsted acidity of the system. This knowledge can be used to effect the overall conversion of **244a** to **245a** in a two step procedure for substrates that require the full Brønsted acidity provided by triflic acid to promote triazoline formation; once its formation is complete, the triazoline can then be converted to oxazolidine dione in a manner that requires both Brønsted acid and a proton transfer agent at low temperature. The effectiveness of amine additives under conditions of excess Brønsted acid also suggests their role as kinetically labile ligands for the proton.

As a final examination of additive performance in the outcome of these

transformations, we investigated whether additive turnover is possible. We were guided by our knowledge of mechanism insofar as the penultimate intermediate in the production of **245a** is oxonium **245a₁**. When water is the additive, hydrolysis of **245a₁** occurs rapidly. We first evaluated the effect of 20 mol% DMF and found that nitrogen evolution was again vigorous, and that all triazoline had been converted to oxazolidine dione (**245a**) upon inspection of the crude reaction mixture by ¹H NMR.

Table 29. Comparison of Stoichiometric and Substoichiometric Additive Effects in the Conversion of Triazolium to Oxazolidine Dione^a



^aThe additive was introduced 30 min following the combination of azide, olefin, and 100 mol% TfOH at -20 °C. Following a 6 h reaction time, Et₃N (100 mol%) was introduced, and the reaction was warmed to ambient temperature, concentrated, and analyzed by ¹H NMR prior to purification. Nitrogen evolution was observed at the point of additive addition for entries 1,3,4 but not at reaction quench or beyond. ^bRatio estimated by ¹H NMR analysis of the crude reaction mixture. Yields represent isolated, analytically pure material.

This establishes the ability of DMF to turn over in the proton transfer step. The isolated yield, however, was only 41% (Table 29, entry 1). This could be attributed to the minimization of a means at -20 °C for **245a₁**, a competent methylating agent, to convert to oxazolidine dione **245a** through a controlled, efficient pathway; the acetonitrile solvent

competitively demethylates **245a₁**, but only at warmer temperatures. We therefore turned to thioanisole as a methyl scavenger, one that does not itself promote triazolium fragmentation (Table 29, entry 2). Using a combination of 60 mol% PhSMe and 20 mol% DMF, a slight improvement was observed both spectroscopically and in the isolated yield (Table 29, entry 3). When used in a stoichiometric amount, DMF may either stabilize **245a₁** until reaction quench, or become methylated itself, leading to an improved yield of **245a** (Table 29, entry 4). The ability to form reactive intermediate **245a₁** using a substoichiometric amount of Brønsted base additive might provide the opportunity to sequence an additional intra- or intermolecular reaction in order to further increase the overall structural complexity generated during the olefin functionalization.

It is interesting to note that the behavior of these additives in bulk solvent parallels observations of the role of peptide side chain functionality performing a similar function, but in the shielded environment of a protein's active site. Although the reaction and conditions here bear little resemblance to biological contexts where proton transfer is rate-limiting, some of the additives examined might be considered reasonable surrogates: acetamide~Gln/Asn, ⁱPr₂NH~Lys, imidazole~His, DBU~Arg, MeOH~Ser, and AcOH~Asp/Glu. In contrast to studies involving enzymes, where the presence of water is inherent to the system, the triazolium fragmentation reaction can be considered a tool to evaluate an *N*→*N* proton transfer under anhydrous conditions.

2.4. Conclusion.

In summary, we have identified the intervening steps in the Brønsted acid-catalyzed conversion of olefin to oxazolidine dione. Significant rate acceleration is provided by triflic acid to the azide-olefin addition step, leading to an intermediate triazoline under

anhydrous conditions that has been characterized by *in situ* IR spectroscopy. Additionally, we have further characterized the effect of water on the triazolinium stability in which it works in concert with triflic acid at low temperature to promote triazoline fragmentation in a nonhydrolytic step.

Chapter 3.

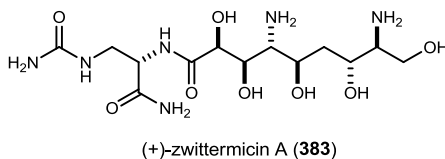
Studies Towards the Synthesis of (+)-Zwittermicin A

3.1. Background

3.1.1 Introduction to (+)-Zwittermicin A and Biosynthesis of (+)-Zwittermicin A

(+)-Zwittermicin A (**383**), a water-soluble aminopolyol antibiotic, was reported in 1994⁸⁹ after isolation from the fermentation broth of the soil-borne bacterium *Bacillus cereus*. (+)-Zwittermicin A (**383**) enhances the activity of the endotoxin from *Bacillus thuringiensis* which is used for the protection of vegetable crops and for the eradication of gypsy moths from forest tree.⁹⁰

Figure 23. (+)-Zwittermicin A



The biosynthesis of zwittermicin A has been an interest of ongoing studies due to the production of exotic “non-natural” aminopolyketides. The biosynthesis originated from a nonribosomal peptide synthetase/polyketide synthase pathway (NRPS/PKS) involving two newly described type 1 PKS extender units: hydroxymalonyl-acyl carrier protein (ACP) and aminomalonyl-ACP.⁹¹

⁸⁹ He, H.; Silo-Suh, L. A.; Handelsman, J.; Clardy, J. *Tetrahedron. Lett.* **1994**, 35, 2499.

⁹⁰ Silo-Suh, L. A.; Stabb, E. V.; Raffel, S. J.; Handelsman, J. *Curr. Microbiol.* **1998**, 37, 6. Broderick, N. A.; Goodman, R. M.; Raffa, K. F.; Handelsman, J. *Environ. Entomol.* **2009**, 29, 101. Stohl, E. A.; Brady, S. F.; Clardy, J.; Handelsman, J. *J. Bacteriol.* **1999**, 181, 5455.

⁹¹ Emmert, E. A. B.; Klimowicz, A. K.; Thomas, M. G.; Handelsman, J. *Appl. Environ. Microbiol.* **2004**, 70, 104

3.1.2. Previous Synthetic Efforts

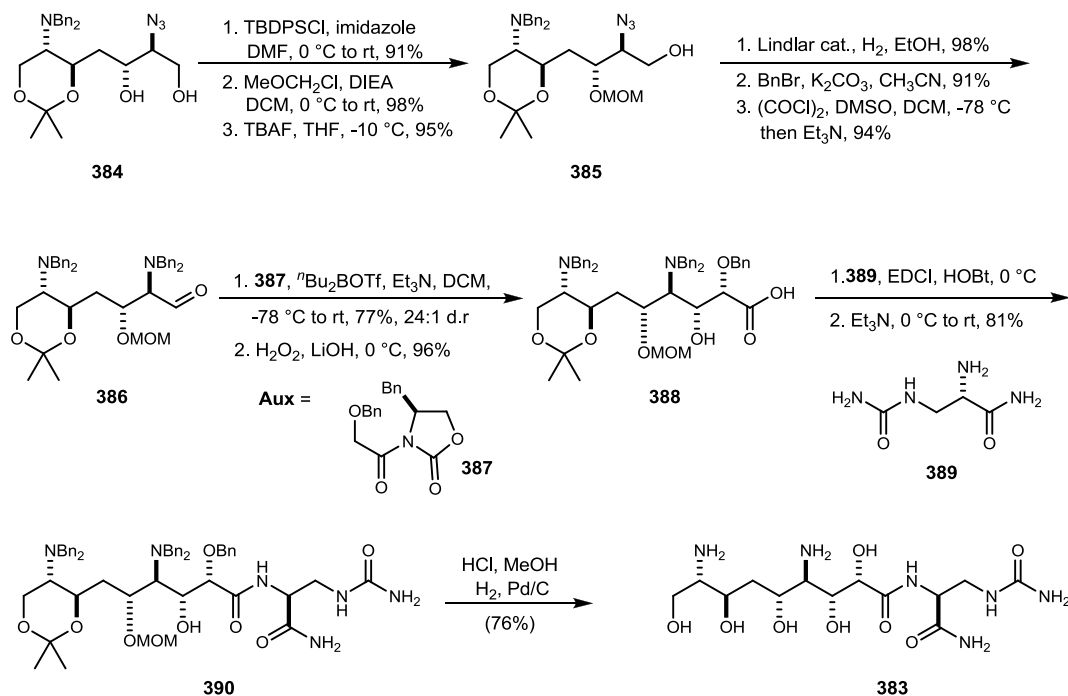
The original isolation and partial structural elucidation were reported in 1994 by the complete relative and absolute configuration were reported in 2007 by Molinski.⁹² In the following year, Molinski reported the first total synthesis of (+)-zwittermicin A.⁹³ The azidodiol **384**, prepared from L-Ser as reported,⁹² was refunctionalized by protection and deprotection to give **385**. Transformation of the azido group of **385** into an amine by hydrogenolysis and subsequent benzylation and oxidation gave aldehyde **386**. Evans' aldol addition of chiral glycolate **387** to aldehyde **386** and subsequent removal of the auxiliary afforded carboxylic acid **388**. Coupling of **388** and **389** gave the amide **390** which was deprotected to afford (+)-zwittermicin A (**383**) (Scheme 61).

104. Stohl, E. A.; Milner, J. L.; Handelsman, J. *Gene* **1999**, *237*, 403. Chan, Y. A.; Boyne, M. T.; Podevels, A. M.; Klimowicz, A. K.; Handelsman, J.; Kelleher, N. L.; Thomas, M. G. *Proc. Natl. Acad. Sci. USA* **2006**, *103*, 14349. Chan, Y. A.; Boyne, M. T.; Podevels, A. M.; Klimowicz, A. K.; Handelsman, J.; Kelleher, N. L.; Thomas, M. G. *Proc. Natl. Acad. Sci. USA* **2006**, *103*, 14349. Chan, Y. A.; Boyne, M. T.; Podevels, A. M.; Klimowicz, A. K.; Handelsman, J.; Kelleher, N. L.; Thomas, M. G. *Proc. Natl. Acad. Sci. USA* **2006**, *103*, 14349. Chan, Y. A.; Boyne, M. T.; Podevels, A. M.; Klimowicz, A. K.; Handelsman, J.; Kelleher, N. L.; Thomas, M. G. *Proc. Natl. Acad. Sci. USA* **2006**, *103*, 14349. Chan, Y. A.; Boyne, M. T.; Podevels, A. M.; Klimowicz, A. K.; Handelsman, J.; Kelleher, N. L.; Thomas, M. G. *Proc. Natl. Acad. Sci. USA* **2006**, *103*, 14349. Chan, Y. A.; Boyne, M. T.; Podevels, A. M.; Klimowicz, A. K.; Handelsman, J.; Kelleher, N. L.; Thomas, M. G. *Proc. Natl. Acad. Sci. USA* **2006**, *103*, 14349.

⁹² Rogers, E. W.; Molinski, T. F. *Org. Lett.* **2007**, *9*, 437.

⁹³ Rogers, Evan W.; Dalisay, Doralyn S.; Molinski, Tadeusz F. *Angew. Chem. Int. Ed.* **2008**, *47*, 8086.

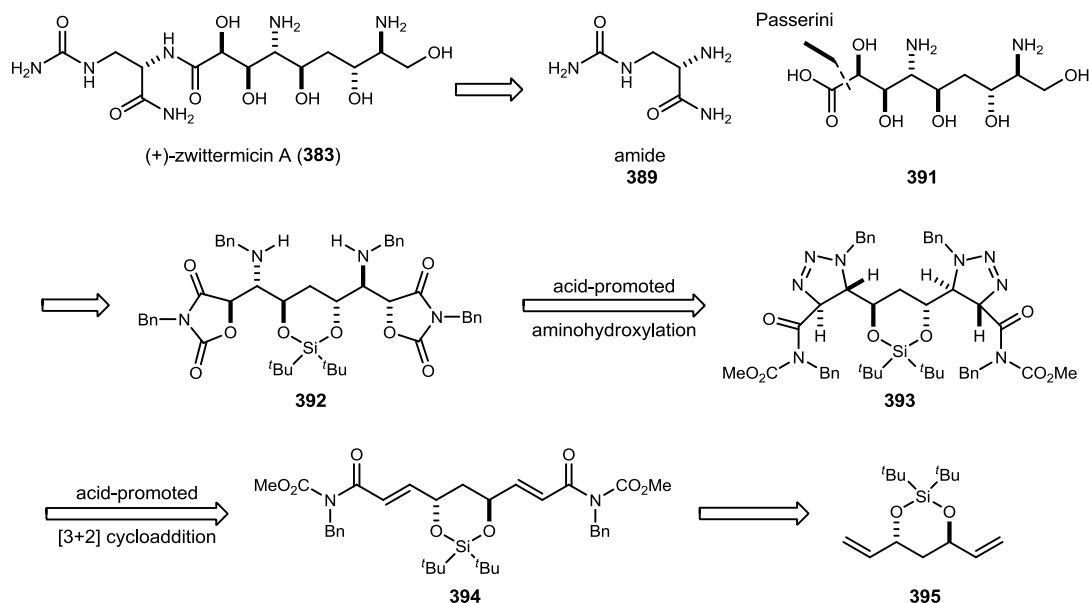
Scheme 61. Molinski's Synthesis of (+)-Zwittermicin A



3.1.3. Retrosynthetic Analysis

Our retrosynthetic analysis for the synthesis of (+)-zwittermicin A is outlined in Scheme 62. The first disconnection is a coupling of known amide **389** and deprotected carboxylic acid **391**. The carboxylic acid **391** is a result of Passerini reaction from the reduced form (hemiaminal) of oxazolidine dione **392**. The Brønsted acid-catalyzed *anti* aminohydroxylation allows for a convergent route to key intermediate **392** which contains the desired four stereocenters of the zwittermicin core. The methods for azide addition to olefins, developed and described previously, are used to form triazoline **393**. The silyl group protection maximizes the size of oxygen substituent for facial selectivity of the azide additions to olefins, and discourages protonation that might lead to elimination of the silylether. The diimide **394** is synthesized in two steps from the known diol **395**.

Scheme 62. Retrosynthetic Analysis



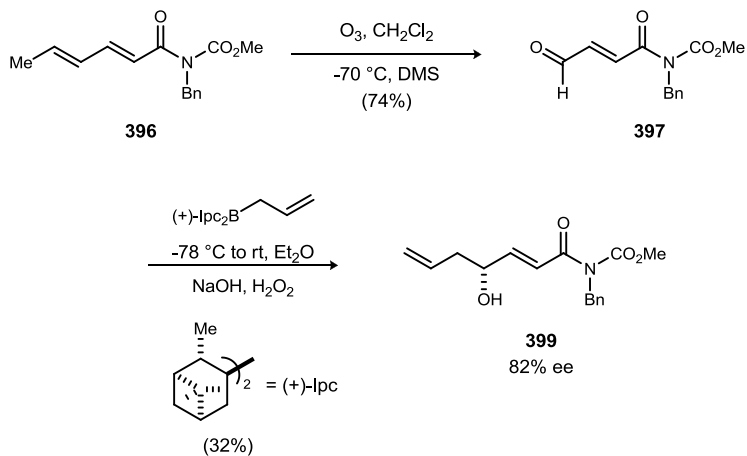
3.2. Results and Discussions

3.2.1 Diastereoselective Intermolecular [3+2] Azide-Olefin Cycloadditions

To this point, we had not explored the question of diastereoselection in intermolecular azide-olefin additions. γ -Acetoxy unsaturated imides were targeted as model substrates for the key step in a proposed zwittermicin A synthesis. Synthesis of the chiral γ -substituted unsaturated imide **399** started from commercially available sorbic acid. This two step protocol involved the synthesis of sorbic imide **396** from sorbic acid and *N*-benzyl carbamate. Selective ozonolysis of the terminal alkene provided α,β -unsaturated aldehyde **397** in 74% yield (Scheme 63). To install the desired hydroxyl chiral center in **399**, Brown allylation was chosen for its ability to achieve moderate enantioselectivity. However, due to the instability of the imide system to hydrolytic conditions, standard oxidative conditions with sodium hydroxide, and peroxide quenching gave an average 32%

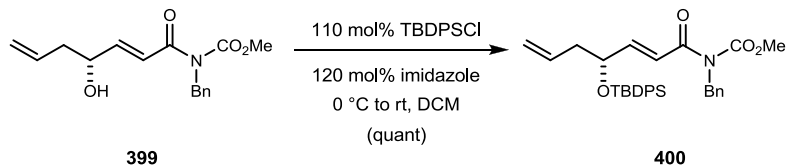
yield of desired γ -substituted unsaturated imide **399** with 82% ee.

Scheme 63.



γ -Hydroxy unsaturated imide **399** was protected by the large tributyl diphenyl silyl group to provide steric hindrance for selective [3+2] cycloaddition (Scheme 64).

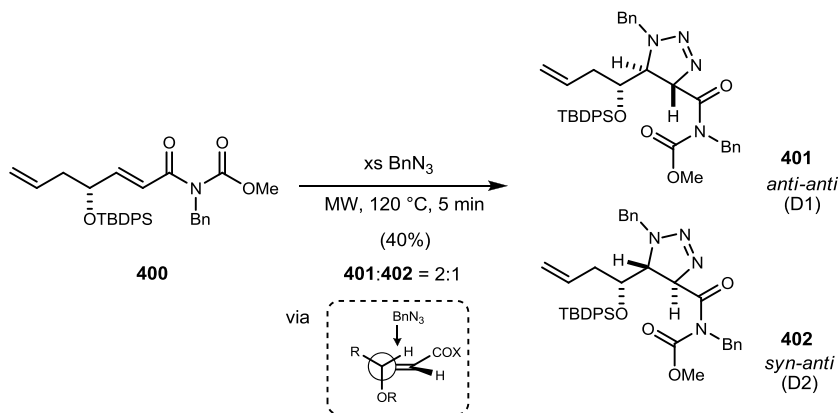
Scheme 64.



With protected unsaturated imide **400**, thermal and Brønsted acid-promoted [3+2] cycloaddition protocols were applied to triazoline synthesis. Using a microwave reactor with benzyl azide as a solvent, thermal conversion was tested first. The predictive model (Scheme 65) minimizes allylic strain and arranges the C-O bond perpendicular to the π -plane. This model was the basis for rationalizing the observed selectivity for

organocuprate⁹⁴ and amide additions to unsaturated esters.⁹⁵ Based on the crude NMR analysis, desired *anti-anti* diastereomer **401** and *syn-anti* diastereomer **402** were obtained in a 2:1 ratio (Scheme 65).

Scheme 65. Thermal [3+2] Cycloaddition

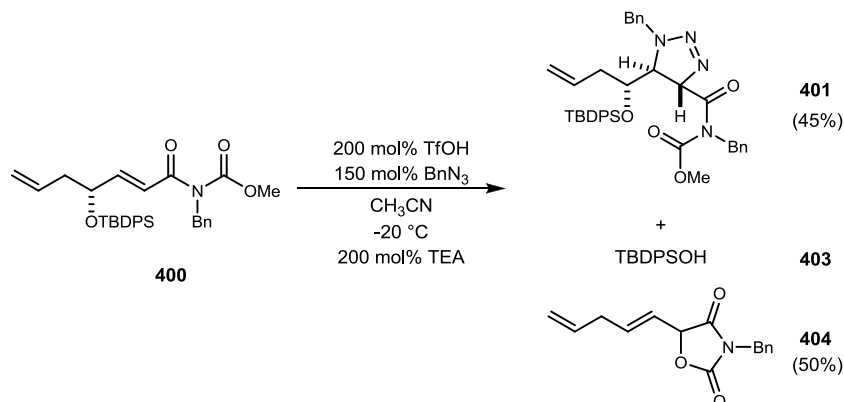


In contrast to thermal conversion, using acid promoted condition, *anti-anti* diastereomer **401** was formed selectively. However, competitive acid-promoted S_N2' cyclization of the carbamate, led to considerable amounts of oxazolidine dione **404** too. A typical Brønsted acid-promoted addition gave only 45% yield of the desired triazoline **401**.

⁹⁴ Kireev, A. S.; Manpadi, M.; Kornienko. *J. Org. Chem.* **2006**, *71*, 2630.

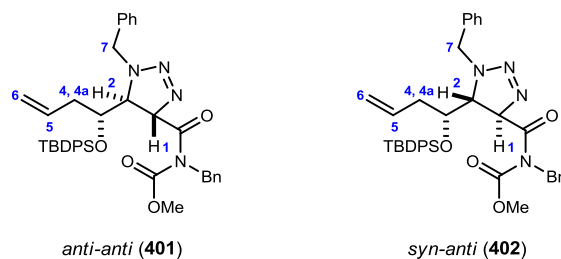
⁹⁵ Cailleau, T.; Cooke, J. W. B.; Davies, S. G.; Ling, K. B.; Naylor, A.; Nicholson, R. L.; Price, P. D.; Roberts, P. M.; Russell, A. J.; Smith, A. D.; Thomson, J. E. *Org. Biomol. Chem.* **2007**, *5*, 3922.

Scheme 66.



The conformational analysis of the *anti-anti* triazoline **401** was evaluated by NMR (1D and 2D) experiments for the relative stereochemistry and conformations. All the proton and carbon chemical shifts of the *anti-anti* triazoline **401** were assigned, using ¹H, ¹³C and HSQC (¹J_{CH}), and NOESY NMR experiments.

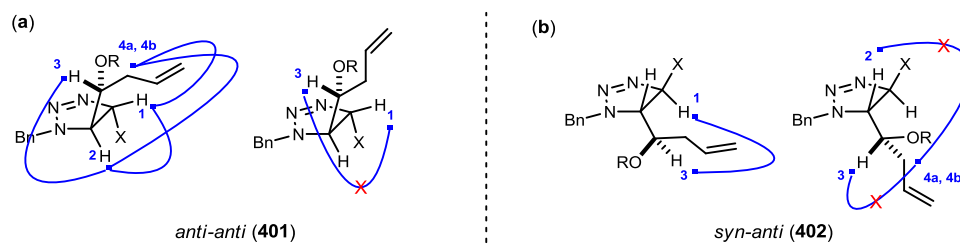
Figure 24. Conformational Depiction of *anti-anti* (**401**) and *syn-anti* Triazoline (**402**)



Beginning from the right next to amide functionality, crosspeaks for H2/H3, H4a and H1, and H4/H5 defined the orientation of all hydrogens and single bond rotations (Figure 25-a). No H3/H1 correlation was observed, supporting the rotamer depicted wherein this hydrogen is oriented away from H1. In contrast, the *syn-anti* diastereomer (Figure 25-b) conformation is not supported by the observed crosspeaks. First of all, to support

crosspeaks for H2/H3, the *syn-anti* diastereomer should have an H3/H1 correlation, which was not observed. Additionally, single bond rotation to avoid this H3/H1 correlation resulted in a proximal orientation between H1 and both of H4/4a which was not consistent with a single H4a crosspeak. Secondly, single bond rotation between C3 and C4 to avoid this H1/ H4a,4b correlation should result in an interaction between H7 and one of H4, which was not observed. Finally, the crosspeaks between H4a,4b and either H2 or H3 are observed. It is not possible to identify whether H2 or H3 sees both H4a and H4b due to the overlapping of H2 and H3, but the correlation of both H4a and H4b to either H2 or H3 are consistent with the *anti-anti* diastereomer. In the *syn-anti* diastereomer, both H2 and H3 would only see H4a or H4b, due to the opposite direction of the H4 hydrogen.

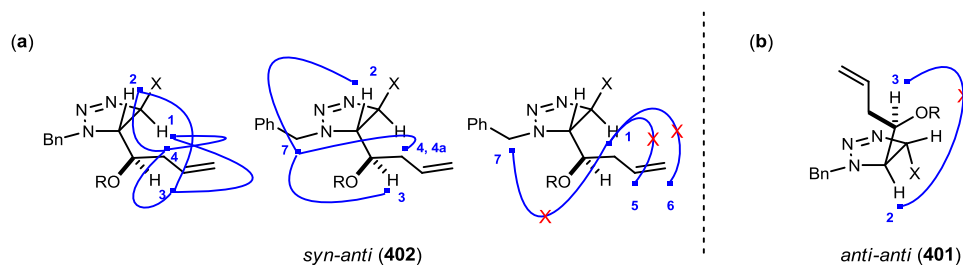
Figure 25. Observed Regional NOESY Correlations for *anti-anti* Triazoline (**401**)



The *syn-anti* triazoline **402** was also evaluated using a NOESY experiment. The *syn-anti* conformation was determined by observation of crosspeaks between H1/H3, H1/H4 (H4a and H4b are overlapping in this diastereomer), H2/H3 and H3/H4, H4/H5 (Figure 26-a). Additionally, H7/H2, H7/H3, H7/H4 correlation was also observed, supporting the orientation depicted. Importantly, no H1/H5 or H1/H6 crosspeaks were observed, consistent with the *syn-anti* configuration shown. In contrast, the *anti-anti* diastereomer

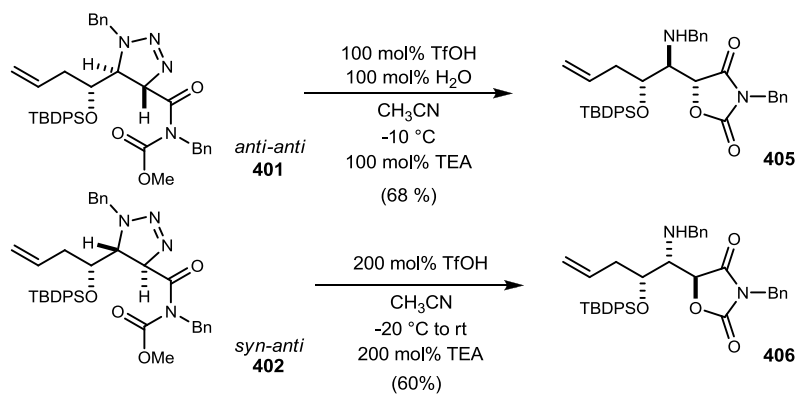
(Figure 26-b) conformation is not consistent with the observed crosspeaks. For example, to maintain the crosspeaks H1/H3, H1/H4 and H7/H3, H7/H4 correlation, an H2 and H3 crosspeak should not be observed due to the anti orientation of H2 and H3.

Figure 26. Observed Regional NOESY Correlations for *syn-anti* Triazoline (**402**)



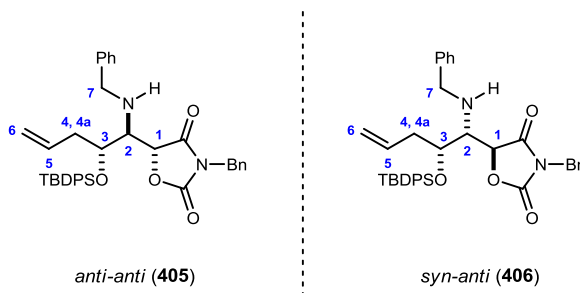
With the *anti-anti* **401** and *syn-anti* triazoline **402** in hand, the acid promoted triazoline ring fragmentation was attempted using both thermal and water-assisted conditions. Both triazolines were converted to the corresponding oxazolidine diones with moderate yield (Scheme 67). The conformational analysis of the *anti-anti* oxazolidine dione **405** was also evaluated by NMR (1D and 2D) experiments to independently determine the relative stereochemistry of the oxazolidine dione.

Scheme 67. Acid Promoted Oxazolidine Dione Formation



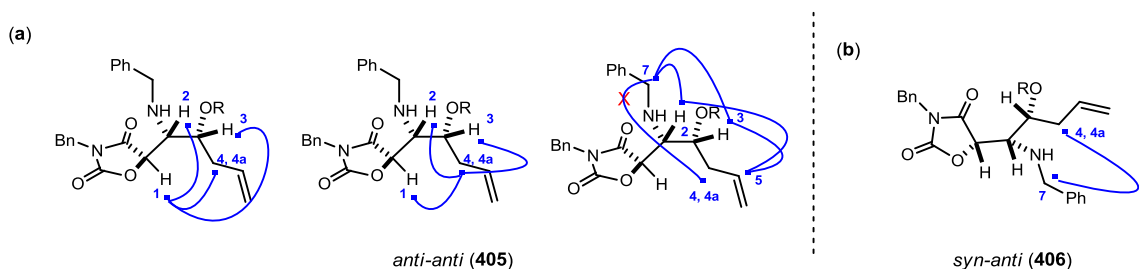
From the ^1H , ^{13}C and HSQC ($^1J_{\text{CH}}$), and NOESY NMR experiments, all the proton and carbon chemical shifts of the *anti-anti* oxazolidinone dione **405** were assigned (Figure 28).

Figure 27. Depiction of *anti-anti* (**405**) and *syn-anti* Oxazolidinone-Dione (**406**)



Beginning from the right next to amide functionality, crosspeaks for H1/H2, H1/H3, H2/H3 and H4/H1, H4/H2, H4/H3 defined the orientation of all hydrogens and single bond rotations. No H5/H1 correlation was observed. Additionally, the observation of H7/H2, H7/H3, and H5/H2, H5/H3, H5/H4 crosspeaks support the orientation of this rotamer (Figure 28).

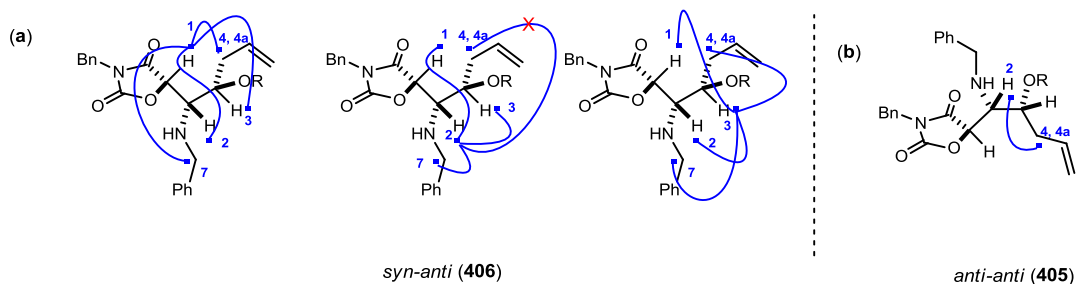
Figure 28. Observed Regional NOESY Correlations for *anti-anti* Oxazolidinone Dione (**405**)



The *syn-anti* oxazolidinone dione **406** was also evaluated by a NOESY experiment to

determine the relative stereochemistry and conformation.

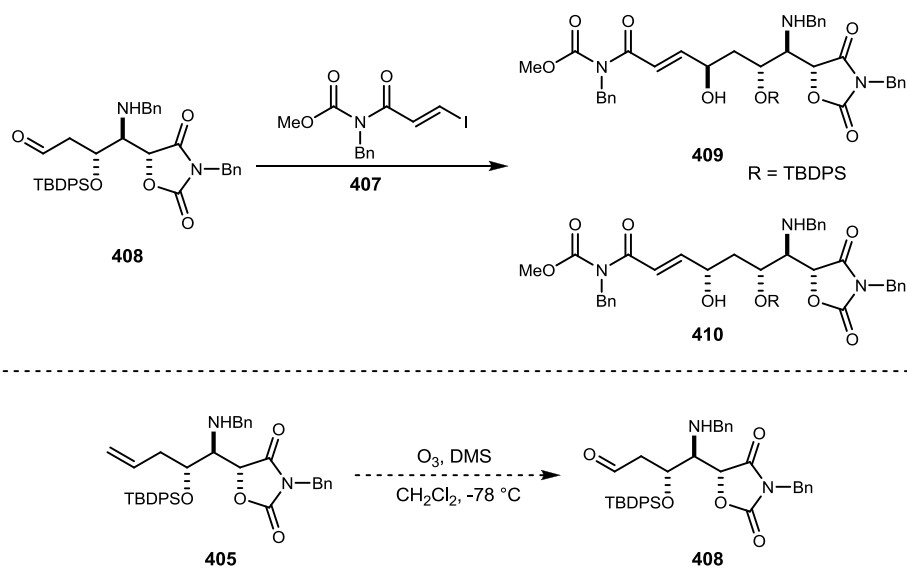
Figure 29. Observed Regional NOESY Correlations for *syn-anti* Oxazolidine Dione (**406**)



Beginning from the right next to amide functionality, crosspeaks for H1/H2, H1/H3, H1/H4a,4b and H1/H7, H2/H7, H2/H3, H3/H4a,4b defined the orientation of all hydrogens and single bond rotations. No H2/H4a,4b correlation was observed. In contrast, the *anti-anti* diastereomer (Figure 29-b) conformation is not consistent with the observed crosspeaks. For example, to maintain the crosspeaks at H1/H2, H1/H3, H1/H4a,4b, and H1/H7, H2/H7, H2/H3, H2 and H4a,4b crosspeaks should be observed due to the *syn* orientation of H2 and H4a,4b.

At this stage, we envisioned a synthesis of the target molecule using an intermolecular Nozaki-Hiyama-Kishi coupling reaction with β -iodo imide **407** and aldehyde **408**. However, ozonolysis of terminal alkene **405** gave multiple products without any desired aldehyde **408** (Scheme 68).

Scheme 68.



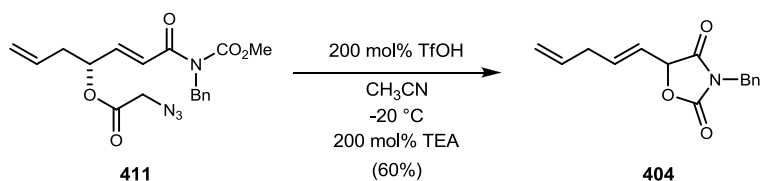
3.2.2 Model System: Intramolecular [3+2] Cycloaddition

It is an alternative to a diastereoselective intermolecular [3+2] cycloadditions, we naturally wondered whether an intramolecular variant could be developed. Acylation of hydroxyl group could provide an intramolecular azide moiety. As described by Lectka⁹⁶, bromoacetic acid was converted to azidoacetic acid. Then the acid chloride was made by treatment with oxalyl chloride and a catalytic amount of DMF. After removal of volatiles, the standard acylation condition was applied to form γ -substituted unsaturated imide **411**. With an intramolecular azide moiety, Brønsted acid-promoted [3+2] cycloaddition was attempted under the standard condition. However, the formation of the desired *trans*-triazoline was not observed. Combined acid-promoted S_N2' type cyclization of carbamate and elimination of the acetoxy group was faster than the desired azide addition to olefin

⁹⁶ Taggi, A. E.; Hafez, A. M.; Wack, H.; Young, B.; Ferraris, D.; Lectka, T. *J. Am. Chem. Soc.* **2002**, *124*, 6626.

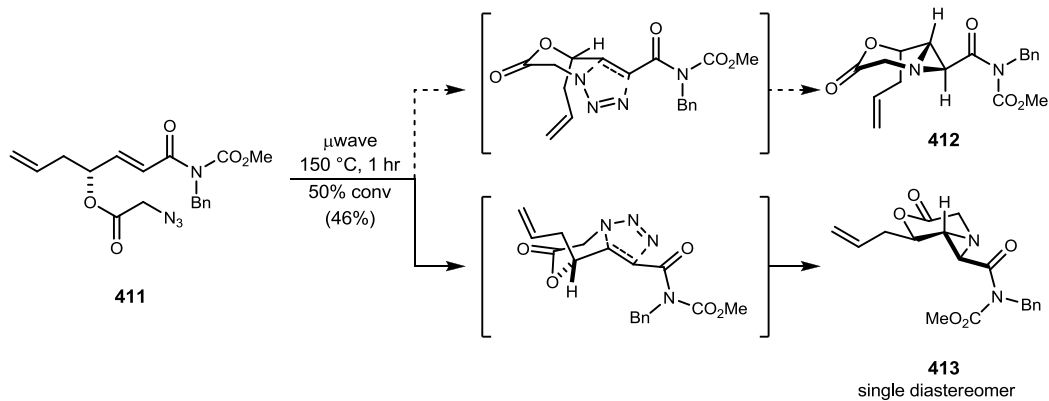
(Scheme 69).

Scheme 69.

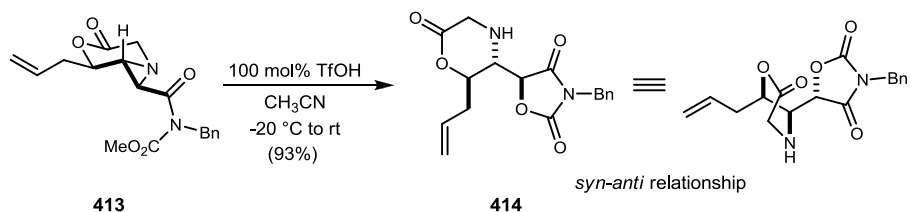


In order to achieve the desired [3+2] cycloaddition, instead of acid-promoted conditions, conventional heating and microwave-assisted protocols were attempted. However, conventional heating such as reflux condition and sealed-tube heating gave no conversion to products from the starting azidoimide system. Additionally, the microwave-assisted protocol produced the undesired *syn*-selective aziridination adduct **413** (Scheme 70). At this stage, even though the undesired *syn*-selective aziridination product was obtained, acid-promoted aziridine opening produced the corresponding oxazolidine dione with excellent yield (Scheme 71).

Scheme 70.

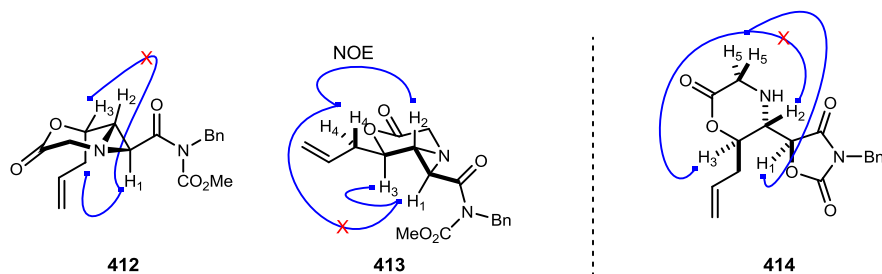


Scheme 71.



The *syn*-aziridine **413** and *syn-anti* oxazolidine dione **414** were also evaluated by NOESY experiments for the relative stereochemistry of structures and conformations (Figure 30-a). Beginning from the right next to amide functionality, crosspeaks for H2/H4, H1/H3 defined the orientation of all hydrogen and single bond rotations. No H1/H4 correlation was observed. In contrast, *anti*-aziridine **412** is not consistent with the observed crosspeaks. For example, H1/H4 should be observed due to the proximal distance between H1 and H4. Additionally, H1/H3 should not be observed due to the opposite orientation of H1 and H3. For the *syn-anti* oxazolidine dione **414**, crosspeaks for H1/H5, H3/H5 defined the orientation of all hydrogen and single bond rotations. No H2/H5 correlation was observed. For an *anti-anti* relationship, an H2/H5 crosspeak should be observed.

Figure 30. Observed NOESY Correlations for *syn*-Aziridine **413** and *syn-anti* Oxazolidine Dione **414**

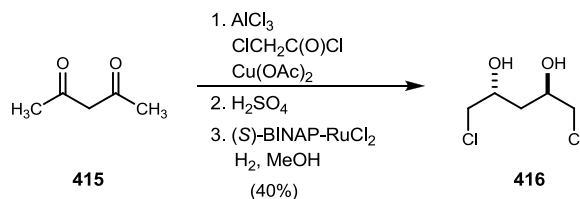


3.2.3 Progress Toward Double-Addition Strategy

3.2.3.1 Optimization of Bisimide Synthesis

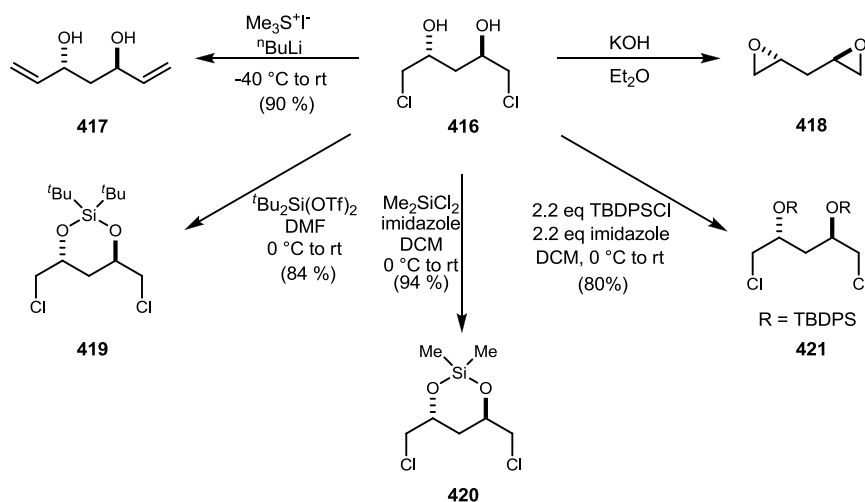
Based on the selectivity of acid promoted triazoline and oxazolidine dione formation from the intra- and intermolecular model systems, we engaged in a bidirectional approach to the zwittermicin core synthesis. Using the Rychnovsky preparation, 2,4-pentanedione was converted to chiral nonracemic (2*R*,4*R*)-1,5-dichloropentane-2,4-diol **416** in three steps with 40% overall yield (Scheme 72).⁹⁷

Scheme 72. Chiral Nonracemic Diol Synthesis



Chiral nonracemic 1,3-diol was considered as the bidirectional starting material due to the flexibility of protecting groups available to the 1,3-diol (Chart 1).

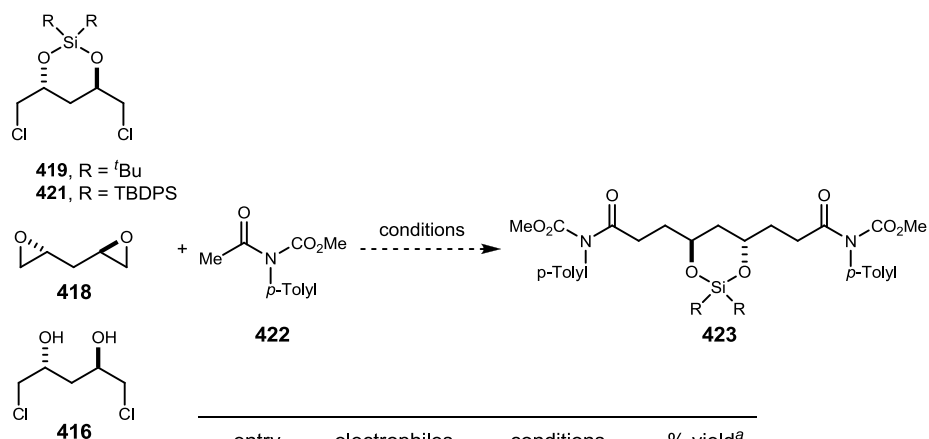
Chart 1. Flexibility of Protecting Group



⁹⁷ Rychnovsky, S. D.; Griesgraber, G.; Powers, J. P. *Org. Syn.* **2000**, *77*, 1.

To obtain the desired bis-imide, we tested different types of olefination approaches. An enolate alkylations was examined using dichloro compound **419** and **421** and readily available acetyl protected carbamate **422** (Table 30). However, only unreacted starting materials were obtained.

Table 30. Enolate Alkylation Approach to Bisimide Synthesis



entry	electrophiles	conditions	% yield ^a
1	419	LDA, THF, -78 °C	0
2		KHMDS, THF, -78 °C	0
3		ⁿ BuLi, THF, -78 °C	0

4	420	LDA, THF, -78 °C	0
5		KHMDS, THF, -78 °C	0
6		ⁿ BuLi, THF, -78 °C	0

7	421	LDA, THF, -78 °C	0
8		KHMDS, THF, -78 °C	0
9		ⁿ BuLi, THF, -78 °C	0

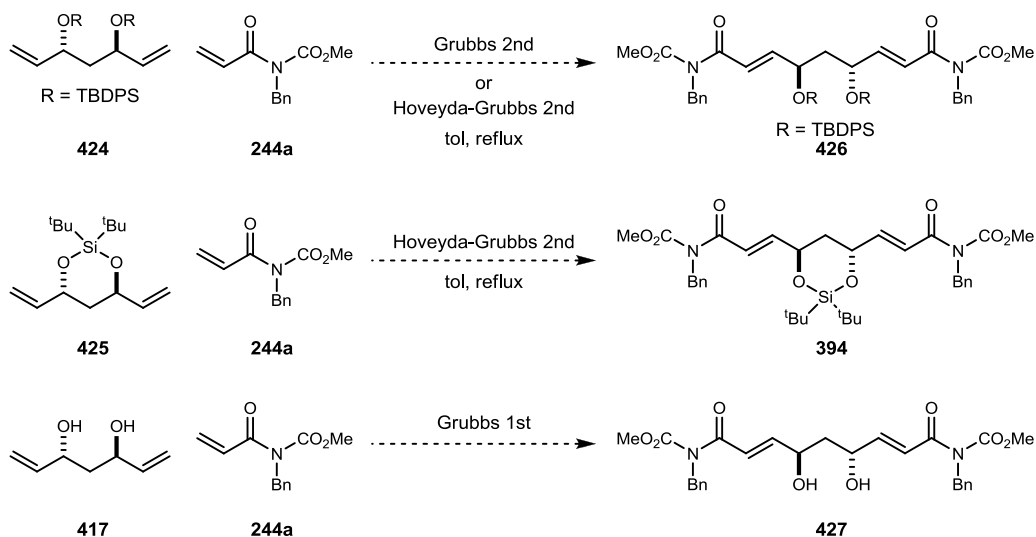
10	416	LDA, THF, -78 °C	0
11	418	LDA, THF, -78 °C	0

^aReactions monitored by ¹H NMR.

Alternative and more direct olefination methodologies were investigated next. The most reasonable and efficient approach to the bis-imide system **394** was the olefin cross metathesis approach (Scheme 73). After homologation of dichloro compound **416** to bisolefin **417**, the diol was protected with two different silyl protecting groups. Based on the intermolecular model system described earlier, bulky TBDPS group would provide

optimal selectivity to the [3+2] cycloaddition and be stable to TfOH conditions. Based on the types of olefin for olefin cross metathesis, protected diols **424**, **425** were considered type II and acryloyl imide **244a** was considered type III olefin. As a result, fast reactivity between the two olefins with no self-dimerization would be expected. However, combination of type II and type III olefins with various cross-metathesis catalyst such as Grubbs II and Hoveyda-Grubbs II catalyst failed to promote olefin cross-metathesis, even under prolonged reaction time and harsh reaction conditions. Additionally, unprotected diol **417** treated with Grubbs I catalyst also failed to promote the desired cross-metathesis reaction. Reactions were monitored by crude NMR analysis, and there was no sign of newly formed olefin peak between 5 ppm and 6 ppm.

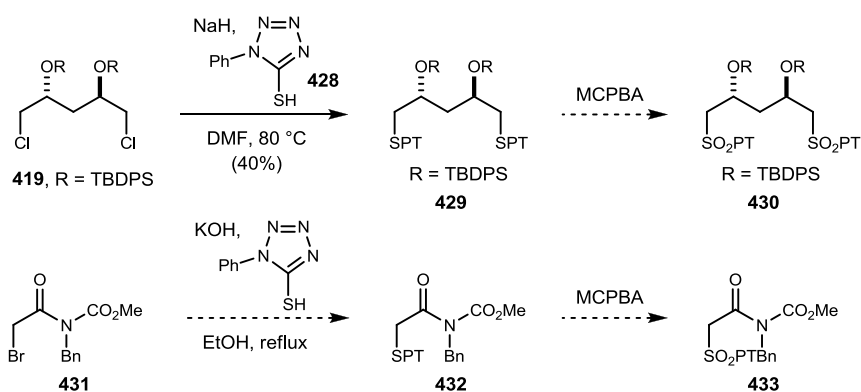
Scheme 73.



Other olefination reactions such as the modified Julia protocol, Wittig protocol, and Horner-Wadsworth-Emmons protocol were investigated. First of all, the modified Julia olefination was considered due to the availability of the starting material. After protection

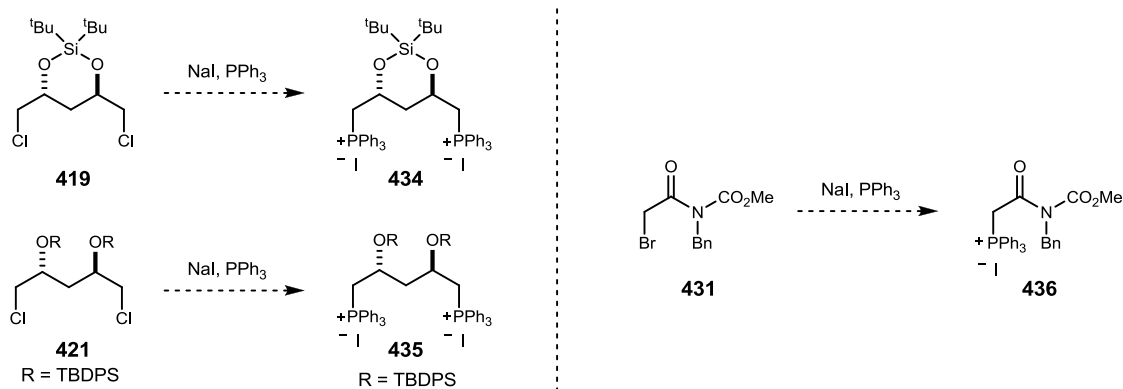
with a silyl group, dichloro-diols **419** and **421** were treated with phenyltetrazolethiol **428**. However, further oxidation of the thiol to the sulfone was not successful with various oxidants such as MCPBA and ammonium molybdate tetrahydrate. Another approach to the modified Julia olefination was to generate imide **433**. However, reaction with phenyltetrazole **428** gave a complex reaction mixture without any desired sulfide (**432**) formation.

Scheme 74.



Additionally, generation of triphenylphosphonium imide **436** or bistrisphenylphosphonium diols **434**, **435** were not successful under various reaction conditions with PPh₃ (Scheme 75).

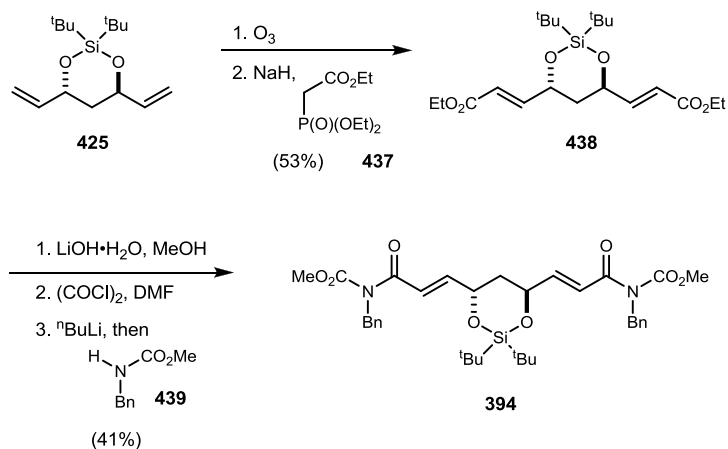
Scheme 75.



3.2.3.2 Horner-Wadsworth-Emmons Approach to Bisimide Synthesis

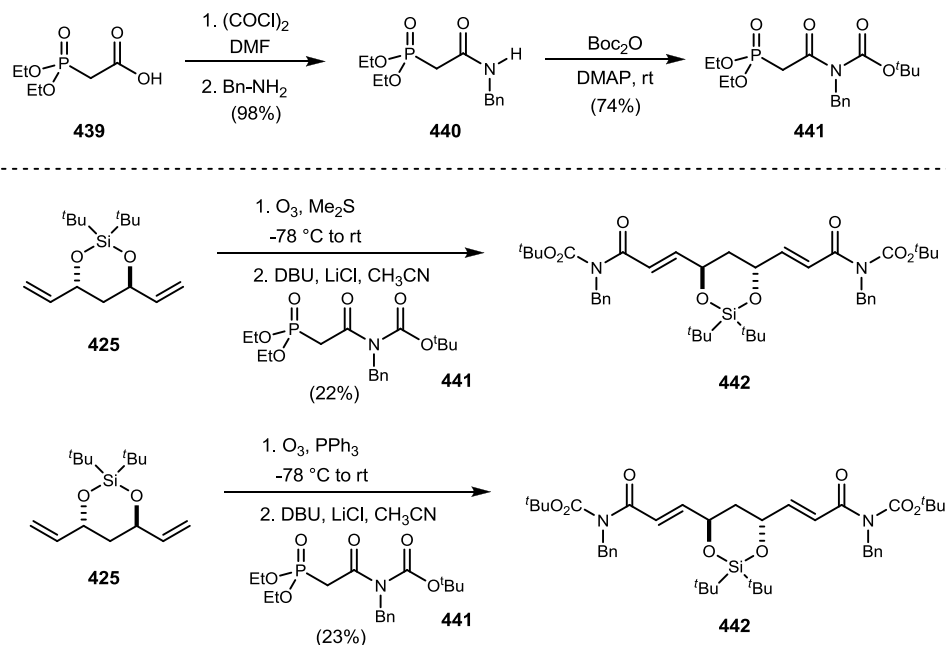
As an alternative to these unsuccessful routes to the needed C₂-symmetric bisimide synthesis, a stepwise Horner-Wadsworth-Emmons protocol was considered. After ozonolysis of bisolefin **425** to bisaldehyde, triethylphosphonoacetate **437** was added. The standard Horner-Wadsworth-Emmons protocol gave 53% yield of the desired bisester **438** (Scheme 76). With ester **438** in hand, functional group modification to the acid chloride was attempted and the crude acid chloride was coupled with *N*-Bn carbamate **439**. An initial test reaction gave 45% yield over three steps, but due to the instability of ester **438**, this sequence exhibited poor reproducibility.

Scheme 76.



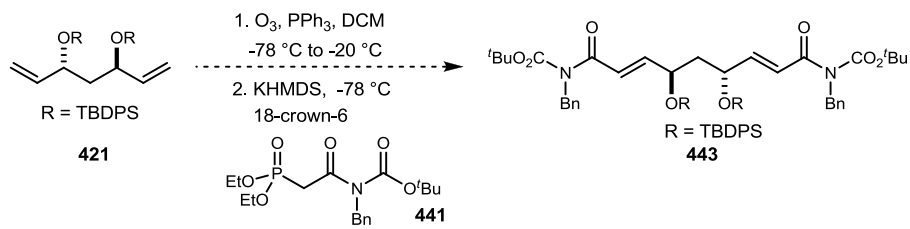
To avoid an unstable intermediate, a different reaction pathway was considered to generate stable phosphonoimide **441** in an easily scalable reaction sequence. To obtain the phosphonate functionality, Arbuzov reaction was considered first due to the accessibility of the required α -haloimide. Under standard reaction conditions, triethyl phosphite reacted with α -haloimide to generate desired phosphonoimide **441**. However, due to the long reaction time, low conversion, and stability of α -haloimide, an alternative route was again considered. Starting from the commercially available 2-(diethoxyphosphoryl)acetic acid **439**, in situ generation of acid chloride and coupling with benzylamine gave a quantitative yield of desired amide **440**. Direct coupling with *N*-Bn carbamate was also attempted, but as before, no desired product was detected. With the phosphonate amide in hand, reaction with di-tert-butyl carbamate and a catalytic amount of DMAP gave desired the phosphonoimide **441**. Compared to the previous approach, this reaction route gave efficient conversion in an easily scalable starting imide synthesis.

Scheme 77.



Next, two different bisolefins were subjected to the Horner-Wadsworth-Emmons reaction with phosphonoimide (Scheme 78). To achieve the desired diastereoselection as seen with the model system (Scheme 66), bulky TBDPS protected bisolefin **424** was also considered. However, various ozonolysis and HWE reaction conditions, still did not produce desired bisimide **443**.

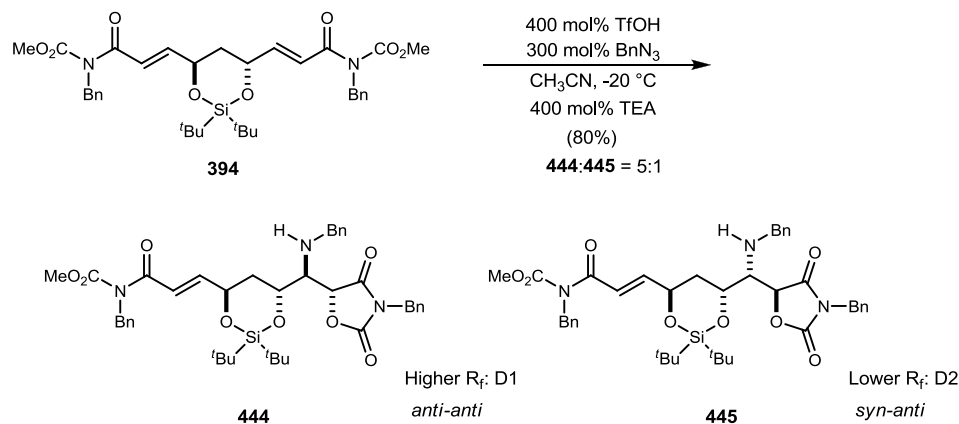
Scheme 78.



3.2.3.3 Progress Toward Double-Addition Strategy

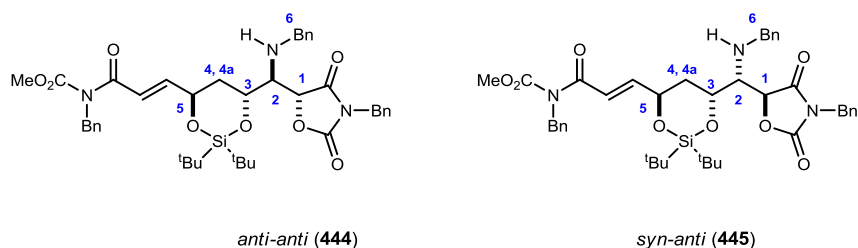
With the bisimide **394** in hand, we tested the acid-promoted [3+2] cycloaddition. Using the standard protocol with 2 equivalents of acid and 1.5 equivalents of benzyl azide for each olefin at -20 °C, the mono-oxazolidine dione **444** was isolated with a 5:1 ratio of desired *anti* addition as the major product, even when using the low temperature quench protocol. Despite the strictly anhydrous conditions applied, no triazoline formation was detected (Scheme 79).

Scheme 79.



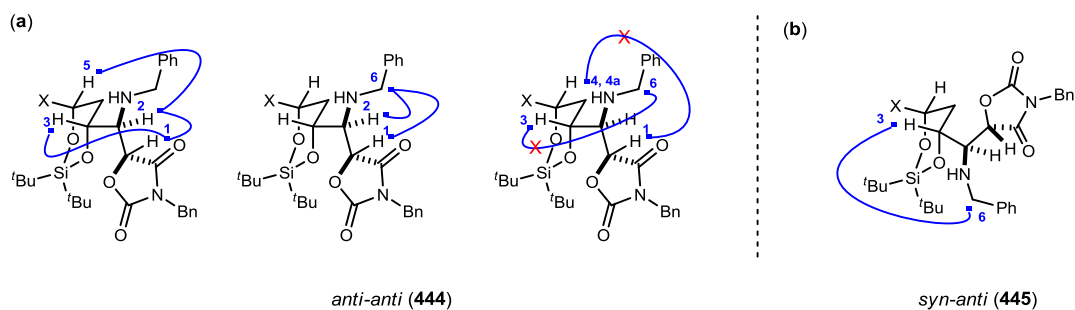
Conformational and configurational analysis of the *anti*-oxazolidine dione **444** was based upon NMR (1D and 2D) experiments. From the ¹H, ¹³C, HSQC (¹J_{CH}), and NOESY NMR experiments, all of the proton and carbon chemical shifts of the *anti*-oxazolidine dione **444** were assigned.

Figure 31. Depiction of *anti-anti* (**444**) and *syn-anti* Oxazolidine-Dione (**445**)



Beginning from C1 next to the amide functionality, crosspeaks for H1/H2, H1/H3, H1/H6, H2/H6, and H2/H5 defined the orientation of all hydrogens and single bond rotations (Figure 32-a). No H1/H4 correlation was observed, supporting the rotamer depicted wherein this hydrogen is oriented away from H1. Additionally, no H3/H6 correlation was observed, supporting the rotamer depicted wherein this hydrogen is oriented away from H3. In contrast, the *syn-anti* diastereomer (Figure 32-b) is not consistent with the observed crosspeaks. First, to support crosspeaks for H2/H5, the *syn-anti* diastereomer would require a proximal orientation between H3 and H6, which was not observed.

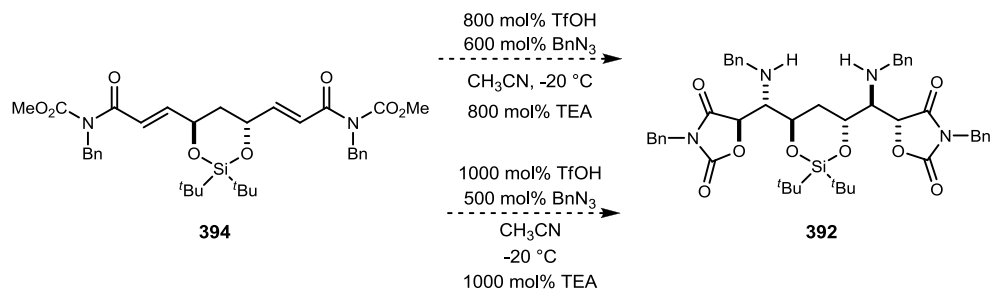
Figure 32. Observed NOESY Correlations for *anti-anti* Oxazolidine Dione (**444**)



Due to the unexpected formation of the mono-oxazolidine dione, we resubjected it to acid promoted cycloaddition conditions. The reaction was monitored by TLC, but there was no sign of any further reaction. After quenching the reaction, all of the starting material was recovered by column chromatography.

Next, we decided to use excess TfOH and benzyl azide for this double [3+2] cycloaddition and fragmentation reaction. By using 10 equivalents of TfOH and 8 equivalents of benzyl azide, the reaction gave two new spots by TLC analysis. However, NMR analysis of the crude reaction mixture revealed that there was no sign of triazoline or oxazolidine dione peaks. Furthermore, after column chromatography, two new compounds were isolated, but neither of them were the desired products.

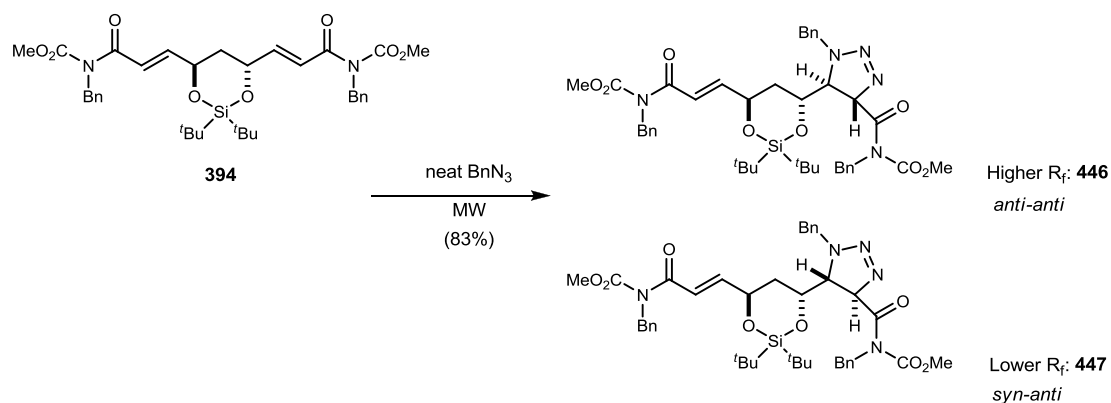
Scheme 80.



Reasoning that those conditions merely lacked the reactivity necessary, we began to investigate the conventional heating and microwave assisted [3+2] cycloaddition. Under conventional heating, prolonged reaction times led to only minor conversion of the starting material. To increase the conversion, a microwave assisted protocol was attempted, and this produced two products by crude NMR analysis (Scheme 81). By TLC analysis, the starting bisimide was fully converted to triazoline products, but the two

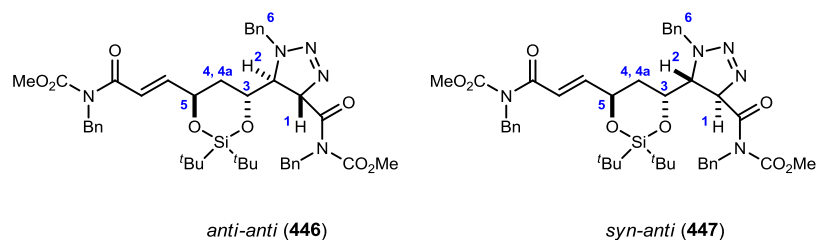
products had similar R_f values by TLC. Following repeated column chromatography, first compound of this mixture was enriched and subsequently characterized as triazoline **446**.

Scheme 81.



Conformational and configurational analysis of the *anti*-triazoline **446** was based upon NMR (1D and 2D) experiments. From the ^1H , ^{13}C , HSQC ($^1J_{\text{CH}}$), and NOESY NMR experiments, all of the proton and carbon chemical shifts of the *anti*- triazoline **446** were assigned.

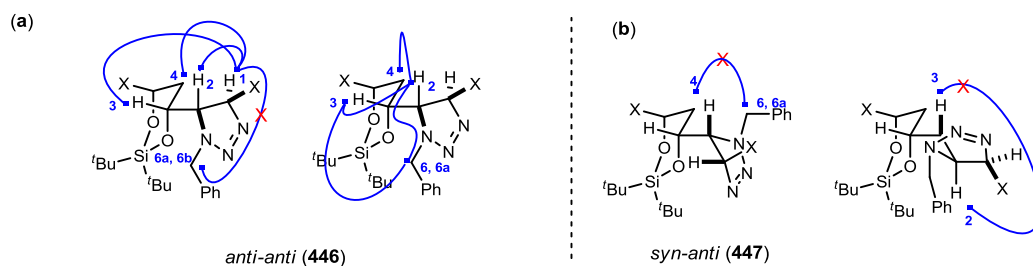
Figure 33. Depiction of *anti-anti* (**446**) and *syn-anti* Triazoline (**447**)



Beginning from C1 next to the amide functionality, crosspeaks for H1/H2, H1/H3, H1/H4, H2/H3, H2/H6, and H3/H6 defined the orientation of all hydrogens and single

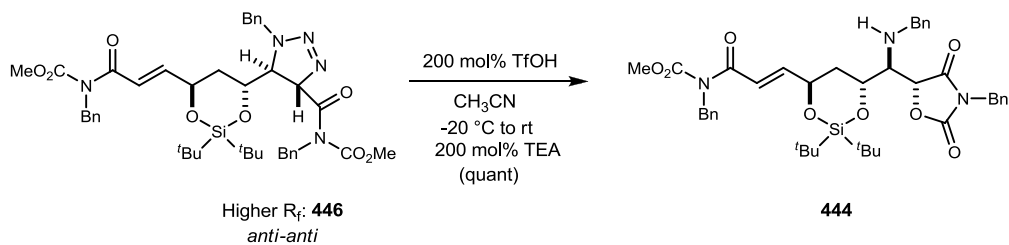
bond rotations (Figure 34-a). No H1/H6 correlation was observed, supporting the rotamer depicted wherein this hydrogen is oriented away from H1. In contrast, *syn-anti* diastereomer (Figure 34-b) is not consistent with the observed crosspeaks. First, to support crosspeaks for H2/H6 and H3/H6, the *syn-anti* diastereomer should have an H4/H6 correlation, which was not observed. Additionally, single bond rotation to avoid this H4/H6 correlation gave opposite orientation between H2 and both of H3 which was not consistent with observative crosspeak between H2 and H3.

Figure 34. Observed NOESY Correlations for *syn-anti* Triazoline (**446**)



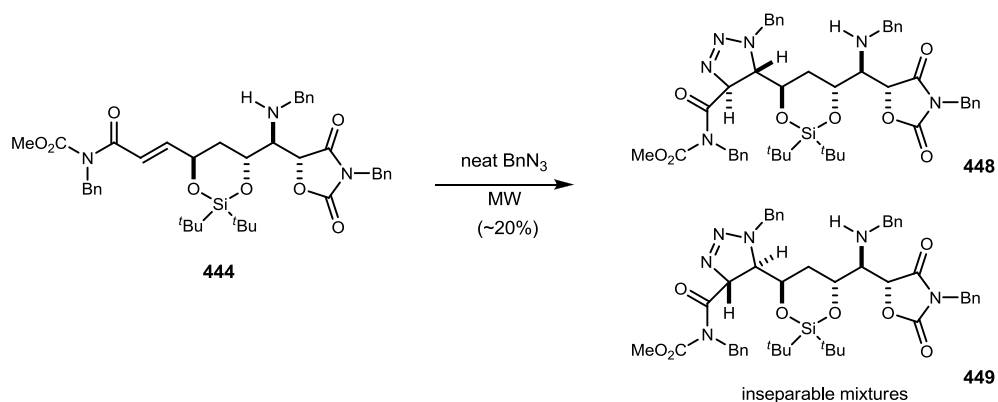
The stereochemical analysis of the *anti*-triazoline was further consistent based on its conversion to **444** utilizing acid promoted triazoline fragmentation. Recall that oxazolidine dione **444** was formed directly using the acid-promoted protocol. (Scheme 79).

Scheme 82.



At this stage, a linear approach to bis-oxazolidine dione was applied utilizing microwave assisted cycloaddition. Unfortunately, the low reactivity of imide **444** with benzyl azide provided a low yield, and produced two diastereomers that were not separable by TLC and column chromatography.

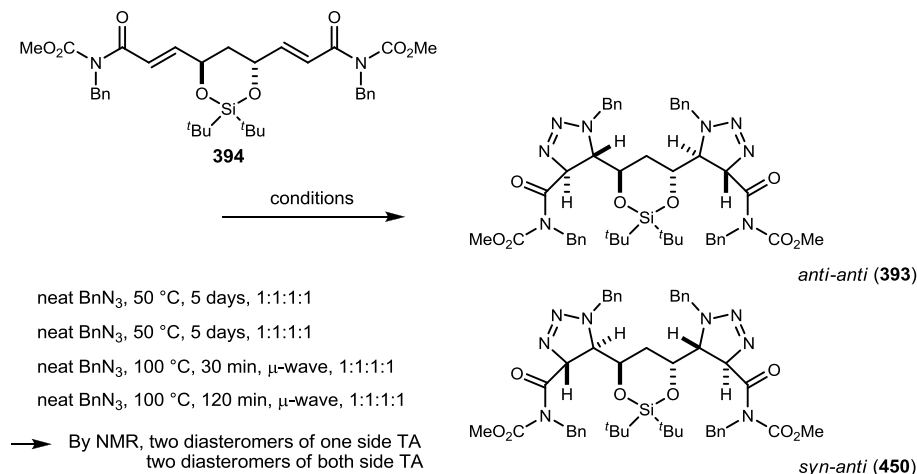
Scheme 83.



Due to the reactivity and selectivity, an extended time microwave assisted cycloaddition was investigated. During the course of the thermal cycloaddition study, it was found that prolonged reaction times could not convert bisimide to bistriazoline adduct. In all cases, the thermal cycloaddition produced two diastereomers of mono

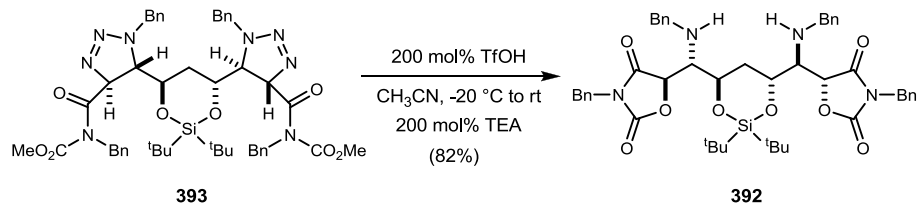
triazoline and two diastereomers of bistriazoline adducts. Furthermore, after isolation of desired bistriazoline **393**, the remaining mixture was resubjected to same reaction conditions but failed to produce additional conversion to the triazoline adduct.

Scheme 84



Even though the efficiency of the thermal [3+2] cycloaddition needs to be improved, the *anti-anti* bistriazoline **393** was converted to the corresponding *anti-anti* bisoxazolidine dione **392** with good efficiency (Scheme 85).

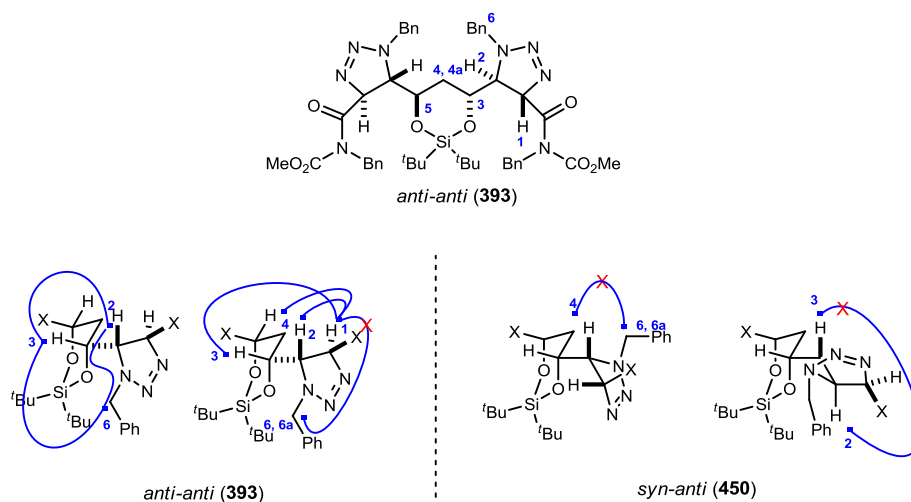
Scheme 85.



The stereochemical analysis of *anti-anti* bistriazoline **393** and *anti-anti* bisoxazolidine dione **392** was examined by NMR (1D and 2D) experiments. Based on the ¹H, ¹³C,

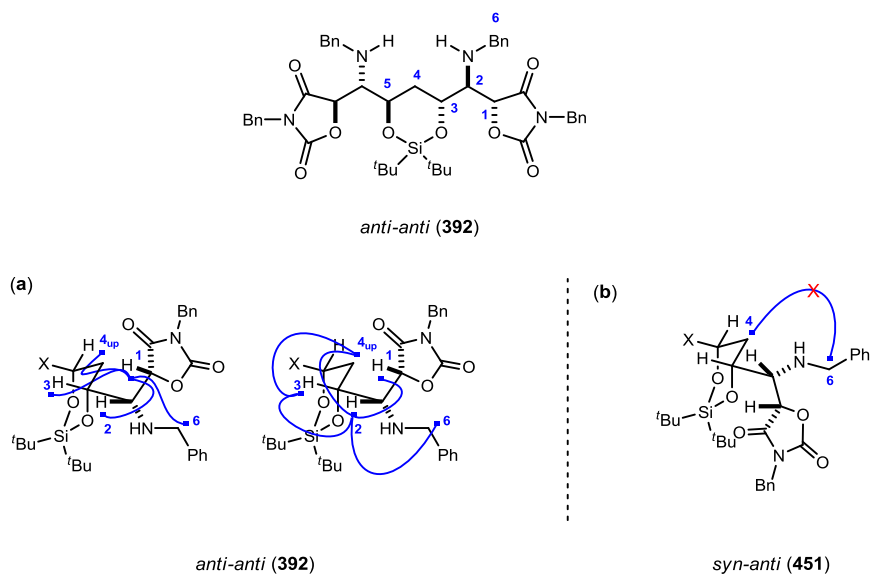
HSQC ($^1J_{\text{CH}}$), and NOESY NMR experiments, all the proton and carbon chemical shifts of **393** and **392** were assigned.

Figure 35. Depiction of *anti-anti* Triazolone (**393**) and Observed NOESY Correlations



Beginning from C1 next to the amide functionality, crosspeaks for H1/H2, H1/H3, H1/H4, H2/H3, H2/H6, and H3/H6 defined the orientation of all hydrogens and single bond rotations (Figure 35-a). No H1/H6 correlation was observed, supporting the rotamer depicted wherein this hydrogen is oriented away from H1. In contrast, the *syn-anti* diastereomer (Figure 35-b) is not consistent with the observed crosspeaks. First, to support crosspeaks for H2/H6 and H3/H6, the *syn-anti* diastereomer should have an H4/H6 correlation, which was not observed. Additionally, single bond rotation to avoid this H4/H6 correlation gave opposite orientation between H2 and both of H3 which was not consistent with observative crosspeak between H2 and H3.

Figure 36. Depiction of *anti-anti* Oxazolidine Dione (**392**) and Observed NOESY Correlations

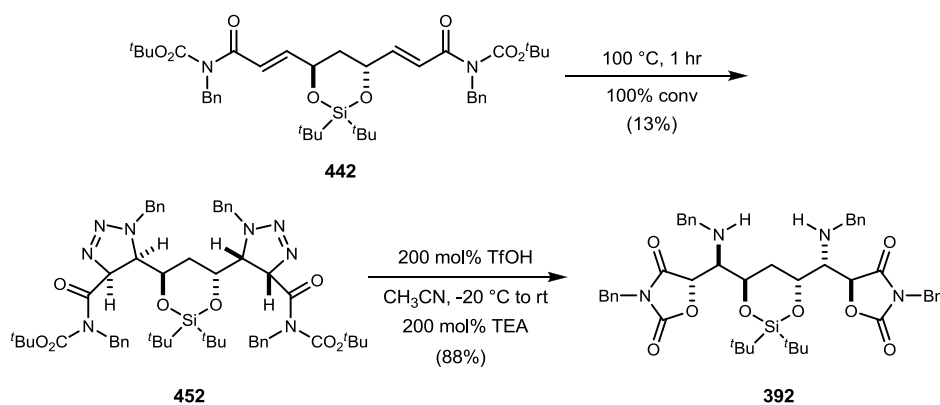


Beginning from C1 next to the amide functionality, crosspeaks for H1/H2, H1/H3, H1/H4, H1/H6, H2/H3, H2/H4, and H2/H6 defined the orientation of all hydrogens and single bond rotations (Figure 36-a). No H4/H6 correlation was observed, supporting the rotamer depicted wherein this hydrogen is oriented away from H4. In contrast, the *syn-anti* diastereomer (Figure 36-b) is not consistent with the observed crosspeaks. First of all, to support crosspeaks for H1/H4 and H2/H4, the *syn-anti* diastereomer should have an H4/H6 correlation, which was not observed. Additionally, single bond rotation to avoid this H4/H6 correlation gave opposite orientation between H1 and both of H6 which was not consistent with observation of only H6 crosspeak.

3.2.3.4 Progress Toward Double-Addition Strategy and Functionalization

Due to the instability of intermediate in the previous bisimide synthesis, an alternative route using phosphonate imide HWE gave a relatively better yield of bisimide **442**. With bisimide **442** in hand, microwave assisted cycloaddition was investigated. Unfortunately, as with previous experiments, crude NMR revealed two diastereomers of mono triazoline and two diastereomers of bistriazoline adducts. The behavior of new bisimide **442** was also the same as the previously used bisimide **394**. However, in this case, *syn-anti* triazoline **452** was easily separated by column chromatography. Additionally, conversion

Scheme 86.

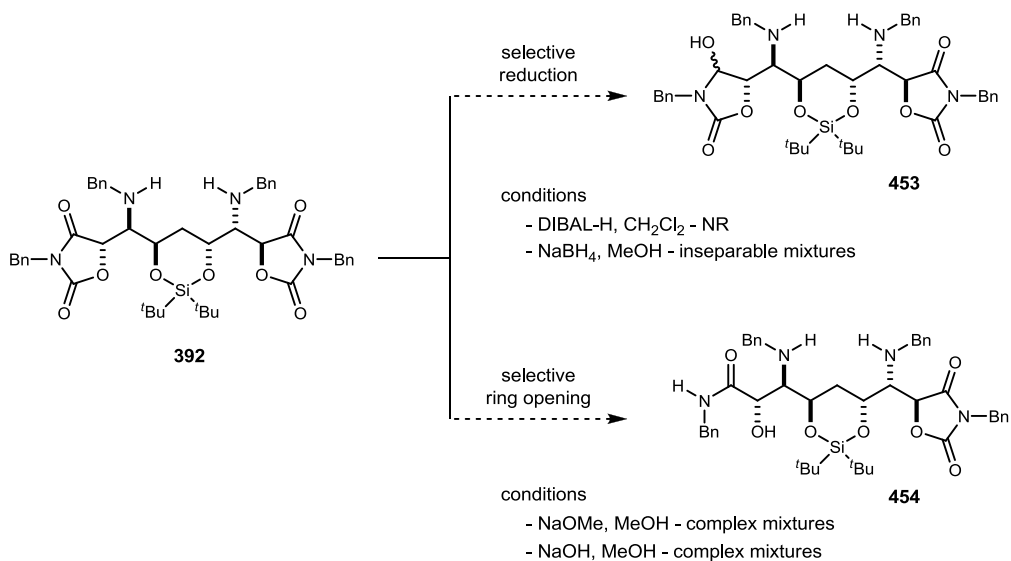


of *syn-anti* bistriazoline **452** to *syn-anti* bisoxazolidinone **392** gave improved yield.

The next step in the synthesis is functionalization of one side of the oxazolidinone dione to either the aminal **453** or the amide **454** (Scheme 87). First, a variety of reduction conditions were attempted using DIBAL and NaBH₄. Amide reduction using DIBAL at low temperature provided no reduction at all, and NaBH₄ reduction gave inseparable mixtures. At this point, excess NaBH₄ reduction was also attempted, however, we were not able to isolate any product of amide reduction. Next, hydroxide mediated hydrolysis of the oxazolidinone dione was attempted to produce α -hydroxy amide **454**. Varying

conditions such as the amount of NaOMe and the molarities of NaOH solution resulted in complex mixture, which after column chromatography, we were still not able to identify due to the complex NMR.

Scheme 87.



3.3. Conclusion

We have developed an efficient bidirectional approach to the synthesis of zwittermicin core. The Brønsted acid-catalyzed *anti* aminohydroxylation allows for a convergent route to key intermediate bis oxazolidinone which contains the desired four stereocenters of the zwittermicin core.

Chapter IV

Experimental Procedures

Flame-dried (under vacuum) glassware was used for all reactions. All reagents and solvents were commercial grade and purified prior to use when necessary. Tetrahydrofuran (THF) and dichloromethane (CH_2Cl_2) were dried by passage through a column of activated alumina as described by Grubbs.⁹⁸

Thin layer chromatography (TLC) was performed using glass-backed silica gel (250 μm) plates and flash chromatography utilized 230–400 mesh silica gel from Scientific Adsorbents. UV light, and/or the use of ceric ammonium molybdate and potassium iodoplatinate solutions were used to visualize products.

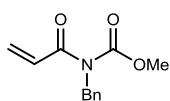
Melting points were recorded on a Laboratory Devices Mel-Temp capillary melting point apparatus or a Stanford Research Systems OptiMelt MPA100 and are reported uncorrected. IR spectra were recorded on a Nicolet Avatar 360 or a Thermo Electron (Nicolet) IR100/IR200 spectrophotometer and are reported in wavenumbers (cm^{-1}). Liquids and oils were analyzed as neat films on a NaCl plate (transmission), whereas solids were applied to a diamond plate (ATR) if a thin film could not be prepared.⁹⁹ Nuclear magnetic resonance spectra (NMR) were acquired on either a Varian instrument: INOVA-400 (400 MHz), VXR-400 (400 MHz) or Bruker instrument: AV-400 (400 MHz), DRX-500 (500 MHz), or AVII-600 (600 MHz). Chemical shifts are measured relative to residual solvent peaks as an internal standard set to δ 7.26 and δ 77.0 (CDCl_3) for ^1H and ^{13}C , respectively. Multiplicities are reported as singlet (s), doublet (d), triplet

⁹⁸ Pangborn, A. B.; Giardello, M.A.; Grubbs, R. H.; Rosen, R. K.; Timmers, F. J. *Organometallics* **1996**, *15*, 1518-1520.

⁹⁹ Note that triazoline N=N stretches are very weak when observed.

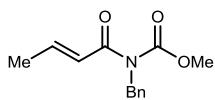
(t), quartet (q) or combinations thereof while higher coupling patterns are not abbreviated. Mass spectra were recorded using a Synapt hybrid quadrupole/oa-TOF Mass Spectrometer (Waters Corp., Milford, MA) equipped with a dual chemical ionization/electrospray (ESCI) source at Vanderbilt University. A post-acquisition gain correction was applied using sodium formate or sodium iodide as the lock mass. Alternatively, mass spectra were obtained by use of chemical ionization (CI) or electrospray ionization (ESI) at Indiana University. Mass spectra were recorded on a Kratos MS-80 spectrometer by use of chemical ionization (CI). Atlantic Microlabs, GA, performed combustion analyses.

General Procedure for Preparation of Imides: To a solution of carbamate (1 equiv) in tetrahydrofuran (0.3 M) cooled in a dry ice/acetone bath was added *n*-butyllithium (1.05 equiv, 2.5 M in hexanes), and stirring continued for 30 min. To the lithiated carbamate was added the acid chloride (1.1 equiv) either neat via syringe or as a solution in tetrahydrofuran (2 M) via cannula. The reaction mixture was stirred cold for 2 h and then water was added. Upon warming to rt, the tetrahydrofuran was removed in vacuo. Water was added to the reaction, and the aqueous phase was extracted with ethyl acetate. The combined organic phases were washed with brine, dried (MgSO₄), filtered, and concentrated in vacuo. The crude residue was triturated with hexanes-diethyl ether (10:1) to afford analytically pure imide.



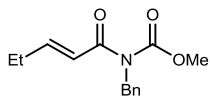
Acryloyl-benzyl-carbamic acid methyl ester (244a). According to the general procedure, *N*-benzylacrylamide (30.0 g, 186 mmol) provided the desired product after flash column chromatography (10% ethyl acetate in hexanes) as a

colorless oil (85%). $R_f = 0.45$ (30% EtOAc/Hexanes); IR (film) 3065, 3034, 2956, 1733, 1683 cm^{-1} ; ^1H NMR (400 MHz, CDCl_3) δ 7.30-7.23 (m, 5H), 7.12 (dd, $J = 16.9, 10.5$ Hz, 1H), 6.40 (dd, $J = 16.9, 1.6$ Hz, 1H), 5.75 (dd, $J = 10.5, 1.6$ Hz, 1H), 4.96 (s, 2H), 3.79 (s, 3H); ^{13}C NMR (100 MHz, CDCl_3) δ 168.4, 155.1, 137.6, 130.9, 129.1, 128.5, 127.8, 127.5, 53.8, 47.7; HRMS (EI) Exact mass calcd for $\text{C}_{12}\text{H}_{13}\text{NO}_3$ $[\text{M}]^+$ 219.0895, found 219.0896.



(E)-Methyl benzyl(but-2-enoyl)carbamate (244b). According to the

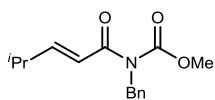
general procedure, (*E*)-*N*-benzylbut-2-enamide (5.50 g, 33.2 mmol) provided the desired product after flash column chromatography (10% ethyl acetate in hexanes) as a colorless oil (87%). $R_f=0.5$ (30% EtOAc/hexanes); IR (film) 3030, 2954, 1732, 1738 cm^{-1} ; ^1H NMR (400 MHz, CDCl_3) δ 7.32-7.22 (m, 5H), 7.05 (dq, $J = 15.5, 6.8$ Hz, 1H), 6.90 (dd, $J = 15.5, 1.6$ Hz, 1H), 4.95 (s, 2H), 3.79 (s, 3H), 1.92 (dd, $J = 6.8, 1.6$ Hz, 3H); ^{13}C NMR (100 MHz, CDCl_3) ppm 168.3, 155.2, 144.3, 137.8, 128.5, 127.7, 127.3, 125.3, 53.7, 47.6, 18.4; HRMS (CI): Exact mass calcd for $\text{C}_{13}\text{H}_{16}\text{NO}_3$ $[\text{M}+\text{H}]^+$ 234.1130, found 234.1130.



Benzyl-pent-2-enoyl-carbamic acid methyl ester (244c). According

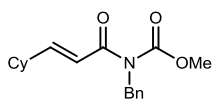
to the general procedure, (*E*)-*N*-benzylpent-2-enamide (5.50 g, 33.2 mmol) provided the desired product after flash column chromatography (10% ethyl acetate in hexanes) as a colorless oil (90%). $R_f = 0.6$ (30% EtOAc/Hexanes); IR (film) 2923, 1734, 1635 cm^{-1} ; ^1H NMR (400 MHz, CDCl_3) δ 7.28-7.18 (m, 5H), 7.06 (dt, $J = 15.6, 6.0$ Hz, 1H), 6.88 (dt, $J = 15.6, 1.6$ Hz, 1H), 4.92 (s, 2H), 3.72 (s, 3H), 2.23 (m, 2H), 1.05 (t, $J = 7.6$ Hz, 3H); ^{13}C NMR (100 MHz, CDCl_3) δ 168.3, 155.1, 150.2, 137.8, 128.3,

127.6, 127.2, 122.9, 53.5, 47.4, 25.6, 12.3; HRMS (EI) Exact mass calcd for C₁₄H₁₇NO₃ [M]⁺ 247.1208, found 247.1208.



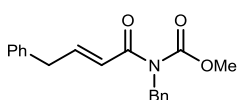
Benzyl-(4-methyl-pent-2-enoyl)-carbamic acid methyl ester (244d).

According to the general procedure, (*E*)-*N*-benzyl-4-methylpent-2-enamide (4.50 g, 39.9 mmol) provided the desired product after flash column chromatography (10% ethyl acetate in hexanes) as a colorless oil (43%). *R_f* = 0.7 (30% EtOAc/Hexanes); IR (film) 2894, 2919, 1735, 1681 cm⁻¹; ¹H NMR (400 MHz, CDCl₃) δ 7.34-7.22 (m, 5H), 7.04 (dd, *J* = 15.2, 6.8 Hz, 1H), 6.89 (dd, *J* = 15.2, 1.2 Hz, 1H), 4.98 (s, 2H), 3.79 (s, 3H), 2.52 (m, 1H), 1.11 (d, *J* = 6.8 Hz, 6H); ¹³C NMR (100 MHz, CDCl₃) δ 168.6, 155.1, 155.0, 137.8, 128.3, 127.7, 127.2, 121.2, 53.5, 47.5, 31.2, 21.4. HRMS (EI) Exact mass calcd for C₁₅H₁₉NO₃ [M]⁺ 261.1365, found 261.1359.



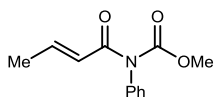
(*E*)-Methyl benzyl(3-cyclohexylacryloyl)carbamate (244e).

According to the general procedure, (*E*)-*N*-benzyl-3-cyclohexylacrylamide (7.00 g, 45.3 mmol) provided the desired product after flash column chromatography (10% ethyl acetate in hexanes) as a white solid (64%). *R_f*=0.6 (30% EtOAc/hexanes); IR (film) 2926, 1738, 1631, 1633 cm⁻¹; ¹H NMR (400 MHz, CDCl₃) δ 7.32-7.25 (m, 5H), 7.02 (dd, *J* = 12.2, 5.4 Hz, 1H), 6.89 (dd, *J* = 12.4, 0.8 Hz, 1H), 4.98 (s, 2H), 3.80 (s, 3H), 2.24-2.19 (m, 1H), 1.84-1.68 (m, 5H), 1.36-1.17 (m, 5H); ¹³C NMR (100 MHz, CDCl₃) ppm 168.6, 155.0, 153.8, 137.6, 128.2, 127.6, 127.1, 121.3, 53.4, 47.4, 40.6, 31.6, 25.8, 25.6; HRMS (CI): Exact mass calcd for C₁₈H₂₃NaNO₃ [M+Na]⁺ 324.1576, found 324.1584.



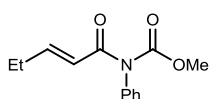
(E)-Methyl benzyl(4-phenylbut-2-enoyl)carbamate (244f).

According to the general procedure, (*E*)-*N*-benzyl-4-phenylbut-2-enamide (7.00 g, 45.3 mmol) provided the desired product after flash column chromatography (10% ethyl acetate in hexanes) as a white solid (25%). $R_f=0.5$ (30% EtOAc/hexanes); IR (film) 1734, 1683 cm^{-1} ; ^1H NMR (400 MHz, CDCl_3) δ 7.36-7.23 (m, 10H), 7.13 (dq, $J = 12.0, 5.6$ Hz, 1H), 6.98 (d, $J = 12.4$ Hz, 1H), 5.00 (s, 2H), 3.81 (s, 3H), 2.85 (t, $J = 6.4$ Hz, 2H), 2.62 (dd, $J = 12.0, 5.6$ Hz, 2H); ^{13}C NMR (100 MHz, CDCl_3) ppm 168.1, 155.0, 147.7, 140.8, 137.6, 129.4, 128.3, 128.2, 127.6, 127.2, 126.0, 124.0, 53.5, 47.4, 34.3, 34.1; HRMS (CI): Exact mass calcd for $\text{C}_{20}\text{H}_{21}\text{NaNO}_3$ $[\text{M}]^+$ 346.1419, found 346.1432.



But-2-enoyl-phenyl-carbamic acid methyl ester (244g).

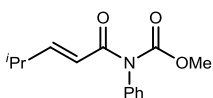
According to the general procedure, (*E*)-*N*-phenylbut-2-enamide (5.00 g, 31.0 mmol) provided the desired product after flash column chromatography (10% ethyl acetate in hexanes) as a white solid (4.82 g, 72%). Mp 110-111 $^\circ\text{C}$; $R_f=0.7$ (20% EtOAc/hexanes); IR (film) 3027, 2967, 1733, 1699, 1695 cm^{-1} ; ^1H NMR (400 MHz, CDCl_3) δ 7.38-7.31 (m, 3H), 7.09 (d, $J = 7.6$ Hz, 2H), 7.04-7.00 (m, 1H), 6.77 (d, $J = 15.2$ Hz, 1H), 3.66 (s, 3H), 1.86 (d, $J = 7.2$ Hz, 3H); ^{13}C NMR (100 MHz, CDCl_3) ppm 167.8, 154.8, 145.2, 138.4, 129.3, 128.5, 128.3, 124.8, 53.9, 18.5; HRMS (CI): Exact mass calcd for $\text{C}_{12}\text{H}_{13}\text{NO}_3$ $[\text{M}]^+$ 220.0968, found 220.0966.



Pent-2-enoyl-phenyl-carbamic acid methyl ester (244h).

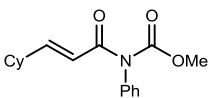
According to the general procedure, (*E*)-*N*-phenylpent-2-enamide (5.00 g, 28.5 mmol) provided the desired product after flash column chromatography (10% ethyl

acetate in hexanes) as a yellow solid (4.71 g, 72%). Mp 45-46 °C; $R_f=0.7$ (30% EtOAc/hexanes); IR (film) 3027, 2967, 1733, 1699, 1695 cm^{-1} ; ^1H NMR (400 MHz, CDCl_3) δ 7.41-7.33 (m, 3H), 7.12-7.06 (m, 3H), 6.75 (d, $J = 15.6$ Hz, 1H), 3.72 (s, 3H), 2.24 (m, 2H), 1.06 (t, $J = 7.2$ Hz, 3H); ^{13}C NMR (100 MHz, CDCl_3) ppm 168.2, 154.9, 151.6, 138.4, 129.3, 128.5, 128.4, 122.4, 54.0, 25.9, 12.4; HRMS (CI): Exact mass calcd for $\text{C}_{13}\text{H}_{15}\text{NO}_3$ $[\text{M}]^+$ 234.1125, found 234.1128.



(4-Methyl-pent-2-enoyl)-phenyl-carbamic acid methyl ester (244i).

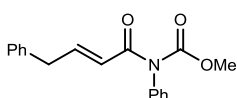
According to the general procedure, (*E*)-4-methyl-*N*-phenylpent-2-enamide (3.02 g, 15.8 mmol) provided the desired product after flash column chromatography (10% ethyl acetate in hexanes) as a white solid (2.31 g, 60%). Mp 55-56 °C; $R_f=0.6$ (30% EtOAc/hexanes); IR (film) 2960, 1732, 1698, 1634 cm^{-1} ; ^1H NMR (400 MHz, CDCl_3) δ 7.65-7.56 (m, 3H), 7.36-7.33 (m, 2H), 7.02 (dd, $J = 15.2, 6.8$ Hz, 1H), 6.73 (d, $J = 15.6$ Hz, 1H), 3.94 (s, 3H), 2.74-2.67 (m, 1H), 1.30 (d, $J = 7.2$ Hz, 3H), 1.27 (d, $J = 6.8$ Hz, 3H); ^{13}C NMR (100 MHz, CDCl_3) ppm 168.3, 156.1, 154.8, 138.5, 129.3, 128.5, 128.3, 120.8, 53.9, 31.4, 21.5; HRMS (CI): Exact mass calcd for $\text{C}_{14}\text{H}_{17}\text{NO}_3$ $[\text{M}]^+$ 248.1281, found 248.1284.



(*E*)-Methyl 3-cyclohexylacryloyl(phenyl)carbamate (244j).

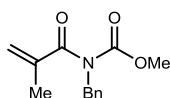
According to the general procedure, (*E*)-3-cyclohexyl-*N*-phenylacrylamide (7.02 g, 45.3 mmol) provided the desired product after flash column chromatography (10% ethyl acetate in hexanes) as a white solid (27%). $R_f=0.6$ (30% EtOAc/hexanes); IR (film) 2929, 1740, 1696 cm^{-1} ; ^1H NMR (400 MHz, CDCl_3) δ 7.46-7.39 (m, 3H), 7.17-7.15 (m, 2H), 7.04 (dd, $J = 12.4, 5.6$ Hz, 1H), 6.75 (d, $J = 12.4$ Hz,

1H), 3.75 (s, 3H), 2.21-2.19 (m, 1H), 1.94-1.51 (m, 5H), 1.36-1.14 (m, 5H); ¹³C NMR (100 MHz, CDCl₃) ppm 168.2, 154.9, 138.2, 129.2, 129.1, 128.3, 128.2, 128.1, 120.7, 53.7, 40.7, 31.6, 25.8, 25.6; HRMS (CI): Exact mass calcd for C₁₇H₂₁NaNO₃ [M]⁺ 310.1419, found 310.1421.



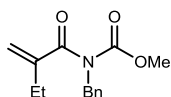
(E)-Methyl phenyl(4-phenylbut-2-enoyl)carbamate (244k).

According to the general procedure, (*E*)-*N*,4-diphenylbut-2-enamide (6.02 g, 23.9 mmol) provided the desired product after flash column chromatography (10% ethyl acetate in hexanes) as a white solid (71%). R_f=0.6 (30% EtOAc/hexanes); IR (film) 1738, 1695 cm⁻¹; ¹H NMR (400 MHz, CDCl₃) δ 7.47-7.14 (m, 10H), 6.84 (d, *J* = 12.4 Hz, 1H), 3.76 (s, 3H), 2.83 (t, *J* = 6.2 Hz, 2H), 2.60 (dd, *J* = 12.0, 6.2 Hz, 2H); ¹³C NMR (100 MHz, CDCl₃) ppm 167.6, 154.5, 148.7, 140.7, 138.0, 129.0, 128.9, 128.3, 128.2, 128.1, 126.0, 123.5, 53.7, 34.2, 34.1; HRMS (CI): Exact mass calcd for C₁₉H₁₉NaNO₃ [M]⁺ 332.1263, found 332.1262.



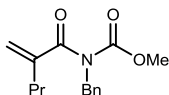
Benzyl-(2-methyl-acryloyl)-carbamic acid methyl ester (262b).

Colorless oil (76%). R_f=0.5 (30% EtOAc/hexanes); IR (film) 3038, 2949, 1743, 1683, 1443 cm⁻¹; ¹H NMR (400 MHz, CDCl₃) δ 7.33-7.26 (m, 5H), 5.19 (s, 1H), 5.15 (s, 1H), 4.88 (s, 2H), 3.74 (s, 3H), 2.00 (s, 3H); ¹³C NMR (100 MHz, CDCl₃) δ 174.0, 155.5, 143.1, 137.4, 128.6, 128.2, 127.7, 116.6, 53.7, 48.3, 19.2; HRMS (EI) Exact mass calcd for C₁₃H₁₅NO₃ [M]⁺ 233.1052, found 233.1057.



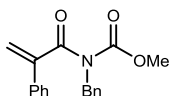
Benzyl-(2-methylene-butyl)-carbamic acid methyl ester (263b).

Colorless oil (98%). $R_f=0.6$ (30% EtOAc/hexanes); IR (film) 2957, 2931, 1768, 1673 cm^{-1} ; ^1H NMR (400 MHz, CDCl_3) δ 7.36-7.08 (m, 5H), 5.12 (d, $J = 6.4$ Hz, 2H), 4.85 (s, 2H), 3.66 (s, 3H), 2.36 (q, $J = 8.0$ Hz, 2H), 1.05 (t, $J = 8.0$ Hz, 3H); ^{13}C NMR (100 MHz, CDCl_3) δ 173.8, 155.3, 148.9, 137.4, 128.5, 128.1, 127.5, 114.1 53.4, 48.1, 25.8, 11.9; HRMS (EI) Exact mass calcd for $\text{C}_{14}\text{H}_{17}\text{NO}_3$ $[\text{M}]^+$ 247.1208, found 247.1210.



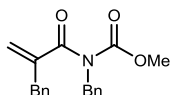
Benzyl-(2-methylene-pentanoyl)-carbamic acid methyl ester (264b).

Colorless oil (89%). $R_f=0.6$ (30% EtOAc/hexanes); IR (film) 2958, 2923, 1742, 1678 cm^{-1} ; ^1H NMR (400 MHz, CDCl_3) δ 7.40-7.14 (m, 5H), 5.20 (s, 1H), 5.03 (s, 1H), 4.90 (s, 2H), 3.74 (s, 3H), 2.34 (tt, $J = 7.6, 1.2$ Hz, 2H), 1.51 (m, 2H), 0.96 (t, $J = 7.6$ Hz, 3H); ^{13}C NMR (100 MHz, CDCl_3) δ 174.0, 155.6, 147.6, 137.6, 137.4, 128.7, 128.4, 128.3, 127.7, 115.7, 53.7, 48.5, 35.2, 21.3, 14.0; HRMS (EI) Exact mass calcd for $\text{C}_{15}\text{H}_{19}\text{NO}_3$ $[\text{M}]^+$ 261.1365, found 261.1363.



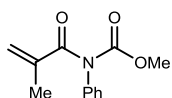
Methyl benzyl(2-phenylacryloyl)carbamate (265b).

White solid (4.82 g, 72%). $R_f=0.45$ (20% EtOAc/hexanes); IR (film) 3032, 2955, 1742, 1674, 1615 cm^{-1} ; ^1H NMR (400 MHz, CDCl_3) δ 7.42-7.22 (m, 10H), 5.52 (s, 1H), 5.04 (s, 1H), 5.04 (s, 2H), 3.53 (s, 3H); ^{13}C NMR (100 MHz, CDCl_3) ppm 171.8, 154.5, 147.1, 137.1, 136.2, 128.5, 128.4, 128.3, 127.7, 126.2, 116.2, 53.5, 48.1; HRMS (CI): Exact mass calcd for $\text{C}_{18}\text{H}_{17}\text{NO}_3$ $[\text{M}]^+$ 295.1208, found 295.1205.



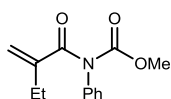
Benzyl-(2-benzyl-acryloyl)-carbamic acid methyl ester (266b).

Colorless oil (57%). $R_f=0.6$ (30% EtOAc/hexanes); IR (film) 2966, 2923, 1745, 1685 cm^{-1} ; ^1H NMR (400 MHz, CDCl_3) δ 7.34-7.12 (m, 10H), 5.27 (s, 1H), 5.03 (s, 1H), 5.25 (s, 2H), 4.88 (s, 2H), 3.71 (s, 3H); ^{13}C NMR (100 MHz, CDCl_3) δ 173.5, 155.5, 147.2, 137.9, 137.4, 129.7, 128.72, 128.69, 127.8, 126.8, 117.2, 53.7, 48.5, 39.2; HRMS (EI) Exact mass calcd for $\text{C}_{15}\text{H}_{19}\text{NO}_3$ $[\text{M}]^+$ 309.1365, found 309.1363.



(2-Methyl-acryloyl)-phenyl-carbamic acid methyl ester (267b).

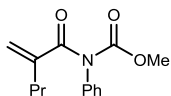
According to the general procedure, *N*-phenylmethacrylamide (23.1 g, 143 mmol) provided the desired product after flash column chromatography (10% ethyl acetate in hexanes) as a yellow oil (23.0 g, 74%). $R_f=0.7$ (30% EtOAc/hexanes); IR (film) 3065, 3033, 2957, 1742, 1732 cm^{-1} ; ^1H NMR (400 MHz, CDCl_3) δ 7.41-7.33 (m, 3H), 7.15-7.13 (m, 2H), 5.50 (s, 1H), 5.37 (s, 1H), 3.74 (s, 3H), 2.03 (s, 3H); ^{13}C NMR (100 MHz, CDCl_3) ppm 173.6, 155.2, 142.4, 138.2, 129.4, 128.3, 127.95, 119.4, 54.0, 19.1; HRMS (CI): Exact mass calcd for $\text{C}_{12}\text{H}_{14}\text{NO}_3$ $[\text{M}+\text{H}]^+$ 220.0968, found 220.0971.



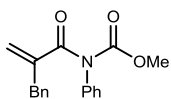
Methyl 2-methylenebutanoyl(phenyl)carbamate (268b).

According to the general procedure, 2-methylene-*N*-phenylbutanamide (10.0 g, 99.8 mmol) provided the desired product after flash column chromatography (10% ethyl acetate in hexanes) as a yellow oil (15.1 g, 65%). $R_f=0.7$ (30% EtOAc/hexanes); IR (film) 1746, 1695, 1439, 1256, 1081 cm^{-1} ; ^1H NMR (400 MHz, CDCl_3) δ 7.38-7.32 (m, 2H), 7.31-7.26 (m, 1H), 7.13-7.08 (m, 2H), 5.46 (s, 1H), 5.31 (s, 1H), 3.68 (s, 3H), 2.37 (q, $J = 7.5$ Hz, 2H), 1.08 (t, $J = 7.4$ Hz, 3H); ^{13}C NMR (100 MHz, CDCl_3) ppm 173.4, 155.0, 148.1, 138.1, 129.2, 128.0, 127.7, 116.9, 53.7, 25.5, 11.9; HRMS (CI): Exact mass calcd

for $C_{13}H_{16}NO_3$ $[M+H]^+$ 234.1052, found 234.1134. *Anal.* Calcd for $C_{13}H_{15}N_1O_3$: C, 66.94; H, 6.48; N, 6.00. Found C, 66.86; H, 6.55; N, 6.31.



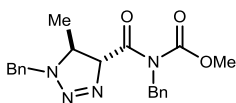
Methyl 2-methylenepentanoyl(phenyl)carbamate (269b). According to the general procedure, 2-methylene-*N*-phenylpentanamide (5.60 g, 29.5 mmol) provided the desired product after flash column chromatography (10% ethyl acetate in hexanes) as a yellow oil (3.7 g, 50%). $R_f=0.7$ (30% EtOAc/hexanes); IR (film) 1746, 1696, 1438, 1255, 1065 cm^{-1} ; 1H NMR (400 MHz, $CDCl_3$) δ 7.36-7.32 (m, 2H), 7.31-7.25 (m, 1H), 7.12-7.08 (m, 2H), 5.49 (s, 1H), 5.32 (s, 1H), 3.69 (s, 3H), 2.30 (t, $J = 7.6$ Hz, 2H), 1.45-1.55 (m, 2H), 0.90 (t, $J = 7.4$ Hz, 3H); ^{13}C NMR (100 MHz, $CDCl_3$) ppm 173.3, 154.9, 146.6, 138.1, 129.2, 128.0, 127.4, 118.3, 53.7, 34.7, 21.0, 13.7; HRMS (CI): Exact mass Calcd for $C_{14}H_{17}NNaO_3$ $[M+Na]^+$ 270.1106, found 270.1117. *Anal.* calcd for $C_{14}H_{17}N_1O_3$: C, 68.00; H, 6.93; N, 5.66. Found C, 67.92; H, 7.09; N, 5.49.



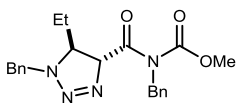
Methyl 2-benzylprop-2-enoyl(phenyl)carbamate (270b). According to the general procedure, 2-benzyl-*N*-phenylacrylamide (12.0 g, 73.9 mmol) provided the desired product after flash column chromatography (10% ethyl acetate in hexanes) as a yellow oil (7.3 g, 33%). $R_f=0.7$ (30% EtOAc/hexanes); IR (film) 1745, 1694, 1494, 1438, 1264, 1071 cm^{-1} ; 1H NMR (400 MHz, $CDCl_3$) δ 7.43-7.24 (m, 5H), 7.23-7.15 (m, 3H), 6.90 (d, $J = 7.6$ Hz, 2H), 5.57 (s, 1H), 5.22 (s, 1H), 3.67 (s, 5H); ^{13}C NMR (100 MHz, $CDCl_3$) ppm 172.6, 154.8, 145.9, 138.0, 137.6, 129.4, 129.1, 128.5, 128.0, 127.7, 126.6, 120.4, 53.7, 38.9; HRMS (CI): Exact mass calcd for $C_{18}H_{17}NNaO_3$ $[M+Na]^+$ 318.1106, found 318.1105. *Anal.* calcd for $C_{18}H_{17}N_1O_3$: C, 73.20; H, 5.80; N, 4.74. Found C, 73.18; H, 5.92; N, 4.85.

General Procedure for Acid Catalyzed Triazoline Formation

A solution of the Michael acceptor (1.0 equiv) in CH₃CN (0.3 M) was cooled to -20 °C and treated with triflic acid (2.0 equiv). Benzyl azide (1.5 equiv) was then added and the reaction was allowed to stir until complete conversion. The reaction mixture was quenched with distilled triethylamine (2.0 equiv) at -20 °C. The solution was dried and concentrated to an oil that was purified by flash chromatography to provide the desired triazoline in analytically pure form.

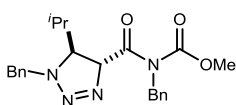


Methyl benzyl((4*R*,5*S*)-1-benzyl-5-methyl-4,5-dihydro-1*H*-1,2,3-triazole-4-carbonyl)carbamate (246b). According to the general procedure, (*E*)-methyl benzyl(but-2-enoyl)carbamate (117 mg, 0.50 mmol) provided the desired product after flash column chromatography (10% ethyl acetate in hexanes) as a colorless oil (134 mg, 73%). IR (film) 3300, 3063, 2933, 2850, 1814, 1733 cm⁻¹; ¹H NMR (400 MHz, CDCl₃) δ 7.31-7.24 (m, 10H), 5.64 (d, *J* = 11.2 Hz, 1H), 4.96 (d, *J* = 14.8 Hz, 1H), 4.94 (d, *J* = 15.2 Hz, 1H), 4.88 (d, *J* = 15.2 Hz, 1H), 4.64 (d, *J* = 15.6 Hz, 1H), 3.83 (s, 3H), 3.80 (dq, *J* = 12.4, 6.0 Hz, 1H), 1.16 (d, *J* = 6.4 Hz, 3H); ¹³C NMR (100 MHz, CDCl₃) ppm 171.7, 155.6, 139.6, 134.7, 129.1, 129.0, 128.9, 128.7, 128.6, 128.4, 128.1, 127.3, 82.0, 53.5, 51.8, 43.7, 15.1; HRMS (ED): Exact mass calcd for C₂₀H₂₂NaN₄O₃ [M+Na]⁺ 367.1765, found 367.1764.



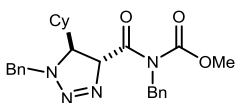
Methyl benzyl((4*R*,5*S*)-1-benzyl-5-ethyl-4,5-dihydro-1*H*-1,2,3-triazole-4-carbonyl)carbamate (246c). According to the general procedure, (*E*)-methyl benzyl(pent-2-enoyl)carbamate (123 mg, 0.50 mmol) provided the desired product after flash column chromatography (10% ethyl acetate in hexanes) as a

colorless oil (150 mg, 78%). IR (film) 3383, 2962, 2853, 1744, 1698 cm^{-1} ; ^1H NMR (400 MHz, CDCl_3) δ 7.41-7.07 (m, 10H), 5.85 (d, $J = 10.4$ Hz, 1H), 4.97 (d, $J = 15.6$ Hz, 1H), 4.96 (d, $J = 15.2$ Hz, 1H), 4.89 (d, $J = 15.2$ Hz, 1H), 4.62 (d, $J = 15.2$ Hz, 1H), 3.84 (s, 3H), 3.82-3.75 (m, 1H), 1.69-1.59 (m, 1H), 1.49-1.38 (m, 1H), 0.76 (t, $J = 7.6$ Hz, 3H); ^{13}C NMR (100 MHz, CDCl_3) ppm 170.2, 155.0, 137.0, 135.8, 128.6, 128.4, 128.0, 127.8, 127.4, 127.3, 83.8, 59.2, 54.0, 52.3, 48.2, 23.8, 9.2; HRMS (CI): Exact mass calcd for $\text{C}_{21}\text{H}_{25}\text{N}_4\text{O}_3$ $[\text{M}+\text{H}]^+$ 381.1921, found 381.1922.



Methyl benzyl((4*R*,5*S*)-1-benzyl-5-isopropyl-4,5-dihydro-1*H*-1,2,3-triazole-4-carbonyl)carbamate (246d). According to the

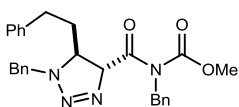
general procedure, (*E*)-methyl benzyl(4-methylpent-2-enoyl)carbamate (125 mg, 0.47 mmol) provided the desired product after flash column chromatography (10% ethyl acetate in hexanes) as a colorless oil (140 mg, 75%). IR (film) 3063, 2958, 1954, 1743, 1700 cm^{-1} ; ^1H NMR (400 MHz, CDCl_3) δ 7.30-7.18 (m, 10H), 6.01 (d, $J = 10.4$ Hz, 1H), 5.06 (d, $J = 15.2$ Hz, 1H), 4.95 (d, $J = 15.2$ Hz, 1H), 4.88 (d, $J = 15.2$ Hz, 1H), 4.58 (d, $J = 15.2$ Hz, 1H), 3.86-3.83 (m, 4H), 1.98-1.90 (m, 1H), 0.77 (d, $J = 6.8$ Hz, 3H), 0.73 (d, $J = 6.8$ Hz, 3H); ^{13}C NMR (100 MHz, CDCl_3) ppm 170.3, 155.0, 137.0, 135.6, 128.6, 128.4, 128.0, 127.8, 127.4, 127.3, 80.5, 62.4, 54.1, 48.2, 27.6, 18.7, 16.4; HRMS (CI): Exact mass calcd for $\text{C}_{22}\text{H}_{27}\text{N}_4\text{O}_3$ $[\text{M}+\text{H}]^+$ 395.2078, found 395.2072.



Methyl benzyl((4*R*,5*S*)-1-benzyl-5-cyclohexyl-4,5-dihydro-1*H*-1,2,3-triazole-4-carbonyl)carbamate (246e). According to the

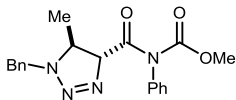
general procedure, (*E*)-methyl benzyl(3-cyclohexylacryloyl)carbamate (150 mg, 0.49 mmol) provided the desired product after flash column chromatography (10% ethyl

acetate in hexanes) as a colorless oil (149 mg, 70%). IR (film) 3063, 2926, 2853, 1744, 1699 cm^{-1} ; ^1H NMR (400 MHz, CDCl_3) δ 7.27-7.16 (m, 10H), 6.00 (d, $J = 10.4$ Hz, 1H), 5.01 (d, $J = 15.2$ Hz, 1H), 4.92 (d, $J = 15.2$ Hz, 1H), 4.86 (d, $J = 15.2$ Hz, 1H), 4.57 (d, $J = 15.2$ Hz, 1H), 3.83 (s, 3H), 3.80 (dd, $J = 10.4, 4.2$ Hz, 1H), 1.68-1.47 (m, 5H), 1.39-1.36 (m, 1H), 1.17-0.98 (m, 3H), 0.85-0.69 (m, 2H); ^{13}C NMR (100 MHz, CDCl_3) ppm 170.2, 155.0, 137.0, 135.6, 128.5, 128.4, 128.0, 127.7, 127.3, 127.2, 81.3, 61.9, 54.0, 52.8, 48.2, 38.1, 29.5, 27.2, 26.1, 25.7; HRMS (CI): Exact mass calcd for $\text{C}_{25}\text{H}_{31}\text{N}_3\text{O}_4$ $[\text{M}+\text{H}]^+$ 434.2318, found 435.2397.



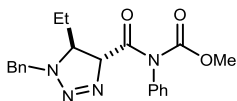
Methyl benzyl((4*R*,5*S*)-1-benzyl-5-phenethyl-4,5-dihydro-1*H*-1,2,3-triazole-4-carbonyl)carbamate (246f). According to the

general procedure, (*E*)-methyl benzyl(5-phenylpent-2-enoyl)carbamate (168 mg, 0.50 mmol) provided the desired product after flash column chromatography (10% ethyl acetate in hexanes) as a colorless oil (175 mg, 76%). IR (film) 3062, 1744, 1697 cm^{-1} ; ^1H NMR (400 MHz, CDCl_3) δ 7.33-7.14 (m, 13H), 7.02 (d, $J = 7.2$ Hz, 2H), 5.94 (d, $J = 10.8$ Hz, 1H), 4.97 (d, $J = 15.2$ Hz, 1H), 4.94 (d, $J = 15.2$ Hz, 1H), 4.92 (d, $J = 14.8$ Hz, 1H), 4.67 (d, $J = 15.2$ Hz, 1H), 3.90 (ddd, $J = 10.6, 7.8, 3.6$ Hz, 1H), 3.84 (s, 3H), 2.55-2.40 (m, 2H), 2.01-1.92 (m, 1H), 1.79-1.69 (m, 1H); ^{13}C NMR (100 MHz, CDCl_3) ppm 169.9, 154.7, 140.5, 136.8, 135.5, 128.5, 128.3, 128.2, 128.1, 128.0, 127.7, 127.3, 127.2, 125.9, 84.4, 58.0, 53.9, 52.4, 48.1, 32.7, 31.2; HRMS (CI): Exact mass calcd for $\text{C}_{27}\text{H}_{29}\text{N}_4\text{O}_3$ $[\text{M}+\text{H}]^+$ 457.2234, found 457.2242.



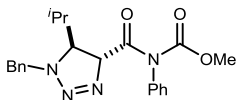
Methyl (4R,5S)-1-benzyl-5-methyl-4,5-dihydro-1H-1,2,3-triazole-4-carbonyl(phenyl)carbamate (246g). According to the

general procedure, (*E*)-methyl but-2-enoyl(phenyl)carbamate (104 mg, 0.47 mmol) provided the desired product after flash column chromatography (10% ethyl acetate in hexanes) as a colorless oil (109 mg, 62%). $R_f=0.50$ (30% EtOAc/hexanes); IR (film) 3063, 3031, 2955, 2086, 1747, 1703, 1683, 1652 cm^{-1} ; ^1H NMR (400 MHz, CDCl_3) δ 7.38-7.07 (m, 10H), 5.72 (d, $J = 11.2$ Hz, 1H), 4.90 (d, $J = 15.2$ Hz, 1H), 4.63 (d, $J = 15.2$ Hz, 1H), 3.79-3.76 (m, 1H), 3.74 (s, 3H), 1.14 (d, $J = 6.4$ Hz, 3H); ^{13}C NMR (100 MHz, CDCl_3) ppm 169.8, 154.2, 137.4, 135.4, 129.0, 128.4, 128.2, 128.0, 127.8, 127.6, 85.7, 54.3, 54.0, 51.9, 16.7; HRMS (CI): Exact mass calcd for $\text{C}_{19}\text{H}_{20}\text{N}_4\text{O}_3$ $[\text{M}]^+$ 352.1530, found 352.1530.



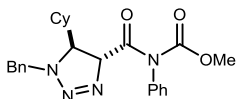
Methyl (4R,5S)-1-benzyl-5-ethyl-4,5-dihydro-1H-1,2,3-triazole-4-carbonyl(phenyl)carbamate (246h). According to the general

procedure, (*E*)-methyl pent-2-enoyl(phenyl)carbamate (115 mg, 0.49 mmol) provided the desired product after flash column chromatography (10% ethyl acetate in hexanes) as a colorless oil (133 mg, 73%). $R_f=0.50$ (30% EtOAc/hexanes); IR (film) 3031, 2963, 2878, 2086, 1746, 1710, 1653, 1598 cm^{-1} ; ^1H NMR (400 MHz, CDCl_3) δ 7.40-7.11 (m, 10H), 5.89 (d, $J = 10.4$ Hz, 1H), 4.95 (d, $J = 15.6$ Hz, 1H), 4.62 (d, $J = 15.2$ Hz, 1H), 3.84-3.78 (m, 1H), 3.73 (s, 3H), 1.68-1.61 (m, 1H), 1.46-1.39 (m, 1H), 0.78 (t, $J = 7.2$ Hz, 3H); ^{13}C NMR (100 MHz, CDCl_3) ppm 170.1, 154.4, 137.7, 135.6, 129.1, 128.5, 128.3, 128.1, 127.9, 127.7, 83.4, 59.1, 54.1, 52.2, 23.6, 9.1; HRMS (CI): Exact mass calcd for $\text{C}_{20}\text{H}_{23}\text{N}_4\text{O}_3$ $[\text{M}+\text{H}]^+$ 367.1765, found 367.1761.



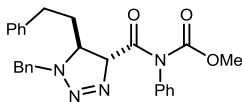
Methyl (4R,5S)-1-benzyl-5-isopropyl-4,5-dihydro-1H-1,2,3-triazole-4-carbonyl(phenyl)carbamate (246i). According to the

general procedure, (*E*)-methyl 4-methylpent-2-enoyl(phenyl)carbamate (123 mg, 0.49 mmol) provided the desired product after flash column chromatography (10% ethyl acetate in hexanes) as a colorless oil (123 mg, 65%). $R_f=0.50$ (30% EtOAc/hexanes); IR (film) 3064, 3032, 2958, 2874, 2117, 1955, 1752, 1696 cm^{-1} ; ^1H NMR (400 MHz, CDCl_3) δ 7.40-7.11 (m, 10H), 6.01 (d, $J = 10.4$ Hz, 1H), 5.04 (d, $J = 15.2$ Hz, 1H), 4.59 (d, $J = 15.2$ Hz, 1H), 3.86 (dd, $J = 10.0, 4.0$ Hz, 1H), 3.75 (s, 3H), 1.99-1.96 (m, 1H), 0.81 (d, $J = 7.2$ Hz, 3H), 0.74 (d, $J = 6.8$ Hz, 3H); ^{13}C NMR (100 MHz, CDCl_3) ppm 170.2, 154.3, 137.7, 135.3, 129.0, 128.4, 128.2, 128.0, 127.8, 127.6, 79.7, 62.5, 53.9, 52.3, 27.2, 18.6, 16.1; HRMS (CI): Exact mass calcd for $\text{C}_{21}\text{H}_{25}\text{N}_4\text{O}_3$ $[\text{M}+\text{H}]^+$ 381.1921, found 381.1927.



Methyl (4R,5S)-1-benzyl-5-cyclohexyl-4,5-dihydro-1H-1,2,3-triazole-4-carbonyl(phenyl)carbamate (246j). According to the

general procedure, (*E*)-methyl 3-cyclohexylacryloyl(phenyl)carbamate (143 mg, 0.50 mmol) provided the desired product after flash column chromatography (10% ethyl acetate in hexanes) as a colorless oil (127 mg, 60%). IR (film) 3031, 2926, 2853, 1747, 1712 cm^{-1} ; ^1H NMR (400 MHz, CDCl_3) δ 7.40-7.21 (m, 8H), 7.12-7.10 (m, 2H), 6.03 (d, $J = 10.4$ Hz, 1H), 5.00 (d, $J = 15.2$ Hz, 1H), 4.60 (d, $J = 15.6$ Hz, 1H), 3.82 (dd, $J = 10.4, 4.0$ Hz, 1H), 3.75 (s, 3H), 1.70-1.49 (m, 5H), 1.41-1.38 (m, 1H), 1.15-0.99 (m, 3H), 0.87-0.76 (m, 2H); ^{13}C NMR (100 MHz, CDCl_3) ppm 170.3, 154.5, 137.9, 135.5, 129.1, 128.6, 128.4, 128.2, 128.0, 127.7, 80.7, 62.2, 54.1, 52.7, 37.8, 29.7, 27.0, 26.1, 25.7; HRMS (CI): Exact mass calcd for $\text{C}_{24}\text{H}_{28}\text{N}_4\text{NaO}_3$ $[\text{M}+\text{Na}]^+$ 443.2059, found 443.2045.

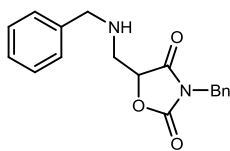


Methyl (4*R*,5*S*)-1-benzyl-5-phenethyl-4,5-dihydro-1*H*-1,2,3-triazole-4-carbonyl(phenyl)carbamate (246k). According to the

general procedure, (*E*)-methyl phenyl(5-phenylpent-2-enoyl)carbamate (162 mg, 0.50 mmol) provided the desired product after flash column chromatography (10% ethyl acetate in hexanes) as a colorless oil (92.0 mg, 41%). IR (film) 3062, 1746, 1711 cm^{-1} ; ^1H NMR (400 MHz, CDCl_3) δ 7.48-7.19 (m, 13H), 7.10 (d, $J = 7.2$ Hz, 2H), 6.06 (d, $J = 10.8$ Hz, 1H), 4.98 (d, $J = 15.2$ Hz, 1H), 4.73 (d, $J = 15.2$ Hz, 1H), 3.98 (ddd, $J = 12.9, 8.0, 3.2$ Hz, 1H), 3.81 (s, 3H), 2.61-2.48 (m, 2H), 2.06-1.97 (m, 1H), 1.84-1.75 (m, 1H); ^{13}C NMR (100 MHz, CDCl_3) ppm 169.9, 154.3, 140.6, 137.6, 135.4, 129.1, 128.6, 128.4, 128.3, 128.1, 128.0, 127.7, 84.2, 58.0, 54.1, 52.5, 31.3; HRMS (CI): Exact mass calcd for $\text{C}_{26}\text{H}_{26}\text{N}_4\text{NaO}_3$ $[\text{M}+\text{Na}]^+$ 465.1903, found 465.1916.

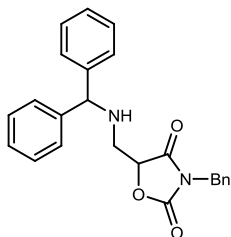
General Procedure for Acid Catalyzed Aminohydroxylation

To a solution of imide (1 equiv) and azide (2 equiv) in acetonitrile (0.3 M) cooled in a -20 $^\circ\text{C}$ bath was added triflic acid (2 equiv). After consumption of the imide as monitored by TLC (silica gel, hexanes-ethyl acetate, 2:1), water (1 equiv) was added to the cold solution with subsequent gas evolution. After 1 h, triethylamine (2 equiv) was added via syringe, the reaction mixture was warmed to room temperature and the solvent was removed in vacuo. The crude material was purified by flash column chromatography (silica gel, hexanes-ethyl acetate, 10:1 \rightarrow 5:1 \rightarrow 2:1 \rightarrow 1:1) to afford the *N*-acylated oxazolidine dione.



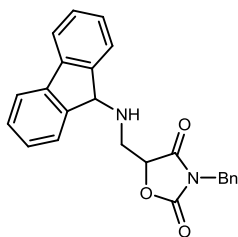
3-Benzyl-5-((benzylamino)methyl)oxazolidine-2,4-dione (245a).

According to the general procedure **245a** was obtained as a yellow oil that slowly crystallized to a light yellow solid (229 mg, 92%). Mp 74-76 °C; IR (neat) 1818, 1737 cm^{-1} ; ^1H NMR (500 MHz, CDCl_3) δ 7.45-7.37 (m, 2H), 7.35-7.29 (m, 4H), 7.26 (d, $J = 7.0$ Hz, 2H), 7.19 (d, $J = 7.0$ Hz, 2H), 4.82 (dd, $J = 3.7$, 3.7 Hz, 1H), 4.73 (d, $J = 14.5$ Hz, 1H), 4.67 (d, $J = 14.5$ Hz, 1H), 3.77 (d, $J = 2.5$ Hz, 2H), 3.21 (dd, $J = 13.5$, 3.5 Hz, 1H), 3.10 (dd, $J = 13.7$, 3.7 Hz, 1H), 1.51 (br s, 1H); ^{13}C NMR (125 MHz, CDCl_3) ppm 172.0, 155.4, 139.3, 134.6, 128.8, 128.7, 128.4, 128.2, 127.9, 127.1, 80.1, 53.8, 47.7, 43.6; HRMS (CI): Exact mass calcd for $\text{C}_{18}\text{H}_{18}\text{N}_2\text{O}_3$ $[\text{M}+\text{H}]^+$ 311.1385, found 311.1390. *Anal.* calcd for $\text{C}_{18}\text{H}_{18}\text{N}_2\text{O}_3$: C, 69.66; H, 5.85; N, 9.03. Found C, 69.26; H, 5.84; N, 8.81.



5-((Benzhydrylamino)methyl)-3-benzylloxazolidine-2,4-dione

(247a). According to the general procedure **247a** was obtained as a colorless oil that crystallized to a white solid (273 mg, 62%). Mp 124-125 °C; IR (film) 1815, 1745, 1494, 1441, 1414, 1348, 1162, 1064 cm^{-1} ; ^1H NMR (500 MHz, CDCl_3) δ 7.55-7.50 (m, 2H), 7.41-7.35 (m, 3H), 7.34-7.22 (m, 10H), 4.87-4.83 (m, 2H), 4.81 (d, $J = 14.5$ Hz, 1H), 4.73 (d, $J = 14.5$ Hz, 1H), 3.18 (dd, $J = 13.7$, 3.2 Hz, 1H), 3.10 (dd, $J = 13.7$, 3.3 Hz, 1H), 1.85 (s, 1H); ^{13}C NMR (125 MHz, CDCl_3) ppm 171.8, 155.4, 143.1, 142.5, 134.7, 128.8, 128.62, 128.58, 128.51, 128.3, 127.28, 127.25, 127.16, 127.07, 79.9, 66.9, 46.3, 43.7; HRMS (CI): Exact mass calcd for $\text{C}_{24}\text{H}_{23}\text{N}_2\text{O}_3$ $[\text{M}+\text{H}]^+$ 387.1709, found 387.1726.



5-((9H-Fluoren-9-ylamino)methyl)-3-benzyloxazolidine-2,4-

dione (247b). According to the general procedure **247b** was

obtained as a white solid (736 mg, 84%). Mp 151-152 °C; IR

(neat) 1815, 1739, 1441, 1413, 1348, 1162, 743 cm^{-1} ; ^1H NMR

(500 MHz, CDCl_3) δ 7.68 (d, $J = 5.5$ Hz, 2H), 7.46 (d, $J = 6.5$

Hz, 2H), 7.43 (d, $J = 7.5$ Hz, 1H), 7.40-7.27 (m, 8H), 4.87 (s, 1H), 4.73 (d, $J = 1.5$ Hz,

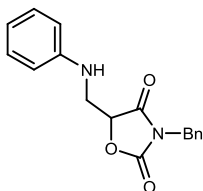
2H), 4.68 (dd, $J = 3.2, 3.2$ Hz, 1H), 2.95 (dd, $J = 13.7, 3.3$ Hz, 1H), 2.77 (dd, $J = 13.7,$

3.3 Hz, 1H), 2.00 (br s, 1H); ^{13}C NMR (125 MHz, CDCl_3) ppm 171.7, 155.5, 144.3,

144.0, 134.6, 128.7, 128.6, 128.40, 128.35, 128.27, 127.41, 127.38, 119.9, 119.8, 79.9,

62.9, 43.7, 43.0; HRMS (ESI): Exact mass calcd for $\text{C}_{24}\text{H}_{20}\text{N}_2\text{O}_3$ $[\text{M}+\text{Na}]^+$ 407.1372,

found 407.1378.



3-Benzyl-5-((phenylamino)methyl)oxazolidine-2,4-dione (247c).

According to the general procedure **247c** was obtained as an off white

solid (43 mg, 63%). Mp 113-115 °C; IR (film) 3389, 1816, 1738, 1603,

1490, 1440, 1414, 1348, 1162, 752 cm^{-1} ; ^1H NMR (500 MHz, CDCl_3) δ 7.33-7.29 (m,

2H), 7.28-7.23 (m, 3H), 7.19 (t, $J = 7.5$ Hz, 2H), 6.79 (t, $J = 7.5$ Hz, 1H), 6.66 (d, $J = 8.0$

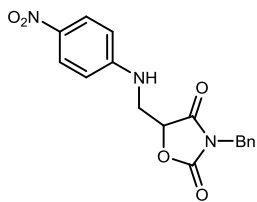
Hz, 2H), 4.95 (dd, $J = 4.0, 4.0$ Hz, 1H), 4.67 (d, $J = 14.5$ Hz, 1H), 4.62 (d, $J = 14.5$ Hz,

1H), 3.91 (br s, 1H), 3.74-3.76 (m, 2H); ^{13}C NMR (100 MHz, CDCl_3) ppm 171.6, 155.0,

146.4, 134.3, 129.4, 128.7, 128.4, 128.3, 119.1, 113.7, 79.0, 44.4, 43.7; HRMS (EI):

Exact mass calcd for $\text{C}_{17}\text{H}_{16}\text{N}_2\text{O}_3$ $[\text{M}]^+$ 296.1161, found 296.1152. *Anal.* calcd for

$\text{C}_{17}\text{H}_{16}\text{N}_2\text{O}_3$: C, 68.91; H, 5.44; N, 9.45. Found C, 68.69; H, 5.41; N, 9.31.



3-Benzyl-5-((4-nitrophenylamino)methyl)oxazolidine-2,4-dione

(247d). According to the general procedure **247d** was obtained as a

light yellow solid (215 mg, 52%). Mp 158-160 °C; IR (neat) 1810,

1730, 1599, 1535, 1484, 1446, 1321 cm^{-1} ; ^1H NMR (500 MHz,

CDCl_3) δ 8.07 (d, $J = 9.5$ Hz, 2H), 7.34-7.21 (m, 5H), 6.58 (d, $J = 9.0$ Hz, 2H), 3.98 (dd,

$J = 3.5, 3.5$ Hz, 1H), 4.69 (d, $J = 14.5$ Hz, 1H), 4.63 (d, $J = 14.5$ Hz, 1H), 4.53 (br s, 1H),

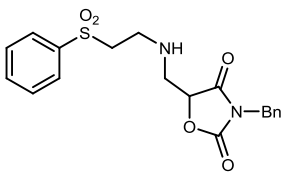
3.89 (br s, 2H); ^{13}C NMR (125 MHz, CDCl_3) ppm 170.9, 154.6, 151.6, 139.5, 134.1,

128.8, 128.5, 126.1, 111.9, 78.5, 43.9, 43.1 (one overlapping C); HRMS (EI): Exact mass

calcd for $\text{C}_{17}\text{H}_{15}\text{N}_3\text{O}_5$ $[\text{M}]^+$ 341.1012, found 341.1015. *Anal.* calcd for $\text{C}_{17}\text{H}_{15}\text{N}_3\text{O}_5$: C,

59.82; H, 4.43; N, 12.31. Found C, 59.85; H, 4.44; N, 12.19.

3-Benzyl-5-((2-(phenylsulfonyl)ethylamino)methyl)oxazolidine-2,4-dione **(247e).**



According to the general procedure **247e** was obtained as a light

yellow oil (181 mg, 93%). IR (film) 3354, 1815, 1739, 1443,

1415, 1349, 1306, 1147, 733 cm^{-1} ; ^1H NMR (500 MHz, CDCl_3)

δ 7.86 (d, $J = 7.5$ Hz, 2H), 7.67 (t, $J = 7.2$ Hz, 1H), 7.57 (t, $J = 7.7$ Hz, 2H), 7.38 (d, $J =$

7.0 Hz, 2H), 7.31-7.24 (m, 3H), 4.75 (dd, $J = 3.2, 3.2$ Hz, 1H), 4.68 (d, $J = 14.5$ Hz, 1H),

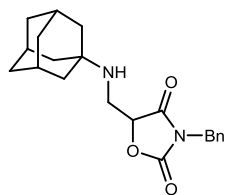
4.62 (d, $J = 14.5$ Hz, 1H), 3.18 (dd, $J = 14.2, 3.3$ Hz, 1H), 3.09-2.90 (m, 5H), 1.64 (br s,

1H); ^{13}C NMR (125 MHz, CDCl_3) ppm 171.8, 155.3, 139.0, 134.6, 133.9, 129.4, 128.7,

128.5, 128.2, 127.9, 79.9, 55.8, 47.9, 43.6, 43.3; HRMS (CI): Exact mass calcd for

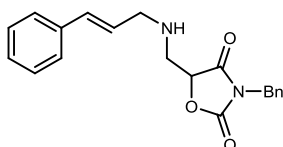
$\text{C}_{19}\text{H}_{21}\text{N}_2\text{O}_5\text{S}$ $[\text{M}+\text{H}]^+$ 389.1166, found 389.1159. *Anal.* calcd for $\text{C}_{19}\text{H}_{20}\text{N}_2\text{O}_5\text{S}$: C, 58.75;

H, 5.19. Found C, 58.63; H, 5.25.



3-Benzyl-5-((adamantylamino)methyl)oxazolidine-2,4-dione

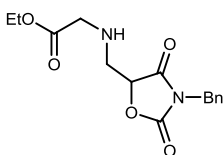
(247f). According to the general procedure **247f** was obtained as a white solid (97 mg, 55%). Mp 159-160 °C; IR (neat) 1810, 1732, 1443, 1171, 730 cm^{-1} ; ^1H NMR (500 MHz, CDCl_3) δ 7.45-7.39 (m, 2H), 7.35-7.28 (m, 3H), 4.78 (br s, 1H), 4.73 (d, $J = 15.0$ Hz, 1H), 4.64 (d, $J = 15.0$ Hz, 1H), 3.17 (dd, $J = 14.0, 3.0$ Hz, 1H), 3.09 (dd, $J = 14.0, 3.0$ Hz, 1H), 2.01 (br s, 3H), 1.68-1.57 (m, 3H), 1.56-1.50 (m, 3H), 1.49-1.38 (m, 6H), 0.99 (br s, 1H); ^{13}C NMR (125 MHz, CDCl_3) ppm 172.4, 155.7, 134.6, 128.6, 128.2, 128.0, 80.7, 50.0, 43.4, 42.5, 39.8, 36.5, 29.4; HRMS (CI): Exact mass calcd for $\text{C}_{21}\text{H}_{27}\text{N}_2\text{O}_3$ $[\text{M}+\text{H}]^+$ 355.1016, found 355.2013. *Anal.* calcd for $\text{C}_{21}\text{H}_{26}\text{N}_2\text{O}_3$: C, 71.16; H, 7.39. Found C, 70.91; H, 7.45.



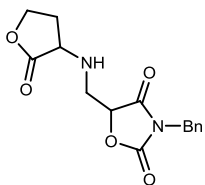
(E)-3-Benzyl-5-((cinnamylamino)methyl)oxazolidine-2,4-

dione (247g). According to the general procedure **247g** was obtained as a light yellow oil (387 mg, 84%). IR (film) 3410, 1814, 1740, 1440, 1414, 1349, 1163, 740 cm^{-1} ; ^1H NMR (500 MHz, CDCl_3) δ 7.45 (d, $J = 7.5$ Hz, 2H), 7.39-7.23 (m, 8H), 6.49 (d, $J = 16.0$ Hz, 1H), 6.13 (ddd, $J = 16.0, 6.5, 6.5$ Hz, 1H), 4.88 (dd, $J = 3.5, 3.5$ Hz, 1H), 4.76 (d, $J = 14.5$ Hz, 1H), 4.71 (d, $J = 14.5$ Hz, 1H), 3.45-3.36 (m, 2H), 3.29 (dd, $J = 13.8, 3.3$ Hz, 1H), 3.17 (dd, $J = 13.7, 3.7$ Hz, 1H), 1.48 (br s, 1H); ^{13}C NMR (125 MHz, CDCl_3) ppm 172.0, 155.4, 136.7, 134.5, 131.7, 128.7, 128.48, 128.45, 128.2, 127.47, 127.46, 126.3, 80.1, 51.7, 47.6, 43.7; HRMS (EI): Exact mass calcd for $\text{C}_{20}\text{H}_{20}\text{N}_2\text{O}_3$ $[\text{M}]^+$ 336.1474, found 336.1478.

Ethyl 2-((3-benzyl-2,4-dioxooxazolidin-5-yl)methylamino)ethanoate (247h).



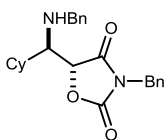
According to the general procedure **247h** was obtained as a colorless oil (48 mg, 69%). IR (film) 3356, 1816, 1739, 1441, 1349, 1200, 1157, 761 cm^{-1} ; ^1H NMR (500 MHz, CDCl_3) δ 7.45-7.38 (m, 2H), 7.37-7.29 (m, 3H), 4.82 (dd, $J = 3.2, 3.2$ Hz, 1H), 4.72 (d, $J = 15.0$ Hz, 1H), 4.68 (d, $J = 14.5$ Hz, 1H), 4.18 (q, $J = 7.2$ Hz, 2H), 3.38 (d, $J = 18.0$ Hz, 1H), 3.34 (d, $J = 18.0$ Hz, 1H), 3.32 (dd, $J = 14.5, 3.0$ Hz, 1H), 3.14 (dd, $J = 14.2, 3.8$ Hz, 1H), 1.92 (br s, 1H), 1.28 (t, $J = 7.0$ Hz, 3H); ^{13}C NMR (125 MHz, CDCl_3) ppm 172.1, 171.9, 155.3, 134.6, 128.8, 128.7, 128.4, 80.2, 60.8, 51.1, 48.2, 43.6, 14.1; HRMS (EI): Exact mass calcd for $\text{C}_{15}\text{H}_{18}\text{N}_2\text{O}_5$ $[\text{M}]^+$ 306.1216, found 306.1210. *Anal.* calcd for $\text{C}_{15}\text{H}_{18}\text{N}_2\text{O}_5$: C, 58.82; H, 5.92; N, 9.15. Found C, 58.92; H, 6.09; N, 9.13.



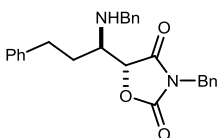
3-Benzyl-5-((2-oxotetrahydrofuran-3-ylamino)methyl)oxazolidine-2,4-dione (247i). According to the general procedure a 1:1 diastereomeric mixture **247i** was obtained as a colorless oil (367 mg, 88%). IR (neat) 3332, 1815, 1731, 1442, 1415, 1349, 1219, 1162, 1018 cm^{-1} ; ^1H NMR (400 MHz, CDCl_3) δ 7.29-7.23 (m, 4H), 7.27-7.15 (m, 6H), 4.74-4.68 (m, 2H), 4.62-4.47 (m, 4H), 4.16-4.06 (m, 2H), 4.10-3.94 (m, 2H), 3.44-3.34 (m, 3H), 3.27 (dd, $J = 14.6, 3.4$ Hz, 1H), 3.12 (dd, $J = 14.4, 3.2$ Hz, 1H), 2.97 (dd, $J = 14.0, 3.2$ Hz, 1H), 2.26-2.15 (m, 2H), 1.87 (s, 2H), 1.79-1.70 (m, 1H), 1.69-1.60 (m, 1H); ^{13}C NMR (100 MHz, CDCl_3) ppm 176.8, 172.1, 171.8, 155.44, 155.38, 134.6, 128.62, 128.60, 128.3, 128.14, 128.08, 80.17, 79.95, 65.6, 65.4, 56.6, 56.2, 46.3, 46.3, 43.5, 30.0, 29.9; HRMS (ESI): Exact mass calcd for $\text{C}_{15}\text{H}_{16}\text{N}_2\text{O}_5$ $[\text{M}]^+$ 304.1059, found 304.1055.

General Procedure for Acid Catalyzed Aminohydroxylation

A solution of the triazoline (1.0 equiv) in the CH₃CN (0.3 M) was cooled to -20 °C and treated with triflic acid (2.0 equiv). The solution was allowed to warm to room temperature until reaction was complete. The reaction mixture was quenched with distilled triethylamine (2.0 equiv). The solution was dried and concentrated to an oil that was purified by flash chromatography to provide the desired oxazolidine dione in analytically pure form.

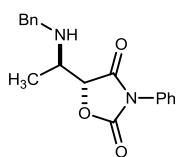


(5R)-3-benzyl-5-((benzylamino)(cyclohexyl)methyl)oxazolidine-2,4-dione (245e). According to the general procedure **245e** was obtained as a yellow oil (80.0 mg, 75%). IR (film) 3046, 2926, 1813, 1737 cm⁻¹; ¹H NMR (400 MHz, CDCl₃) δ 7.40-7.21 (m, 8H), 7.46-7.16 (m, 10H), 5.03 (s, 1H), 4.72 (d, *J* = 14.4 Hz, 1H), 4.65 (d, *J* = 14.4 Hz, 1H), 3.84 (d, *J* = 12.4 Hz, 1H), 3.79 (d, *J* = 12.4 Hz, 1H), 2.89 (d, *J* = 7.2 Hz, 1H), 1.91-1.65 (m, 5H), 1.27-1.00 (m, 6H), the NH was not observed; ¹³C NMR (100 MHz, CDCl₃) ppm 171.7, 155.8, 134.6, 128.6, 128.5, 128.4, 128.1, 127.2, 81.2, 54.9, 43.5, 38.9, 30.4, 30.0, 26.0, 25.8, 25.7; HRMS (CI): Exact mass calcd for C₂₄H₂₉N₂O₃ [M+H]⁺ 393.2178, found 393.2197.



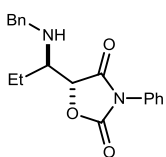
(R)-3-Benzyl-5-((R)-1-(benzylamino)-3-phenylpropyl)oxazolidine-2,4-dione (245f). According to the general procedure **245f** was obtained as a yellow oil (176 mg, 74%). IR (film) 3343, 1813, 1738 cm⁻¹; ¹H NMR (400 MHz, CDCl₃) δ 7.46-7.40 (m, 2H), 7.38-7.20 (m, 11H), 7.10-7.08 (d, *J* = 7.2 Hz, 2H), 5.02 (d, *J* = 2.8 Hz, 1H), 4.89 (d, *J* = 2.8 Hz, 1H), 4.71 (d, *J* = 14.4 Hz, 1H), 4.66 (d, *J* = 14.4 Hz, 1H), 3.86 (d, *J* = 12.8 Hz, 1H), 3.79 (d, *J* = 12.8 Hz, 1H), 3.17

(ddd, $J = 8.5, 5.0, 2.8$ Hz, 1H), 2.78 (ddd, $J = 14.2, 9.0, 5.6$ Hz, 1H), 2.65 (ddd, $J = 13.8, 9.0, 6.8$ Hz, 1H), 1.91-1.75 (m, 2H), the NH was not recorded; ^{13}C NMR (100 MHz, CDCl_3) ppm 171.5, 155.4, 140.7, 134.5, 128.6, 128.5, 128.4, 128.3, 128.2, 128.1, 127.1, 126.0, 81.0, 57.4, 52.3, 43.5, 32.1, 31.3; HRMS (CI): Exact mass calcd for $\text{C}_{26}\text{H}_{27}\text{N}_2\text{O}_3$ $[\text{M}]^+$ 415.2022, found 415.2011.



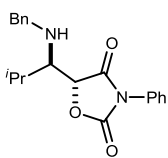
(R)-5-((R)-1-(benzylamino)ethyl)-3-phenyloxazolidine-2,4-dione (246g).

colorless oil (103 mg, 67%). $R_f = 0.30$ (30% EtOAc/hexanes); IR (film) 3298, 1752, 1683 cm^{-1} ; ^1H NMR (400 MHz, CDCl_3) δ 7.19-7.37 (m, 10H), 4.96 (d, $J = 3.2$ Hz, 1H), 3.93 (d, $J = 13.2$ Hz, 1H), 3.88 (d, $J = 13.2$ Hz, 1H), 3.39 (dq, $J = 6.8, 3.2$ Hz, 1H), 1.30 (d, $J = 6.8$ Hz, 3H), the NH was not observed; ^{13}C NMR (100 MHz, CDCl_3) ppm 170.7, 154.3, 139.5, 130.7, 129.2, 128.8, 128.4, 127.9, 127.1, 125.6, 81.6, 53.5, 51.7, 15.0; HRMS (CI): Exact mass calcd for $\text{C}_{18}\text{H}_{18}\text{N}_2\text{O}_3$ $[\text{M}+\text{H}]^+$ 311.1390. Found 311.1394.

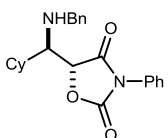


(R)-5-((R)-1-(benzylamino)propyl)-3-phenyloxazolidine-2,4-dione (246h).

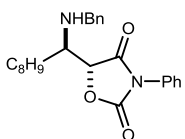
Colorless oil (115 mg, 63%). IR (film) 1735, 1646 cm^{-1} ; ^1H NMR (400 MHz, CDCl_3) δ 7.49-7.20 (m, 10H), 4.97 (d, $J = 2.8$ Hz, 1H), 3.92 (d, $J = 12.8$ Hz, 1H), 3.87 (d, $J = 12.8$ Hz, 1H), 3.13 (dt, $J = 7.2, 2.8$ Hz, 1H), 1.73 (dq, $J = 7.8, 7.8$ Hz, 2H), 1.08 (t, $J = 7.2$ Hz, 3H); ^{13}C NMR (100 MHz, CDCl_3) ppm 171.0, 154.6, 139.8, 130.8, 129.3, 128.8, 128.4, 128.1, 127.2, 125.7, 81.3, 60.1, 53.1, 23.3, 10.8; HRMS (EI): Exact mass calcd for $\text{C}_{19}\text{H}_{19}\text{N}_2\text{O}_3$ $[\text{M}-\text{H}]^+$ 323.1390, found 323.1391.



(R)-5-((R)-1-(benzylamino)-2-methylpropyl)-3-phenyloxazolidine-2,4-dione (246i). Colorless oil (80 mg, 54%). $R_f = 0.20$ (30% EtOAc/hexane s); IR (film) 1756, 1720 cm^{-1} ; ^1H NMR (400 MHz, CDCl_3) δ 7.51-7.26 (m, 10H), 5.13 (d, $J = 2.8$ Hz, 1H), 3.96 (d, $J = 12.4$, Hz, 1H), 3.91 (d, $J = 12.4$, Hz, 1H), 2.93 (dd, $J = 8.8, 3.2$ Hz, 1H), 2.12 (qq, $J = 6.8, 6.8$ Hz, 1H), 1.15 (d, $J = 6.8$ Hz, 3H), 1.07 (d, $J = 6.4$ Hz, 3H); ^{13}C NMR (100 MHz, CDCl_3) ppm 171.1, 154.8, 139.8, 131.0, 129.2, 128.8, 128.4, 128.3, 127.2, 125.8, 81.3, 65.4, 55.2, 29.7, 20.5, 19.9; HRMS (EI) Exact mass calcd for $\text{C}_{19}\text{H}_{22}\text{N}_2\text{O}$ $[\text{M}-\text{CO}_2]^+$ 294.1630, found 294.1803.

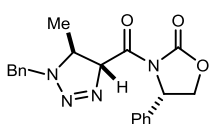


(R)-5-((S)-(benzylamino)(cyclohexyl)methyl)-3-phenyloxazolidine-2,4-dione (245j). According to the general procedure **x** was obtained as a yellow oil (72.0 mg, 50%). IR (film) 3031, 2926, 2853, 1747, 1712 cm^{-1} ; ^1H NMR (400 MHz, CDCl_3) δ 7.43-7.18 (m, 10H), 5.07 (d, $J = 2.4$ Hz, 1H), 3.87 (d, $J = 12.4$ Hz, 1H), 3.82 (d, $J = 12.0$ Hz, 1H), 2.90 (dd, $J = 8.8, 2.4$ Hz, 1H), 1.94-1.88 (m, 2H), 1.76-1.64 (m, 4H), 1.31-1.02 (m, 5H), the NH was not observed; ^{13}C NMR (100 MHz, CDCl_3) ppm 171.1, 154.9, 139.8, 131.1, 129.2, 128.7, 128.4, 128.3, 127.2, 125.8, 81.2, 64.5, 55.5, 39.2, 30.6, 30.2, 26.1, 25.9, 25.8; HRMS (CI): Exact mass calcd for $\text{C}_{23}\text{H}_{27}\text{N}_2\text{O}_3$ $[\text{M}+\text{H}]^+$ 379.2016, found 379.2017.



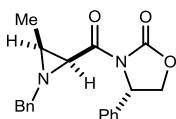
(R)-5-((R)-1-(benzylamino)-3-phenylpropyl)-3-phenyloxazolidine-2,4-dione (245k). According to the general procedure **x** was obtained as a yellow oil (100 mg, 51%). IR (film) 3343, 1813, 1738 cm^{-1} ; ^1H NMR (400 MHz, CDCl_3) δ 7.51-7.16 (m, 15H), 5.02 (d, $J = 2.8$ Hz, 1H), 3.94 (d, $J = 13.2$ Hz, 1H), 3.87 (d, $J = 13.2$ Hz, 1H), 3.27 (dt, $J = 8.4, 2.8$ Hz, 1H), 2.88-2.71 (m, 2H),

2.06-1.95 (m, 2H), 1.36 (bs, 1H); ^{13}C NMR (100 MHz, CDCl_3) ppm 170.8, 154.4, 140.7, 139.6, 130.8, 129.2, 128.8, 128.5, 128.3, 128.2, 127.2, 126.2, 125.6, 81.2, 57.9, 52.8, 32.3, 31.7; HRMS (CI): Exact mass calcd for $\text{C}_{25}\text{H}_{25}\text{N}_2\text{O}_3$ $[\text{M}+\text{H}]^+$ 401.1860, found 401.1859



(S)-3-((4R,5S)-1-Benzyl-5-methyl-4,5-dihydro-1H-1,2,3-triazole-4-carbonyl)-4-phenyloxazolidin-2-one (253). White solid (110 mg, 46%). IR (film) 1781, 1707 cm^{-1} ; ^1H NMR (400 MHz, CDCl_3) δ 7.37-

7.19 (m, 10H), 5.83 (d, $J = 10.0$ Hz, 1H), 5.37 (dd, $J = 8.4, 2.8$ Hz, 1H), 4.97 (d, $J = 15.2$ Hz, 1H), 4.74 (t, $J = 8.8$ Hz, 1H), 4.60 (d, $J = 15.2$ Hz, 1H), 4.32 (dd, $J = 8.8, 2.8$ Hz, 1H), 3.72-3.68 (m, 1H), 1.11 (d, $J = 6.4$ Hz, 3H); ^{13}C NMR (125 MHz, CDCl_3) ppm 166.5, 138.7, 135.5, 129.2, 128.8, 128.7, 128.6, 127.9, 127.8, 125.8, 83.4, 77.3, 76.9, 76.6, 70.3, 58.0, 53.8, 51.8, 16.7; HRMS (CI): Exact mass calcd for $\text{C}_{20}\text{H}_{21}\text{N}_4\text{O}_3$ $[\text{M}+\text{H}]^+$ 365.1614, found 365.1602.

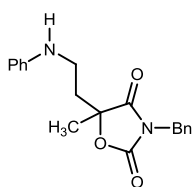


(S)-3-((2S,3S)-1-Benzyl-3-methylaziridine-2-carbonyl)-4-phenyloxazolidin-2-one (257). Colorless oil (10 mg, 30%). IR (film)

1811, 1735 cm^{-1} ; ^1H NMR (400 MHz, CDCl_3) δ 7.41-7.19 (m, 10H), 5.47 (dd, $J = 8.6, 4.2$ Hz, 1H), 4.69 (t, $J = 9.0$ Hz, 2H), 4.29 (dd, $J = 9.2, 4.4$ Hz, 1H), 3.61 (dd, $J = 13.6, 2.8$ Hz, 2H), 3.38 (d, $J = 6.8$ Hz, 1H), 2.22 (dq, $J = 6.0, 6.0$ Hz, 1H), 1.21 (d, $J = 5, 6$ Hz, 3H); ^{13}C NMR (125 MHz, CDCl_3) ppm 168.1, 155.7, 138.4, 138.2, 129.1, 128.7, 128.2, 127.6, 126.9, 126.0, 103.3, 70.2, 63.5, 57.5, 43.7, 13.2; HRMS (CI): Exact mass calcd for $\text{C}_{20}\text{H}_{21}\text{N}_2\text{O}_3$ $[\text{M}+\text{H}]^+$ 337.1552, found 337.1550.

General Procedure for Acid Catalyzed Iminoacetoxylation

To a vial, the Michael acceptor (1.0 equiv) was added with solvent to generate a 0.3 M solution. The solution was cooled to $-20\text{ }^{\circ}\text{C}$ and benzyl azide (2.0 equiv) was added. Triflic acid (2.0 equiv) was then added, and the reaction mixture was stirred until complete conversion (generally 12-48 hours). The reaction was diluted with triethyl amine (5 equiv) and concentrated to an oil that was purified by flash chromatography to give the analytically pure amine.

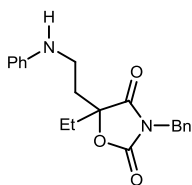


3-Benzyl-5-methyl-5-(2-(phenylamino)ethyl)oxazolidine-2,4-dione

(272a). According to the general procedure **272a** was prepared as a colorless oil (123 mg, 88%). $R_f = 0.6$ (50% EtOAc/hexanes); IR (film)

3400, 3046, 2937, 2844, 1804, 1733, 1411 cm^{-1} ; ^1H NMR (400 MHz,

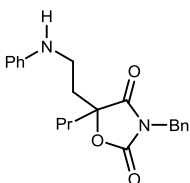
CDCl_3) δ 7.36-7.31 (m, 2H), 7.30-7.24 (m, 3H), 7.17 (d, $J = 7.6$ Hz, 1H), 7.15 (d, $J = 7.3$ Hz, 1H), 6.73 (t, $J = 7.2$ Hz, 1H), 6.47 (d, $J = 8.0$ Hz, 2H), 4.60 (d, $J = 14.6$ Hz, 1H), 4.54 (d, $J = 14.6$ Hz, 1H), 3.47 (bs, 1H), 3.41 (t, $J = 6.7$ Hz, 2H), 2.21 (dq, $J = 14.6, 7.3$ Hz, 2H), 1.58 (s, 3H); ^{13}C NMR (100 MHz, CDCl_3) ppm 175.4, 154.7, 147.5, 134.9, 129.5, 129.1, 128.7, 128.5, 118.3, 113.2, 85.2, 43.9, 38.6, 36.3, 23.3; HRMS (EI) Exact mass calcd for $\text{C}_{19}\text{H}_{20}\text{N}_2\text{O}_3$ $[\text{M}]^+$, 324.1474. Found 324.1463. *Anal.* Calcd for $\text{C}_{19}\text{H}_{20}\text{N}_2\text{O}_3$: C, 70.35; H, 6.21; N, 8.64. Found: C, 70.54; H, 6.22; N, 8.62.



3-Benzyl-5-ethyl-5-(2-(phenylamino)ethyl)oxazolidine-2,4-dione

(272b). According to the general procedure **272b** was prepared as a colorless oil (35 mg, 61%). $R_f = 0.14$ (20% EtOAc/hexanes); IR (film)

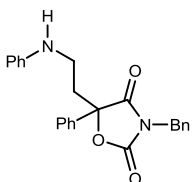
3403, 3033, 2927, 1810, 1733, 1603 cm^{-1} ; ^1H NMR (400 MHz, CDCl_3) δ 7.37-7.32 (m, 2H), 7.28-7.24 (m, 3H), 7.18-7.13 (m, 2H), 6.75-6.71 (m, 1H), 6.50-6.45 (m, 2H), 4.56 (AB q, $J = 14.4$ Hz, 2H), 3.50 (br s, 1H), 3.14 (t, $J = 6.6$ Hz, 2H), 2.28-2.13 (m, 2H) 1.98-1.89 (m, 2H), 0.82 (t, $J = 7.6$ Hz, 3H); ^{13}C NMR (100 MHz, CDCl_3) ppm 175.0, 155.2, 147.5, 134.9, 129.5, 129.0, 128.8, 128.5, 118.3, 113.2, 88.3, 43.9, 38.5, 35.3, 29.9; HRMS (ED): Exact mass calcd for $\text{C}_{20}\text{H}_{22}\text{N}_2\text{O}_3$ $[\text{M}]^+$, 338.1630. Found 338.1625. *Anal.* Calcd for $\text{C}_{20}\text{H}_{22}\text{N}_2\text{O}_3$: C, 70.99; H, 6.55; N, 8.28. Found: C, 70.85; H, 6.49; N, 8.20.



3-Benzyl-5-(2-(phenylamino)ethyl)-5-propyloxazolidine-2,4-dione

(272c). According to the general procedure **272c** was prepared as a colorless oil (35 mg, 60%). $R_f = 0.13$ (10% EtOAc/hexanes); IR (film)

3394, 2962, 2924, 1810, 1734 cm^{-1} ; ^1H NMR (400 MHz, CDCl_3) δ 7.42-7.22 (m, 5H), 7.17-7.11 (m, 2H), 6.72 (tt, $J = 7.6, 1.2$ Hz, 1H), 6.46 (m, 2H), 4.55 (AB q, $J = 14.4$ Hz, 2H), 3.12 (t, $J = 7.2$ Hz, 2H), 2.18 (m, 2H), 1.84 (m, 2H), 1.32 (m, 1H), 1.16 (m, 1H), 0.86 (t, $J = 7.2$ Hz, 3H); ^{13}C NMR (100 MHz, CDCl_3) ppm 175.0, 155.1, 147.5, 134.9, 129.5, 129.0, 128.8, 128.5, 118.3, 113.2, 88.0, 43.9, 38.7, 38.5, 35.5, 16.1, 13.9; HRMS (CI): Exact mass calcd for $\text{C}_{21}\text{H}_{24}\text{N}_2\text{O}_3$ $[\text{M}]^+$, 352.1783. Found 352.1787. *Anal.* Calcd for $\text{C}_{21}\text{H}_{24}\text{N}_2\text{O}_3$: C, 71.57; H, 6.86; N, 7.95. Found: C, 71.59; H, 6.86; N, 7.90.

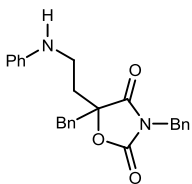


3-Benzyl-5-phenyl-5-(2-(phenylamino)ethyl)oxazolidine-2,4-dione

(272d). According to the General Procedure, **272d** was prepared as a colorless oil (28 mg, 86%). $R_f = 0.46$ (20% EtOAc/hexanes); IR (film)

3034, 2955, 1742, 1674, 1615 cm^{-1} ; ^1H NMR (400 MHz, CDCl_3) δ 7.64-7.58 (m, 2H),

7.45-7.38 (m, 3H), 7.34-7.24 (m, 5H), 7.18-7.12 (m, 2H), 6.73 (t, $J = 7.4$ Hz, 1H), 6.45 (d, $J = 8.8$ Hz, 2H), 4.60 (dd, $J = 14.8, 4.0$ Hz, 2H), 3.48 (br s, 1H), 3.18 (m, 2H), 2.50 (m, 2H); ^{13}C NMR (100 MHz, CDCl_3) ppm 173.5, 154.6, 147.4, 137.8, 134.6, 129.5, 129.3, 129.2, 129.1, 128.61, 128.56, 124.7, 118.3, 113.3, 87.4, 44.2, 38.8, 38.4; HRMS (CI): Exact mass calcd for $\text{C}_{24}\text{H}_{22}\text{N}_2\text{O}_3$ $[\text{M}]^+$ 386.1630. Found 386.1629.



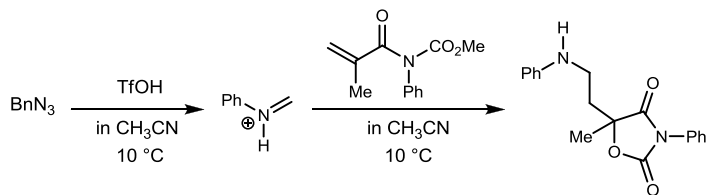
3,5-Dibenzyl-5-(2-(phenylamino)ethyl)oxazolidine-2,4-dione (272e).

Compound **272e** was prepared according to the general procedure except it was allowed to react in a sealed tube and heated at 50 °C for 7 days. Colorless oil (27 mg, 46%). $R_f = 0.15$ (20% EtOAc/hexanes); IR (film) 3403, 3031, 2924, 1815, 1734, 1603 cm^{-1} ; ^1H NMR (400 MHz, CDCl_3) δ 7.20-7.11 (m, 10H), 6.93-6.89 (m, 2H), 6.77-6.71 (m, 1H), 6.53-6.48 (m, 2H), 4.24 (AB q, $J = 14.4$ Hz, 2H), 3.50 (br s, 1H), 3.23 (m, 2H), 3.17 (s, 2H), 2.44-2.36 (m, 1H), 2.32-2.24 (m, 1H); ^{13}C NMR (100 MHz, CDCl_3) ppm 174.2, 154.6, 147.5, 134.4, 132.3, 130.4, 129.5, 128.9, 128.8, 128.1, 128.0, 118.4, 113.2, 54.2, 43.6, 42.5, 38.6, 35.7; HRMS (CI): Exact mass calcd for $\text{C}_{25}\text{H}_{24}\text{N}_2\text{O}_3$ $[\text{M}]^+$, 400.1787. Found 400.1794. *Anal.* Calcd for $\text{C}_{25}\text{H}_{24}\text{N}_2\text{O}_3$: C, 74.98; H, 6.04; N, 7.00. Found: C, 74.96; H, 6.13; N, 6.85.

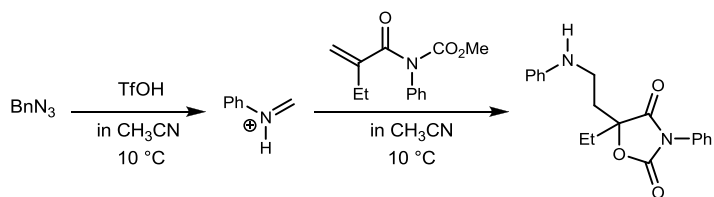
General Procedure for Acid Catalyzed Iminoacetoxylation

To a vial, the Michael acceptor (1.0 equiv) was added with solvent to generate a 0.3 M solution. The solution was cooled to -20 °C and benzyl azide (2.0 equiv) was added. Triflic acid (2.0 equiv) was then added, and the reaction mixture was stirred until complete conversion (generally 12-48 hours). The reaction was diluted with triethyl

amine (5 equiv) and concentrated to an oil that was purified by flash chromatography to give the analytically pure amine.

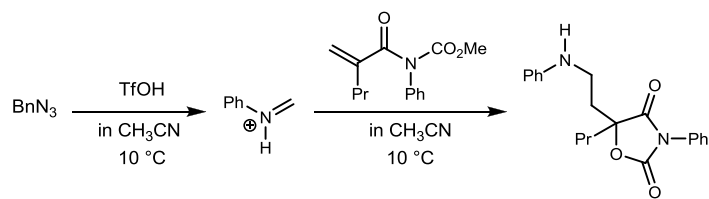


5-Methyl-3-phenyl-5-(2-(phenylamino)ethyl)oxazolidine-2,4-dione (272f). According to the general procedure, the oxazolidine dione was prepared as a colorless oil (200 mg, 64%). $R_f=0.30$ (30% EtOAc/hexanes); IR (film) 3290, 1727, 1692, 1599 cm^{-1} ; ^1H NMR (400 MHz, CDCl_3) δ 7.67 (d, $J = 8.0$ Hz, 2H), 7.48 (br s, 1H), 7.38-7.31 (m, 4H), 7.23-7.14 (m, 3H), 6.98 (t, $J = 7.2$ Hz, 1H), 3.93 (dt, $J = 16.8, 4.8$ Hz, 1H), 3.76 (dd, $J = 17.2, 8.0$ Hz, 1H), 2.86-2.78 (m, 1H), 2.34 (dq, $J = 13.2, 3.7$ Hz, 1H), 1.62 (s, 3H); ^{13}C NMR (100 MHz, CDCl_3) ppm 172.1, 152.1, 139.0, 137.6, 128.8, 128.7, 125.0, 123.2, 119.9, 118.9, 80.8, 44.4, 30.5, 23.1; HRMS (EI) Exact mass calcd for $\text{C}_{18}\text{H}_{18}\text{N}_2\text{O}_3$ $[\text{M}]^+$ 310.1312, found 310.1324.

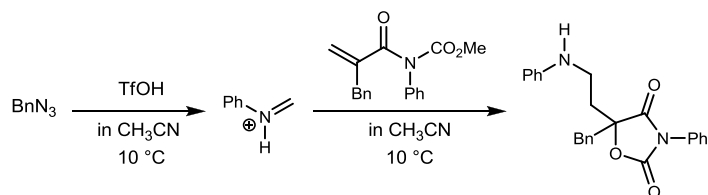


5-Ethyl-3-phenyl-5-(2-(phenylamino)ethyl)oxazolidine-2,4-dione (272g). According to the general procedure, the oxazolidine dione was prepared as a colorless oil (247 mg, 76%). $R_f=0.30$ (30% EtOAc/hexanes); IR (film) 3291, 1726, 1691, 1599 cm^{-1} ; ^1H NMR (400 MHz, CDCl_3) δ 7.69 (d, $J = 8.0$ Hz, 2H), 7.41-7.32 (m, 4H), 7.26-7.16 (m, 3H), 7.02 (t, $J = 7.2$ Hz, 1H), 4.00 (dt, $J = 16.4, 4.9$ Hz, 1H), 3.77 (dd, $J = 16.0, 9.2$ Hz, 1H), 2.74

(dq, $J = 13.6, 4.5$ Hz, 1H), 2.41 (ddd, $J = 13.3, 9.2, 3.2$ Hz, 1H), 2.09-1.91 (m, 2H), 1.06 (t, $J = 7.2$ Hz, 3H), the NH was not observed; ^{13}C NMR (100 MHz, CDCl_3) ppm 171.6, 152.1, 139.1, 137.5, 128.9, 128.8, 125.0, 123.4, 120.1, 118.9, 83.5, 44.8, 29.8, 27.6, 7.3; HRMS (EI) Exact mass calcd for $\text{C}_{19}\text{H}_{20}\text{NaN}_2\text{O}_3$ $[\text{M}+\text{Na}]^+$, 347.1372, found 347.1376.



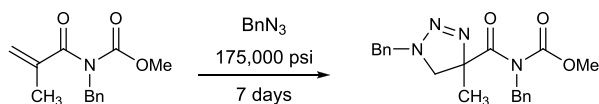
3-Phenyl-5-(2-(phenylamino)ethyl)-5-propyloxazolidine-2,4-dione (272h). According to the general procedure, the oxazolidinone was prepared as a colorless oil (190 mg, 56%). $R_f=0.30$ (30% EtOAc/hexanes); IR (film) 3291, 1726, 1691, 1599 cm^{-1} ; ^1H NMR (400 MHz, CDCl_3) δ 7.69 (d, $J = 8.0$ Hz, 2H), 7.40-7.25 (m, 4H), 7.27-7.23 (m, 2H), 7.18 (dd, $J = 7.6, 7.6$ Hz, 1H), 7.04 (dd, $J = 7.2, 7.2$ Hz, 1H), 6.86 (br s, 1H), 3.99 (ddd, $J = 9.6, 9.6, 3.2$ Hz, 1H), 3.77 (ddd, $J = 8.8, 8.8, 7.2$ Hz, 1H), 2.75 (ddd, $J = 13.6, 10.4, 7.2$ Hz, 1H), 2.43 (ddd, $J = 13.6, 8.4, 7.2$ Hz, 1H), 2.02-1.85 (m, 2H), 1.64-1.39 (m, 2H), 0.98 (t, $J = 7.2$ Hz, 3H); ^{13}C NMR (100 MHz, CDCl_3) ppm 171.4, 152.0, 139.1, 137.4, 128.8, 124.9, 123.5, 118.8, 83.3, 44.7, 38.9, 28.2, 16.3, 14.1; HRMS (EI) Exact mass calcd for $\text{C}_{20}\text{H}_{22}\text{N}_2\text{O}_3$ $[\text{M}]^+$, 338.1625, found 338.1627.



5-Benzyl-3-phenyl-5-(2-(phenylamino)ethyl)oxazolidine-2,4-dione (270i). According to the general procedure, the oxazolidine dione was prepared as a colorless oil (183 mg, 47%). $R_f=0.30$ (30% EtOAc/hexanes); $^1\text{H NMR}$ (400 MHz, CDCl_3) δ 7.61 (br s, 1H), 7.46 (d, $J = 8.0$ Hz, 2H), 7.39-7.16 (m, 12H), 7.03 (t, $J = 7.2$ Hz, 1H), 3.60 (dq, $J = 9.6, 2.4$ Hz, 1H), 3.35 (d, $J = 13.2$ Hz, 1H), 3.28 (d, $J = 13.2$ Hz, 1H), 2.83-2.67 (m, 2H), 2.56 (ddd, $J = 13.3, 8.0, 2.4$ Hz, 1H); $^{13}\text{C NMR}$ (100 MHz, CDCl_3) ppm 171.3, 152.1, 138.6, 137.6, 133.7, 130.3, 128.7, 128.3, 127.3, 125.2, 123.4, 120.6, 119.5, 83.5, 44.6, 42.5, 27.6; HRMS (EI) Exact mass calcd for $\text{C}_{24}\text{H}_{23}\text{N}_2\text{O}_3$ $[\text{M}+\text{H}]^+$, 387.1709, found 387.1699.

General Procedure for High Pressure Assisted [3+2] Cycloaddition

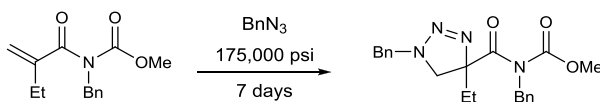
A solution of the olefin in azide 1.1 mL was sealed in a 5-mL plastic Luerlok syringe and subjected to 175,000 psi of pressure for 7 days at ambient temperature in a LECO Model PG-200-HPC apparatus. The solvent was removed in vacuo, and the residue was purified using flash chromatography to provide the product.



Methyl-benzyl(1-benzyl-4-methyl-4,5-dihydro-1H-1,2,3-triazole-4-carbonyl)

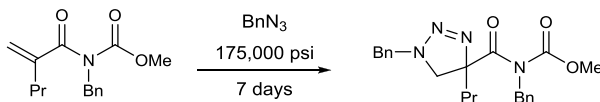
Carbamate (273a). According to the general procedure, methyl benzyl(methacryloyl)carbamate (42.2 mg, 0.18 mmol) provided the desired product after flash column chromatography (10% ethyl acetate in hexanes) as a colorless oil (47.1 mg,

70%). $R_f=0.50$ (30% EtOAc/hexanes); IR (film) 3088, 3031, 2954, 1957, 1747, 1683 cm^{-1} ; ^1H NMR (400 MHz, CDCl_3) δ 7.31-7.18 (m, 10H), 4.90 (d, $J = 14.8$ Hz, 1H), 4.79 (s, 2H), 4.49 (d, $J = 14.8$ Hz, 1H), 3.74 (s, 3H), 3.22 (d, $J = 10.0$ Hz, 1H), 2.96 (d, $J = 10.4$ Hz, 1H), 1.51 (s, 3H); ^{13}C NMR (100 MHz, CDCl_3) ppm 175.5, 155.2, 136.8, 135.4, 128.6, 128.3, 128.0, 127.7, 127.6, 127.3, 86.5, 55.7, 54.3, 53.8, 49.5, 23.0; HRMS (CI): Exact mass calcd for $\text{C}_{20}\text{H}_{23}\text{N}_4\text{O}_3$ $[\text{M}+\text{H}]^+$ 367.1765. Found 367.1767.



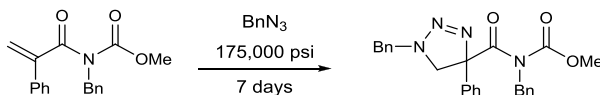
Methyl-benzyl(1-benzyl-4-ethyl-4,5-dihydro-1H-1,2,3-triazole-4-carbonyl)

carbamate (273b). According to the general procedure, methyl benzyl(2-methylenebutanoyl)carbamate (150 mg, 0.61 mmol) provided the desired product after flash column chromatography (10% ethyl acetate in hexanes) as a colorless oil (47.1 mg, 23%). $R_f=0.50$ (30% EtOAc/hexanes); IR (film) 3064, 2954, 2933, 2880, 2096, 1747, 1683 cm^{-1} ; ^1H NMR (400 MHz, CDCl_3) δ 7.30-7.18 (m, 10H), 4.94 (d, $J = 14.8$ Hz, 1H), 4.81, 4.78 (AB_q , $J_{\text{AB}} = 15.0$ Hz, 2H), 4.45 (d, $J = 14.8$ Hz, 1H), 3.73 (s, 3H), 3.21 (d, $J = 10.4$ Hz, 1H), 3.00 (d, $J = 10.4$ Hz, 1H), 2.01 (m, 2H), 0.73 (t, $J = 7.2$ Hz, 3H); ^{13}C NMR (100 MHz, CDCl_3) ppm 175.1, 155.3, 136.9, 135.6, 128.6, 128.3, 128.1, 128.0, 127.8, 127.4, 90.6, 54.4, 53.9, 53.0, 49.6, 29.8, 7.9; HRMS (CI): Exact mass calcd for $\text{C}_{21}\text{H}_{25}\text{N}_4\text{O}_3$ $[\text{M}+\text{H}]^+$ 381.1921. Found 381.1926.



Methyl-benzyl(1-benzyl-4-propyl-4,5-dihydro-1H-1,2,3-triazole-4-carbonyl)

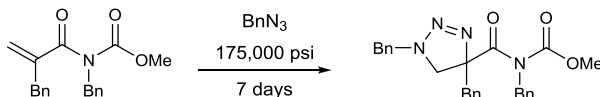
carbamate (273c). According to the general procedure, methyl benzyl(2-methylenepentanoyl)carbamate (207 mg, 0.79 mmol) provided the desired product after flash column chromatography (10% ethyl acetate in hexanes) as a colorless oil (47.1 mg, 15%). $R_f=0.50$ (30% EtOAc/hexanes); IR (film) 2958, 2923, 2851, 1747, 1683, 1674 cm^{-1} ; ^1H NMR (400 MHz, CDCl_3) δ 7.29-7.18 (m, 10H), 4.92 (d, $J = 14.8$ Hz, 1H), 4.81, 4.78 (AB_q, $J_{\text{AB}} = 15.0$ Hz, 2H), 4.46 (d, $J = 15.2$ Hz, 1H), 3.73 (s, 3H), 3.21 (d, $J = 10.4$ Hz, 1H), 3.00 (d, $J = 10.4$ Hz, 1H), 2.90 (m, 2H), 1.15 (m, 2H), 0.80 (t, $J = 7.6$ Hz, 3H); ^{13}C NMR (100 MHz, CDCl_3) ppm 175.2, 155.3, 136.9, 135.6, 128.7, 128.4, 128.1, 127.8, 127.4, 90.4, 54.5, 53.9, 53.6, 49.7, 38.9, 29.6, 16.9, 14.1; HRMS (CI): Exact mass calcd for $\text{C}_{22}\text{H}_{27}\text{N}_4\text{O}_3$ $[\text{M}+\text{H}]^+$ 395.2078. Found 395.2082.



Methyl-benzyl(1-benzyl-4-phenyl-4,5-dihydro-1H-1,2,3-triazole-4-carbonyl)

carbamate (273d). According to the general procedure, methyl benzyl(2-phenylacryloyl)carbamate (89.0 mg, 0.30 mmol) provided the desired product after flash column chromatography (10% ethyl acetate in hexanes) as a colorless oil (70.0 mg, 54%). $R_f=0.50$ (30% EtOAc/hexanes); IR (film) 3063, 3031, 2951, 2850, 1956, 1814, 1742, 1677 cm^{-1} ; ^1H NMR (400 MHz, CDCl_3) δ 7.26-7.08 (m, 15H), 4.86, 4.83 (AB_q, $J_{\text{AB}} = 14.8$ Hz, 2H), 4.75, 4.70 (AB_q, $J_{\text{AB}} = 14.8$ Hz, 2H), 3.82 (d, $J = 10.8$ Hz, 1H), 3.42 (s,

3H), 3.00 (d, $J = 10.8$ Hz, 1H); ^{13}C NMR (100 MHz, CDCl_3) ppm 172.6, 155.1, 139.7, 136.9, 135.0, 128.7, 128.5, 128.3, 128.1, 127.9, 127.8, 127.5, 127.4, 124.3, 92.8, 57.3, 54.4, 53.5, 49.6; HRMS (CI): Exact mass calcd for $\text{C}_{25}\text{H}_{25}\text{N}_4\text{O}_3$ $[\text{M}+\text{H}]^+$ 429.1921. Found 429.1940.



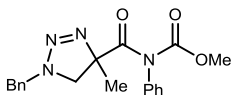
Methyl-benzyl(1,4-dibenzyl-4,5-dihydro-1H-1,2,3-triazole-4-carbonyl)carbamate

(273e). According to the general procedure, methyl benzyl(2-benzylacryloyl)carbamate (195 mg, 0.63 mmol) provided the desired product after flash column chromatography (10% ethyl acetate in hexanes) as a colorless oil (143 mg, 52%). $R_f=0.50$ (30% EtOAc/hexanes); IR (film) 3062, 3030, 2954, 1747, 1683 cm^{-1} ; ^1H NMR (400 MHz, CDCl_3) δ 7.25-6.76 (m, 13H), 6.78-6.76 (m, 2H), 4.80, 4.76 (AB_q , $J_{\text{AB}} = 14.8$ Hz, 2H), 4.71 (d, $J = 15.2$ Hz, 1H), 4.22 (d, $J = 14.8$ Hz, 1H), 3.78 (s, 3H), 3.42 (d, $J = 13.6$ Hz, 1H), 3.19 (d, $J = 14.0$ Hz, 1H), 3.16, 3.11 (AB_q , $J_{\text{AB}} = 11.8$ Hz, 2H); ^{13}C NMR (100 MHz, CDCl_3) ppm 175.0, 155.2, 136.8, 135.3, 134.8, 130.5, 128.4, 128.3, 128.1, 127.7, 127.5, 127.4, 126.9, 90.7, 54.0, 53.9, 52.1, 49.6, 41.5; HRMS (CI): Exact mass calcd for $\text{C}_{26}\text{H}_{27}\text{N}_4\text{O}_3$ $[\text{M}+\text{H}]^+$ 443.2078. Found 443.2062.

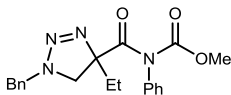
General Procedure for Acid Promoted [3+2] Cycloaddition.

A 0.1 M solution of the the triazoline (1.0 equiv) in acetonitrile was prepared in a 5 ml vial. This was cooled to -20 °C and triflic acid (2.0 equiv) was added and allowed to stir until reaction was complete. The cooled solution was first treated with triethylamine (2.0 equiv), then diluted in ethyl acetate and washed with saturated aq NaHCO_3 . The organic

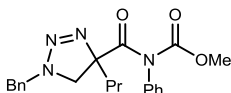
layers were dried and concentrated, and the crude oil was purified using flash chromatography to provide the product.



Methyl 1-benzyl-4-methyl-4,5-dihydro-1H-1,2,3-triazole-4-carbonyl(phenyl) carbamate (273f). IR (film) 3031, 1751, 1684 cm^{-1} ; ^1H NMR (400 MHz, CDCl_3) δ 7.38-7.27 (m, 8H), 7.09-7.07 (m, 2H), 4.97 (d, $J = 14.8$ Hz, 1H), 4.64 (d, $J = 14.8$ Hz, 1H), 3.75 (s, 3H), 3.44 (d, $J = 10.1$ Hz, 1H), 3.02 (d, $J = 10.1$ Hz, 1H), 1.62 (s, 3H); ^{13}C NMR (100 MHz, CDCl_3) ppm 175.9, 154.7, 138.1, 135.5, 129.2, 128.7, 128.2, 128.0, 127.9, 86.6, 55.9, 54.5, 54.2, 23.3; HRMS (CI): Exact mass calcd for $\text{C}_{19}\text{H}_{21}\text{N}_4\text{O}_3$ $[\text{M}+\text{H}]^+$ 353.1608. Found 353.1614.

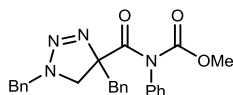


Methyl 1-benzyl-4-ethyl-4,5-dihydro-1H-1,2,3-triazole-4-carbonyl(phenyl) carbamate (273g). IR (film) 3064, 2955, 1748, 1698 cm^{-1} ; ^1H NMR (400 MHz, CDCl_3) δ 7.38-7.27 (m, 8H), 7.10-7.08 (m, 2H), 5.00 (d, $J = 14.8$ Hz, 1H), 4.61 (d, $J = 14.8$ Hz, 1H), 3.74 (s, 3H), 3.43 (d, $J = 10.3$ Hz, 1H), 3.07 (d, $J = 10.3$ Hz, 1H), 2.19-1.97 (m, 2H), 0.86 (t, $J = 7.4$ Hz, 3H); ^{13}C NMR (100 MHz, CDCl_3) ppm 175.5, 154.8, 138.2, 135.6, 129.1, 128.7, 128.2, 128.0, 127.9, 90.6, 54.5, 54.2, 53.0, 30.2, 8.7; HRMS (CI): Exact mass calcd for $\text{C}_{20}\text{H}_{23}\text{N}_4\text{O}_3$ $[\text{M}+\text{H}]^+$ 367.1770. Found 367.1757.



Methyl 1-benzyl-4-propyl-4,5-dihydro-1H-1,2,3-triazole-4-carbonyl(phenyl) carbamate (273h). IR (film) 3063, 2959, 1747, 1696 cm^{-1} ; ^1H NMR (400 MHz, CDCl_3) δ 7.38-7.27 (m, 8H), 7.10-7.08 (m, 2H), 4.98 (d, $J = 14.8$ Hz, 1H), 4.62 (d, $J = 14.8$ Hz, 1H), 3.74 (s, 3H), 3.43 (d, $J = 10.2$ Hz, 1H), 3.07

(d, $J = 10.2$ Hz, 1H), 2.10-1.91 (m, 2H), 1.40-1.16 (m, 2H), 0.88 (t, $J = 7.3$ Hz, 3H); ^{13}C NMR (100 MHz, CDCl_3) ppm 175.4, 154.7, 138.1, 135.5, 129.1, 128.6, 128.1, 127.9, 127.8, 90.2, 54.4, 54.1, 53.5, 39.2, 16.9, 14.1; HRMS (CI): Exact mass calcd for $\text{C}_{21}\text{H}_{25}\text{N}_4\text{O}_3$ $[\text{M}+\text{H}]^+$ 381.1927. Found 381.1911.

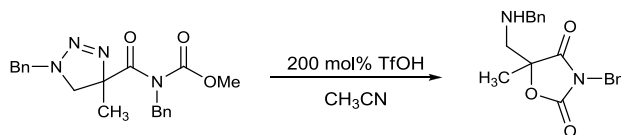


Methyl 1,4-dibenzyl-4,5-dihydro-1H-1,2,3-triazole-4-carbonyl(phenyl)carbamate (273i). IR (film) 3062, 3030, 1747,

1697 cm^{-1} ; ^1H NMR (400 MHz, CDCl_3) δ 7.31-7.16 (m, 11H), 6.91-6.87 (m, 4H), 4.80 (d, $J = 15.0$ Hz, 1H), 4.37 (d, $J = 15.0$ Hz, 1H), 3.72 (s, 3H), 3.51 (d, $J = 13.7$ Hz, 1H), 3.37 (d, $J = 10.5$ Hz, 1H), 3.19 (d, $J = 13.7$ Hz, 1H), 3.18 (d, $J = 10.5$ Hz, 1H); ^{13}C NMR (100 MHz, CDCl_3) ppm 175.0, 154.7, 138.1, 135.4, 134.9, 130.7, 129.0, 128.5, 128.1, 127.8, 127.7, 127.6, 126.9, 90.4, 54.2, 54.1, 52.6, 42.3; HRMS (CI): Exact mass calcd for $\text{C}_{25}\text{H}_{25}\text{N}_4\text{O}_3$ $[\text{M}+\text{H}]^+$ 429.1927. Found 429.1944.

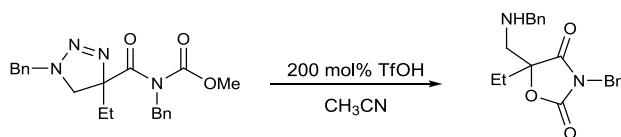
General Procedure for Acid Promoted Triazoline Decomposition.

A 0.1 M solution of the the triazoline (1.0 equiv) in acetonitrile was prepared in a 5 ml vial. This was cooled to -20 $^\circ\text{C}$ and triflic acid (2.0 equiv) was added and allowed to stir until reaction was complete. The cooled solution was first treated with triethylamine (2.0 equiv), then diluted in ethyl acetate and washed with saturated aq NaHCO_3 . The organic layers were dried and concentrated, and the crude oil was purified using flash chromatography to provide the product.



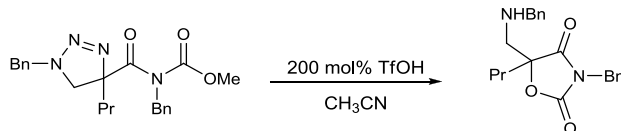
3-Benzyl-5-(benzylamino-methyl)-5-methyl-oxazolidine-2,4-dione (114a).

According to the general procedure, methyl benzyl(1-benzyl-4-methyl-4,5-dihydro-1H-1,2,3-triazole-4-carbonyl)carbamate (50.1 mg, 0.13 mmol) provided the desired product after flash column chromatography (10% ethyl acetate in hexanes) as a colorless oil (38.1 mg, 90%). $R_f=0.5$ (30% EtOAc/hexanes); IR (film) 3352, 2924, 2852, 1813, 1738 cm^{-1} ; ^1H NMR (500 MHz, CDCl_3) δ 7.49-7.12 (m, 10H), 4.73, 4.69 (AB_q , $J_{\text{AB}} = 11.8$ Hz, 2H), 3.72 (s, 2H), 3.05, 3.01 (AB_q , $J_{\text{AB}} = 10.8$ Hz, 2H), 1.48 (s, 3H); ^{13}C NMR (100 MHz, CDCl_3) ppm 175.1, 155.1, 139.5, 134.8, 129.3, 128.7, 128.4, 128.3, 127.9, 127.1, 53.9, 53.4, 43.7, 29.6, 19.7; HRMS (EI): Exact mass calcd for $\text{C}_{19}\text{H}_{21}\text{N}_2\text{O}_3$ $[\text{M}+\text{H}]^+$ 325.1547. Found 325.1545. *Anal.* Calcd for $\text{C}_{19}\text{H}_{20}\text{N}_2\text{O}_3$: C, 70.35; H, 6.21; N, 8.64. Found C, 70.27; H, 6.20; N, 8.21.

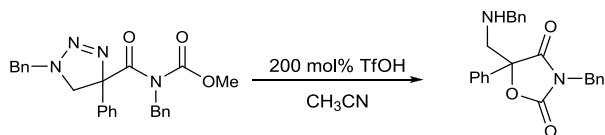


3-Benzyl-5-(benzylamino-methyl)-5-ethyl-oxazolidine-2,4-dione (114b). According to the general procedure, methyl benzyl(1-benzyl-4-ethyl-4,5-dihydro-1H-1,2,3-triazole-4-carbonyl)carbamate (85.1 mg, 0.22 mmol) provided the desired product after flash column chromatography (10% ethyl acetate in hexanes) as a colorless oil (52.2 mg, 70%). $R_f=0.49$ (30% EtOAc/hexanes); IR (film) 3390, 2924, 2849, 1811, 1739 cm^{-1} ; ^1H NMR (500 MHz, CDCl_3) δ 7.45-7.42 (m, 2H), 7.36-7.25 (m, 6H), 7.16-7.15 (m, 2H), 4.75, 4.72 (AB_q , $J_{\text{AB}} = 11.8$ Hz, 2H), 3.74 (s, 2H), 3.05, 3.03 (AB_q , $J_{\text{AB}} = 10.8$ Hz, 2H), 1.92-1.80 (m, 2H) 1.41 (br s, 1H), 0.86 (t, $J = 7.5$ Hz, 3H); ^{13}C NMR (100 MHz, CDCl_3) ppm

174.6, 155.4, 139.5, 134.8, 128.7, 128.6, 128.4, 128.3, 128.1, 127.9, 127.1, 90.6, 53.9, 52.4, 43.6, 26.5, 6.9; HRMS (EI): Exact mass calcd for C₂₀H₂₃N₂O₃ [M+H]⁺ 339.1703. Found 339.1700. *Anal.* Calcd for C₂₀H₂₂N₂O₃: C, 70.99; H, 6.55; N, 8.28. Found C, 71.10; H, 6.73; N, 8.17.

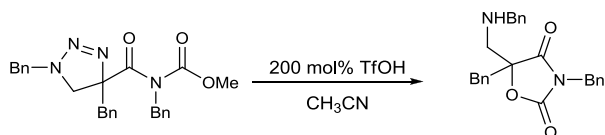


3-Benzyl-5-(benzylamino-methyl)-5-propyl-oxazolidine-2,4-dione (114c). According to the general procedure, methyl benzyl(1-benzyl-4-propyl-4,5-dihydro-1H-1,2,3-triazole-4-carbonyl)carbamate (28.1 mg, 0.07 mmol) provided the desired product after flash column chromatography (10% ethyl acetate in hexanes) as a colorless oil (17.0 mg, 71%). *R_f*=0.51 (30% EtOAc/hexanes); IR (film) 3403, 2962, 2931, 2875, 1811, 1734 cm⁻¹, ¹H NMR (500 MHz, CDCl₃) δ 7.49–7.41 (m, 2H), 7.36–7.24 (m, 6H), 7.20–7.15 (m, 2H), 4.70, 4.74 (AB_q, *J*_{AB} = 11.6 Hz, 2H), 3.73 (s, 2H), 3.03 (s, 2H), 1.84–1.73 (m, 2H), 1.42–1.32 (m, 2H), 1.20–1.12 (m, 1H), 0.86 (t, *J* = 7.5 Hz, 3H); ¹³C NMR (100 MHz, CDCl₃) ppm 174.7, 155.4, 139.4, 134.8, 128.7, 128.4, 128.3, 128.1, 127.9, 127.1, 90.3, 53.9, 52.6, 43.6, 35.4, 15.9, 13.8; HRMS (CI): Exact mass calcd for C₂₁H₂₅N₂O₃ [M+H]⁺ 353.1860. Found 353.1855. *Anal.* Calcd for C₂₁H₂₄N₂O₃: C, 71.57; H, 6.86; N, 7.95. Found C, 71.79; H, 7.06; N, 7.79.



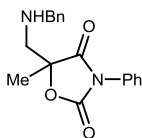
3-Benzyl-5-(benzylamino-methyl)-5-phenyl-oxazolidine-2,4-dione (114d).

According to the general procedure, methyl benzyl(1-benzyl-4-phenyl-4,5-dihydro-1H-1,2,3-triazole-4-carbonyl)carbamate (36.1 mg, 0.08 mmol) provided the desired product after flash column chromatography (10% ethyl acetate in hexanes) as a colorless oil (17.2 mg, 54%). $R_f=0.46$ (30% EtOAc/hexanes); IR (film) 3352, 2922, 2849, 2360, 1740 cm^{-1} ; ^1H NMR (500 MHz, CDCl_3) δ 7.62-7.60 (m, 2H), 7.45-7.41 (m, 5H), 7.30-7.24 (m, 6H), 7.16-7.14 (m, 2H), 4.76, 4.71 (AB_q, $J_{AB} = 16$ Hz, 2H), 3.79 (s, 2H), 3.40 (d, $J = 12.0$ Hz, 1H), 3.22 (d, $J = 12.0$ Hz, 1H); ^{13}C NMR (100 MHz, CDCl_3) ppm 173.2, 154.9, 139.4, 134.5, 133.9, 129.1, 128.7, 128.6, 128.4, 128.2, 128.0, 127.8, 127.1, 124.7, 89.5, 55.6, 53.9, 43.8, 29.7; HRMS (CI): Exact mass calcd for $\text{C}_{24}\text{H}_{23}\text{N}_2\text{O}_3$ $[\text{M}+\text{H}]^+$ 387.1730. Found 387.1697. *Anal.* Calcd for $\text{C}_{24}\text{H}_{22}\text{N}_2\text{O}_3$: C, 74.59; H, 5.74; N, 7.25. Found C, 74.55; H, 5.93; N, 7.11.



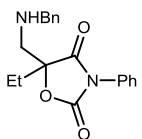
3,5-Dibenzyl-5-(benzylamino-methyl)-oxazolidine-2,4-dione (114e). According to the general procedure, methyl benzyl(1,4-dibenzyl-4,5-dihydro-1H-1,2,3-triazole-4-carbonyl)carbamate (57.1 mg, 0.13 mmol) provided the desired product after flash column chromatography (10% ethyl acetate in hexanes) as a colorless oil (42.1 mg, 80%). $R_f=0.45$ (30% EtOAc/hexanes); IR (film) 3352, 2922, 1815, 1736 cm^{-1} ; ^1H NMR (500 MHz, CDCl_3) δ 7.34-7.15 (m, 13H), 7.00-6.99 (m, 2H), 4.46 (s, 2H), 3.79 (s, 2H), 3.20 (d, $J = 13.5$ Hz, 1H), 3.13 (d, $J = 13.5$ Hz, 1H), 3.11 (s, 2H); ^{13}C NMR (100 MHz,

CDCl₃) ppm 173.8, 154.9, 139.4, 134.3, 132.3, 130.0, 128.7, 128.6, 128.5, 128.3, 127.9, 127.7, 127.6, 127.2, 53.9, 52.7, 43.3, 39.1; HRMS (CI): Exact mass calcd for C₂₅H₂₅N₂O₃ [M+H]⁺ 401.1860. Found 401.1855. *Anal.* Calcd for C₂₅H₂₄N₂O₃: C, 74.98; H, 6.04; N, 7.00. Found C, 75.14; H, 6.09; N, 6.98.



5-((Benzylamino)methyl)-5-methyl-3-phenyloxazolidine-2,4-dione

(274f). According to the general procedure, methyl 1-benzyl-4-methyl-4,5-dihydro-1*H*-1,2,3-triazole-4-carbonyl(phenyl)carbamate (165 mg, 0.46 mmol) provided the desired product after flash column chromatography (10% ethyl acetate in hexanes) as a colorless oil (80.0 mg, 56%). *R_f* = 0.6 (30% EtOAc/hexanes); IR (film) 3344, 2841, 1814, 1746 cm⁻¹; ¹H NMR (400 MHz, CDCl₃) δ 7.42-7.31 (m, 5H), 7.24-7.14 (m, 5H), 3.76 (d, *J* = 13.6 Hz, 1H), 3.72 (d, *J* = 13.6 Hz, 1H), 3.05 (d, *J* = 13.6 Hz, 1H), 3.01 (d, *J* = 13.6 Hz, 1H), 1.50 (s, 3H), the NH was not observed; ¹³C NMR (100 MHz, CDCl₃) ppm 174.4, 154.1, 139.5, 131.1, 129.2, 128.8, 128.5, 127.9, 127.2, 125.8, 87.0, 54.1, 53.6, 19.6; HRMS (EI): Exact mass calcd for C₁₈H₁₉N₂O₃ [M+H]⁺ 311.1396. Found 311.1385.



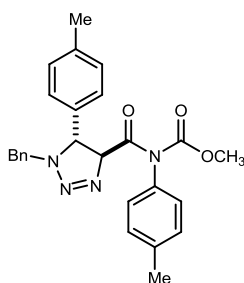
5-((Benzylamino)methyl)-5-ethyl-3-phenyloxazolidine-2,4-dione (274g).

According to the general procedure, methyl 1-benzyl-4-ethyl-4,5-dihydro-1*H*-1,2,3-triazole-4-carbonyl(phenyl)carbamate (226 mg, 0.61 mmol) provided the desired product after flash column chromatography (10% ethyl acetate in hexanes) as a colorless oil (147 mg, 74%). *R_f* = 0.6 (30% EtOAc/hexanes); IR (film) 3353, 3062, 1814, 1747 cm⁻¹; ¹H NMR (400 MHz, CDCl₃) δ 7.42-7.31 (m, 5H), 7.23-7.15 (m, 5H), 3.76 (d, *J* = 13.6 Hz, 1H), 3.72 (d, *J* = 13.6 Hz, 1H), 3.03 (s, 2H), 1.86 (dq, *J* = 14.8,

7.2 Hz, 2H), 0.93 (t, $J = 7.4$ Hz, 3H), the NH was not observed; ^{13}C NMR (100 MHz, CDCl_3) ppm 174.9, 154.4, 139.5, 131.1, 129.2, 128.8, 128.4, 127.8, 127.1, 125.8, 90.5, 54.0, 52.6, 26.4, 7.0; HRMS (EI): Exact mass calcd for $\text{C}_{19}\text{H}_{21}\text{N}_2\text{O}_3$ $[\text{M}+\text{H}]^+$ 325.1552. Found 325.1536.

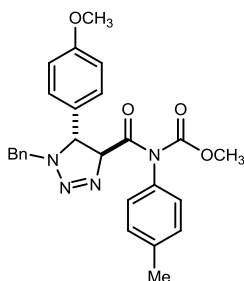
General Procedure for Microwave Promoted Azide-Olefin Cycloaddition.

A solution of the imide (1.0 equiv.) in the benzyl azide (10 equiv.) was subjected to 120-150 °C for 5-10 minutes in a Biotage microwave. The mixture was purified using flash chromatography to provide the product.

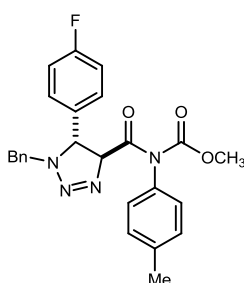


Methyl (4*S*,5*R*)-1-benzyl-5-*p*-tolyl-4,5-dihydro-1*H*-1,2,3-triazole-4-carboxyl(*p*-tolyl)carbamate (275a). According to the general procedure, (*E*)-methyl *p*-tolyl(3-*p*-tolylprop-2-enoyl)carbamate (42 mg, 0.13 mmol) provided the desired product after flash column chromatography (10% ethyl acetate in hexanes) as a colorless oil

(47 mg, 81%). $R_f=0.50$ (30% EtOAc/hexanes); IR (film) 3029, 2955, 2838, 1749, 1708, 1511, 1438 cm^{-1} ; ^1H NMR (400 MHz, CDCl_3) δ 7.28-7.24 (m, 4H), 7.20 (d, $J = 8.0$ Hz, 2H), 7.17-7.10 (m, 5H), 7.00 (d, $J = 8.0$ Hz, 2H), 6.10 (d, $J = 12.0$ Hz, 1H), 5.13 (d, $J = 15.2$ Hz, 1H), 4.78 (d, $J = 12.0$ Hz, 1H), 4.24 (d, $J = 15.2$ Hz, 1H), 3.73 (s, 3H), 2.37 (s, 3H), 2.36 (s, 3H); ^{13}C NMR (100 MHz, CDCl_3) ppm 169.4, 154.2, 138.4, 138.1, 134.9, 134.8, 134.4, 129.8, 129.6, 128.5, 128.4, 127.8, 127.7, 127.5, 88.1, 62.0, 54.1, 51.8, 21.1, 21.0; HRMS (CI): Exact mass calcd for $\text{C}_{26}\text{H}_{27}\text{N}_4\text{O}_4$ $[\text{M}+\text{H}]^+$ 443.2078, found 443.2077.

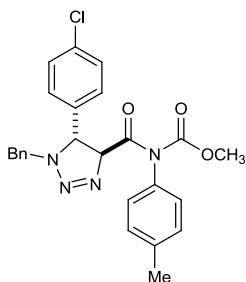


Methyl (4*S*,5*R*)-1-benzyl-5-(4-methoxyphenyl)-4,5-dihydro-1*H*-1,2,3-triazole-4-carbonyl(*p*-tolyl)carbamate (275b). According to the general procedure, (*E*)-methyl 3-(4-methoxyphenyl)prop-2-enoyl(*p*-tolyl)carbamate (46 mg, 0.14 mmol) provided the desired product after flash column chromatography (10% ethyl acetate in hexanes) as a colorless oil (53 mg, 82%). $R_f=0.50$ (30% EtOAc/hexanes); IR (film) 3031, 2955, 2838, 1749, 1716, 1611, 1512 cm^{-1} ; ^1H NMR (400 MHz, CDCl_3) δ 7.29-7.25 (m, 3H), 7.20 (d, $J = 8.0$ Hz, 2H), 7.11-7.12 (m, 4H), 7.00 (d, $J = 8.0$ Hz, 2H), 6.86 (d, $J = 8.8$ Hz, 2H), 6.08 (d, $J = 12.0$ Hz, 1H), 5.11 (d, $J = 14.8$ Hz, 1H), 4.76 (d, $J = 12.0$ Hz, 1H), 4.24 (d, $J = 15.2$ Hz, 1H), 3.81 (s, 3H), 3.73 (s, 3H), 2.36 (s, 3H); ^{13}C NMR (100 MHz, CDCl_3) ppm 169.4, 159.6, 154.3, 138.4, 135.0, 134.9, 129.8, 128.9, 128.5, 128.4, 127.9, 127.7, 125.8, 114.3, 88.0, 61.8, 55.2, 54.1, 51.8, 21.1(two overlapping C); HRMS (CI): Exact mass calcd for $\text{C}_{26}\text{H}_{26}\text{N}_4\text{O}_4$ [M] $^+$ 458.1949, found 458.1949.



Methyl (4*S*,5*R*)-1-benzyl-5-(4-fluorophenyl)-4,5-dihydro-1*H*-1,2,3-triazole-4-carbonyl(*p*-tolyl)carbamate (275c). According to the general procedure, (*E*)-methyl 3-(4-fluorophenyl)acryloyl(*p*-tolyl)carbamate (44 mg, 0.14 mmol) provided the desired product after flash column chromatography (10% ethyl acetate in hexanes) as a colorless oil (32 mg, 50%). $R_f=0.46$ (30% EtOAc/hexanes); IR (film) 3031, 2093, 1749, 1708, 1510 cm^{-1} ; ^1H NMR (400 MHz, CDCl_3) δ 7.25-7.11 (m, 7H), 7.10-7.09 (m, 2H), 7.08-6.97 (m, 4H), 6.07 (d, $J = 12.0$ Hz, 1H), 5.07 (d, $J = 15.2$ Hz, 1H), 4.76 (d, $J = 12.0$ Hz, 1H), 4.27 (d, $J = 15.2$ Hz, 1H), 3.72 (s, 3H), 2.35 (s, 3H); ^{13}C NMR (100 MHz,

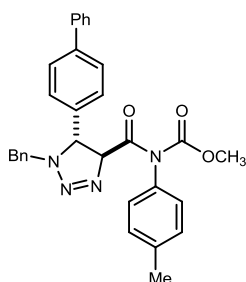
CDCl₃) ppm 169.2, 163.8, 161.3, 154.3, 138.5, 134.8, 134.5, 129.9, 129.4, 129.3, 128.5, 128.4, 116.0, 115.8, 88.4, 61.6, 54.2, 52.2, 21.1; HRMS (CI): Exact mass calcd for C₂₅H₂₄FN₄O₃ [M+H]⁺ 447.1832, found 447.1839.



Methyl (4S,5R)-1-benzyl-5-(4-chlorophenyl)-4,5-dihydro-1H-

1,2,3-triazole-4-carbonyl(p-tolyl)carbamate (275d).

According to the general procedure, (*E*)-methyl 3-(4-chlorophenyl)acryloyl(*p*-tolyl)carbamate (64 mg, 0.2 mmol) provided the desired product after flash column chromatography (10% ethyl acetate in hexanes) as a colorless oil (45 mg, 48%). *R*_f=0.40 (30% EtOAc/hexanes); IR (film) 3031, 2954, 1901, 1749, 1707, 1190 cm⁻¹; ¹H NMR (400 MHz, CDCl₃) δ 7.32-7.25 (m, 5H), 7.21 (d, *J* = 8.0 Hz, 2H), 7.16-7.10 (m, 4H), 7.00 (d, *J* = 8.0 Hz, 2H), 6.07 (d, *J* = 12.0 Hz, 1H), 5.10 (d, *J* = 15.2 Hz, 1H), 4.76 (d, *J* = 12.0 Hz, 1H), 4.29 (d, *J* = 15.2 Hz, 1H), 3.75 (s, 3H), 2.38 (s, 3H); ¹³C NMR (100 MHz, CDCl₃) ppm 169.2, 154.3, 138.5, 136.2, 134.8, 134.5, 134.2, 129.9, 129.0, 128.6, 128.5, 127.9, 127.8, 88.5, 61.7, 54.2, 52.3, 21.1; HRMS (CI): Exact mass calcd for C₂₅H₂₄ClN₄O₃ [M+H]⁺ 463.1537, found 463.1541.

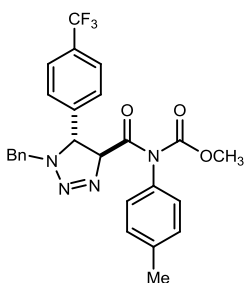


Methyl (4S,5R)-1-benzyl-5-(biphenyl-4-yl)-4,5-dihydro-1H-

1,2,3-triazole-4-carbonyl(p-tolyl)carbamate (275e).

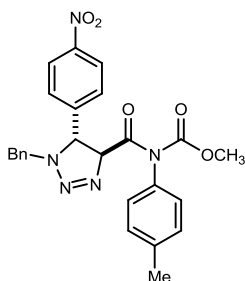
According to the general procedure, (*E*)-methyl 3-(biphenyl-4-yl)acryloyl(*p*-tolyl)carbamate (74 mg, 0.2 mmol) provided the desired product after flash column chromatography (10% ethyl acetate in hexanes) as a colorless oil (30 mg, 29%). *R*_f=0.46 (30% EtOAc/hexanes); IR (film) 3030, 2093, 1749, 1708, 1252 cm⁻¹; ¹H NMR (400 MHz, CDCl₃) δ 7.61-7.56 (m, 4H), 7.49-7.36 (m,

4H), 7.31-7.26 (m, 4H), 7.22 (d, $J = 8.0$ Hz, 2H), 7.17-7.15 (m, 2H), 7.02 (d, $J = 8.4$ Hz, 2H), 6.17 (d, $J = 12.0$ Hz, 1H), 5.16 (d, $J = 14.8$ Hz, 1H), 4.86 (d, $J = 12.0$ Hz, 1H), 4.34 (d, $J = 14.8$ Hz, 1H), 3.75 (s, 3H), 2.38 (s, 3H); ^{13}C NMR (100 MHz, CDCl_3) ppm 169.4, 154.3, 141.3, 140.3, 138.5, 136.6, 134.9, 134.8, 129.9, 128.8, 128.6, 128.5, 128.1, 127.9, 127.8, 127.6, 127.5, 127.0, 88.4, 62.1, 54.2, 52.2, 21.6; HRMS (CI): Exact mass calcd for $\text{C}_{31}\text{H}_{29}\text{N}_4\text{O}_3$ $[\text{M}+\text{H}]^+$ 505.2235, found 505.2244.

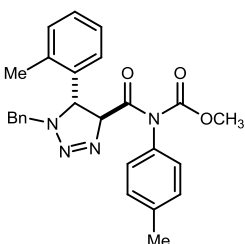


Methyl (4*S*,5*R*)-1-benzyl-5-(4-(trifluoromethyl)phenyl)-4,5-dihydro-1*H*-1,2,3-triazole-4-carbonyl(*p*-tolyl)carbamate (275f).

According to the general procedure, (*E*)-methyl *p*-tolyl(3-(4-(trifluoromethyl)phenyl)acryloyl)carbamate (72 mg, 0.2 mmol) provided the desired product after flash column chromatography (10% ethyl acetate in hexanes) as a colorless oil (43 mg, 43%). $R_f=0.48$ (30% EtOAc/hexanes); IR (film) 3032, 2956, 1750, 1707, 1511, 1325 cm^{-1} ; ^1H NMR (400 MHz, CDCl_3) δ 7.56 (d, $J = 8.4$ Hz, 2H), 7.31 (d, $J = 8.0$ Hz, 2H), 7.23-7.17 (m, 5H), 7.09-7.07 (m, 2H), 6.97 (d, $J = 8.0$ Hz, 2H), 6.08 (d, $J = 12.4$ Hz, 1H), 5.07 (d, $J = 14.8$ Hz, 1H), 4.79 (d, $J = 12.4$ Hz, 1H), 4.30 (d, $J = 14.8$ Hz, 1H), 3.72 (s, 3H), 2.35 (s, 3H); ^{13}C NMR (100 MHz, CDCl_3) ppm 169.4, 154.3, 141.9, 138.6, 134.8, 134.3, 129.9, 128.6, 128.5, 128.0, 127.8, 126.0, 125.9, 88.8, 62.0, 54.2, 52.6, 21.1; HRMS (CI): Exact mass calcd for $\text{C}_{26}\text{H}_{23}\text{F}_3\text{N}_4\text{O}_3$ $[\text{M}]^+$ 496.1717, found 496.1715.

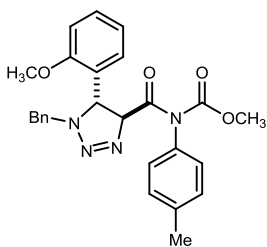


Methyl (4*S*,5*R*)-1-benzyl-5-(4-nitrophenyl)-4,5-dihydro-1*H*-1,2,3-triazole-4-carbonyl(*p*-tolyl)carbamate (275g). According to the general procedure, (*E*)-methyl 3-(4-nitrophenyl)acryloyl(*p*-tolyl)carbamate (68 mg, 0.2 mmol) provided the desired product after flash column chromatography (10% ethyl acetate in hexanes) as a colorless oil (78 mg, 82%). $R_f=0.49$ (30% EtOAc/hexanes); IR (film) 3030, 2955, 2094, 1749, 1706, 1521, 1253 cm^{-1} ; ^1H NMR (400 MHz, CDCl_3) δ 8.16 (d, $J = 8.4$ Hz, 2H), 7.39 (d, $J = 8.8$ Hz, 2H), 7.26-7.21 (m, 5H), 7.11-7.09 (m, 2H), 7.00 (d, $J = 8.4$ Hz, 2H), 6.12 (d, $J = 12.4$ Hz, 1H), 5.06 (d, $J = 15.2$ Hz, 1H), 4.85 (d, $J = 12.4$ Hz, 1H), 4.40 (d, $J = 15.2$ Hz, 1H), 3.75 (s, 3H), 2.38 (s, 3H); ^{13}C NMR (100 MHz, CDCl_3) ppm 168.8, 154.3, 147.8, 145.3, 138.7, 134.7, 134.0, 130.0, 128.7, 128.5, 128.2, 127.7, 124.1, 89.1, 61.9, 54.3, 53.0, 21.1; HRMS (CI): Exact mass calcd for $\text{C}_{25}\text{H}_{23}\text{N}_5\text{O}_5$ $[\text{M}]^+$ 473.1694, found 473.1713.



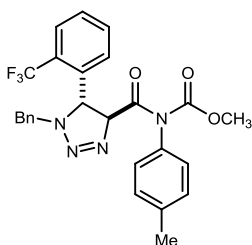
Methyl (4*S*,5*R*)-1-benzyl-5-*o*-tolyl-4,5-dihydro-1*H*-1,2,3-triazole-4-carbonyl(*p*-tolyl)carbamate (275h). According to the general procedure, (*E*)-methyl *p*-tolyl(3-*o*-tolylacryloyl)carbamate (60 mg, 0.2 mmol) provided the desired product after flash column chromatography (10% ethyl acetate in hexanes) as a colorless oil (60 mg, 67%). $R_f=0.46$ (30% EtOAc/hexanes); IR (film) 3029, 2922, 1749, 1707, 1511, 1290 cm^{-1} ; ^1H NMR (400 MHz, CDCl_3) δ 7.28-7.20 (m, 8H), 7.12-7.09 (m, 3H), 7.01 (d, $J = 8.4$ Hz, 2H), 6.19 (d, $J = 11.2$ Hz, 1H), 5.20 (d, $J = 14.8$ Hz, 1H), 5.14 (d, $J = 11.2$ Hz, 1H), 4.25 (d, $J = 15.2$ Hz, 1H), 3.74 (s, 3H), 2.37 (s, 3H), 2.06 (s, 3H); ^{13}C NMR (100 MHz, CDCl_3) ppm

169.6, 154.3, 138.4, 136.9, 135.1, 134.8, 130.7, 129.9, 128.5, 128.3, 127.9, 127.8, 126.7, 88.2, 57.9, 54.2, 21.1, 19.0; HRMS (CI): Exact mass calcd for C₂₆H₂₇N₄O₃ [M+H]⁺ 443.2083, found 443.2086.



Methyl (4*S*,5*R*)-1-benzyl-5-(2-methoxyphenyl)-4,5-dihydro-1*H*-1,2,3-triazole-4-carbonyl(*p*-tolyl)carbamate (275i).

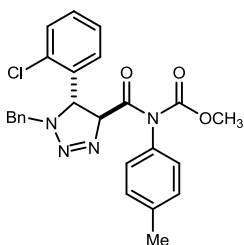
According to the general procedure, (*E*)-methyl 3-(2-methoxyphenyl)prop-2-enoyl(*p*-tolyl)carbamate (64 mg, 0.2 mmol) provided the desired product after flash column chromatography (10% ethyl acetate in hexanes) as a colorless oil (50 mg, 54%). *R_f*=0.50 (30% EtOAc/hexanes); IR (film) 3029, 2954, 2840, 1747, 1708, 1600, 1288 cm⁻¹; ¹H NMR (400 MHz, CDCl₃) δ 7.30-7.19 (m, 6H), 7.13 (dd, *J* = 6.8, 1.6 Hz, 2H), 7.07 (dd, *J* = 8.4, 1.6 Hz, 1H), 7.02 (d, *J* = 8.0 Hz, 2H), 6.91 (ddd, *J* = 7.6, 6.4, 0.8 Hz, 1H), 6.84 (d, *J* = 8.0 Hz, 1H), 6.22 (d, *J* = 9.6 Hz, 1H), 5.20 (d, *J* = 8.0 Hz, 1H), 5.09 (d, *J* = 15.2 Hz, 1H), 4.35 (d, *J* = 15.2 Hz, 1H), 3.72 (s, 6H), 2.37 (s, 3H); ¹³C NMR (100 MHz, CDCl₃) ppm 170.1, 157.5, 154.3, 138.3, 135.5, 135.2, 129.8, 129.4, 128.9, 128.4, 128.1, 127.9, 127.5, 125.8, 110.8, 88.2, 57.7, 55.3, 54.0, 51.9, 21.1; HRMS (CI): Exact mass calcd for C₂₆H₂₇N₄O₄ [M+H]⁺ 459.2027, found 459.2021.



Methyl (4*S*,5*R*)-1-benzyl-5-(2-(trifluoromethyl)phenyl)-4,5-dihydro-1*H*-1,2,3-triazole-4-carbonyl(*p*-tolyl)carbamate (275j).

According to the general procedure, (*E*)-methyl *p*-tolyl(3-(2-(trifluoromethyl)phenyl)acryloyl)carbamate (72 mg, 0.2 mmol) provided the desired product after flash column chromatography (10% ethyl acetate in

hexanes) as a colorless oil (57 mg, 57%). $R_f=0.46$ (30% EtOAc/hexanes); IR (film) 3031, 2956, 1747, 1710, 1510, 1350 cm^{-1} ; ^1H NMR (400 MHz, CDCl_3) δ 7.62 (d, $J = 7.6$ Hz, 1H), 7.54 (dd, $J = 7.6, 7.6$ Hz, 1H), 7.39 (dd, $J = 7.6, 7.6$ Hz, 1H), 7.28 (dd, $J = 7.6, 7.6$ Hz, 1H), 7.24-7.11 (m, 5H), 7.00 (d, $J = 8.4$ Hz, 2H), 6.30 (d, $J = 7.6$ Hz, 2H), 5.39 (d, $J = 7.6$ Hz, 1H), 5.10 (d, $J = 14.8$ Hz, 1H), 4.50 (d, $J = 14.8$ Hz, 1H), 3.69 (s, 3H), 2.37 (s, 3H); ^{13}C NMR (100 MHz, CDCl_3) ppm 169.0, 154.3, 138.4, 137.7, 134.9, 134.7, 132.6, 129.9, 128.4, 128.1, 128.0, 127.7, 125.9, 125.8, 125.1, 122.4, 88.8, 57.7, 54.1, 52.2, 21.1; HRMS (CI): Exact mass calcd for $\text{C}_{26}\text{H}_{23}\text{F}_3\text{N}_4\text{O}_3$ $[\text{M}+\text{H}]^+$ 496.1717, found 496.1713.

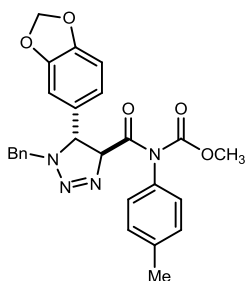


Methyl (4*S*,5*R*)-1-benzyl-5-(2-chlorophenyl)-4,5-dihydro-1*H*-

1,2,3-triazole-4-carbonyl(*p*-tolyl)carbamate (275k). According to

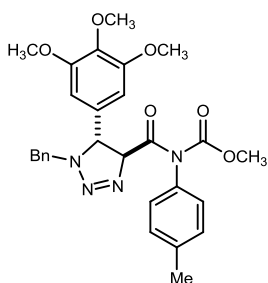
the general procedure, (*E*)-methyl 3-(2-chlorophenyl)acryloyl(*p*-tolyl)carbamate (66 mg, 0.2 mmol) provided the desired product after flash column chromatography (10% ethyl acetate in hexanes)

as a colorless oil (43 mg, 46%). $R_f=0.46$ (30% EtOAc/hexanes); IR (film) 3030, 2954, 1747, 1709, 1510, 1253 cm^{-1} ; ^1H NMR (400 MHz, CDCl_3) δ 7.32-7.30 (m, 1H), 7.24-7.11 (m, 10H), 6.23 (d, $J = 10.0$ Hz, 2H), 5.32 (d, $J = 10.0$ Hz, 1H), 5.08 (d, $J = 15.2$ Hz, 1H), 4.39 (d, $J = 15.2$ Hz, 1H), 3.67 (s, 3H), 2.34 (s, 3H); ^{13}C NMR (100 MHz, CDCl_3) ppm 169.3, 154.3, 138.5, 135.0, 134.7, 133.6, 130.0, 129.9, 129.3, 128.5, 128.3, 127.9, 127.8, 127.4, 88.5, 59.3, 54.2, 52.4, 21.1; HRMS (CI): Exact mass calcd for $\text{C}_{25}\text{H}_{23}\text{ClN}_4\text{O}_3$ $[\text{M}+\text{H}]^+$ 462.1453, found 462.1442.



Methyl (4*S*,5*R*)-5-(benzo[d][1,3]dioxol-5-yl)-1-benzyl-4,5-dihydro-1*H*-1,2,3-triazole-4-carbonyl(*p*-tolyl)carbamate (275l).

According to the general procedure, (*E*)-methyl 3-(benzo[d][1,3]dioxol-5-yl)acryloyl(*p*-tolyl)carbamate (66 mg, 0.2 mmol) provided the desired product after flash column chromatography (10% ethyl acetate in hexanes) as a colorless oil (85 mg, 45%). $R_f=0.44$ (30% EtOAc/hexanes); IR (film) 3032, 2956, 1750, 1707, 1511, 1325 cm^{-1} ; ^1H NMR (400 MHz, CDCl_3) δ 7.27-7.22 (m, 3H), 7.18 (d, $J = 8.4$ Hz, 2H), 7.12-7.11 (m, 2H), 6.98 (d, $J = 8.0$ Hz, 2H), 6.72 (d, $J = 8.0$ Hz, 1H), 6.67-6.64 (m, 2H), 6.05 (d, $J = 12.0$ Hz, 1H), 5.94 (s, 2H), 5.09 (d, $J = 15.2$ Hz, 1H), 4.70 (d, $J = 11.6$ Hz, 1H), 4.26 (d, $J = 15.2$ Hz, 1H), 3.72 (s, 3H), 2.36 (s, 3H); ^{13}C NMR (100 MHz, CDCl_3) ppm 169.3, 154.3, 148.2, 147.6, 138.5, 134.9, 134.7, 131.2, 129.8, 128.5, 128.4, 127.9, 127.8, 121.4, 108.4, 107.5, 101.2, 88.1, 62.1, 54.2, 51.9, 21.1; HRMS (CI): Exact mass calcd for $\text{C}_{26}\text{H}_{24}\text{N}_4\text{O}_5$ $[\text{M}]^+$ 472.1741. Found 472.1718.



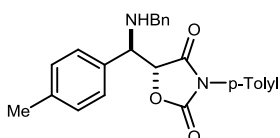
Methyl (4*S*,5*R*)-1-benzyl-5-(3,4,5-trimethoxyphenyl)-4,5-dihydro-1*H*-1,2,3-triazole-4-carbonyl(*p*-tolyl)carbamate (275m).

According to the general procedure, (*E*)-methyl *p*-tolyl(3-(3,4,5-trimethoxyphenyl)prop-2-enoyl)carbamate (77 mg, 0.2 mmol) provided the desired product after flash column chromatography (10% ethyl acetate in hexanes) as a colorless oil (35 mg, 35%). $R_f=0.50$ (30% EtOAc/hexanes); IR (film) 3029, 3000, 2938, 2839, 1749, 1706, 1592, 1509 cm^{-1} ; ^1H NMR (400 MHz, CDCl_3) δ 7.27-7.24 (m, 3H), 7.21 (d, $J = 8.4$ Hz, 2H), 7.16-7.14 (m, 2H), 7.01 (d, $J = 8.4$ Hz, 2H), 6.38 (s, 2H), 6.10 (d, $J = 12.4$ Hz, 1H), 5.03 (d, $J = 15.2$ Hz,

1H), 4.74 (d, $J = 12.0$ Hz, 1H), 4.42 (d, $J = 14.8$ Hz, 1H), 3.84 (s, 3H), 3.78 (s, 6H), 3.76 (s, 3H), 2.37 (s, 3H); ^{13}C NMR (100 MHz, CDCl_3) ppm 169.4, 154.3, 153.5, 138.5, 137.7, 134.9, 133.1, 129.9, 128.6, 128.5, 127.8, 104.3, 88.3, 62.9, 60.7, 56.1, 54.2, 52.4, 21.1; HRMS (CI): Exact mass calcd for $\text{C}_{28}\text{H}_{30}\text{N}_4\text{O}_6$ $[\text{M}]^+$ 518.2165, found 518.1970.

General Procedure for Acid Promoted Conversion of Triazoline to Oxazolidine Dione

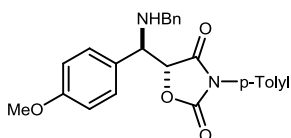
A 0.1 M solution of the the triazoline (1.0 equiv) in acetonitrile was prepared in a 5 ml vial. This was cooled to -20 °C and triflic acid (2.0 equiv) was added and allowed to stir until reaction was complete. The cooled solution was first treated with triethylamine (2.0 equiv), then diluted in ethyl acetate and washed with saturated aq NaHCO_3 . The organic layers were dried and concentrated, and the crude oil was purified using flash chromatography to provide the product.



(R)-5-((R)-(Benzylamino)(p-tolyl)methyl)-3-p-tolyloxazolidine-2,4-dione (276a). According to the general procedure, methyl (4*S*,5*R*)-1-benzyl-5-*p*-tolyl-4,5-dihydro-1*H*-1,2,3-triazole-4-carbonyl(*p*-tolyl)carbamate (130 mg, 0.29 mmol) provided the desired product after flash column chromatography (10% ethyl acetate in hexanes) as a colorless oil (56.0 mg, 62%). $R_f = 0.5$ (30% EtOAc/hexanes); IR (film) 1812, 1746, 1516 cm^{-1} ; ^1H NMR (600 MHz, CDCl_3) δ 7.36-7.25 (m, 8H), 7.22 (d, $J = 7.8$ Hz, 2H), 7.16 (d, $J = 8.4$ Hz, 1H), 6.69 (d, $J = 8.4$ Hz, 2H), 5.27 (d, $J = 3.0$ Hz, 1H), 4.29 (d, $J = 3.0$ Hz, 1H), 3.84 (d, $J = 13.2$ Hz, 1H), 3.66 (d, $J = 13.2$ Hz, 1H), 2.38 (s, 3H), 2.33 (s, 3H), the NH was not observed; ^{13}C NMR (150 MHz, CDCl_3) ppm 170.1, 154.1, 139.2, 139.1, 138.7, 131.7,

129.8, 129.5, 128.5, 128.3, 128.1, 127.6, 127.3, 125.5, 82.2, 62.0, 51.0, 21.2, 21.1;

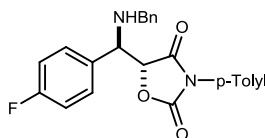
HRMS (EI): Exact mass calcd for C₂₅H₂₅N₂O₃ [M+H]⁺ 402.1865, found 402.1901.



(R)-5-((R)-(Benzylamino)(4-methoxyphenyl)methyl)-3-p-

tolyloxazolidine-2,4-dione (276b). According to the general procedure, methyl (4*S*,5*R*)-1-benzyl-5-(4-methoxyphenyl)-4,5-

dihydro-1*H*-1,2,3-triazole-4-carbonyl(*p*-tolyl)carbamate (134 mg, 0.29 mmol) provided the desired product after flash column chromatography (10% ethyl acetate in hexanes) as a colorless oil (90 mg, 95%). *R_f*=0.5 (30% EtOAc/hexanes); IR (film) 3330, 3029, 2925, 1812, 1609, 1515 cm⁻¹; ¹H NMR (400 MHz, CDCl₃) δ 7.34-7.24 (m, 7H), 7.13 (d, *J* = 8.0 Hz, 2H), 6.90 (d, *J* = 8.8 Hz, 2H), 6.70 (d, *J* = 8.4 Hz, 2H), 5.23 (d, *J* = 3.2 Hz, 1H), 4.25 (d, *J* = 2.8 Hz, 1H), 3.80 (d, *J* = 13.2 Hz, 1H), 3.70 (s, 3H), 3.64 (d, *J* = 13.2 Hz, 1H), 2.30 (s, 3H), the NH was not observed; ¹³C NMR (100 MHz, CDCl₃) ppm 170.1, 159.9, 154.1, 139.2, 139.1, 129.8, 129.4, 128.5, 128.2, 127.5, 125.3, 126.6, 125.5, 114.2, 82.2, 61.6, 55.3, 50.9, 21.1; HRMS (EI): Exact mass calcd for C₂₅H₂₅N₂O₄ [M+H]⁺ 417.1814, found 417.1816.

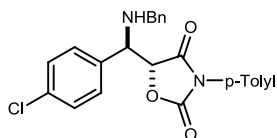


(R)-5-((R)-(Benzylamino)(4-fluorophenyl)methyl)-3-p-

tolyloxazolidine-2,4-dione (276c). According to the general procedure, methyl (4*S*,5*R*)-1-benzyl-5-(4-fluorophenyl)-4,5-

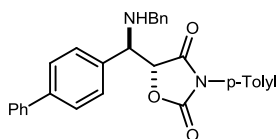
dihydro-1*H*-1,2,3-triazole-4-carbonyl(*p*-tolyl)carbamate (157 mg, 0.35 mmol) provided the desired product after flash column chromatography (10% ethyl acetate in hexanes) as a colorless oil (80 mg, 56%). *R_f*=0.5 (30% EtOAc/hexanes); IR (film) 3330, 3030, 1897, 1813, 1746 cm⁻¹; ¹H NMR (400 MHz, CDCl₃) δ 7.36-7.23 (m, 7H), 7.15 (d, *J* = 8.4 Hz,

2H), 7.08 (dd, $J = 8.8, 8.4$ Hz, 2H), 6.73 (d, $J = 8.4$ Hz, 2H), 5.21 (d, $J = 2.8$ Hz, 1H), 4.29 (d, $J = 3.2$ Hz, 1H), 3.80 (d, $J = 13.2$ Hz, 1H), 3.61 (d, $J = 13.2$ Hz, 1H), 2.31 (s, 3H), the NH was not observed; ^{13}C NMR (100 MHz, CDCl_3) ppm 169.9, 164.1, 161.6, 153.8, 139.2, 138.9, 130.0, 129.9, 128.5, 128.1, 127.3, 125.3, 115.9, 115.7, 81.7, 61.5, 50.9, 21.0; HRMS (EI): Exact mass calcd for $\text{C}_{24}\text{H}_{22}\text{FN}_2\text{O}_3$ $[\text{M}+\text{H}]^+$ 405.1614, found 405.1630.



(R)-5-((R)-(Benzylamino)(4-chlorophenyl)methyl)-3-p-tolyloxazolidine-2,4-dione (276d) According to the general procedure, methyl (4*S*,5*R*)-1-benzyl-5-(4-chlorophenyl)-4,5-

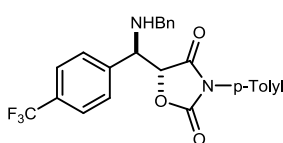
dihydro-1*H*-1,2,3-triazole-4-carbonyl(*p*-tolyl)carbamate (100 mg, 0.21 mmol) provided the desired product after flash column chromatography (10% ethyl acetate in hexanes) as a colorless oil (64 mg, 72%). $R_f=0.5$ (30% EtOAc/hexanes); IR (film) 3328, 3029, 1813, 1746, 1516 cm^{-1} ; ^1H NMR (400 MHz, CDCl_3) δ 7.40-7.26 (m, 9H), 7.18 (d, $J = 8.0$ Hz, 2H), 6.75 (d, $J = 8.4$ Hz, 2H), 5.24 (d, $J = 3.2$ Hz, 1H), 4.30 (d, $J = 2.8$ Hz, 1H), 3.82 (d, $J = 13.2$ Hz, 1H), 3.63 (d, $J = 13.2$ Hz, 1H), 2.34 (s, 3H), the NH was not observed; ^{13}C NMR (100 MHz, CDCl_3) ppm 169.8, 153.7, 139.3, 138.7, 134.8, 133.5, 129.9, 129.6, 129.0, 128.5, 128.1, 127.4, 126.5, 125.3, 81.6, 61.5, 50.9, 21.1; HRMS (EI): Exact mass calcd for $\text{C}_{24}\text{H}_{22}\text{ClN}_2\text{O}_3$ $[\text{M}+\text{H}]^+$ 421.1319, found 421.1321.



(R)-5-((R)-(Benzylamino)(biphenyl-4-yl)methyl)-3-p-tolyloxazolidine-2,4-dione (276e). According to the general procedure, methyl (4*S*,5*R*)-1-benzyl-5-(biphenyl-4-yl)-4,5-

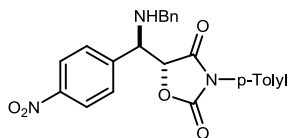
dihydro-1*H*-1,2,3-triazole-4-carbonyl(*p*-tolyl)carbamate (135 mg, 0.26 mmol) provided the desired product after flash column chromatography (10% ethyl acetate in hexanes) as

a colorless oil (72 mg, 60%). $R_f=0.5$ (30% EtOAc/hexanes); IR (film) 3330, 3029, 1812, 1745, 1516 cm^{-1} ; ^1H NMR (400 MHz, CDCl_3) δ 7.62 (d, $J = 8.0$ Hz, 2H), 7.58 (d, $J = 7.6$ Hz, 2H), 7.47-7.28 (m, 10H), 7.09 (d, $J = 8.0$ Hz, 2H), 6.66 (d, $J = 8.0$ Hz, 2H), 5.29 (d, $J = 2.8$ Hz, 1H), 4.35 (d, $J = 2.8$ Hz, 1H), 3.87 (d, $J = 13.2$ Hz, 1H), 3.69 (d, $J = 13.2$ Hz, 1H), 2.28 (s, 3H), the NH was not observed; ^{13}C NMR (100 MHz, CDCl_3) ppm 170.0, 156.2, 153.9, 141.8, 140.2, 139.2, 139.0, 133.8, 129.8, 128.8, 128.6, 128.5, 127.6, 127.5, 127.3, 127.0, 125.5, 82.0, 61.9, 51.0, 21.0; HRMS (EI): Exact mass calcd for $\text{C}_{30}\text{H}_{27}\text{N}_2\text{O}_3$ $[\text{M}+\text{H}]^+$ 463.2022, found 463.2009.



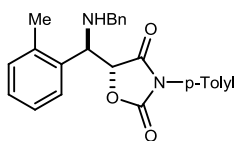
(R)-5-((R)-(Benzylamino)(4-(trifluoromethyl)phenyl)

methyl)-3-p-tolylloxazolidine-2,4-dione (276f). According to the general procedure, methyl (4*S*,5*R*)-1-benzyl-5-(4-(trifluoromethyl)phenyl)-4,5-dihydro-1*H*-1,2,3-triazole-4-carbonyl(*p*-tolyl)carbamate (154 mg, 0.31 mmol) provided the desired product after flash column chromatography (10% ethyl acetate in hexanes) as a colorless oil (100 mg, 70%). $R_f = 0.5$ (30% EtOAc/hexanes); IR (film) 3332, 3030, 1842, 1814, 1517 cm^{-1} ; ^1H NMR (400 MHz, CDCl_3) δ 7.65 (d, $J = 8.0$ Hz, 2H), 7.50 (d, $J = 8.0$ Hz, 2H), 7.35-7.24 (m, 5H), 7.13 (d, $J = 8.0$ Hz, 2H), 6.65 (d, $J = 8.4$ Hz, 2H), 5.23 (d, $J = 3.2$ Hz, 1H), 4.35 (d, $J = 3.2$ Hz, 1H), 3.81 (d, $J = 13.2$ Hz, 1H), 3.62 (d, $J = 13.2$ Hz, 1H), 2.31 (s, 3H), the NH was not observed; ^{13}C NMR (100 MHz, CDCl_3) ppm 169.7, 153.6, 139.4, 139.3, 138.6, 129.9, 128.7, 128.5, 128.1, 127.4, 125.8, 125.78, 125.75, 125.71, 125.2, 81.4, 61.8, 50.9, 21.0; HRMS (EI): Exact mass calcd for $\text{C}_{25}\text{H}_{22}\text{F}_3\text{N}_2\text{O}_3$ $[\text{M}+\text{H}]^+$ 455.1583, found 455.1581.



(R)-5-((R)-(Benzylamino)(4-nitrophenyl)methyl)-3-p-tolyloxazolidine-2,4-dione (276g). According to the general

procedure, methyl (4*S*,5*R*)-1-benzyl-5-(4-nitrophenyl)-4,5-dihydro-1*H*-1,2,3-triazole-4-carbonyl(*p*-tolyl)carbamate (84 mg, 0.17 mmol) provided the desired product after flash column chromatography (10% ethyl acetate in hexanes) as a colorless oil (47 mg, 64%). R_f = 0.5 (30% EtOAc/hexanes); IR (film) 3337, 3029, 1813, 1745, 1518 cm^{-1} ; ^1H NMR (400 MHz, CDCl_3) δ 8.23 (d, J = 8.4 Hz, 2H), 7.57 (d, J = 8.4 Hz, 2H), 7.32-7.22 (m, 5H), 7.15 (d, J = 8.4 Hz, 2H), 6.79 (d, J = 8.4 Hz, 2H), 5.21 (d, J = 3.6 Hz, 1H), 4.39 (d, J = 3.6 Hz, 1H), 3.80 (d, J = 13.2 Hz, 1H), 3.60 (d, J = 13.2 Hz, 1H), 2.31 (s, 3H), the NH was not observed; ^{13}C NMR (100 MHz, CDCl_3) ppm 169.5, 153.3, 148.1, 142.7, 139.4, 138.3, 129.9, 129.3, 128.6, 128.0, 127.5, 127.2, 125.0, 123.9, 81.0, 61.6, 50.9, 21.0; HRMS (EI): Exact mass calcd for $\text{C}_{24}\text{H}_{22}\text{N}_3\text{O}_5$ $[\text{M}+\text{H}]^+$ 432.1559, found 432.1573.

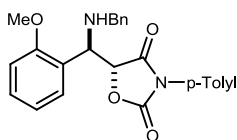


(R)-5-((R)-(benzylamino)(*o*-tolyl)methyl)-3-p-tolyloxazolidine-2,4-dione (276h) According to the general procedure, methyl

(4*S*,5*R*)-1-benzyl-5-*o*-tolyl-4,5-dihydro-1*H*-1,2,3-triazole-4-carbonyl(*p*-tolyl)carbamate (95 mg, 0.21 mmol) provided the desired product after flash column chromatography (10% ethyl acetate in hexanes) as a colorless oil (42 mg, 50%). R_f = 0.5 (30% EtOAc/hexanes); IR (film) 3338, 3061, 1813, 1746, 1517 cm^{-1} ; ^1H NMR (400 MHz, CDCl_3) δ 7.53 (d, J = 8.4 Hz, 2H), 7.33-7.23 (m, 8H), 7.16 (d, J = 7.2 Hz, 1H), 6.66 (d, J = 8.0 Hz, 1H), 5.28 (d, J = 3.2 Hz, 1H), 4.62 (d, J = 3.6 Hz, 1H), 3.79 (d, J = 13.2 Hz, 1H), 3.61 (d, J = 13.2 Hz, 1H), 2.29 (s, 3H), 2.19 (s, 3H), the NH was not observed; ^{13}C NMR (100 MHz, CDCl_3) ppm 170.0, 154.1, 139.2, 139.1, 137.3, 133.8,

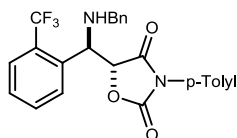
131.0, 129.8, 128.5, 128.3, 128.1, 127.5, 127.3, 126.6, 125.6, 81.9, 56.3, 50.8, 21.1, 19.6;

HRMS (EI): Exact mass calcd for C₂₅H₂₅N₂O₃ [M+H]⁺ 401.1865, found 401.1853.



(R)-5-((R)-(Benzylamino)(2-methoxyphenyl)methyl)-3-*p*-

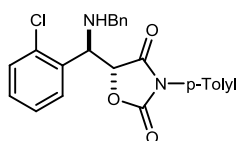
tolyloxazolidine-2,4-dione (276i). According to the general procedure, methyl (4*S*,5*R*)-1-benzyl-5-(2-methoxyphenyl)-4,5-dihydro-1*H*-1,2,3-triazole-4-carbonyl(*p*-tolyl)carbamate (95 mg, 0.20 mmol) provided the desired product after flash column chromatography (10% ethyl acetate in hexanes) as a colorless oil (48 mg, 57%). *R_f*=0.5 (30% EtOAc/hexanes); IR (film) 1811, 1749, 1515 cm⁻¹; ¹H NMR (600 MHz, CDCl₃) δ 7.35 (dd, *J* = 7.8, 1.8 Hz, 1H), 7.33-7.23 (m, 7H), 7.16 (d, *J* = 8.4 Hz, 2H), 6.99 (ddd, *J* = 7.8, 7.8, 0.6 Hz, 1H), 6.91 (d, *J* = 8.4 Hz, 1H), 6.85 (d, *J* = 8.4 Hz, 2H), 5.24 (d, *J* = 3.0 Hz, 1H), 4.76 (d, *J* = 3.6 Hz, 1H), 3.80 (d, *J* = 13.2 Hz, 1H), 3.79 (s, 3H), 3.65 (d, *J* = 13.2 Hz, 1H), 2.31 (s, 3H); ¹³C NMR (150 MHz, CDCl₃) ppm 170.1, 157.6, 154.4, 139.4, 139.0, 129.8, 129.6, 128.6, 128.4, 128.2, 127.9, 127.2, 125.6, 120.9, 111.0, 82.0, 56.9, 55.5, 51.6, 21.1; HRMS (EI): Exact mass calcd for C₂₅H₂₅N₂O₄ [M+H]⁺ 417.1815, found 417.1814.



(R)-5-((R)-(Benzylamino)(2-(trifluoromethyl)phenyl)

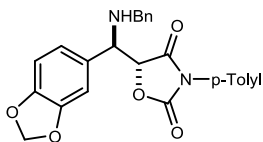
methyl)-3-*p*-tolyloxazolidine-2,4-dione (276j). According to the general procedure, methyl (4*S*,5*R*)-1-benzyl-5-(2-(trifluoromethyl)phenyl)-4,5-dihydro-1*H*-1,2,3-triazole-4-carbonyl(*p*-tolyl)carbamate (129 mg, 0.25 mmol) provided the desired product after flash column chromatography (10% ethyl acetate in hexanes) as a colorless oil (102 mg, 86%). *R_f*=0.5 (30% EtOAc/hexanes); IR (film) 3321, 3030, 1842, 1814, 1745 cm⁻¹; ¹H NMR (400 MHz,

CDCl₃) δ 7.99 (d, *J* = 8.0 Hz, 1H), 7.74 (d, *J* = 8.0 Hz, 1H), 7.66 (dd, *J* = 7.6, 7.6 Hz, 1H), 7.49 (dd, *J* = 7.6, 7.6 Hz, 1H), 7.33-7.19 (m, 9H), 5.04 (d, *J* = 5.2 Hz, 1H), 4.79 (d, *J* = 5.2 Hz, 1H), 3.69 (d, *J* = 13.2 Hz, 1H), 3.64 (d, *J* = 13.2 Hz, 1H), 2.39 (s, 3H), the NH was not observed; ¹³C NMR (100 MHz, CDCl₃) ppm 170.2, 153.7, 139.2, 139.0, 136.0, 132.4, 129.9, 128.7, 129.8, 128.5, 128.4, 127.9, 127.7, 127.2, 126.1, 126.0, 125.4, 81.1, 58.0, 51.3, 21.0; HRMS (EI): Exact mass calcd for C₂₅H₂₂F₃N₂O₃ [M+H]⁺ 455.1583, found 455.1578.

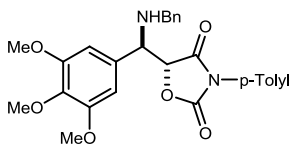


(R)-5-((R)-(Benzylamino)(2-chlorophenyl)methyl)-3-p-tolyloxazolidine-2,4-dione (276k). According to the general procedure, methyl (4*S*,5*R*)-1-benzyl-5-(2-chlorophenyl)-4,5-

dihydro-1*H*-1,2,3-triazole-4-carbonyl(*p*-tolyl)carbamate (165 mg, 0.35 mmol) provided the desired product after flash column chromatography (10% ethyl acetate in hexanes) as a colorless oil (125 mg, 81%). *R_f*=0.5 (30% EtOAc/hexanes); IR (film) 1813, 1747, 1516 cm⁻¹; ¹H NMR (600 MHz, CDCl₃) δ 7.61 (dd, *J* = 7.8, 1.2 Hz, 1H), 7.42 (dd, *J* = 8.4, 1.2 Hz, 1H), 7.35-7.24 (m, 7H), 7.19 (d, *J* = 8.4 Hz, 2H), 6.97 (d, *J* = 8.4 Hz, 2H), 5.18 (d, *J* = 3.6 Hz, 1H), 4.94 (d, *J* = 4.2 Hz, 1H), 3.76 (d, *J* = 13.2 Hz, 1H), 3.64 (d, *J* = 13.2 Hz, 1H), 2.33 (s, 3H), the NH was not observed; ¹³C NMR (150 MHz, CDCl₃) ppm 169.6, 154.0, 139.2, 138.9, 134.5, 133.5, 130.1, 129.9, 129.7, 128.7, 128.5, 128.2, 127.7, 127.3, 125.4, 81.1, 58.1, 51.3, 21.1; HRMS (EI): Exact mass calcd for C₂₄H₂₂ClN₂O₃ [M+H]⁺ 421.1310, found 421.1329.

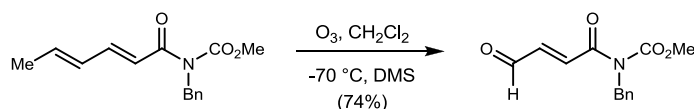


(R)-5-((R)-Benzo[d][1,3]dioxol-5-yl(benzylamino)methyl)-3-p-tolyloxazolidine-2,4-dione (276l). According to the general procedure, methyl (4*S*,5*R*)-5-(benzo[d][1,3]dioxol-5-yl)-1-benzyl-4,5-dihydro-1*H*-1,2,3-triazole-4-carbonyl(*p*-tolyl)carbamate (124 mg, 0.26 mmol) provided the desired product after flash column chromatography (10% ethyl acetate in hexanes) as a colorless oil (53 mg, 47%). R_f = 0.5 (30% EtOAc/hexanes); IR (film) 3327, 3029, 1813, 1745, 1606 cm^{-1} ; ^1H NMR (400 MHz, CDCl_3) δ 7.32-7.25 (m, 5H), 7.16 (d, J = 8.0 Hz, 2H), 6.88 (s, 1H), 6.83-6.80 (m, 4H), 5.94 (dd, J = 3.6, 1.2 Hz, 2H), 5.18 (d, J = 3.2 Hz, 1H), 4.21 (d, J = 3.2 Hz, 1H), 3.80 (d, J = 13.2 Hz, 1H), 3.61 (d, J = 13.2 Hz, 1H), 2.31 (s, 3H), the NH was not observed; ^{13}C NMR (100 MHz, CDCl_3) ppm 170.0, 153.9, 148.1, 147.9, 139.2, 139.0, 129.8, 128.7, 128.5, 128.2, 127.6, 127.3, 125.4, 121.9, 108.5, 108.2, 101.2, 82.0, 61.9, 50.9, 21.1; HRMS (EI): Exact mass calcd for $\text{C}_{25}\text{H}_{22}\text{Na N}_2\text{O}_5$ $[\text{M}+\text{Na}]^+$ 453.1426, found 453.1425.

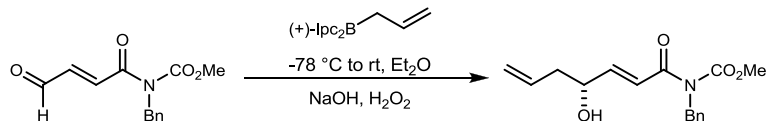


(R)-5-((R)-(Benzylamino)(3,4,5-trimethoxyphenyl)methyl)-3-p-tolyloxazolidine-2,4-dione (276m). According to the general procedure, methyl (4*S*,5*R*)-1-benzyl-5-(3,4,5-trimethoxyphenyl)-4,5-dihydro-1*H*-1,2,3-triazole-4-carbonyl(*p*-tolyl)carbamate (94 mg, 0.18 mmol) provided the desired product after flash column chromatography (10% ethyl acetate in hexanes) as a colorless oil (32 mg, 37%). R_f = 0.5 (30% EtOAc/hexanes); IR (film) 3325, 3001, 2938, 1813, 1746, 1590, 1515 cm^{-1} ; ^1H NMR (400 MHz, CDCl_3) δ 7.33-7.26 (m, 5H), 7.12 (d, J = 8.0 Hz, 2H), 6.66 (d, J = 8.4 Hz, 2H), 6.51 (s, 2H), 5.24 (d, J = 2.8 Hz, 1H), 4.19 (d, J = 3.2 Hz, 1H), 3.85 (m, 4H), 3.80 (s, 6H), 3.67 (d, J = 13.2 Hz, 1H), 2.29 (s, 3H), the NH was not observed; ^{13}C NMR (100 MHz, CDCl_3) ppm 170.0,

154.1, 153.5, 139.4, 139.0, 138.2, 130.5, 129.9, 128.5, 128.2, 127.5, 127.4, 125.5, 105.0, 81.9, 62.4, 60.8, 56.2, 51.0, 21.1; HRMS (EI): Exact mass calcd for C₂₇H₂₈Na N₂O₆ [M+Na]⁺ 499.1845, found 499.1824.



(E)-Methyl benzyl(4-oxobut-2-enyl)carbamate (397). A 1 L round bottom flask equipped with a magnetic stir bar and gas purging glass tube was charged with carbamate (50.0 g, 192 mmol) and dichloromethane (500 mL). The solution was cooled to -78 °C and maintained throughout the reaction. O₂ was then introduced to the solution for 10 minutes, followed by the addition of O₃ until the solution turned blue. Ozone addition was then discontinued and the solution was purged with O₂ for an additional 10 minutes. Dimethyl sulfide (56.0 mL, 770 mmol) was then added dropwise at -78 °C and allowed to warm to rt overnight. The solution was concentrated, diluted with EtOAc, washed with water and satd aq NaHCO₃, and then dried, filtered, and concentrated to brown oil. Flash column chromatography (SiO₂, 10-25-30% ethyl acetate in hexanes) yielded a yellow oil (34.5 g, 74%); R_f=0.20 (30% EtOAc/hexanes); IR (film) 2958, 1739, 1694, 1229 cm⁻¹; ¹H NMR (400 MHz, CDCl₃) δ 7.75 (d, *J* = 15.6 Hz, 1H), 7.34-7.27 (m, 5H), 6.87 (dd, *J* = 15.6, 7.6 Hz, 1H), 4.99 (s, 2H), 3.86 (s, 3H); ¹³C NMR (100 MHz, CDCl₃) ppm 192.7, 166.9, 154.7, 142.9, 137.6, 128.4, 127.7, 127.6, 54.1, 47.5; HRMS (CI): Exact mass calcd for C₁₃H₁₀NO₄ [M-H]⁺ 246.0761, found 246.0768.

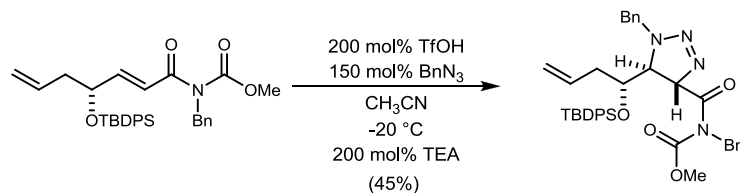


(*R,E*)-Methyl benzyl(4-hydroxyhepta-2,6-dienoyl)carbamate (399). A 500 mL round bottom flask was charged with (+)-Ipc₂BOMe (11.4 g, 36.0 mmol) and ether (100 mL) at -78 °C. A solution of allyl magnesium bromide (36 mL, 1 M in ether) was added dropwise and stirred for 15 minutes. The reaction mixture was removed from a dry ice-acetone bath and allowed to warm to 25 °C for 1 h. The formation of borane reagent was indicated by precipitation of the magnesium salts. The reagent was isolated as the neat liquid by passing the reaction mixture through a filtration. To a solution of the borane reagent in ether (100 mL) was added aldehyde (7.0 g, 30 mmol) and the reaction mixture was stirred for 3 h at -78 °C and then allowed to warm to 25 °C. After 1 h of stirring, the reaction mixture was quenched with 1 M Rochelle salt solution (50 mL). The reaction was extracted with EtOAc and the combined organic layers were dried, filtered, and concentrated to a colorless oil. Flash column chromatography (SiO₂, 20-30-40% ethyl acetate in hexanes) provided the alcohol as a colorless oil (3.39 g, 40%). $R_f=0.40$ (30% EtOAc/hexanes); $[\alpha]_D^{24} -2.25$ (*c* 3.1, CHCl₃); IR (film) 3391, 2957, 1737, 1689, 1211 cm⁻¹; ¹H NMR (500 MHz, CDCl₃) δ 7.29-7.21 (m, 5H), 7.08 (dd, *J* = 15.0, 1.5 Hz, 1H), 6.96 (dd, *J* = 15.5, 4.5 Hz, 1H), 5.88-5.80 (m, 1H), 5.18 (dd, *J* = 3.0, 1.5 Hz, 1H), 5.16 (d, *J* = 1.0 Hz, 1H), 4.93 (s, 2H), 4.42 (m, 1H), 3.81 (s, 3H), 2.43 (m, 1H), 2.31 (ddd, *J* = 14.0, 7.5, 7.5 Hz, 1H), 1.86 (s, 1H); ¹³C NMR (125 MHz, CDCl₃) ppm 168.0, 155.0, 148.2, 137.5, 133.3, 128.4, 127.7, 127.3, 122.9, 118.1, 70.2, 53.7, 47.6, 41.1; HRMS (CI): Exact mass calcd for C₁₆H₁₉NO₄Na [M+Na]⁺ 312.1212, found 312.1208.

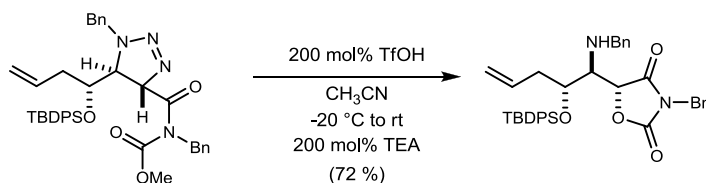


(*R,E*)-Methyl benzyl(4-(*tert*-butyldiphenylsilyloxy)hepta-2,6-dienoyl)carbamate

(400). The alcohol (1.76 g, 6.08 mmol) and imidazole (0.50 g, 7.29 mmol) were dissolved in CH_2Cl_2 (50 mL) and cooled to 0 °C. TBDPSCl (2.1 g, 7.29 mmol) was added and the reaction was stirred for 10 min at 0 °C and at least 4 h at rt. Water was added and the reaction was extracted with EtOAc. The combined organic layers were washed with brine and then dried, filtered, and concentrated to a crude oil. Flash column chromatography of the oil (SiO_2 , 5-10-20% ethyl acetate in hexanes) provided the unsaturated imide as a colorless oil (3.02 g, 99%). $R_f=0.80$ (30% EtOAc/hexanes); $[\alpha]_D^{24} -13.9$ (c 1.15, CHCl_3); IR (film) 3955, 2931, 2361, 1738, 1683 cm^{-1} ; $^1\text{H NMR}$ (400 MHz, CDCl_3) δ 7.70 (d, $J = 6.8$ Hz, 2H), 7.64 (d, $J = 6.8$ Hz, 2H), 7.44-7.27 (m, 9H), 7.00-6.92 (m, 2H), 5.67 (dddd, $J = 17.2, 10.4, 7.2, 7.2$ Hz, 1H), 4.95-4.90 (m, 3H), 4.45 (ddd, $J = 6.0, 3.2, 3.2$ Hz, 1H), 3.74 (s, 3H), 2.23 (t, $J = 6.8$ Hz, 2H), 1.10 (s, 9H); $^{13}\text{C NMR}$ (125 MHz, CDCl_3) ppm 168.2, 154.8, 149.0, 137.6, 135.8, 135.1, 134.7, 133.8, 133.4, 133.0, 129.6, 128.4, 127.8, 127.7, 127.6, 127.5, 122.7, 117.9, 53.7, 47.7, 41.4, 31.6, 26.9, 26.5, 21.1, 14.1; HRMS (CI): Exact mass calcd for $\text{C}_{32}\text{H}_{37}\text{NNaO}_4$ $[\text{M}+\text{Na}]^+$ 550.2390, found 550.2393.



Methyl benzyl((4*S*,5*S*)-1-benzyl-5-(1-(*tert*-butyldiphenylsilyloxy)but-3-enyl)-4,5-dihydro-1*H*-1,2,3-triazole-4-carbonyl)carbamate (401). A 0.1 M solution of the unsaturated imide (1.30 g, 2.46 mmol) in acetonitrile was cooled to $-20\text{ }^{\circ}\text{C}$ and triflic acid (436 μL , 4.93 mmol) was added, and stirring was continued for 10 min. To the solution was added benzyl azide (491 μL , 3.69 mmol) via syringe. The reaction was stirred for 18 h before quenching with triethylamine (687 μL , 4.93 mmol) via syringe. The mixture was concentrated and chromatographed (SiO_2 , 5-10-20% ethyl acetate in hexanes) to provide the triazolone as a colorless oil (723 mg, 45%). $R_f=0.20$ (10% EtOAc/hexanes); $[\alpha]_D^{24}$ 32.6 (c 1.50, CHCl_3); IR (film) 2927, 1815, 1742, 1688 cm^{-1} ; ^1H NMR (400 MHz, CDCl_3) δ 7.69 (d, $J = 6.4$ Hz, 2H), 7.64 (d, $J = 6.8$ Hz, 2H), 7.52-7.16 (m, 14H), 6.91 (d, $J = 6.8$ Hz, 2H), 6.57 (d, $J = 10.0$ Hz, 1H), 5.41 (dddd, $J = 17.6, 10.4, 7.2, 7.2$ Hz, 1H), 4.97 (s, 2H), 4.96 (d, $J = 16.8$ Hz, 1H), 4.80 (d, $J = 10.4$ Hz, 1H), 4.70 (d, $J = 17.2$ Hz, 1H), 3.94 (s, 3H), 3.93-3.86 (m, 3H), 2.11-1.96 (m, 2H), 1.08 (s, 9H); ^{13}C NMR (100 MHz, CDCl_3) ppm 169.9, 154.9, 137.1, 136.3, 135.9, 134.9, 133.9, 132.8, 132.4, 130.0, 129.7, 128.5, 128.4, 128.1, 127.7, 127.5, 127.2, 118.4, 80.6, 69.6, 60.4, 54.2, 51.6, 48.4, 39.4, 26.8, 19.2; HRMS (CI): Exact mass calcd for $\text{C}_{39}\text{H}_{45}\text{N}_4\text{O}_4\text{Si}$ $[\text{M}+\text{H}]^+$ 661.3210, found 661.3239.



(R)-3-Benzyl-5-((1S,2R)-1-(benzylamino)-2-(tert-butyldiphenylsilyloxy)pent-4-

enyl)oxazolidine-2,4-dione (405). A 0.1 M solution of the triazolone (410 mg, 620 μmol)

in acetonitrile was cooled to $-20\text{ }^{\circ}\text{C}$ and triflic acid (110 μL , 1.24 mmol) was added, and stirring was continued for 10 min and then allowed to warm to $25\text{ }^{\circ}\text{C}$. The reaction was stirred for 18 h before quenching with triethylamine (172 μL , 1.24 mmol) via syringe.

The mixture was concentrated, and the residue was chromatographed (SiO_2 , 5-10-20% ethyl acetate in hexanes) to provide desired the oxazolidinone product as a yellow oil

(278 mg, 72%). $R_f=0.30$ (10% EtOAc/hexanes); $[\alpha]_D^{24}$ 5.33 (c 1.50, CHCl_3); IR (film)

2918, 1825, 1741, 1600 cm^{-1} ; ^1H NMR (600 MHz, CDCl_3) δ 7.71 (dd, $J = 7.8, 1.2$ Hz,

2H), 7.69 (dd, $J = 7.8, 1.2$ Hz, 2H), 7.42-7.33 (m, 8H), 7.25-7.17 (m, 6H), 6.98-6.96 (m,

2H), 5.47 (dddd, $J = 17.4, 10.2, 7.2, 7.2$ Hz, 1H), 5.20 (d, $J = 3.6$ Hz, 1H), 4.85 (d, $J =$

10.2 Hz, 1H), 4.80 (dd, $J = 17.4, 1.8$ Hz, 1H), 4.67 (d, $J = 14.4$ Hz, 1H), 4.60 (d, $J = 15.0$

Hz, 1H), 4.10 (dd, $J = 12.0, 6.0$ Hz, 1H), 3.65 (d, $J = 12.6$ Hz, 1H), 3.55 (d, $J = 12.6$ Hz,

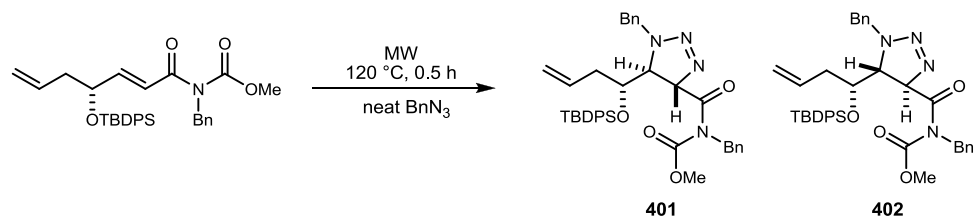
1H), 3.16-3.14 (m, 1H), 2.28 (t, $J = 6.6$ Hz, 2H), 1.02 (s, 9H); ^{13}C NMR (125 MHz,

CDCl_3) ppm 171.5, 155.6, 139.5, 136.0, 135.9, 134.7, 133.6, 133.2, 132.8, 129.9, 129.7,

128.7, 128.5, 128.3, 128.1, 128.0, 127.7, 127.6, 127.0, 118.1, 80.7, 72.3, 62.9, 53.3, 43.4,

38.8, 27.0, 19.4; HRMS (CI): Exact mass calcd for $\text{C}_{38}\text{H}_{43}\text{N}_2\text{O}_4\text{Si}$ $[\text{M}+\text{H}]^+$ 619.2992,

found 619.2995.



Methyl benzyl((4*R*,5*R*)-1-benzyl-5-((*R*)-1-(*tert*-butyldiphenylsilyloxy)but-3-enyl)-4,5-

dihydro-1*H*-1,2,3-triazole-4-carbonyl)carbamate (402). The unsaturated carbamate

(264 mg, 0.50 mmol) was weighed in a 2 mL glass pressure microwave tube equipped with a magnetic stir bar. Benzyl azide (1 mL) was added, the tube was closed with a septum, and the reaction mixture was subjected to microwave irradiation for 0.5 h at 120

°C. The reaction tube was allowed to cool to rt, and the reaction mixture was concentrated to a crude oil that was chromatographed (SiO₂, 10-20-30% ethyl acetate in

hexanes) to give a colorless oil (130 mg, 40%). $R_f=0.20$ (10% EtOAc/hexanes); $[\alpha]_D^{24} -$

2.00 (c 1.00, CHCl₃); IR (film) 1742, 1715 cm⁻¹; ¹H NMR (600 MHz, CDCl₃) δ 7.55 (d, J

= 7.2 Hz, 2H), 7.54 (d, J = 7.8 Hz, 2H), 7.39 (d, J = 7.6 Hz, 2H), 7.31 (d, J = 7.8 Hz, 2H),

7.30 (d, J = 7.8 Hz, 2H), 7.25-7.11 (m, 8H), 7.01 (d, J = 7.8 Hz, 2H), 6.51 (d, J = 8.4 Hz,

1H), 5.29 (dddd, J = 17.4, 10.2, 7.2, 7.2 Hz, 1H), 4.86 (s, 2H), 4.74 (dd, J = 10.2, 0.6 Hz,

1H), 4.68 (d, J = 15.0 Hz, 1H), 4.67 (dd, J = 16.8, 1.2 Hz, 1H), 4.60 (d, J = 15.0 Hz, 1H),

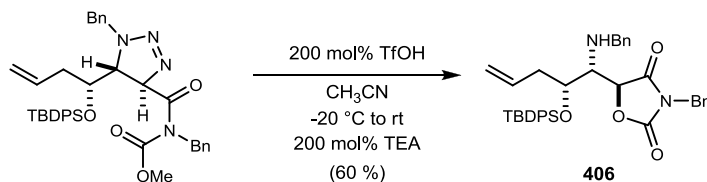
4.09 (dd, J = 8.4, 4.2 Hz, 1H), 3.85 (s, 3H), 3.68 (dd, J = 10.2, 5.4 Hz, 1H), 1.99-1.90 (m,

2H), 0.98 (s, 9H); ¹³C NMR (100 MHz, CDCl₃) ppm 169.5, 154.7, 136.9, 135.9, 135.8,

135.5, 133.7, 133.5, 133.0, 129.8, 129.7, 128.5, 128.4, 128.3, 127.6, 127.5, 127.3, 127.2,

117.5, 82.3, 71.7, 60.9, 54.0, 53.6, 48.1, 37.2, 26.8, 19.2; HRMS (CI): Exact mass calcd

for C₃₉H₄₅N₄O₄Si [M+H]⁺ 661.3210, found 661.3204.



(S)-3-Benzyl-5-((1R,2R)-1-(benzylamino)-2-(tert-butyldiphenylsilyloxy)pent-4-

enyl)oxazolidine-2,4-dione (406). A 0.1 M solution of the triazolone (25.1 mg, 378 μmol)

in acetonitrile was cooled to $-20 \text{ }^\circ\text{C}$ and triflic acid (6.71 μL , 756 μmol) was added. The

mixture was stirred for 10 min and then allowed to warm to $25 \text{ }^\circ\text{C}$. The reaction was

stirred for 18 h before addition of triethylamine (10.1 μL , 756 μmol) via syringe. The

mixture was concentrated, and the residue was chromatographed (SiO_2 , 5-10-20% ethyl

acetate in hexanes) to provide the desired oxazolidine dione product as a yellow oil (14.1

mg, 60%). $R_f=0.30$ (10% EtOAc/hexanes); $[\alpha]_D^{24} -5.60$ (c 2.50, CHCl_3); IR (film) 3070,

1824, 1747 cm^{-1} ; $^1\text{H NMR}$ (600 MHz, CDCl_3) δ 7.70-7.69 (m, 2H), 7.62-7.61 (m, 2H),

7.41-7.17 (m, 14H), 6.99-6.97 (m, 2H), 5.59 (dddd, $J = 17.4, 15.6, 7.2, 7.2$ Hz, 1H), 5.01

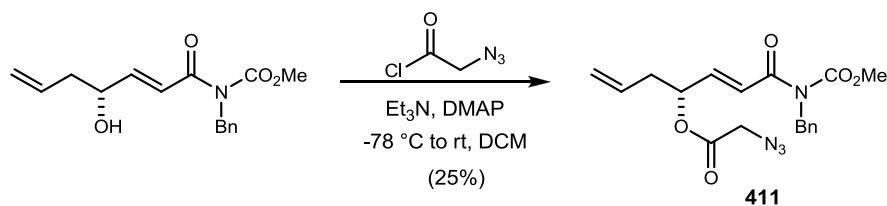
(d, $J = 4.2$ Hz, 1H), 4.93 (d, $J = 10.2$ Hz, 1H), 4.89 (dd, $J = 17.4, 1.8$ Hz, 1H), 4.66 (d, J

$= 14.4$ Hz, 1H), 4.58 (d, $J = 15.0$ Hz, 1H), 4.12-4.05 (m, 1H), 3.61 (s, 2H), 3.11 (dd, $J =$

6.0, 4.2 Hz, 1H), 2.50 (ddd, $J = 14.4, 6.6, 6.6$ Hz, 1H), 2.23-2.18 (m, 1H), 1.02 (s, 9H),

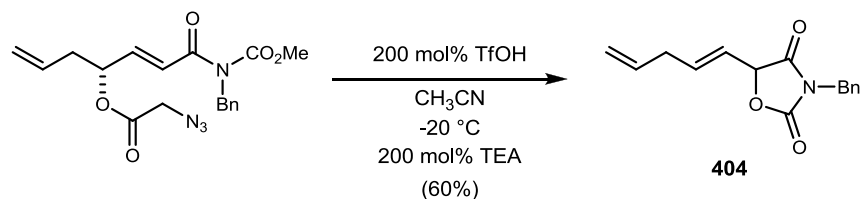
the NH was not observed; HRMS (CI): Exact mass calcd for $\text{C}_{38}\text{H}_{43}\text{N}_2\text{O}_4\text{Si}$ $[\text{M}+\text{H}]^+$

619.2992, found 619.2986.

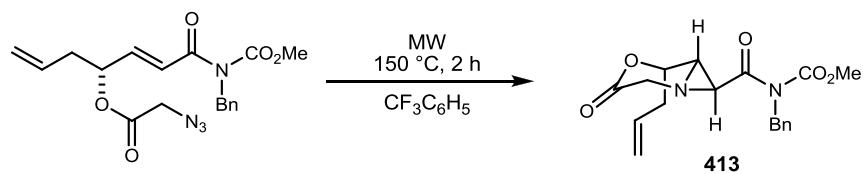


(*R,E*)-7-(Benzyl(methoxycarbonyl)amino)-7-oxohepta-1,5-dien-4-yl 2-azidoacetate

(411). To the alcohol (860 mg, 2.97 mmol) in triethylamine (497 μ L, 3.56 mmol) and CH₂Cl₂ (30 mL) was added azidoacetyl chloride (1.77 g, 14.8 mmol) at 0 °C. The reaction was stirred for 3 h before quenching with satd aq NaHCO₃ and extraction with EtOAc. The combined organic layers were dried, filtered, and concentrated to a yellow oil. Flash column chromatography (SiO₂, 5-10% ethyl acetate in hexanes) provided the acylated compound as a colorless oil (274 mg, 25%). $R_f=0.75$ (30% EtOAc/hexanes); $[\alpha]_D^{24} -16.2$ (c 1.85, CHCl₃); IR (film) 2957, 2361, 1738, 1682 cm⁻¹; ¹H NMR (500 MHz, CDCl₃) δ 7.34-7.26 (m, 5H), 7.10 (dd, $J = 15.5, 1.5$ Hz, 1H), 6.87 (dd, $J = 15.0, 5.5$ Hz, 1H), 5.77 (dddd, $J = 17.0, 10.5, 7.0, 7.0$ Hz, 1H), 5.62 (dd, $J = 15.5, 5.5$ Hz, 1H), 5.18 (d, $J = 7.0$ Hz, 1H), 5.16 (s, 1H), 4.97 (s, 2H), 3.95 (d, $J = 17.5$ Hz, 1H), 3.90 (d, $J = 17.5$ Hz, 1H), 3.82 (s, 3H), 2.56-2.50 (m, 2H); ¹³C NMR (125 MHz, CDCl₃) ppm 167.4, 154.9, 142.0, 137.3, 131.8, 128.4, 127.8, 127.4, 125.3, 119.2, 73.6, 53.8, 50.3, 47.6, 38.2.

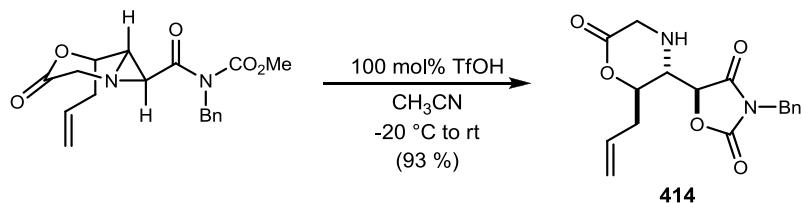


(E)-3-benzyl-5-(penta-1,4-dienyl)oxazolidine-2,4-dione (404). A 0.1 M solution of the unsaturated carbamate (50.0 mg, 0.13 mmol) in acetonitrile was cooled to $-20 \text{ }^\circ\text{C}$ and triflic acid (24 μL , 0.26 mmol) was added. The solution was allowed to stir until reaction was complete at $-20 \text{ }^\circ\text{C}$. The reaction was stirred for 1 h before quenching with triethylamine (36.0 μL , 0.26 mmol), and then diluted with ethyl acetate and washed with sat aq NaHCO_3 . The organic layers were dried and concentrated to a crude oil. Flash column chromatography (SiO_2 , 10-20-30% ethyl acetate in hexanes) provided the cyclized compound as a colorless oil (26.0 mg, 60%). $R_f=0.60$ (30% EtOAc/hexanes); IR (film) 2918, 1814, 1739, 1666 cm^{-1} ; ^1H NMR (500 MHz, CDCl_3) δ 7.38-7.36 (m, 2H), 7.34-7.29 (m, 3H), 6.04 (dddd, $J = 15.5, 6.5, 6.5, 1.0$ Hz, 1H), 5.76 (dddd, $J = 17.0, 10.5, 6.5, 6.5$ Hz, 1H), 5.47 (dddd, $J = 15.5, 6.5, 1.5, 1.5$ Hz, 1H), 5.16 (dd, $J = 6.5, 0.5$ Hz, 1H), 5.06 (s, 1H), 5.03 (dd, $J = 8.5, 1.5$ Hz, 1H), 4.65 (s, 3H), 2.88 (t, $J = 6.5$ Hz, 1H); ^{13}C NMR (150 MHz, CDCl_3) ppm 171.0, 154.9, 137.2, 134.6, 134.5, 128.9, 128.8, 128.5, 120.6, 116.9, 79.8, 43.9, 36.1, 29.7; HRMS (CI): Exact mass calcd for $\text{C}_{15}\text{H}_{15}\text{NNaO}_3$ $[\text{M}+\text{Na}]^+$ 280.0950, found 280.0990.

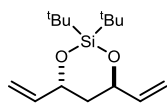


Methyl 5-allyl-3-oxo-4-oxa-1-azabicyclo[4.1.0]heptane-7-carbonyl(benzyl)carbamate

(413). The unsaturated carbamate (61 mg, 0.16 mmol) was weighed in a 2 mL glass pressure microwave tube quipped with a magnetic stir bar. Trifluorotoluene (1 mL) was added, the tube was closed with a septum, and the reaction mixture was subjected to microwave irradiation for 2 h at 150 °C. The reaction tube was allowed to cool to rt, and the reaction mixture was transferred into a round bottomed flask. The solution was concentrated to crude oil that was chromatographed (SiO₂, 10-20-30% ethyl acetate in hexanes) to give a colorless oil (19 mg, 45% brsm). *R*_f=0.15 (30% EtOAc/hexanes); [α]_D²⁴ -16 (*c* 0.25, CHCl₃); IR (film) 3063, 2926, 2853, 1744, 1699 cm⁻¹; ¹H NMR (600 MHz, CDCl₃) δ 7.33-7.26 (m, 5H), 5.89 (dddd, *J* = 16.8, 10.2, 7.8, 6.6 Hz, 1H), 5.28 (dd, *J* = 16.8, 1.2 Hz, 1H), 5.26 (d, *J* = 10.2 Hz, 1H), 4.93 (s, 2H), 4.89 (ddd, *J* = 6.8, 1.3, 1.3 Hz, 1H), 3.90 (d, *J* = 18.1 Hz, 1H), 3.86 (d, *J* = 18.1 Hz, 1H), 3.85 (s, 3H), 3.51 (d, *J* = 2.4 Hz, 1H), 2.79 (dd, *J* = 2.8, 1.6 Hz, 1H), 2.74-2.65 (m, 2H); ¹³C NMR (150 MHz, CDCl₃) ppm 170.3, 166.5, 154.8, 136.8, 131.1, 128.5, 128.0, 127.6, 120.4, 74.8, 54.1, 50.4, 47.6, 39.7, 38.6; HRMS (CI): Exact mass calcd for C₁₈H₂₀N₂NaO₅ [M+Na]⁺ 367.1270, found 367.1269.



(S)-5-((2R,3S)-2-allyl-6-oxomorpholin-3-yl)-3-benzyloxazolidine-2,4-dione (414). A 0.1 M solution of the aziridine (18.0 mg, 0.05 mmol) in acetonitrile was cooled to $-20\text{ }^{\circ}\text{C}$ and triflic acid (4.60 μL , 0.05 mmol) was added. The stirring was continued for 10 min and then allowed to warm to $25\text{ }^{\circ}\text{C}$. The reaction was stirred for 18 h before quenching with triethylamine (7.20 μL , 0.05 mmol), then diluted with ethyl acetate and washed with sat aq NaHCO_3 . The organic layers were dried and concentrated to a crude oil that was chromatographed (SiO_2 , 10-20-40% ethyl acetate in hexanes) to provide the oxazolidinone dione as a colorless oil (16.0 mg, 93%). $R_f=0.55$ (40% EtOAc/hexanes); $[\alpha]_D^{24} -42.8$ (c 0.35, CHCl_3); IR (film) 2919, 2850, 1816, 1733, 1442 cm^{-1} ; ^1H NMR (600 MHz, CDCl_3) δ 7.37 (dd, $J = 7.8, 2.4$ Hz, 2H), 7.33-7.29 (m, 3H), 5.87 (dddd, $J = 16.8, 10.2, 7.2, 7.2$ Hz, 1H), 5.21 (dd, $J = 9.0, 1.2$ Hz, 1H), 5.19 (dd, $J = 17.4, 1.2$ Hz, 1H), 4.84 (ddd, $J = 10.2, 5.4, 4.2$ Hz, 1H), 4.75 (d, $J = 3.0$ Hz, 1H), 4.68 (s, 2H), 3.45 (ddd, $J = 10.8, 7.8, 3.0$ Hz, 1H), 3.27 (dd, $J = 17.4, 10.2$ Hz, 1H), 3.22 (dd, $J = 17.4, 6.0$ Hz, 1H), 2.68-2.60 (m, 1H), 2.51-2.47 (m, 1H), 1.85 (dd, $J = 15.6, 8.4$ Hz, 1H); ^{13}C NMR (150 MHz, CDCl_3) ppm 171.0, 170.1, 155.0, 134.2, 131.1, 128.8, 128.6, 128.5, 119.9, 77.9, 74.0, 55.1, 44.5, 43.9, 36.3; HRMS (CI): Exact mass calcd for $\text{C}_{17}\text{H}_{18}\text{N}_2\text{NaO}_5$ $[\text{M}+\text{Na}]^+$ 353.1114, found 353.1123.



(4R,6R)-2,2-Di-tert-butyl-4,6-divinyl-1,3,2-dioxasilinane (425). $R_f =$

0.70 (30% EtOAc/hexanes); $[\alpha]_D^{24}$ 11.4 (*c* 3.50, CHCl₃); IR (film) 3014,

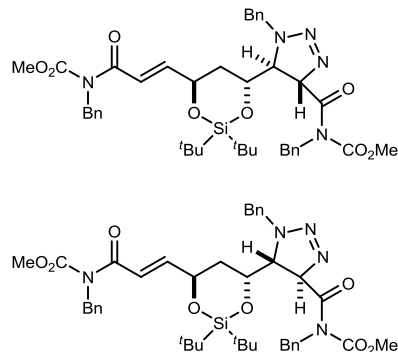
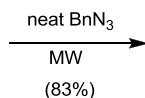
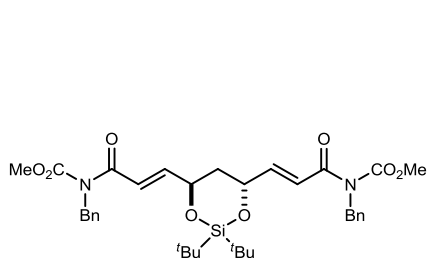
2963, 2859, 1645, 1474, 1151, 825 cm⁻¹; ¹H NMR (400 MHz, CDCl₃) δ 5.93 (dd, *J* =

10.8, 5.2 Hz, 2H), 5.89 (dd, *J* = 10.8, 5.2 Hz, 1H), 5.29 (ddd, *J* = 17.2, 1.6, 1.6 Hz, 2H),

5.10 (ddd, *J* = 10.4, 1.6, 1.6 Hz, 2H), 4.64-4.59 (m, 2H), 1.88 (dd, *J* = 3.2 Hz, 2H), 1.00

(s, 18H); ¹³C NMR (100 MHz, CDCl₃) ppm 140.5, 114.0, 70.7, 39.8, 27.2, 21.1; HRMS

(CI): Exact mass calcd for C₁₅H₂₇O₂Si [M-H]⁺ 267.1775, found 267.1775.



Higher R_f : **446**
anti-anti

Lower R_f : **447**
syn-anti

***anti-anti* Triazoline(446).** $[\alpha]_D^{24}$ -7.15 (*c* 1.50, CHCl₃); IR (film) 2932, 1739, 1733, 1717,

1705, 1699, 1683 cm⁻¹; ¹H NMR (600 MHz, CDCl₃) δ 7.38-7.19 (m, 15H), 7.09 (dd, *J* =

15.0, 1.2 Hz, 1H), 6.89 (dd, *J* = 15.0, 4.2 Hz, 1H), 6.26 (d, *J* = 10.2 Hz, 1H), 5.08 (d, *J* =

15.6 Hz, 1H), 4.99 (s, 2H), 4.92 (s, 2H), 4.87-4.84 (m, 1H), 4.67 (d, *J* = 15.6 Hz, 1H),

4.26 (d, *J* = 10.2 Hz, 1H), 3.88 (s, 3H), 3.85 (dd, *J* = 10.2, 3.6 Hz, 1H), 3.78 (s, 3H), 1.90

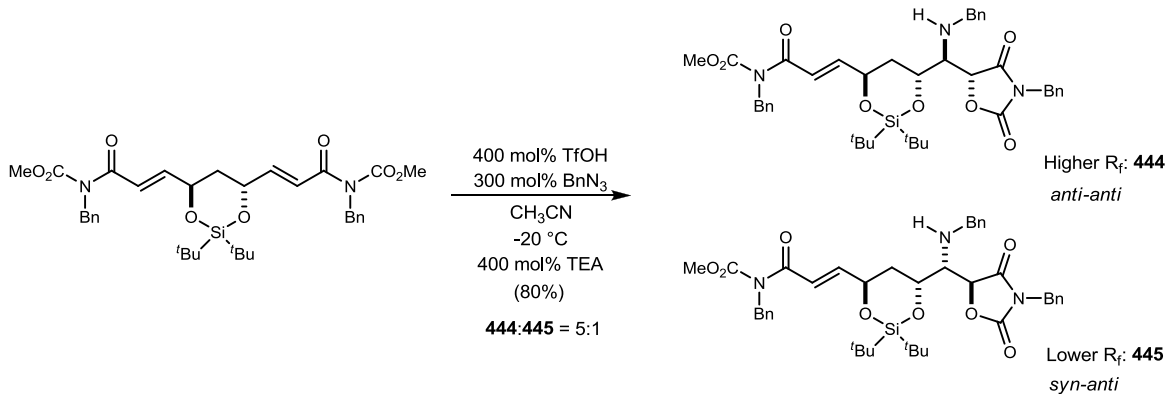
(ddd, *J* = 14.4, 10.2, 6.6 Hz, 1H), 1.63-1.60 (m, 1H), 1.02 (s, 9H), 1.01 (s, 9H); ¹³C NMR

(125 MHz, CDCl₃) ppm 169.8, 167.8, 154.8, 148.3, 137.5, 136.9, 135.5, 128.7, 128.4,

128.0, 127.8, 127.6, 127.5, 123.4, 123.4, 81.2, 70.4, 66.3, 62.9, 54.2, 53.7, 52.6, 48.5,

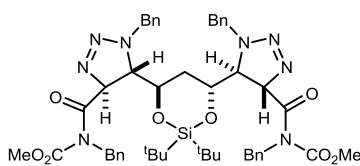
47.6, 35.7, 29.6, 27.1, 26.9, 21.5, 20.8; HRMS (CI): Exact mass calcd for C₄₂H₅₄N₅O₈Si

[M+H]⁺ 784.3742, found 784.3735.



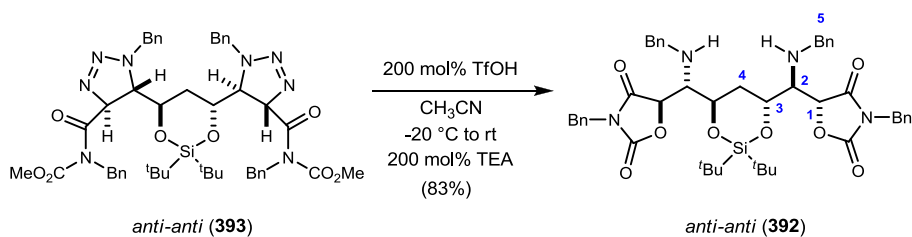
***anti-anti* Oxazolidine Dione (444).** A 0.1 M solution of the imide (57.1 mg, 87.1 μmol) in acetonitrile was cooled to $-20\text{ }^{\circ}\text{C}$ and triflic acid (31.1 μL , 0.35 mmol) was added, and stirring was continued for 10 min and then benzyl azide (34.1 μL , 261 μmol) was then added and the reaction was allowed to stir until complete conversion. The reaction mixture was quenched with triethylamine (48.7 μL , 0.35 mmol) via syringe. The mixture was concentrated, and the residue was chromatographed (SiO_2 , 5-10-20% ethyl acetate in hexanes) to provide desired the oxazolidine dione product as a yellow oil (51.88 mg, 80%). $R_f=0.30$ (10% EtOAc/hexanes); ^1H NMR (600 MHz, CDCl_3) δ 7.38-7.36 (m, 2H), 7.28-7.14 (m, 13H), 7.09 (dd, $J = 15.0, 1.8$ Hz, 1H), 6.92 (dd, $J = 15.6, 4.2$ Hz, 1H), 5.17 (d, $J = 1.8$ Hz, 1H), 4.92 (s, 2H), 4.78-4.77 (m, 1H), 4.65 (d, $J = 14.4$ Hz, 1H), 4.58 (d, $J = 14.4$ Hz, 1H), 4.16 (ddd, $J = 9.6, 9.6, 2.4$ Hz, 1H), 3.81 (d, $J = 13.2$ Hz, 1H), 3.69 (d, $J = 13.2$ Hz, 1H), 3.67 (s, 3H), 3.12 (dd, $J = 9.6, 1.2$ Hz, 1H), 2.24 (ddd, $J = 15.0, 3.0, 3.0$ Hz, 1H), 2.03 (ddd, $J = 14.4, 8.4, 6.0$ Hz, 1H), 0.98 (s, 9H), 0.96 (s, 9H), the NH was not observed; ^{13}C NMR (125 MHz, CDCl_3) ppm 171.5, 167.9, 155.6, 148.4, 139.0, 137.5, 134.8, 128.7, 128.5, 128.4, 128.3, 128.2, 127.6, 127.3, 123.2, 79.4, 70.2, 69.2, 53.6, 52.3, 47.6, 43.6, 36.4, 29.6, 27.0, 26.9, 21.3, 20.8; HRMS (CI): Exact mass calcd for $\text{C}_{41}\text{H}_{52}\text{N}_3\text{O}_8\text{Si}$ $[\text{M}+\text{H}]^+$ 742.3524, found 742.3524.

***syn-anti* Oxazolidine dion (445).** $[\alpha]_D^{24} -26.0$ (*c* 0.50, CHCl₃); IR (film) 2933, 1743, 1717, 1699, 1683 cm⁻¹; ¹H NMR (600 MHz, CDCl₃) δ 7.40-7.37 (m, 2H), 7.33-7.15 (m, 13H), 7.12 (dd, *J* = 15.0, 1.8 Hz, 1H), 6.94 (dd, *J* = 15.0, 4.2 Hz, 1H), 4.98-4.97 (m, 2H), 4.95 (d, *J* = 4.2 Hz, 2H), 4.66 (d, *J* = 14.4 Hz, 1H), 4.63 (d, *J* = 14.4 Hz, 1H), 4.34-4.27 (m, 1H), 3.90 (d, *J* = 12.6 Hz, 1H), 3.74 (s, 3H), 3.73 (d, *J* = 12.6 Hz, 1H), 3.00 (t, *J* = 4.2 Hz, 1H), 4.23 (ddd, *J* = 14.4, 7.8, 6.0 Hz, 1H), 1.76 (ddd, *J* = 15.0, 4.2, 4.2 Hz, 1H), 1.00 (s, 9H), 0.96 (s, 9H), the NH was not observed; ¹³C NMR (125 MHz, CDCl₃) ppm 171.6, 167.9, 155.1, 148.4, 139.4, 137.5, 134.6, 129.4, 128.8, 128.7, 128.5, 128.4, 128.3, 128.2, 127.7, 127.3, 123.2, 119.2, 113.7, 79.1, 70.4, 68.8, 62.5, 53.7, 52.9, 47.7, 43.7, 36.2, 27.1, 27.0, 21.3, 21.1; HRMS (CI): Exact mass calcd for C₄₁H₅₂N₃O₈Si [M+H]⁺ 742.3524, found 742.3524.



anti-anti (**393**)

***anti-anti* Bistriazoline (393).** $[\alpha]_D^{24} -44.0$ (*c* 0.50, CHCl₃); ¹H NMR (600 MHz, CDCl₃) δ 7.25-7.11 (m, 20H), 5.92 (d, *J* = 10.2 Hz, 2H), 5.10 (d, *J* = 15.0 Hz, 2H), 4.88 (d, *J* = 15.0 Hz, 2H), 4.82 (d, *J* = 15.0 Hz, 2H), 4.72 (d, *J* = 15.0 Hz, 2H), 4.15 (dd, *J* = 13.2, 6.0 Hz, 2H), 4.00 (dd, *J* = 10.2, 7.8 Hz, 2H), 3.78 (s, 6H), 1.58-1.53 (m, 2H), 0.92 (s, 18H); ¹³C NMR (125 MHz, CDCl₃) ppm 169.5, 154.9, 136.8, 136.1, 128.4, 128.0, 127.5, 127.3, 127.2, 83.0, 72.5, 62.0, 54.1, 54.0, 48.4, 32.2, 29.7, 21.2; HRMS (CI): Exact mass calcd for C₄₉H₆₁N₈O₈Si [M+H]⁺ 917.4382, found 917.4404.



(5*R*,5'*R*)-5,5'-((1*S*,1'*S*)-((4*R*,6*R*)-2,2-di-*tert*-butyl-1,3,2-dioxasilinane-4,6-

diyl)bis((benzylamino)methylene))bis(3-benzylloxazolidine-2,4-dione) (392). A 0.1 M

solution of the triazolone (400 μg , 4.36 μmol) in acetonitrile was cooled to $-20\text{ }^\circ\text{C}$ and triflic acid (0.70 μL , 8.7 μmol). Stirring was continued for 10 min before allowed to

warm to $25\text{ }^\circ\text{C}$. The reaction was stirred for 18 h before quenching with triethylamine (1.2 μL , 8.72 μmol) via syringe. The mixture was concentrated, and the residue was

chromatographed (SiO_2 , 5-10-20% ethyl acetate in hexanes) to provide the desired

oxazolidine dione as a yellow oil (3 mg, 83%). $R_f=0.30$ (10% EtOAc/hexanes); $[\alpha]_D^{24} -$

49.3 (c 1.50, CHCl_3); IR (film) 1814, 1738 cm^{-1} ; $^1\text{H NMR}$ (600 MHz, CDCl_3) δ 7.44-7.18

(m, 20H), 5.00 (d, $J = 3.6$ Hz, 2H), 4.70 (d, $J = 6.6$ Hz, 2H), 4.69 (s, 4H), 4.49 (dd, $J =$

10.0, 5.4 Hz, 2H), 3.93 (d, $J = 12.6$ Hz, 2H), 3.76 (d, $J = 12.6$ Hz, 2H), 3.08 (dd, $J = 6.0,$

4.2 Hz, 2H), 1.98 (t, $J = 5.4$ Hz, 2H), 0.96 (s, 18H); $^{13}\text{C NMR}$ (125 MHz, CDCl_3) ppm

171.8, 155.2, 139.5, 134.5, 128.9, 128.9, 128.8, 128.7, 128.6, 128.5, 128.4, 127.2, 79.5,

69.6, 67.8, 62.7, 53.6, 43.8, 43.7, 33.8, 27.2, 27.1, 14.1; HRMS (CI): Exact mass calcd

for $\text{C}_{47}\text{H}_{57}\text{N}_4\text{O}_8\text{Si}$ $[\text{M}+\text{H}]^+$ 833.3946, found 833.3970.

Chapter V

Appendix

A.1 ReactIR Experiments

A Mettler-Toledo ReactIR iC-10 equipped with a K-6 conduit immersible probe with SiComp ATR probe tip connected to a liquid nitrogen cooled MCT detector was used for in situ reaction monitoring at 8 wavenumber resolution. The instrument was outfitted with a Dell Latitude D505 laptop running iC IR version 2.0. Industrial grade nitrogen was used to continually purge the system. The external temperature of the isopropanol bath was maintained at -20 °C monitored by thermometer using a Thermo Electron Corporation NESLAB CC 100 Immersion Cooler with the controller set to -25 °C. The acetonitrile was subtracted from the reaction and all 3D spectra were baseline corrected with baseline offset at 1985 cm⁻¹. The raw data was exported into Microsoft Excel to produce the IR spectra. The trendlines for the 1830 cm⁻¹ and 1711 cm⁻¹ peaks were formatted to height to single point at 1985 cm⁻¹. The data corresponding to the conversion time period of 1 hour for each experiment was chosen and the time was then converted into minutes and subsequently into a relative time period.

General Procedure for Triazoline Free Base (246a) Formation: To acetonitrile (8.0 mL) in the reaction vessel cooled to -20 °C was added imide **3** (850 μL, 4.56 mmol), followed by triflic acid (800 μL, 9.12 mmol) via syringe, and stirring was continued for 75 min. To the solution was added benzyl azide (610 μL, 4.56 mmol) via syringe. After 40 min, the reaction mixture was quenched with triethylamine (2.80 mL, 9.12 mmol) via syringe. The solvent was removed in vacuo. The residue was purified by chromatography

10%→20%→30% ethyl acetate in hexanes using a jacketed column circulating ice-water to give triazoline **1** as a faint yellow oil that solidified after being triturated with 1 mL of hexanes-ethyl acetate (10:1) (868 mg, 54%). Characterization data of this compound has been reported previously.¹⁰⁰

General Procedure for Oxazolidine Dione (245a) Formation: To acetonitrile (8.0 mL) in the reaction vessel cooled to -20 °C was added imide **3** (850 µL, 4.56 mmol), followed by triflic acid (800 µL, 9.12 mmol) via syringe and stirring was continued for 75 min. To the solution was added benzyl azide (610 µL, 4.56 mmol) via syringe. After 75 min, the additive (distilled or recrystallized¹⁰¹, 4.56 mmol) was added via syringe and stirring continued for 5 h. The reaction mixture was quenched with triethylamine (2.80 mL, 9.12 mmol) via syringe. The solvent was removed in vacuo, and the residue was chromatographed (10%→20%→30% ethyl acetate in hexanes), furnishing oxazolidine dione **2** (150 mg, 60%) as a white solid. Characterization data of this compound has been reported previously.¹⁰⁰

General Procedure for Additive Purification: D₂O (99.9% atom product of Isotec) was used as received from Cambridge Isotope Laboratories. 3-Methyl-2-oxazolidinone (99.5%) was used as received from Aldrich. Methanol, trifluoroethanol, DMF, pyridine, DBU, and isopropyl amine were distilled from calcium hydride. Acetic acid, acetamide, *N*-methyl-imidazole, and imidazole were purified by the procedure of Perrin.¹⁰²

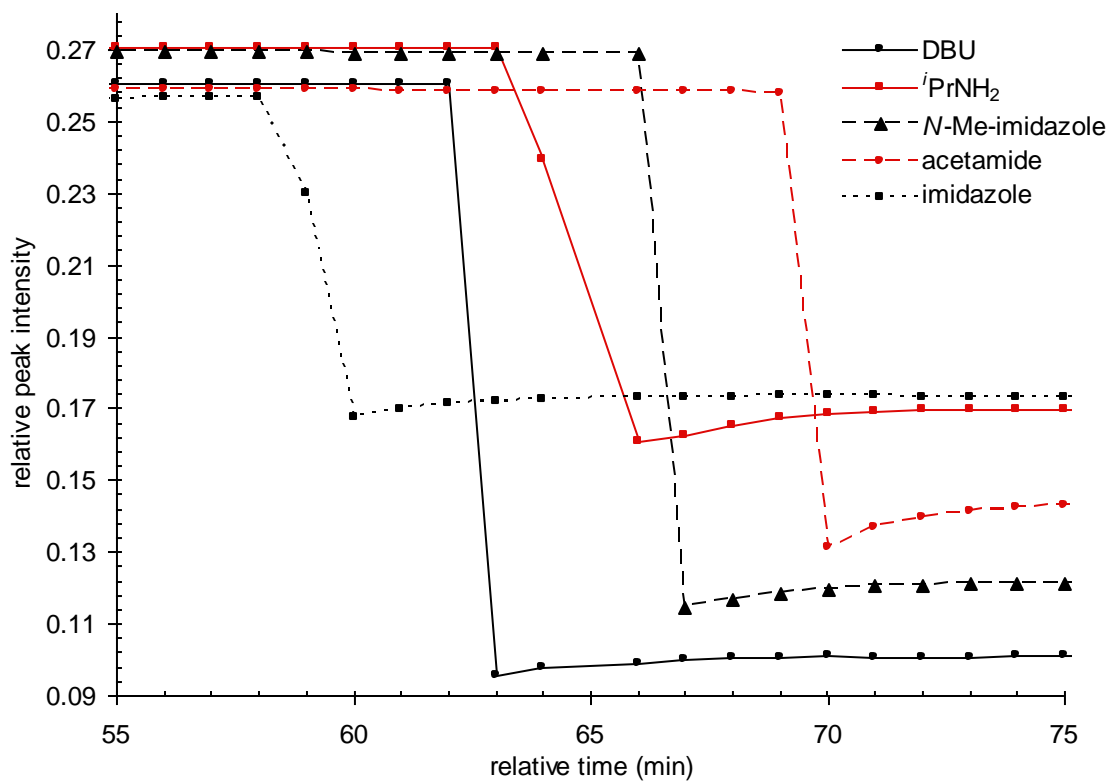
¹⁰⁰ Hong, K. B.; Donahue, M. G.; Johnston, J. N. *J. Am. Chem. Soc.* **2008**, *130*, 2323.

¹⁰¹ Solid additives were added as a solution in CH₃CN (1 mL).

¹⁰² Armarego, W. L.; Perrin, D. D. *Purification of Laboratory Chemicals*, 4th Ed.; Butterworth-Heinemann, 1996.

Effect of Additives in the Conversion of Triazolinium to Oxazolidine Dione by Monitoring the Decomposition of the Triazoline (1711 cm^{-1}).

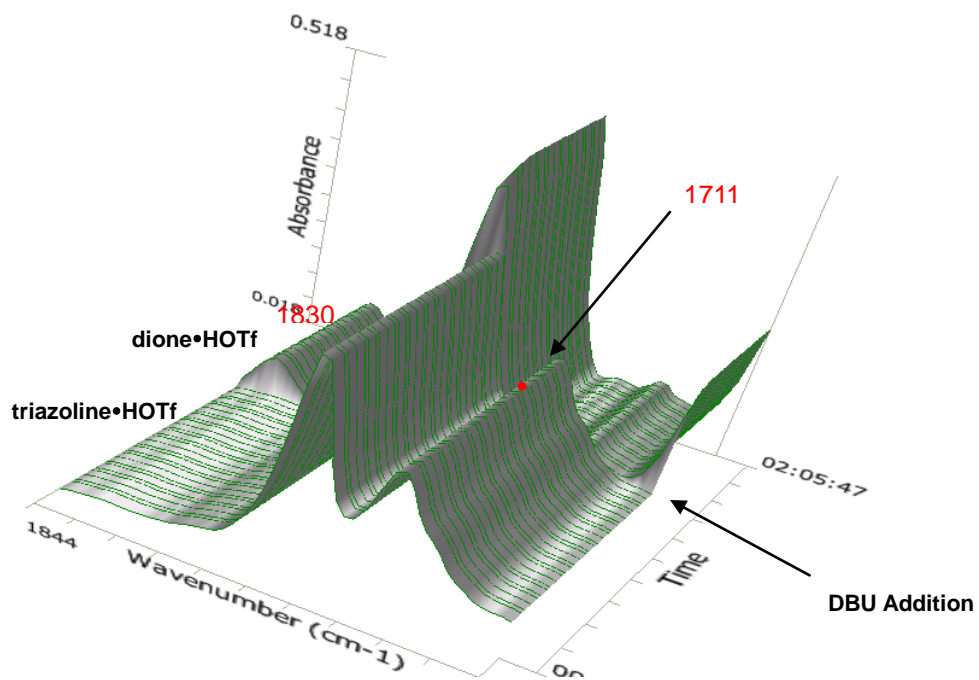
Figure A1. Effect of Additions on the Catalysis of Triazoline Fragmentation; Monitoring by in situ IR at 1711 cm^{-1} .^a



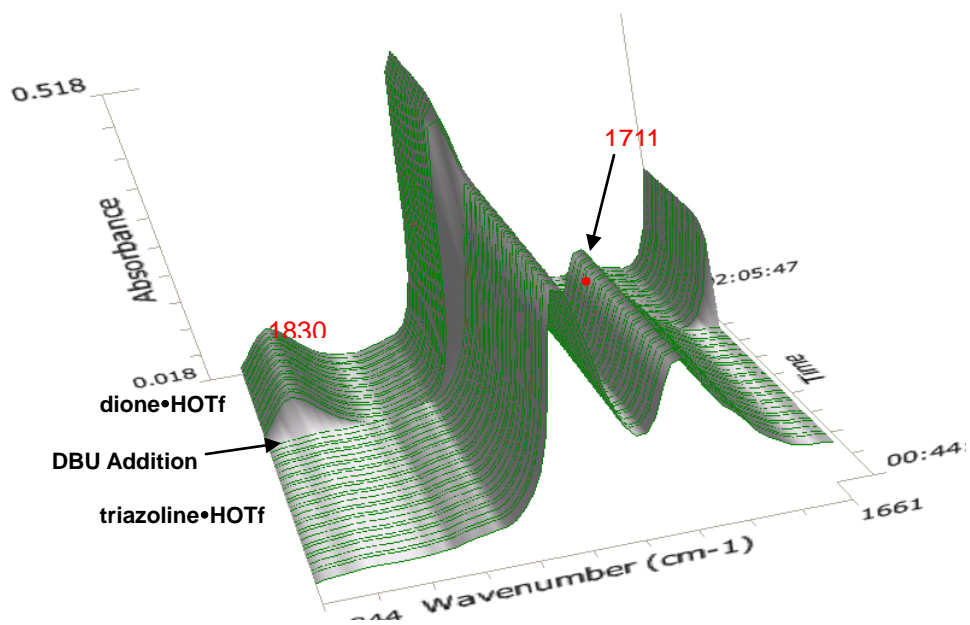
^aAbsorption at 1711 cm^{-1} corresponds to amide carbonyl stretch of the triazoline.

Additive: DBU

Right Perspective

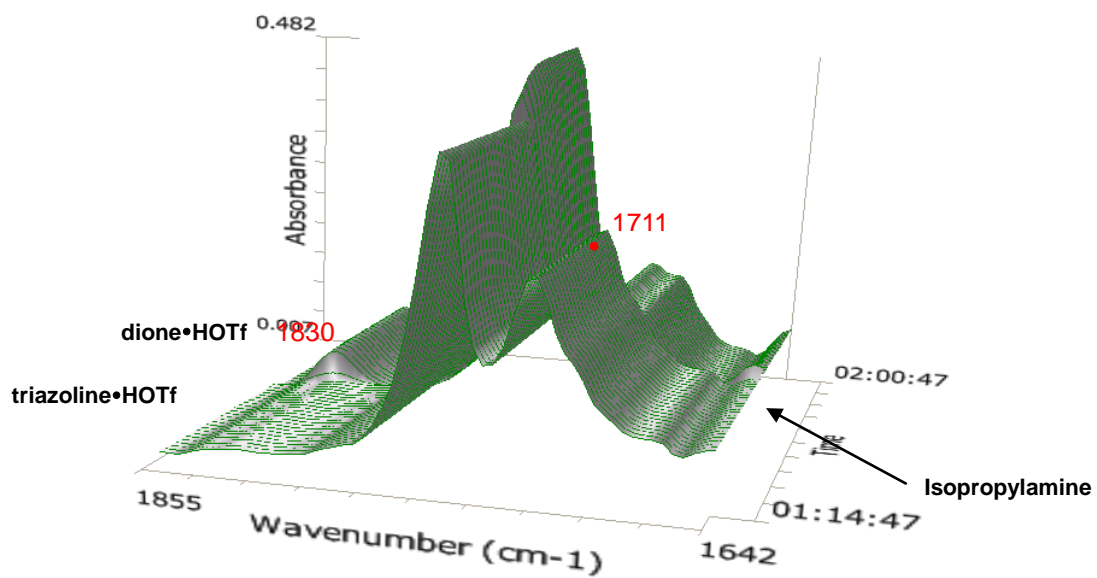


Left Perspective

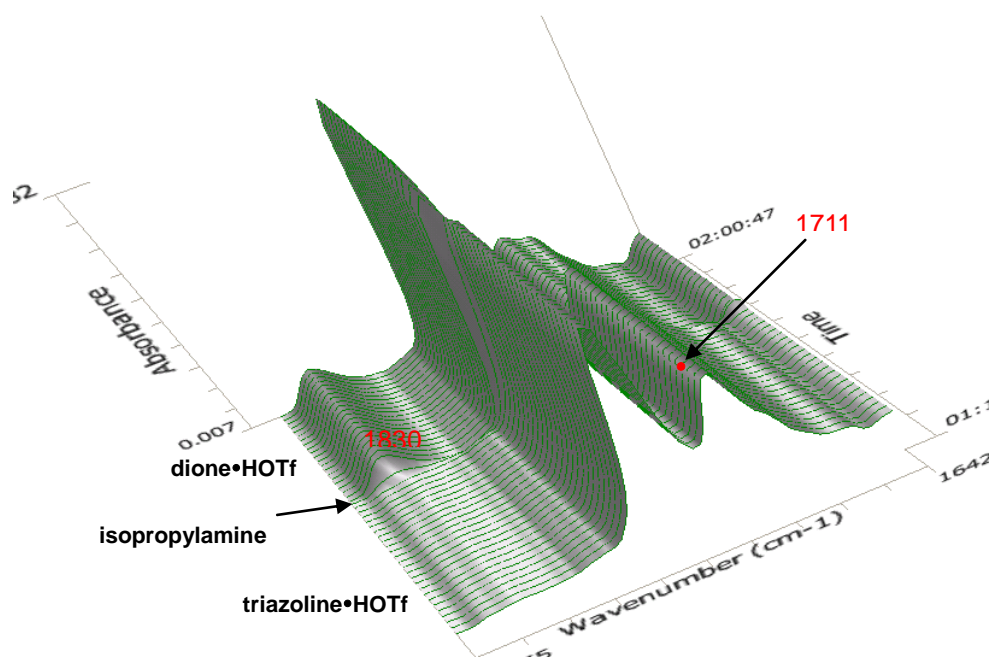


Additive: $i\text{PrNH}_2$

Right Perspective

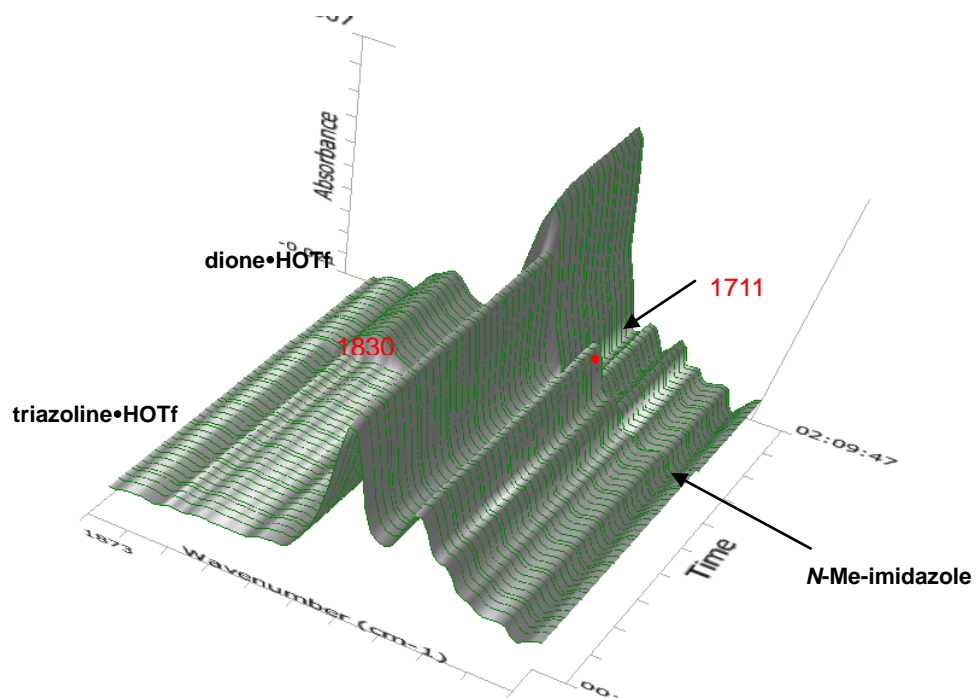


Left Perspective

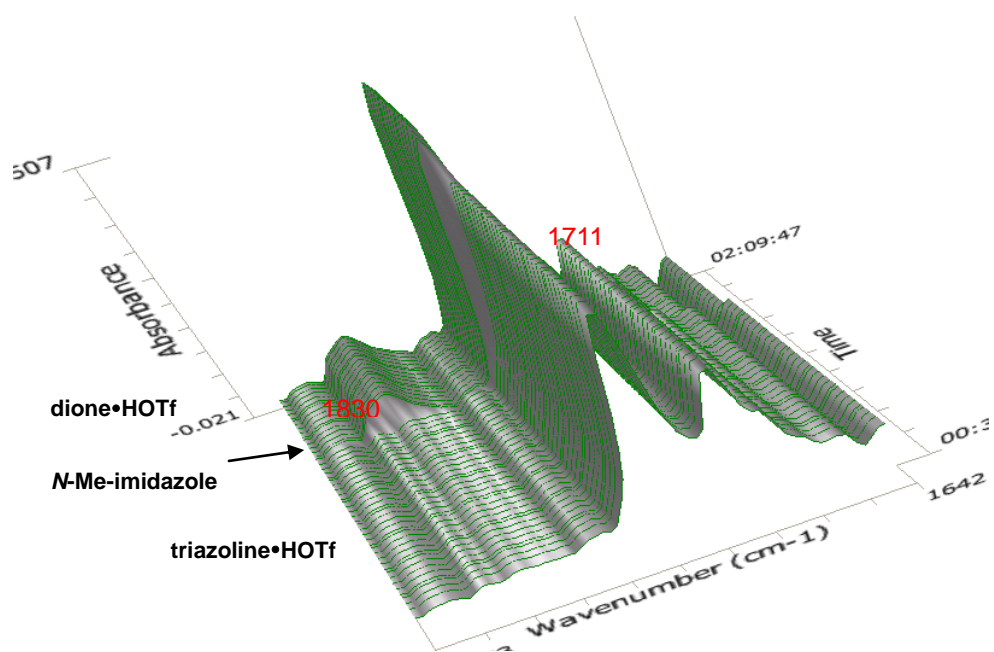


Additive: *N*-Me-imidazole

Right Perspective

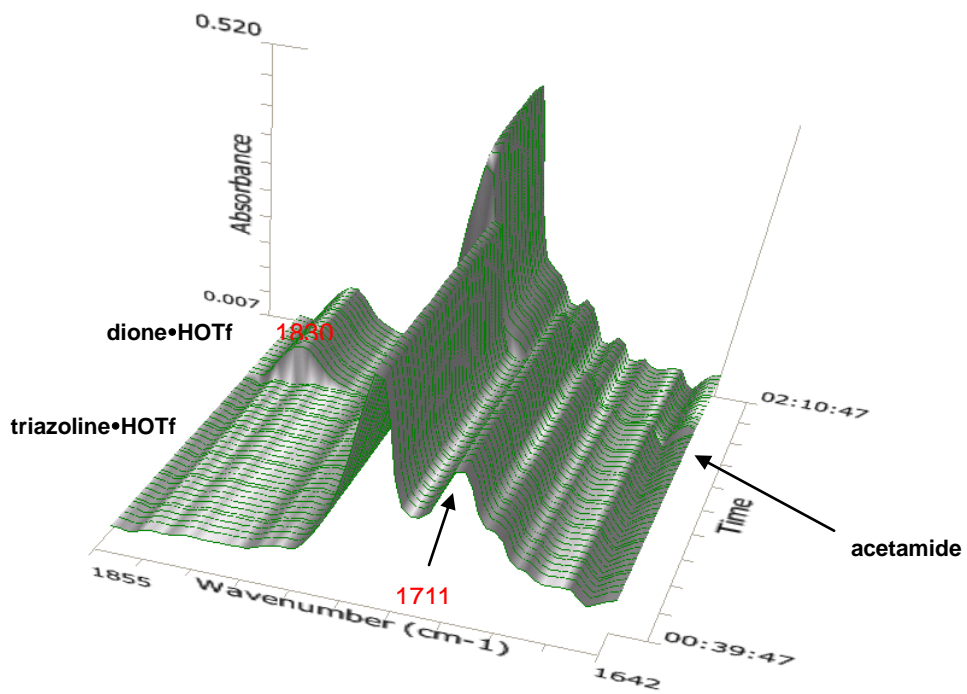


Left Perspective

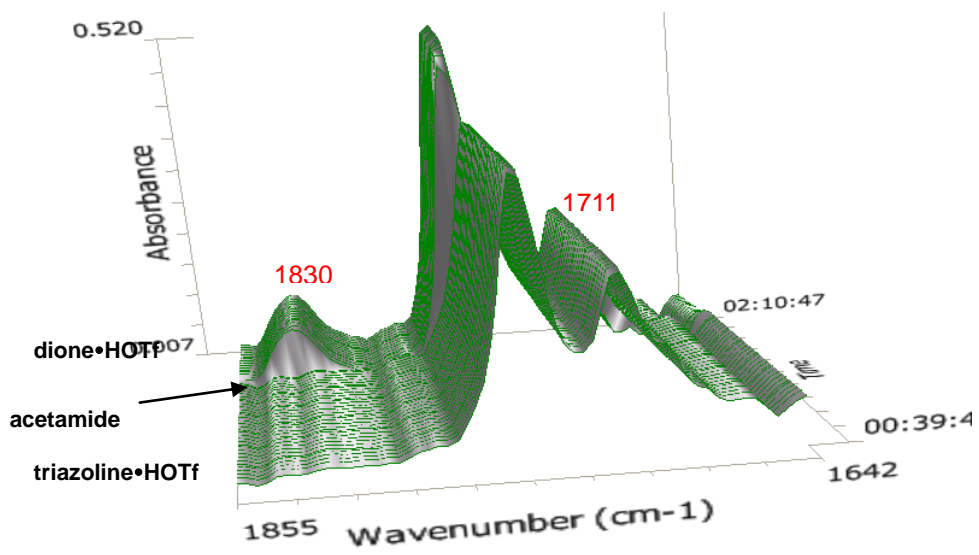


Additive: Acetamide

Right Perspective

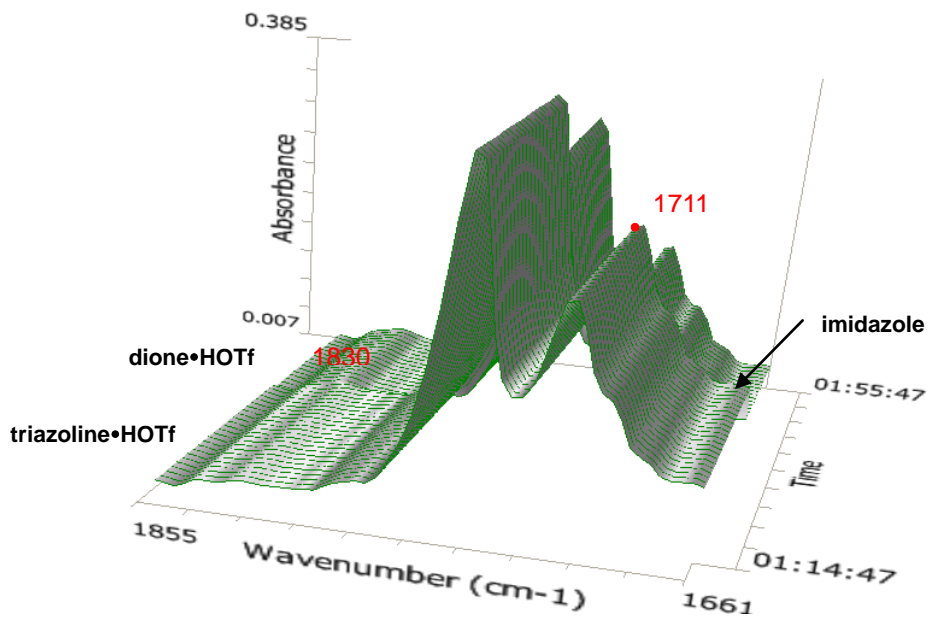


Left Perspective

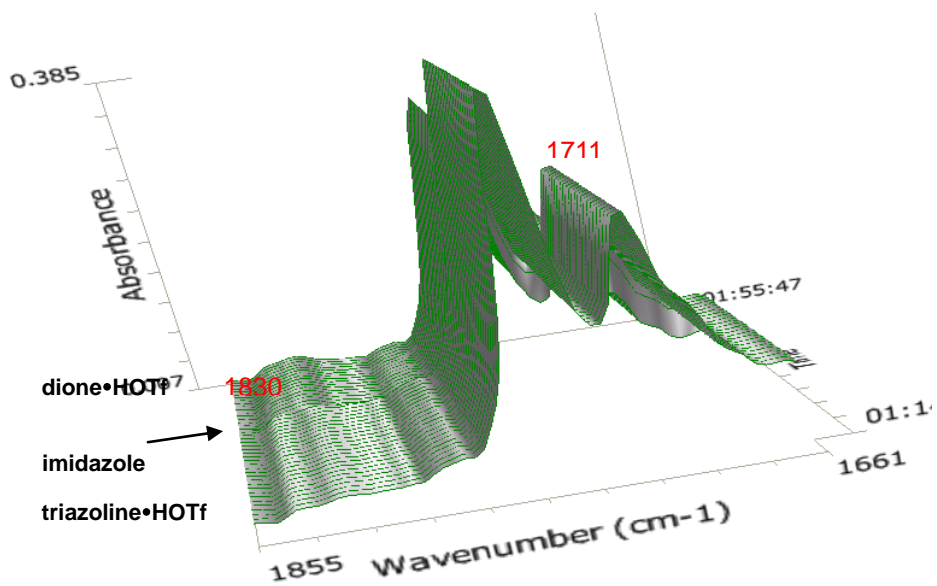


Additive: Imidazole

Right Perspective

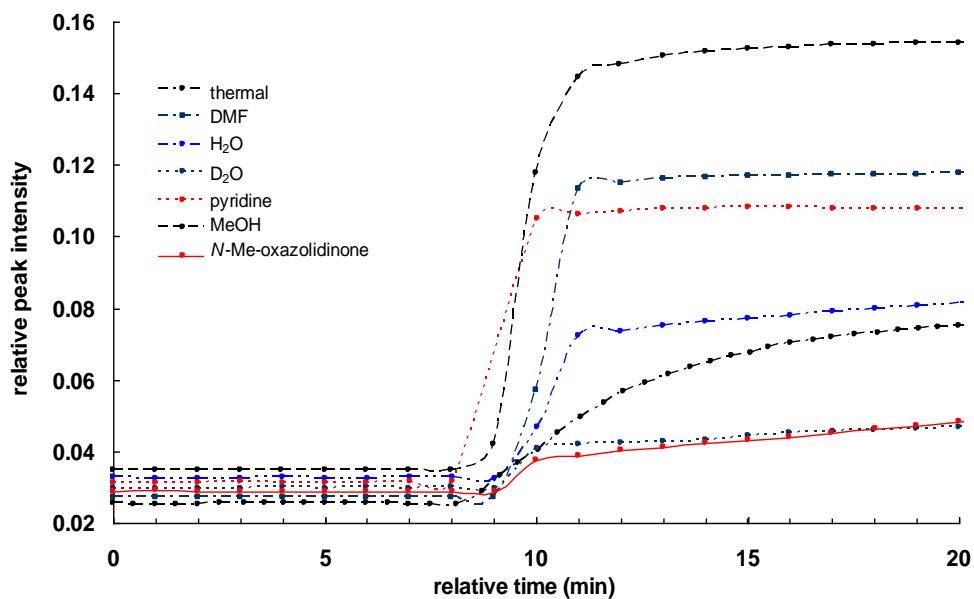


Left Perspective



Effect of Additives in the Conversion of Triazolinium to Oxazolidine Dione by Monitoring the Formation of Oxazolidine Dione (1830 cm^{-1}).

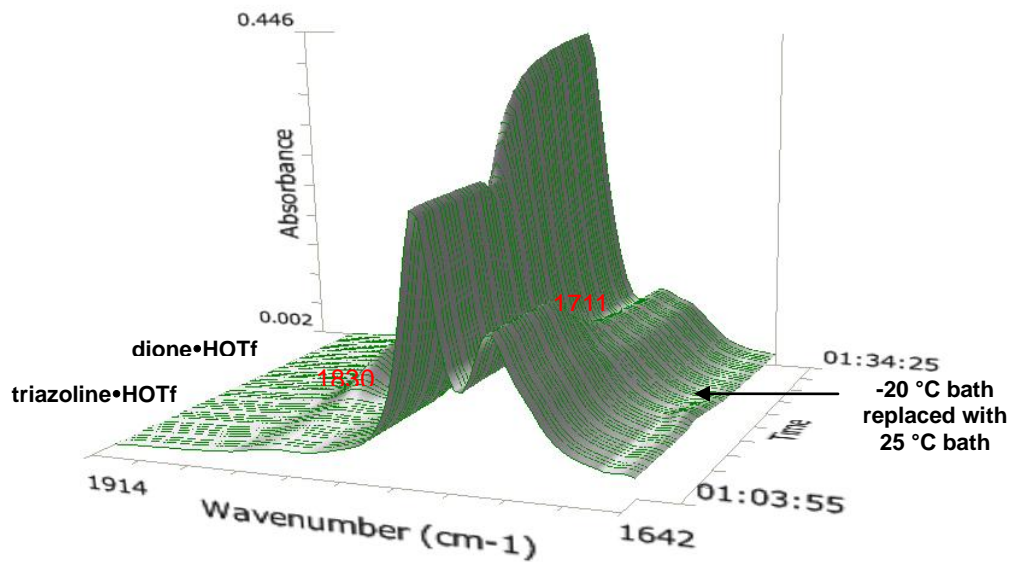
Figure A2. Effect of Additions on the Catalysis of Triazoline Fragmentation; Monitoring by in situ IR at 1830 cm^{-1} .^a



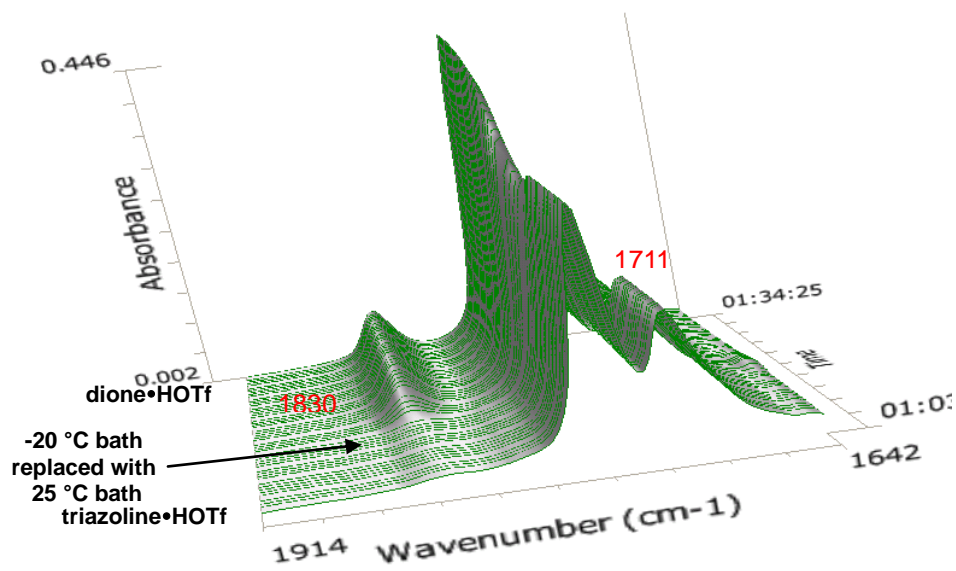
^aAbsorption at 1830 cm^{-1} corresponds to carbamate carbonyl stretch of the oxazolidine dione. Sampling is at 1 minute intervals. The following were added neat: DMF, H₂O, D₂O, pyridine, MeOH. *N*-Methyl oxazolidinone was added as a solution in acetonitrile (1 mL).

Thermal

Right Perspective

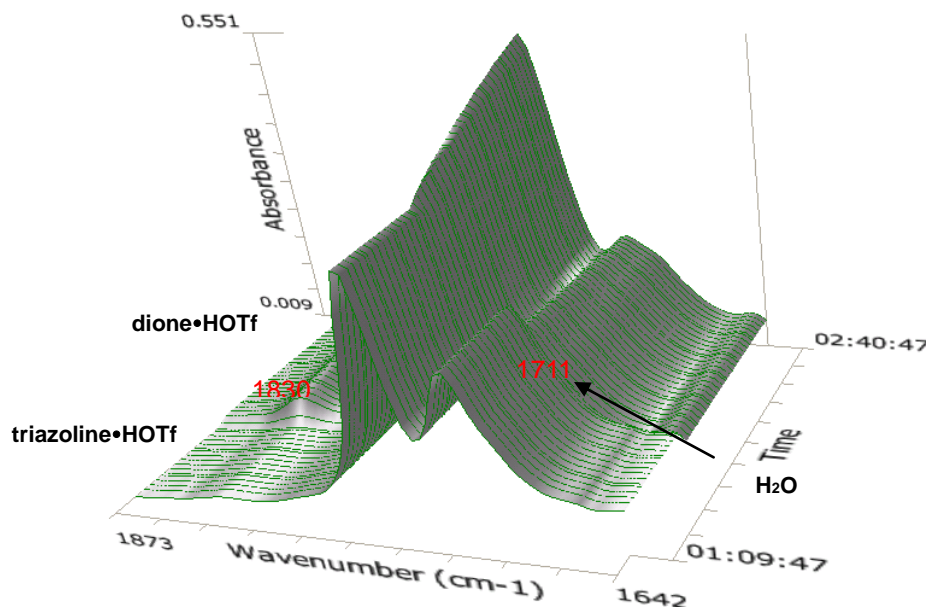


Left Perspective

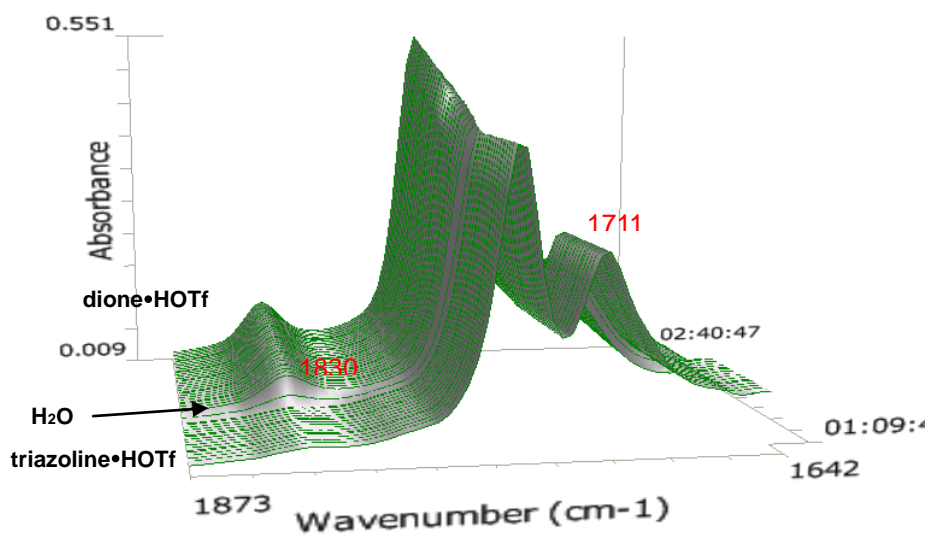


Additive: H₂O

Right Perspective

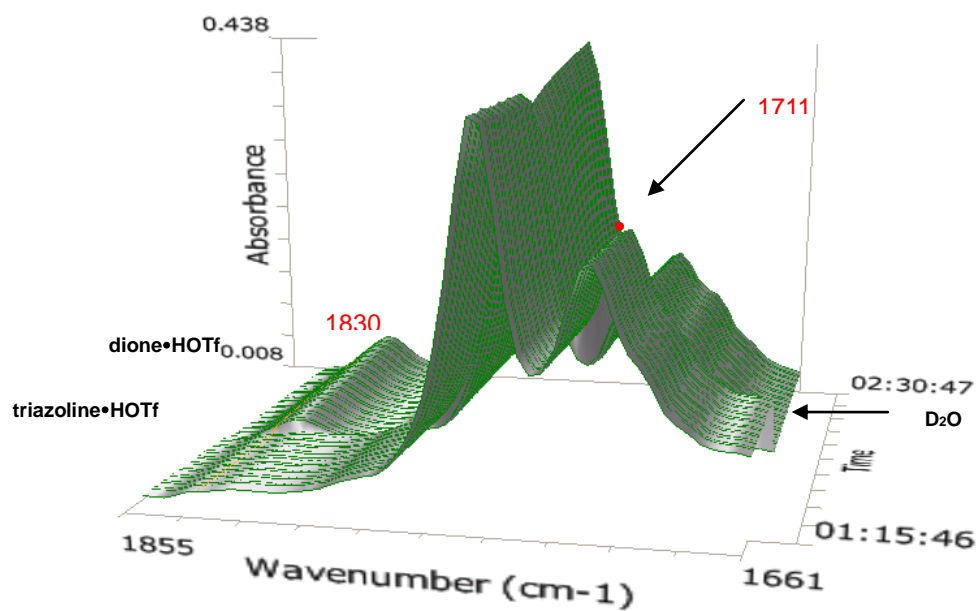


Left Perspective

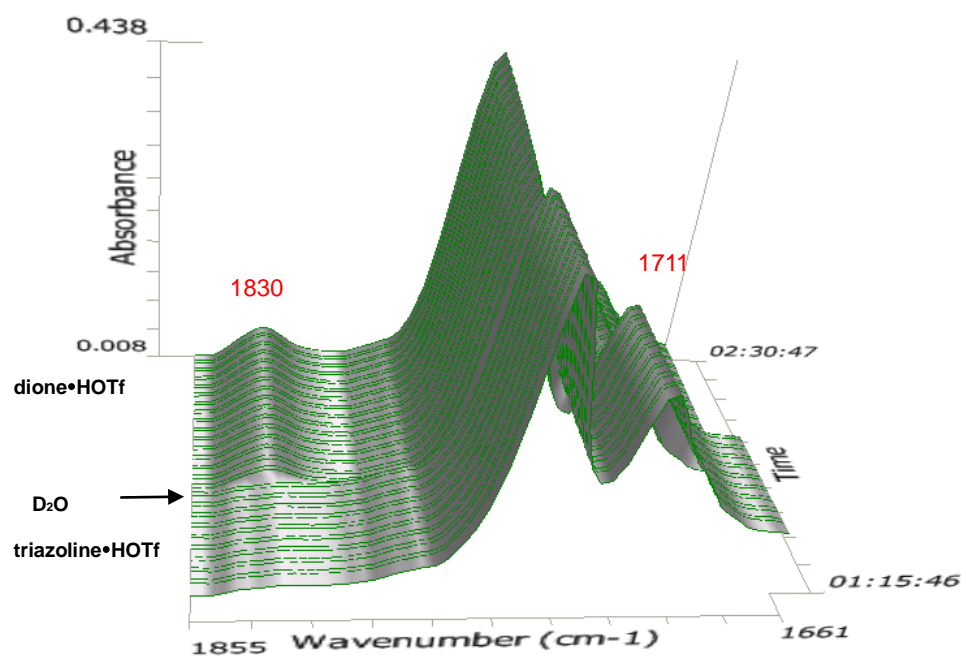


Additive: D₂O

Right Perspective

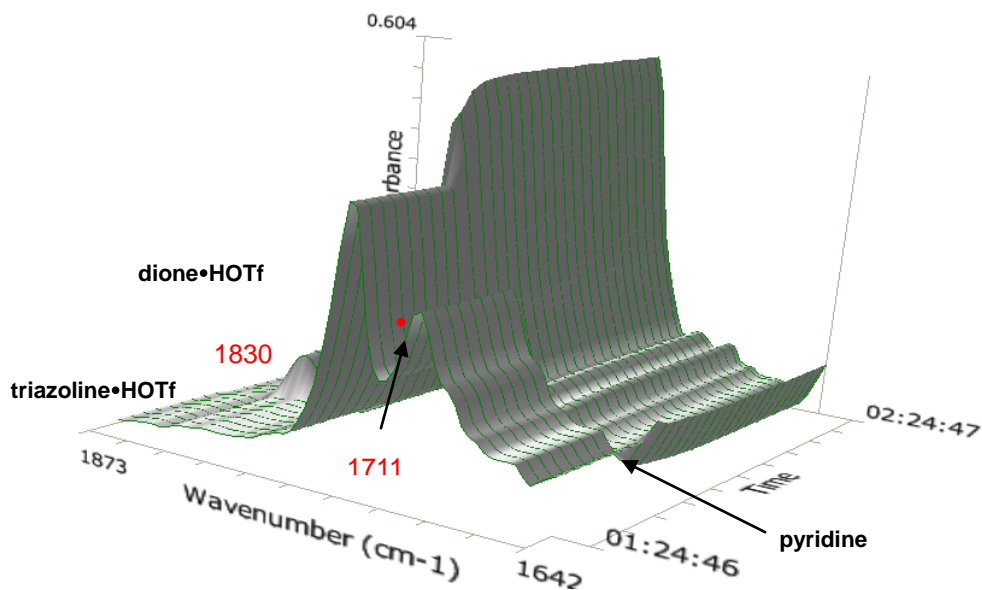


Left Perspective

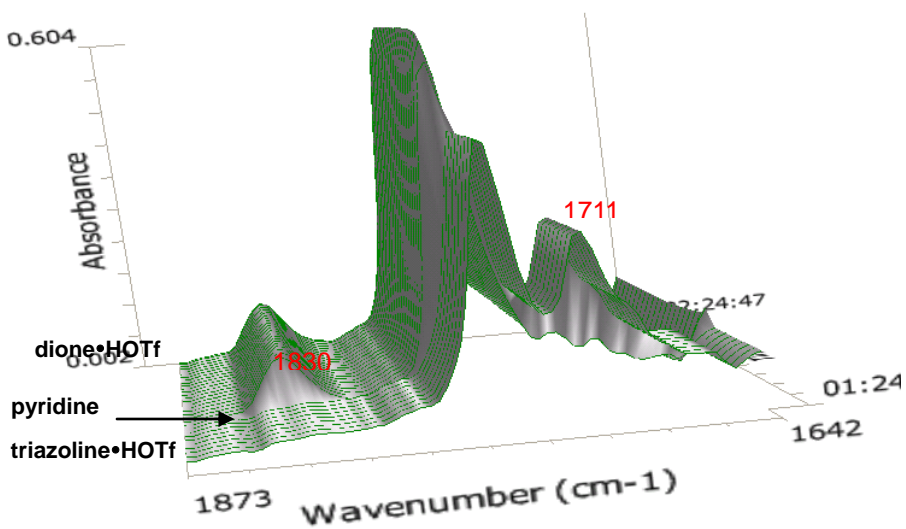


Additive: Pyridine

Right Perspective

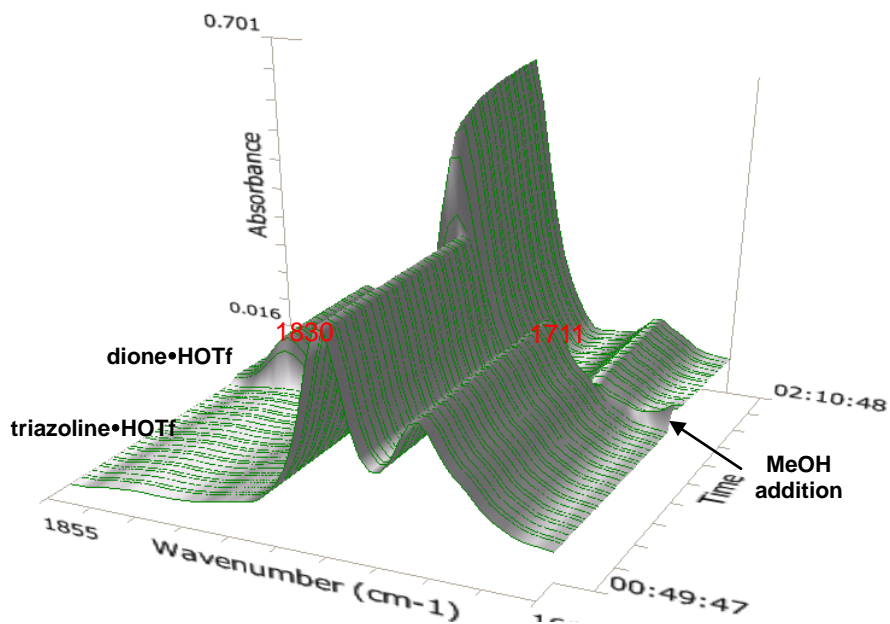


Left Perspective

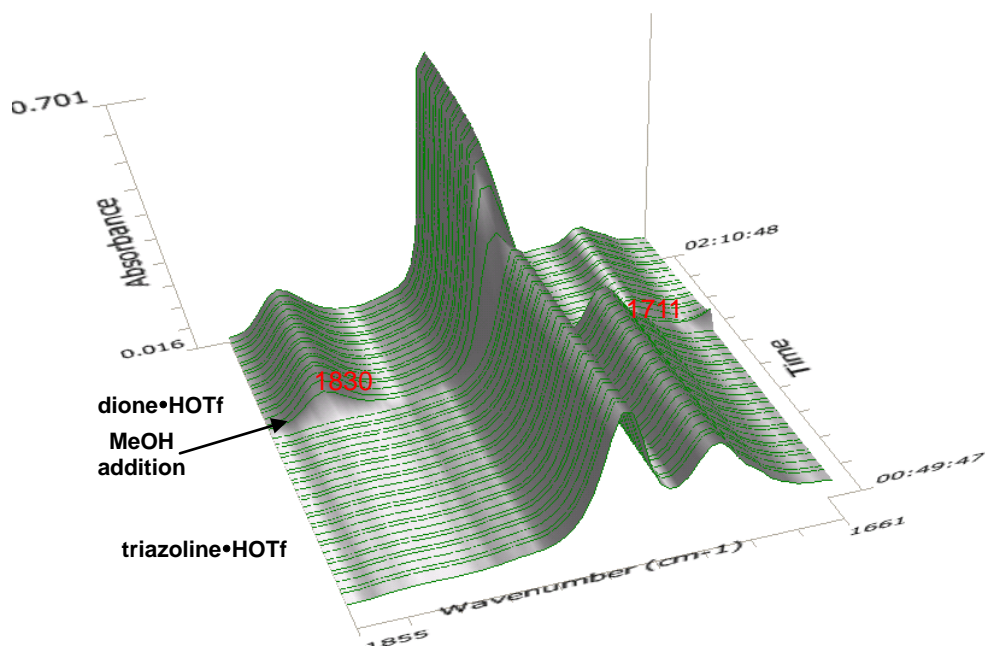


Additive: MeOH

Right Perspective

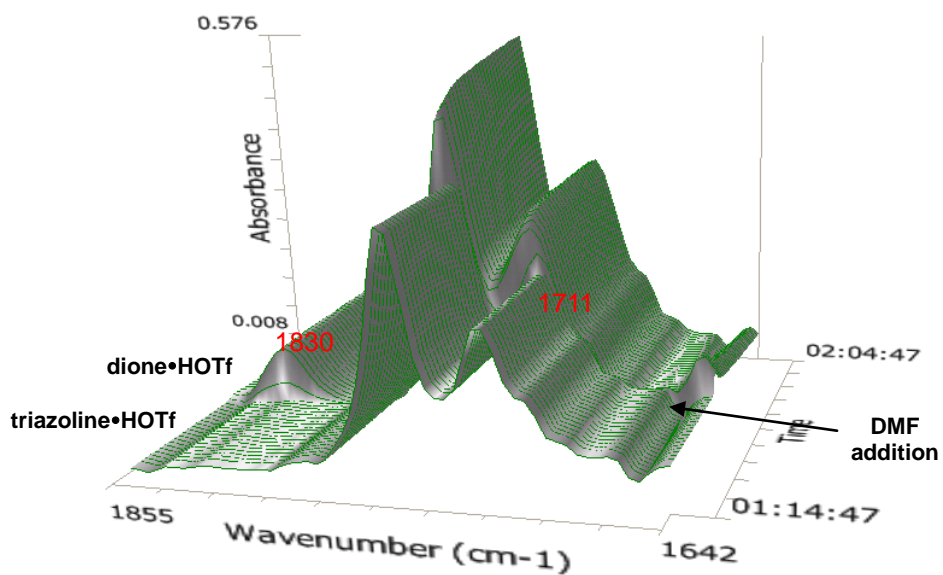


Left Perspective

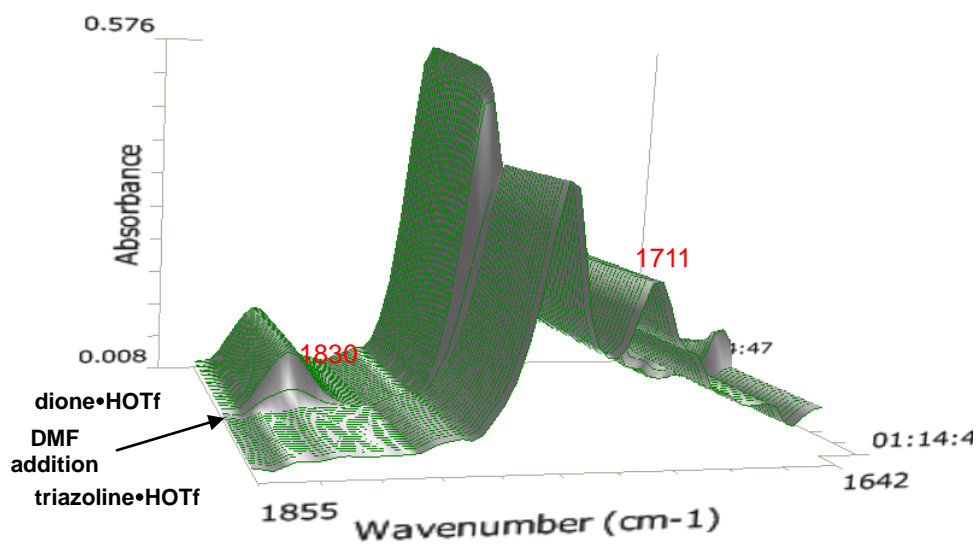


Additive: DMF

Right Perspective

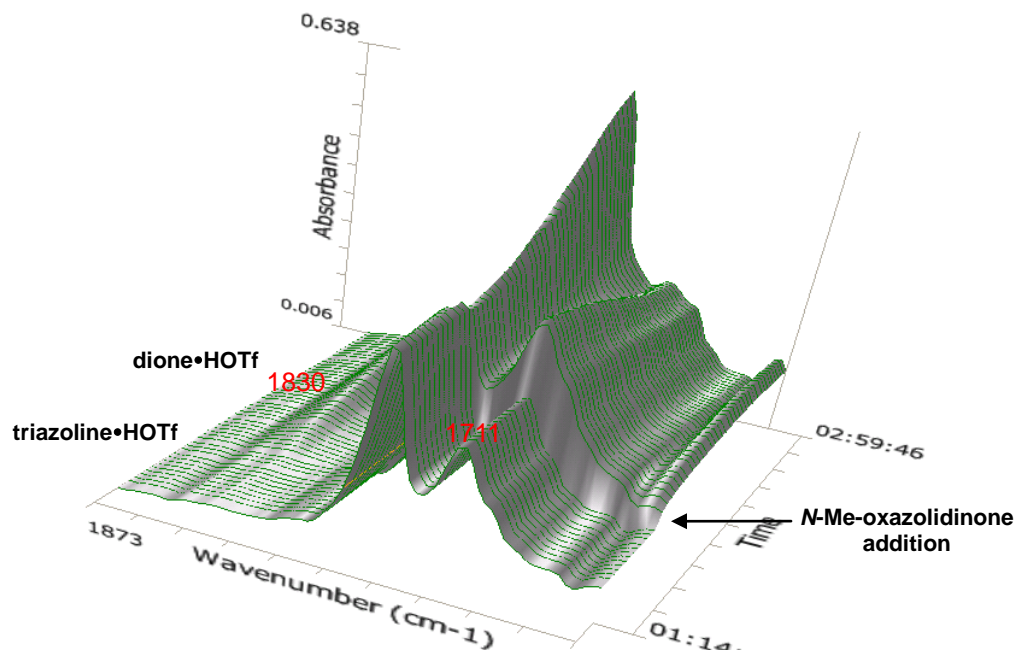


Left Perspective

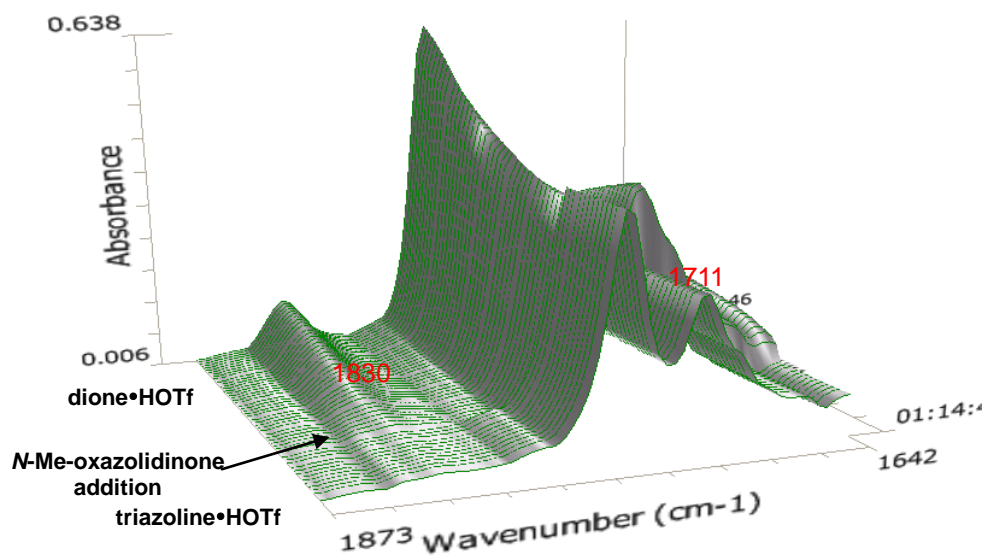


Additive: *N*-Me-oxazolidinone

Right Perspective



Left Perspective



A.2 X-Ray Crystallography Data

The sample was submitted by Ki Bum Hong (research group of J. Johnston, Department of Chemistry, Vanderbilt University). A colorless crystal (approximate dimensions $0.32 \times 0.12 \times 0.11 \text{ mm}^3$) was placed onto the tip of a 0.1 mm diameter glass capillary and mounted on a Bruker platform diffractometer equipped with a SMART6000 CCD detector at 130(2) K.

Data collection

The data collection was carried out using Mo $K\alpha$ radiation (graphite monochromator) with a frame time of 7 seconds and a detector distance of 5.0 cm. A randomly oriented region of reciprocal space was surveyed to the extent of a sphere. Four major sections of frames were collected with 0.30° steps in ω at different ϕ settings and a detector position of -43° in 2θ . Data to a resolution of 0.77 \AA were considered in the reduction. Final cell constants were calculated from the xyz centroids of 6253 strong reflections from the actual data collection after integration (SAINT).¹⁰³ The intensity data were corrected for absorption (SADABS).¹⁰⁴ Please refer to Table 1 for additional crystal and refinement information.

Structure solution and refinement

The space group $P2_1$ was determined based on intensity statistics and systematic absences. The structure was solved using SIR-2004¹⁰⁵ and refined with SHELXL-97.¹⁰⁶ A direct-methods solution was calculated, which provided most non-hydrogen atoms from the E-map. Full-matrix least squares / difference Fourier cycles were performed which located the remaining non-hydrogen atoms. All non-hydrogen atoms were refined with anisotropic displacement parameters. The hydrogen atoms were placed in ideal positions and refined as riding atoms with individual isotropic displacement parameters. The final full matrix least squares refinement converged to $R1 = 0.0287$ and $wR2 = 0.0725$ (F^2 , all data). The remaining electron density is minuscule and located on bonds.

¹⁰³ SAINT, Bruker Analytical X-Ray Systems, Madison, WI, current version.

¹⁰⁴ An empirical correction for absorption anisotropy, R. Blessing, *Acta Cryst.* A51, 33 - 38 (1995).

¹⁰⁵ Sir2004, A Program for Automatic Solution and Refinement of Crystal Structure. M. C. Burla, R. Caliendo, M. Carnalli, B. Carrozzini, G. L. Cascarano, L. De Caro, C. Giacovazzo, G. Polidori, R. Sagna, version 1.0 (2004).

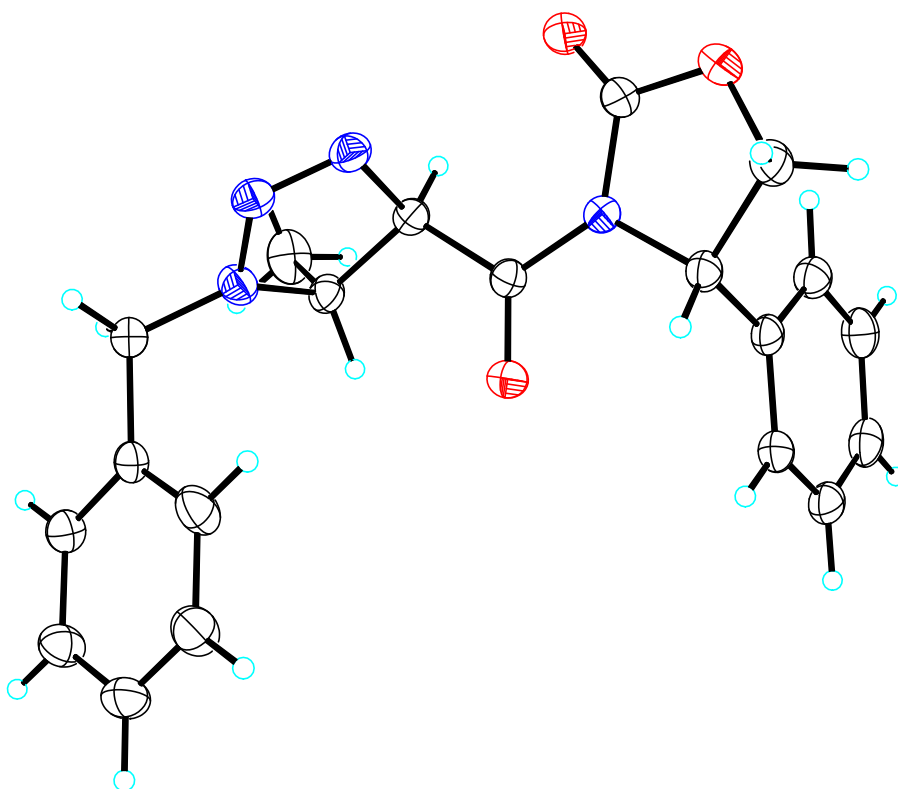
¹⁰⁶ SHELXTL-Plus, Bruker Analytical X-Ray Systems, Madison, WI, current version.

Structure description

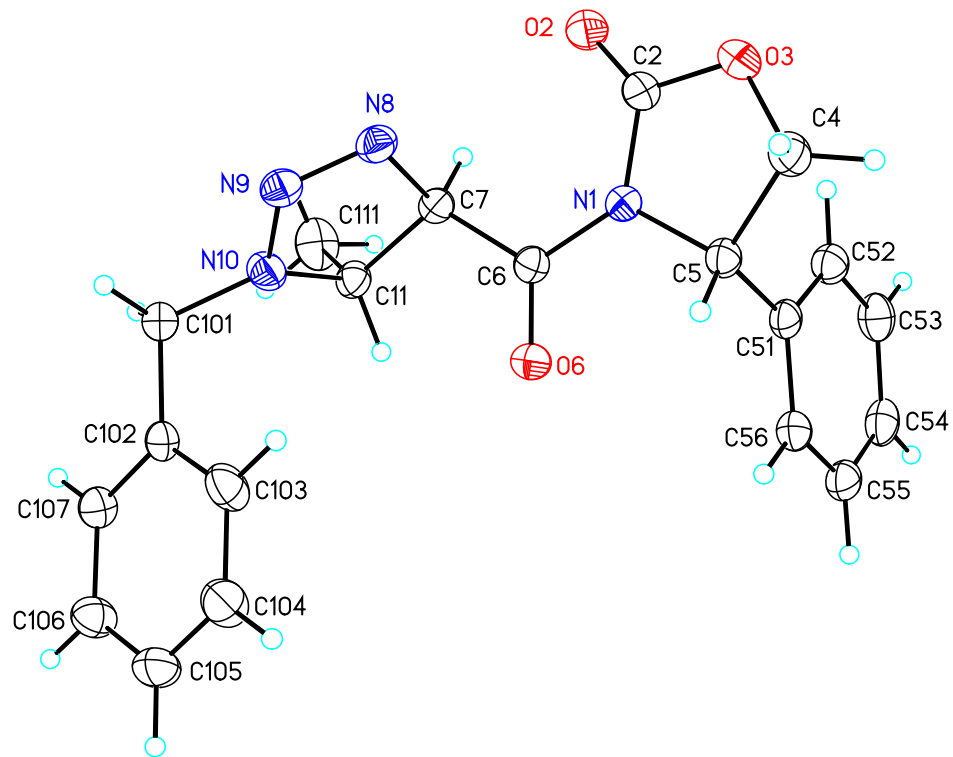
The structure was found as. The absolute configuration cannot be established for a light atom structure using Mo radiation. The refined enantiomer was chosen arbitrarily. Non-classical H-bonding was observed.



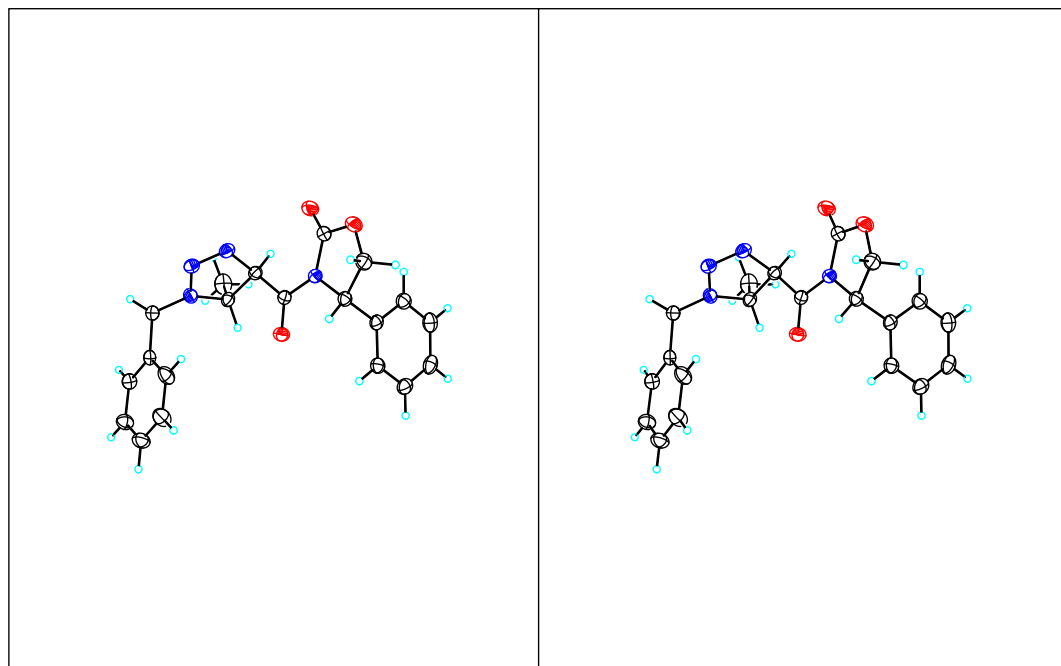
Bulk Material.



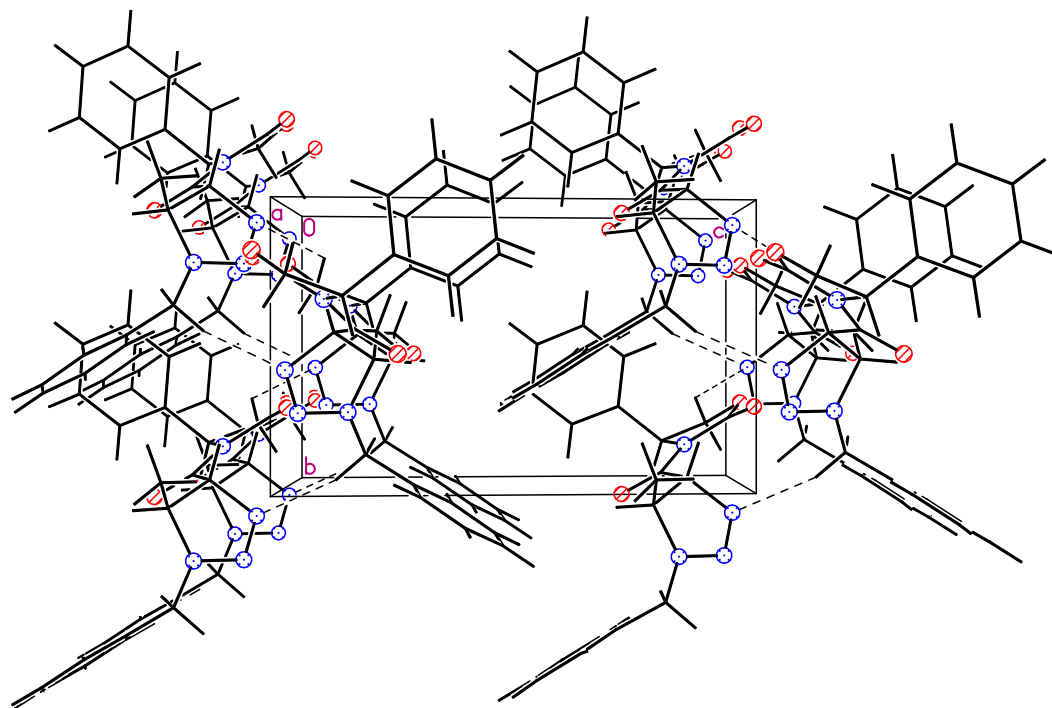
Formula unit.



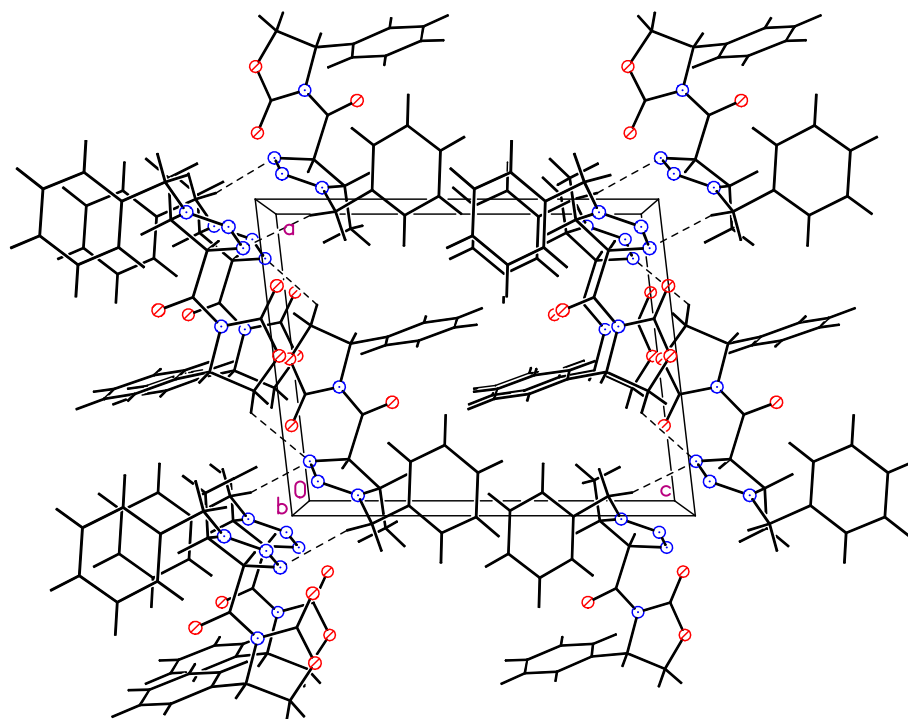
Formula unit.



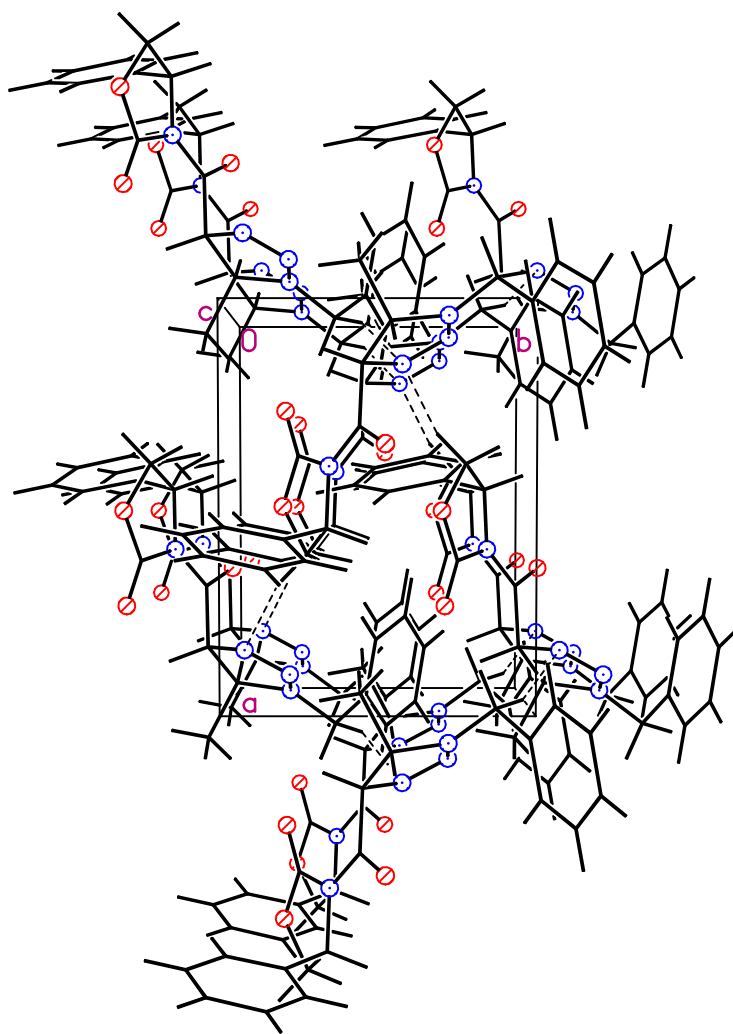
Stereo view of formula unit.



Cell plot, view along *a*.



Cell plot, view along *b*.



Cell plot, view along *c*.

Table 1. Crystal data and structure refinement for 07023.

Empirical formula	C ₂₀ H ₂₀ N ₄ O ₃
Formula weight	364.40
Crystal color, shape, size	colorless block, 0.32 × 0.12 × 0.11 mm ³
Temperature	130(2) K
Wavelength	0.71073 Å
Crystal system, space group	Monoclinic, P2(1)
Unit cell dimensions	a = 9.8678(6) Å α = 90°. b = 7.4604(5) Å β = 96.5463(16)°. c = 12.2936(8) Å γ = 90°.
Volume	899.13(10) Å ³
Z	2
Density (calculated)	1.346 Mg/m ³
Absorption coefficient	0.093 mm ⁻¹
F(000)	384

Data collection

Diffractometer	SMART6000 Platform CCD, Bruker
Theta range for data collection	2.08 to 27.51°.
Index ranges	-12 ≤ h ≤ 12, -9 ≤ k ≤ 9, -15 ≤ l ≤ 15
Reflections collected	26974
Independent reflections	4124 [R(int) = 0.0286]
Observed Reflections	4005
Completeness to theta = 27.51°	100.0 %

Solution and Refinement

Absorption correction	Semi-empirical from equivalents
Max. and min. transmission	0.9898 and 0.9708
Solution	Direct methods
Refinement method	Full-matrix least-squares on F ²
Weighting scheme	w = [σ ² Fo ² + AP ² + BP] ⁻¹ , with P = (Fo ² + 2 Fc ²)/3, A = 0.0360, B = 0.1817
Data / restraints / parameters	4124 / 1 / 265
Goodness-of-fit on F ²	1.033
Final R indices [I > 2σ(I)]	R1 = 0.0287, wR2 = 0.0712
R indices (all data)	R1 = 0.0298, wR2 = 0.0725
Absolute structure parameter	0.3(7)

Largest diff. peak and hole

0.208 and -0.166 e.Å⁻³

Goodness-of-fit = $[\sum[w(F_o^2 - F_c^2)^2]/N_{\text{observns}} - N_{\text{params}}]^{1/2}$, all data.

$R1 = \sum(|F_o| - |F_c|) / \sum |F_o|$. $wR2 = [\sum[w(F_o^2 - F_c^2)^2] / \sum [w(F_o^2)^2]]^{1/2}$.

* For a light atom structure such as this measured with MoK α radiation this value is meaningless. The absolute structure was not established.

Table S.2.1. Atomic coordinates ($\times 10^4$) and equivalent isotropic displacement parameters ($\text{\AA}^2 \times 10^3$) for 07023. U(eq) is defined as one third of the trace of the orthogonalized U^{ij} tensor.

x	y	z	U(eq)	
N1	4007(1)	3503(1)	1308(1)	23(1)
O2	2671(1)	2112(2)	-144(1)	37(1)
C2	3745(1)	2524(2)	340(1)	27(1)
O3	4948(1)	2021(1)	10(1)	32(1)
C4	6083(1)	2801(2)	714(1)	28(1)
C5	5466(1)	3435(2)	1738(1)	22(1)
O6	3515(1)	5237(1)	2702(1)	30(1)
C6	3092(1)	4452(2)	1869(1)	22(1)
C7	1606(1)	4532(2)	1370(1)	22(1)
N8	1577(1)	5770(2)	401(1)	25(1)
N9	970(1)	7194(2)	613(1)	24(1)
N10	519(1)	7178(2)	1594(1)	26(1)
C11	673(1)	5416(2)	2124(1)	23(1)
C51	5706(1)	2180(2)	2710(1)	22(1)
C52	5427(1)	350(2)	2592(1)	26(1)
C53	5592(1)	-783(2)	3497(1)	30(1)
C54	6048(1)	-96(2)	4522(1)	30(1)
C55	6354(1)	1708(2)	4641(1)	29(1)
C56	6179(1)	2843(2)	3740(1)	25(1)
C101	-328(1)	8628(2)	1912(1)	28(1)
C102	304(1)	9613(2)	2917(1)	23(1)
C103	1705(1)	9934(2)	3090(1)	32(1)
C104	2255(1)	10910(2)	3997(1)	37(1)
C105	1421(1)	11566(2)	4737(1)	34(1)
C106	26(1)	11261(2)	4566(1)	30(1)
C107	-524(1)	10282(2)	3664(1)	25(1)
C111	-699(1)	4470(2)	2123(1)	37(1)

Table S.2.2. Bond lengths [Å] and angles [°] for 07023.

N1-C6	1.3902(14)	N1-C2	1.3948(15)
N1-C5	1.4773(14)	O2-C2	1.1952(16)
C2-O3	1.3507(16)	O3-C4	1.4556(16)
C4-C5	1.5344(16)	C4-H4A	0.9900
C4-H4B	0.9900	C5-C51	1.5153(16)
C5-H5	1.0000	O6-C6	1.2125(14)
C6-C7	1.5253(15)	C7-N8	1.5049(15)
C7-C11	1.5287(15)	C7-H7	1.0000
N8-N9	1.2616(15)	N9-N10	1.3317(13)
N10-C101	1.4477(16)	N10-C11	1.4671(16)
C11-C111	1.5261(18)	C11-H11	1.0000
C51-C56	1.3902(16)	C51-C52	1.3971(18)
C52-C53	1.3923(18)	C52-H52	0.9500
C53-C54	1.3870(19)	C53-H53	0.9500
C54-C55	1.383(2)	C54-H54	0.9500
C55-C56	1.3886(18)	C55-H55	0.9500
C56-H56	0.9500	C101-C102	1.5099(16)
C101-H10A	0.9900	C101-H10B	0.9900
C102-C107	1.3900(16)	C102-C103	1.3947(17)
C103-C104	1.3893(19)	C103-H103	0.9500
C104-C105	1.3844(19)	C104-H104	0.9500
C105-C106	1.3874(19)	C105-H105	0.9500
C106-C107	1.3866(18)	C106-H106	0.9500
C107-H107	0.9500	C111-H11A	0.9800
C111-H11B	0.9800	C111-H11C	0.9800
C6-N1-C2	128.49(10)	C6-N1-C5	120.08(9)
C2-N1-C5	111.42(9)	O2-C2-O3	122.64(12)
O2-C2-N1	128.80(12)	O3-C2-N1	108.53(10)
C2-O3-C4	110.73(10)	O3-C4-C5	105.08(9)
O3-C4-H4A	110.7	C5-C4-H4A	110.7
O3-C4-H4B	110.7	C5-C4-H4B	110.7
H4A-C4-H4B	108.8	N1-C5-C51	111.20(9)
N1-C5-C4	100.30(9)	C51-C5-C4	114.55(10)
N1-C5-H5	110.1	C51-C5-H5	110.1
C4-C5-H5	110.1	O6-C6-N1	119.03(10)
O6-C6-C7	122.92(10)	N1-C6-C7	117.97(10)
N8-C7-C6	105.82(9)	N8-C7-C11	104.84(9)
C6-C7-C11	113.03(9)	N8-C7-H7	111.0
C6-C7-H7	111.0	C11-C7-H7	111.0
N9-N8-C7	108.66(9)	N8-N9-N10	113.28(10)

N9-N10-C101	120.02(10)	N9-N10-C11	112.42(10)
C101-N10-C11	125.68(10)	N10-C11-C111	111.56(10)
N10-C11-C7	99.02(9)	C111-C11-C7	113.29(10)
N10-C11-H11	110.8	C111-C11-H11	110.8
C7-C11-H11	110.8	C56-C51-C52	118.95(11)
C56-C51-C5	120.33(11)	C52-C51-C5	120.71(10)
C53-C52-C51	120.43(12)	C53-C52-H52	119.8
C51-C52-H52	119.8	C54-C53-C52	119.89(12)
C54-C53-H53	120.1	C52-C53-H53	120.1
C55-C54-C53	119.97(12)	C55-C54-H54	120.0
C53-C54-H54	120.0	C54-C55-C56	120.23(12)
C54-C55-H55	119.9	C56-C55-H55	119.9
C55-C56-C51	120.52(12)	C55-C56-H56	119.7
C51-C56-H56	119.7	N10-C101-C102	112.76(10)
N10-C101-H10A	109.0	C102-C101-H10A	109.0
N10-C101-H10B	109.0	C102-C101-H10B	109.0
H10A-C101-H10B	107.8	C107-C102-C103	119.03(11)
C107-C102-C101	119.73(10)	C103-C102-C101	121.18(11)
C104-C103-C102	120.12(12)	C104-C103-H103	119.9
C102-C103-H103	119.9	C105-C104-C103	120.39(12)
C105-C104-H104	119.8	C103-C104-H104	119.8
C104-C105-C106	119.77(13)	C104-C105-H105	120.1
C106-C105-H105	120.1	C107-C106-C105	119.92(12)
C107-C106-H106	120.0	C105-C106-H106	120.0
C106-C107-C102	120.76(11)	C106-C107-H107	119.6
C102-C107-H107	119.6	C11-C111-H11A	109.5
C11-C111-H11B	109.5	H11A-C111-H11B	109.5
C11-C111-H11C	109.5	H11A-C111-H11C	109.5
H11B-C111-H11C	109.5		

Table S.2.3. Anisotropic displacement parameters ($\text{\AA}^2 \times 10^3$) for 07023. The anisotropic displacement factor exponent takes the form: $-2\pi^2 [h^2 a^{*2} U^{11} + \dots + 2 h k a^* b^* U^{12}]$

	U ¹¹	U ²²	U ³³	U ²³	U ¹³	U ¹²
N1	21(1)	24(1)	23(1)	-3(1)	-1(1)	2(1)
O2	32(1)	40(1)	36(1)	-16(1)	-8(1)	8(1)
C2	31(1)	26(1)	25(1)	-3(1)	0(1)	7(1)
O3	31(1)	37(1)	27(1)	-9(1)	4(1)	7(1)
C4	26(1)	31(1)	27(1)	0(1)	6(1)	2(1)
C5	19(1)	23(1)	25(1)	-1(1)	2(1)	1(1)
O6	26(1)	35(1)	26(1)	-9(1)	-1(1)	5(1)
C6	23(1)	22(1)	21(1)	1(1)	2(1)	3(1)
C7	21(1)	24(1)	21(1)	0(1)	1(1)	1(1)
N8	24(1)	32(1)	20(1)	1(1)	2(1)	2(1)
N9	24(1)	26(1)	21(1)	1(1)	2(1)	-1(1)
N10	33(1)	22(1)	23(1)	1(1)	6(1)	3(1)
C11	23(1)	26(1)	21(1)	3(1)	3(1)	4(1)
C51	16(1)	26(1)	24(1)	0(1)	3(1)	3(1)
C52	22(1)	27(1)	29(1)	-2(1)	2(1)	1(1)
C53	25(1)	25(1)	41(1)	5(1)	8(1)	1(1)
C54	23(1)	37(1)	31(1)	10(1)	8(1)	8(1)
C55	22(1)	40(1)	25(1)	-1(1)	3(1)	7(1)
C56	20(1)	27(1)	28(1)	-3(1)	3(1)	3(1)
C101	29(1)	27(1)	27(1)	-3(1)	-2(1)	7(1)
C102	24(1)	19(1)	25(1)	2(1)	2(1)	3(1)
C103	25(1)	30(1)	41(1)	-8(1)	9(1)	2(1)
C104	22(1)	36(1)	52(1)	-14(1)	2(1)	-1(1)
C105	31(1)	34(1)	37(1)	-11(1)	-2(1)	-2(1)
C106	30(1)	34(1)	28(1)	-4(1)	7(1)	0(1)
C107	21(1)	26(1)	28(1)	1(1)	5(1)	-1(1)
C111	31(1)	36(1)	46(1)	8(1)	16(1)	0(1)

Table S.2.4. Hydrogen coordinates ($\times 10^4$) and isotropic displacement parameters ($\text{\AA}^2 \times 10^3$) for 07023.

	x	y	z	U(eq)
H4A	6482	3821	345	33(4)
H4B	6804	1896	908	34(4)
H5	5804	4664	1949	20(3)
H7	1263	3313	1138	22(3)
H11	1143	5526	2885	36(4)
H52	5122	-124	1889	31(4)
H53	5394	-2025	3413	39(4)
H54	6149	-864	5142	39(4)
H55	6684	2172	5340	29(4)
H56	6385	4082	3829	33(4)
H10A	-1222	8138	2057	41(5)
H10B	-491	9487	1297	41(4)
H103	2283	9484	2586	43(4)
H104	3209	11128	4109	47(5)
H105	1803	12222	5360	44(5)
H106	-551	11723	5067	33(4)
H107	-1479	10065	3555	29(4)
H11A	-1269	5135	2587	48(5)
H11B	-551	3251	2408	68(7)
H11C	-1157	4419	1373	45(5)

Table S.2.5. Torsion angles [°] for 07023.

C6-N1-C2-O2	-9.8(2)	C5-N1-C2-O2	169.60(14)
C6-N1-C2-O3	171.95(11)	C5-N1-C2-O3	-8.64(14)
O2-C2-O3-C4	176.58(13)	N1-C2-O3-C4	-5.05(14)
C2-O3-C4-C5	15.88(14)	C6-N1-C5-C51	75.20(13)
C2-N1-C5-C51	-104.27(11)	C6-N1-C5-C4	-163.23(10)
C2-N1-C5-C4	17.30(13)	O3-C4-C5-N1	-19.06(12)
O3-C4-C5-C51	100.10(11)	C2-N1-C6-O6	-179.61(12)
C5-N1-C6-O6	1.02(17)	C2-N1-C6-C7	-2.62(18)
C5-N1-C6-C7	178.02(11)	O6-C6-C7-N8	104.19(13)
N1-C6-C7-N8	-72.68(13)	O6-C6-C7-C11	-10.00(17)
N1-C6-C7-C11	173.13(10)	C6-C7-N8-N9	-110.55(10)
C11-C7-N8-N9	9.17(12)	C7-N8-N9-N10	-1.22(13)
N8-N9-N10-C101	-173.21(11)	N8-N9-N10-C11	-7.94(13)
N9-N10-C11-C111	-106.96(12)	C101-N10-C11-C111	57.32(15)
N9-N10-C11-C7	12.59(12)	C101-N10-C11-C7	176.87(11)
N8-C7-C11-N10	-12.22(11)	C6-C7-C11-N10	102.56(11)
N8-C7-C11-C111	106.03(11)	C6-C7-C11-C111	-139.19(11)
N1-C5-C51-C56	-115.31(11)	C4-C5-C51-C56	131.85(11)
N1-C5-C51-C52	63.26(14)	C4-C5-C51-C52	-49.58(14)
C56-C51-C52-C53	1.39(17)	C5-C51-C52-C53	-177.19(10)
C51-C52-C53-C54	-0.50(18)	C52-C53-C54-C55	-0.89(18)
C53-C54-C55-C56	1.37(18)	C54-C55-C56-C51	-0.45(17)
C52-C51-C56-C55	-0.92(17)	C5-C51-C56-C55	177.67(10)
N9-N10-C101-C102	-119.55(12)	C11-N10-C101-C102	77.27(15)
N10-C101-C102-C107	-145.01(12)	N10-C101-C102-C103	37.78(17)
C107-C102-C103-C104	0.0(2)	C101-C102-C103-C104	177.21(13)
C102-C103-C104-C105	0.2(2)	C103-C104-C105-C106	-0.6(2)
C104-C105-C106-C107	0.9(2)	C105-C106-C107-C102	-0.7(2)
C103-C102-C107-C106	0.26(19)	C101-C102-C107-C106	-177.01(12)